Identification of novel transcription factors involved in regulating the production of lignocellulolytic enzymes in *Myceliophthora thermophila*

Yapeng Lai

A thesis submitted to

Auckland University of Technology

in fulfilment of the requirements for the degree of

Doctor of Philosophy (PhD)

2026

Faculty of Health and Environmental Sciences

School of Science

Abstract

Fossil fuels such as crude oil, coal, and natural gas are non-renewable energy resources that are increasingly depleted due to heavy exploitation driven by global population and industrialisation. Their combustion also contributes to global warming and environmental pollution, posing significant threats to human health and the environment. Therefore, the exploitation of renewable and environmentally friendly alternatives to fossil fuel is urgently required. Lignocellulosic biomass, the most abundant renewable resource on Earth, can be converted into biochemicals such as glycolic acid, xylitol, xylonic acid, and xylo-oligosaccharides, and into fermentable sugars for the production of biofuels, making it a potential substitute for fossil fuels. The thermophilic filamentous fungus *Myceliophthora thermophila* secretes large amounts of thermostable lignocellulolytic enzymes, including cellulases and xylanases, which enable efficient degradation of lignocellulose. However, the native production levels of these enzymes in this fungus are generally lower than those of mesophilic fungi such as *Trichoderma* and *Aspergillus* species. Lignocellulose degradation in filamentous fungi is regulated by a complex transcriptional network involving various transcriptional activators and repressors. To date, only a limited number of transcription factors have been identified in *M. thermophila* that regulate cellulase and xylanase biosynthesis, and the underlying mechanisms remain unclear, impeding rational strain engineering. The aim of this thesis was to identify and characterise transcription factors involved in cellulase and xylanase regulation in *M. thermophila* and to elucidate their molecular mechanisms. Comparative transcriptomic analysis of *M. thermophila* grown in Avicel and glucose was firstly performed to identify candidate transcription factors. To facilitate functional studies, a CRISPR/Cas9-based gene editing tool and a constitutive promoter (P*pdc*)-driven overexpression system were developed. Using these approaches, three transcription factors, MtFKH1, MtHAC-1, and MtCLR-2, were shown to regulate cellulase and/or xylanase production. Through molecular genetic analyses and comparative transcriptomic profiling, the regulatory roles of these

transcription factors were elucidated. MtFKH1 is the first forkhead transcription factor identified in *M. thermophila*, which negatively regulates the expression of major cellulase and xylanase genes and plays an important role in fungal sporulation. The EMSAs indicated that MtFKH1 directly binds to the promoter regions of *bgl1*, *cbh1*, and *xyn1*. The bZIP transcription factor MtHAC-1 exerts dual regulatory effects on cellulase and xylanase production. It plays a positive role during the early phase of growth on Avicel (48 h) but acts as a repressor in the middle and later stages (72 and 96 h). The EMSAs suggested that MtHAC-1 can bind to the promoter regions of both *bgl1*, *cbh1*, *egl2*, *xyn1*, and *xyr1*. Thus, it regulates cellulase and xylanase gene expression through two mechanisms: direct binding, and modulation of the crucial xylanolytic activator *Mtxyr1*. MtHAC-1 was also found to be associated with the expression of genes of the 26S proteasome system. The Zn2Cys6-type transcription factor MtCLR-2 acts as a pivotal activator of cellulase production. The EMSAs and RT-qPCR analyses indicated that MtCLR-2 regulates cellulase gene expression by directly binding to the promoter regions of major cellulase genes *egl2* and *bgl1*. Moreover, MtCLR-2 is involved in the transcriptional regulation of approximately half of the ribosomal protein genes. This thesis contributes to a deeper understanding of the transcriptional regulation associated with lignocellulose degradation in *M. thermophila*. The findings expand the repertoire of known transcription factors involved in cellulase and xylanase expression and provide novel targets for engineering of *M. thermophila* to elevate lignocellulolytic enzyme production.

Keywords: *Myceliophthora thermophila*; cellulase; xylanase; gene expression; transcription factor; MtFKH1; MtHAC-1; MtCLR-2; CRISPR/Cas9; comparative transcriptomic analysis

Table of Content

List of Figures

List of Tables

Attestation of Authorship

I hereby declare that this submission is my own work and that, to the best of my knowledge and belief, it contains no material previously published or written by another person (except where explicitly defined in the acknowledgements), nor used artificial intelligence tools or generative artificial intelligence tools (unless it is clearly stated, and referenced, along with the purpose of use), nor material which to a substantial extent has been submitted for the award of any other degree or diploma of a university or other institution of higher learning.

10 December 2025

Co-authorship Contributions within this Thesis

Please copy the box below into your thesis, repeated for each manuscript included in the thesis.

STUDENT AND SUPERVISOR APPROVALS

By signing you are confirming that the co-author contributions stated in the table(s) below are accurate.

Student Name	Yapeng Lai	**Signature**	Ya Peng Lai	**Date**	08.12.2025
Supervisor Name	Donnabella Lacap-Bugler	**Signature**		**Date**	10.12.2025

Chapter Number:	**Chapter 2**
Manuscript Title:	Identification of a novel forkhead transcription factor MtFKH1 for cellulase and xylanase gene expression in *Myceliophthora thermophila* (ATCC 42464)
Publication Status:	**Published**
Reference if published:	https://doi.org/10.1016/j.micres.2025.128097.

AUTHOR SURNAME:	CONTRIBUTION
Yapeng Lai	Conception and design of the project or output Acquisition of research data where the acquisition has required significant intellectual judgement, planning, design, or input Analysis or interpretation of research data Drafting significant parts of the research output or critically revising it, to contribute to its quality and interpretation
Juan Wang	Conception and design of the project or output Contribution of knowledge, where justified, including Indigenous knowledge Analysis or interpretation of research data
Ning Xie	Conception and design of the project or output Contribution of knowledge, where justified, including Indigenous knowledge
Gang Liu	Conception and design of the project or output Acquisition of research data where the acquisition has required significant intellectual judgement, planning, design, or input Contribution of knowledge, where justified, including Indigenous knowledge Drafting significant parts of the research output or critically revising it, to contribute to its quality and interpretation.
Donnabella Lacap-Bugler	Conception and design of the project or output Acquisition of research data where the acquisition has required significant intellectual judgement, planning, design, or input Contribution of knowledge, where justified, including Indigenous knowledge Drafting significant parts of the research output or critically revising it, to contribute to its quality and interpretation.

Chapter Number:	**Chapter 3**
Manuscript Title:	Dual Role of MtHAC-1 in regulating cellulase and xylanase production in *Myceliophthora thermophila*.
Publication Status:	**Published**
Reference if published:	https://doi.org/10.1111/1751-7915.70203.

AUTHOR SURNAME:	CONTRIBUTION
Yapeng Lai	Conception and design of the project or output Acquisition of research data where the acquisition has required significant intellectual judgement, planning, design, or input Analysis or interpretation of research data Drafting significant parts of the research output or critically revising it, to contribute to its quality and interpretation
Juan Wang	Conception and design of the project or output Contribution of knowledge, where justified, including Indigenous knowledge Analysis or interpretation of research data
Ning Xie	Conception and design of the project or output Contribution of knowledge, where justified, including Indigenous knowledge
Gang Liu	Conception and design of the project or output Acquisition of research data where the acquisition has required significant intellectual judgement, planning, design, or input Contribution of knowledge, where justified, including Indigenous knowledge Drafting significant parts of the research output or critically revising it, to contribute to its quality and interpretation.
Donnabella Lacap-Bugler	Conception and design of the project or output Acquisition of research data where the acquisition has required significant intellectual judgement, planning, design, or input Contribution of knowledge, where justified, including Indigenous knowledge Drafting significant parts of the research output or critically revising it, to contribute to its quality and interpretation.

Chapter Number:	**Chapter 4**
Manuscript Title:	Transcription factor MtCLR-2 regulates cellulase production via direct modulation of *Mtegl2* and *Mtbgl1* expression in *Myceliophthora thermophila*
Publication Status:	**Published**
Reference if published:	https://doi.org/10.1186/s12934-026-02976-1

AUTHOR SURNAME:	CONTRIBUTION
Yapeng Lai	Conception and design of the project or output Acquisition of research data where the acquisition has required significant intellectual judgement, planning, design, or input Analysis or interpretation of research data Drafting significant parts of the research output or critically revising it, to contribute to its quality and interpretation
Juan Wang	Conception and design of the project or output Contribution of knowledge, where justified, including Indigenous knowledge Analysis or interpretation of research data
Ning Xie	Conception and design of the project or output Contribution of knowledge, where justified, including Indigenous knowledge
Gang Liu	Conception and design of the project or output Acquisition of research data where the acquisition has required significant intellectual judgement, planning, design, or input Contribution of knowledge, where justified, including Indigenous knowledge Drafting significant parts of the research output or critically revising it, to contribute to its quality and interpretation.
Donnabella Lacap-Bugler	Conception and design of the project or output Acquisition of research data where the acquisition has required significant intellectual judgement, planning, design, or input Contribution of knowledge, where justified, including Indigenous knowledge Drafting significant parts of the research output or critically revising it, to contribute to its quality and interpretation.

Acknowledgements

I am deeply grateful to the many individuals whose support and guidance contributed to the successful completion of this PhD thesis. First and foremost, I would like to express my sincere gratitude to my supervisors, Professor Donnabella Lacap-Bugler, Associate Professor Juan Wang, and Professor Gang Liu. They have provided invaluable assistance and insightful advice throughout every stage of my research, including project conception, experimental design, financial support, troubleshooting during experiments, data analysis, and manuscript revision and publication.

I am also deeply grateful to Shenzhen University (SZU) and Auckland University of Technology (AUT) for giving me the opportunity to pursue my doctoral degree. Without the financial support and scholarships provided by both institutions, it would not have been possible for me to complete my PhD studies so smoothly. I also acknowledge the assistance of ChatGPT in grammar checking and language refinement during the preparation of this thesis.

My heartfelt thanks go to the members of the microbiology research group at SZU for their help and support in both study and daily life. I would also like to thank Brent Seale from Food Science and Microbiology research group in AUT for his encouragement and assistance. I am equally grateful to the friends I have made in New Zealand; your companionship has brought warmth and strength during my time away from home.

Finally, I extend my deepest gratitude to my family. Thank you for your unconditional love and support; you have been my greatest source of motivation throughout this journey.

As I look forward to the future, I hope to continue exploring and contributing within my professional field.

Chapter 1 Introduction and Literature Review

1.1 The introduction of biofuels

As the world population continues to grow, the demand of energy is increasing globally. Currently, the prime resources of energy are the non-renewable fossil fuels such a s crude oil, coal and natural gas (Gupta and Verma, 2015; Taha et al., 2016; Joyia et al., 2024). It has been realized that the fossil resources would be depleted in the near future since they are heavily exploited for the production of multiple products such as fuel, electricity and other goods to meet the increasing population and industrialisation (Naik et al., 2010; Gupta and Verma, 2015). In addition, the combustion of fossil fuels results in the increased level of CO_2 in the atmosphere, which directly relates to global warming (Naik et al., 2010; Bhatia et al., 2017). Therefore, the exploitation of renewable, widely distributed and environmentally benign candidate for replacement of fossil fuel reserves as the major energy source is urgently needed (Himmel et al., 2007; Naik et al., 2010; Bhatia et al., 2017).

Biofuels are derived from renewable biological materials, can be an appropriate alternative to conventional fossil fuels (Naik et al., 2010; Bhatia et al., 2017; Nanda et al., 2018). The application of biofuels would reduce the reliance on crude oil consumption and helps to mitigate the environmental pollution caused by fossil fuel burning, as well as provide employment opportunities in bio-based sectors in rural areas (Naik et al., 2010; Gupta and Verma, 2015). Biofuel includes solid, liquid and gas form of energy, and the primary biofuels contain bioethanol, biodiesel, biogas, and bio-oil, among which, bioethanol and biodiesel belong to liquid transportation fuels, that can be used as blended petroleum-based fuels (Gupta and Verma, 2015; Taha et al., 2016; Nanda et al., 2018). Biofuels can be produced from a wide range of feedstocks including food crops, agricultural residues, forestry biomass, animal fats, municipal solid waste, industrial effluents, sewage sludge, and other organic matters, by using diverse thermochemical and biochemical technologies (Nanda et al., 2018). Depending on the raw material used and the production technique, biofuels are generally categorized into the first, second and third generation, while the fourth-generation biofuel relies on

synthetic biology and just remains at the early research stage (Aro, 2016; Nanda et al., 2018).

The first-generation biofuels are produced using food crops such as corn, wheat, and sugarcane (starch-based and sugar-rich crops); second-generation biofuels are produced from agricultural crop residues (wheat straw, rice straw, corn stover, corncob, and sugarcane bagasse), forest residues (stems, barks, sawdust, wood chips), and dedicated energy crops (switchgrass); third-generation biofuel are generated from algae-based feedstock (microalgae and macroalgae). While the fourth-generation biofuels, known as photobiological solar fuels, empowering conversion of solar energy to fuel from sunlight, water and CO_2 in engineered photosynthetic microorganisms (cyanobacteria), are expected to realize fundamental breakthroughs in the bioenergy field (Aro, 2016; Nanda et al., 2018). Presently, the fuel ethanol produced worldwide is mainly the first-generation from sugar-rich and starchy crops (Himmel et al., 2007; Gupta and Verma, 2015; Mohanty and Swain, 2019). The United States of America (USA) and Brazil are global leaders in renewable fuel ethanol production. While the USA produces bioethanol primarily from corn with a total production capacity of ~57.7 billion liters annually, Brazil produces about ~27.6 billion liters of fuel ethanol mainly from sugarcane as feedstock (Mohanty and Swain, 2019). However, concerns have been raised about the sourcing of the first-generation biofuel owing to the negative impact on biodiversity connected with deforestation for sugar rich and starch-based feedstock cultivation to promote the biofuel industry, and on food security resulting from the competition for arable land use between biofuel crops and food crops (Naik et al., 2010; Taha et al., 2016; Bhatia et al., 2017). By contrast, the second-generation biofuel such as cellulosic ethanol can avoid the existing conflict between crops for food supply and for biofuels production. This is because the second-generation biofuels stem from inedible plant biomass, especially lignocellulosic feedstocks, which do not pose a threat to food security or compete with food crops for the cultivated land (Nanda et al., 2018). In addition, open-field burning of agricultural crop residues is a universally common practice since it is an easy, cheap, and workable method of preparing the arable land for

the next crop. Nevertheless, the air emissions from the combustion process of this lignocellulosic waste not only threats public health but also poses a waste of material energy (Taha et al., 2016; Li et al., 2022c). This adverse effect could also be mitigated by the effective utilisation of agricultural wastes. The utilisation of the second-generation biofuels would decrease the demand for the first-generation biofuels and minimize competition with food crops for land use.

1.2 Composition of lignocellulose and its enzymatic hydrolysis

Lignocellulosic biomass, particularly agricultural crop residues such as corn stover, wheat and rice straw, and sugarcane bagasse, is an abundant renewable resource on the planet and therefore has been regarded as a promising alternative raw material for producing biofuels and value-added biochemicals (Agrawal et al., 2021; Meng et al., 2021; Ashokkumar et al., 2022) (Figure 1.1). It has also been considered a sustainable resource with carbon-neutral potential to reduce CO_2 emission and alleviate global warming (Naik et al., 2010; Ashokkumar et al., 2022). Lignocellulose is mainly from plant cell walls, synthesized by plants via photosynthesis, which is a recalcitrant heterogenic polymeric material. It comprised mainly of 1) cellulose (40-50%): a linear polymer of β-1,4 linked glucose monomers, and is the main component of cell wall polysaccharides; 2) hemicellulose (25-30%): a heteropolymer of hexoses, pentoses and uronic acids, is the second most rich polysaccharide of plant cell wall; and 3) lignin (15-20%): composed of three aromatic alcohols imparting an impenetrable barrier, substantially hinder the enzymatic hydrolysis of plant biomass (Sanchez, 2009; Gupta et al., 2016; Saldarriaga-Hernandez et al., 2020). Pectin is also a component of lignocellulose, but its amount depends on the plant species and tissue (Gupta et al., 2016; Benocci et al., 2017). These components of lignocellulose, form a heterogenous complex of carbohydrate polymers (cellulose-hemicellulose complex), and aromatic polymers (lignin), to create a firmly packed and water-insoluble structure (Taha et al., 2016). However, this type of material is recalcitrant to chemical and microbial attack,

and thus pretreatment is required for their destruction to separate the cellulose and hemicellulose components from lignin so that enzymatic degradation can be carried out more efficiently to release monosaccharides for subsequent fermentation for bioethanol generation (Liu et al., 2019a; Zhao et al., 2024b).

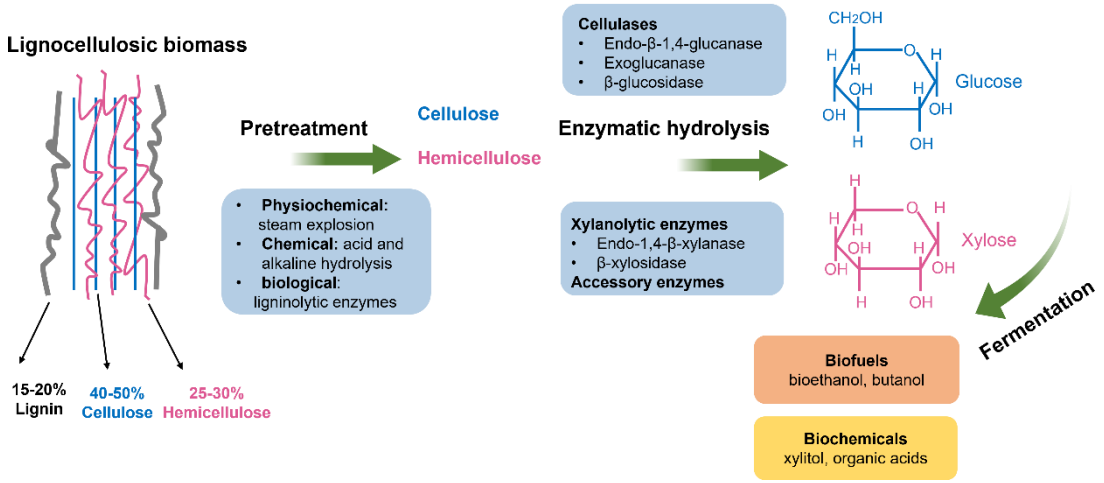

Figure 1.1. The process of conversion of lignocellulosic biomass to produce biofuels and biochemicals. The schematic diagram is based on (Meng et al., 2021).

During the pretreatment process, the lignin is removed, making cellulose and hemicellulose more accessible to enzymatic hydrolysis. There are chemical, physical, physicochemical, and biological approaches employed for pretreatment of lignocellulosic biomass, among which, thermochemical processes (such as steam explosion) are more practical and efficient (Ashokkumar et al., 2022; Zhao et al., 2024b). Biological pretreatment is performed by using various fungi that can secrete lignin-degrading enzymes, such as white rot fungi, or by using a cocktail of ligninolytic enzymes (laccase and peroxidase), which specifically decompose lignin in lignocellulosic residues (Meng et al., 2021). Biological pretreatment methods are more environmentally friendly, but require long incubation time (10-14 days), which makes this not suitable for industrial scale (Taha et al., 2016; Bhatia et al., 2017). After pretreatment, lignocellulosic biomass then undergoes biological hydrolysis, namely the saccharification of the complex lignocellulosic substrates into fermentable sugars,

which requires a diverse range of lignocellulolytic enzymes. These enzymes have been identified and classified into different families in the Carbohydrate Active Enzymes database (CAZy, https://www.cazy.org/) (Drula et al., 2022), based on amino acid sequences and structural features.

For cellulose hydrolysis, the synergistic manner of multiple cellulase components is required. Cellulases include endo-1,4-β-glucanase (EG; EC 3.2.1.4), cellobiohydrolase (CBH; EC 3.2.1.91), and β-glucosidase (BGL; EC 3.2.1.21). During the process of cellulose degradation, EGs randomly break internal β-1,4-glycosidic bonds in amorphous areas of cellulose and generate new reducing and non-reducing ends. CBHs including CBH I and CBH II attack reducing and non-reducing of cellulose fragments respectively, to release cellobiose. Both cellobiose and cello-oligosaccharides are finally hydrolysed by BGLs to yield glucose, which can be utilized to generate large numbers of value-added products such as bioethanol and biochemicals by fermentation performed by microbes (Gupta et al., 2016; Zhang et al., 2024b) (Figure 1.2). The microorganisms primarily used for cellulosic bioethanol fermentation are *Saccharomyces cerevisiae* and *Zymomonas mobilis* (Gupta et al., 2016).

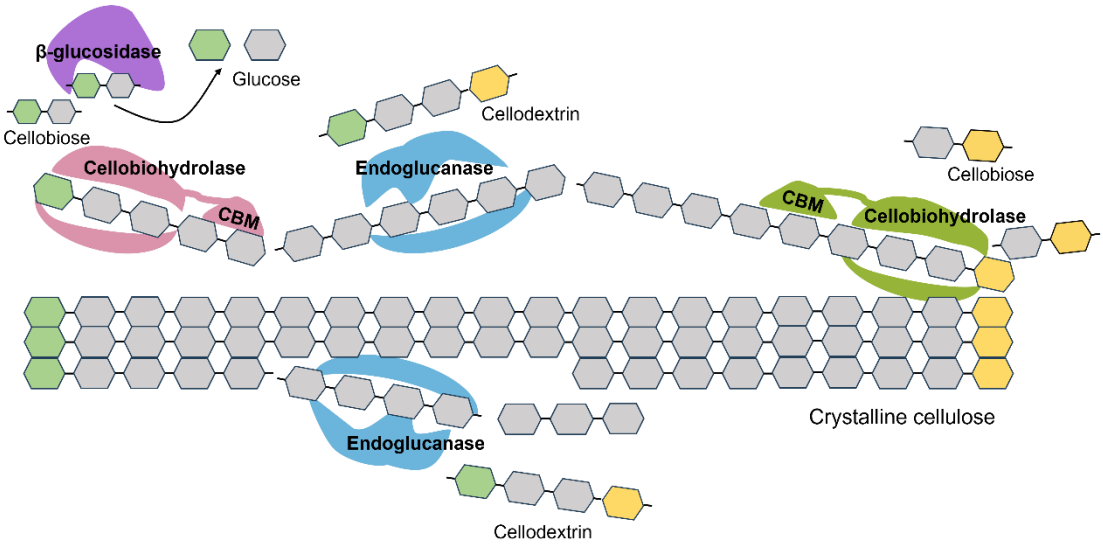

Figure 1.2. Degradation of cellulose by cellulolytic enzymes. The figure was redrawn and modified from (Gupta et al., 2016).

In contrast to cellulose, hemicellulose is more heterogeneous, requiring multiple enzymes, including both backbone and side-chain degrading enzymes, acting synergistically to depolymerisation of hemicellulose into xylose, arabinose, mannose, galactose, glucose and uronic acids (Gupta et al., 2016; Zhang et al., 2024b). For example, endo-1,4-β-xylanase, β-xylosidase, acetylxylan esterase, feruloyl esterase, α-L-arabinofuranosidase, endo-1,4-mannanase, β-mannosidase, α-galactosidase, α-glucuronidase, and other enzymes are all required for the complete degradation of hemicellulose (Li et al., 2022b). Among xylanolytic enzyme systems, endo-1,4-β-xylanase (EC 3.2.1.8) and β-xylosidase (EC 3.2.1.37) are the two crucial enzymes used for the hydrolysis of xylan, the primary constituent of hemicellulose. Endo-1,4-β-xylanase randomly hydrolyse the internal β-1,4-xylosidic linkages of xylan backbone to release xylo-oligosaccharides with different degrees of polymerization (DP), while β-xylosidase cleaves from the non-reducing end of xylo-oligosaccharides releasing xylose monomers (Mendonca et al., 2023). Xylose serves as a precursor for xylitol synthesis, which is widely used as sweetener and nutraceutical ingredient (Kumar et al., 2018). Moreover, xylo-oligosaccharides (XOS) from xylan hydrolysis present substantial potential for application in functional foods, animal feed, cosmetics, and pharmaceutical industries as prebiotics (Amorim et al., 2019). Additionally, *S. cerevisiae* has been engineered with pentose metabolism pathway through the heterologous expression of either xylose reductase and xylitol dehydrogenase or xylose isomerase, which enables the co-fermentation of glucose and xylose derived from lignocellulosic hydrolysates for cellulosic ethanol production, thereby further improving the economic feasibility of biomass utilisation (Gupta et al., 2016; Zhang et al., 2024b; Zhao et al., 2024b).

Besides cellulases and hemicellulases, several accessory proteins are also engaged in lignocellulose decomposition. Among them, lytic polysaccharide monooxygenases (LPMOs), classified as members of auxiliary activity (AA) family in the CAZy database, catalyse the oxidative cleavage of cellulose at the C1 and/or C4 positions of the glycosidic bond in glucose units. This oxidative mechanism increases cellulose

accessibility to cellulases and thereby enhancing the overall hydrolysis efficiency (Gupta et al., 2016; Zhang et al., 2024b). LPMOs are copper-containing enzymes, which reduce the divalent copper ion at their active site to a monovalent state, in the presence of an electron donor, such as glutathione or ascorbate, enabling the oxidative cleavage of polysaccharides (Gupta et al., 2016; Saldarriaga-Hernandez et al., 2020). In addition, cellobiose dehydrogenase (CDH), an oxidative enzyme responsible for cellobiose oxidation, is considered the main electron donor to the catalytic centre of LPMOs, working synergistically to facilitate lignocellulose degradation (Saldarriaga-Hernandez et al., 2020; Agrawal et al., 2021). More recently, LPMOs have also been shown to oxidatively cleave isolated xylan substrates and cellulose-associated xylan (Li et al., 2022b).

Cellulases and xylanases are important industrial enzymes that have been applied in a variety of biotechnological processes, including textile and detergent industry, pulp and paper industry, food and feed industry (bread making, brewing and fruit juice industry and animal feed processing), and pharmaceutical and nutraceutical industry (Juturu and Wu, 2012; Juturu and Wu, 2014; Li et al., 2022b). The combination of cellulase with xylanases and pectinases is used for extracting and clarifying fruits and vegetable juices, resulting in elevated quality and quantity (Alokika and Singh, 2019). In addition, cellulases and xylanases have been used as additives in bread and biscuit making to improve the texture and taste (Juturu and Wu, 2014). Moreover, cellulases and xylanases along with amylases and proteases are being used for making semi-digested feeds, in which cellulase and xylanase play roles in digesting cellulose and hemicellulose components present in the cell wall of silage and cereal grains, to improve digestibility by the animal (Bajaj and Mahajan, 2019). Also, synergistic use of cellulase and xylanase for bio-deinking of wastepaper, leading to an enhancement in brightness and better quality (Alokika and Singh, 2019; Bajaj and Mahajan, 2019). Due to the limited reserves of fossil fuels and the increasing demand for production of biofuels and biochemicals from renewable resources such as lignocellulosic biomass, the application of cellulases and xylanases in lignocellulose biorefinery for generating

fermentable sugars have been attracting attentions worldwide (Juturu and Wu, 2014; Saldarriaga-Hernandez et al., 2020; Li et al., 2022b; Zhao et al., 2024b). However, the high cost of cellulase and xylanase is still a bottleneck for the biochemical conversion of lignocellulosic biomass to biofuels (Bajaj and Mahajan, 2019; Sperandio and Filho, 2021; Zhao et al., 2024b; Meng et al., 2025).

1.3 *Myceliophthora thermophila* as a model fungus for producing thermostable lignocellulolytic enzymes

Filamentous fungi are ubiquitous in the environment and play an essential role in nature by decomposing dead organic materials, and many of them use lignocellulolytic biomass as the main carbon source (Meng et al., 2021; Lubeck and Lubeck, 2022). Their filamentous pattern of growth empowers effective colonization of substrates and provides a large surface to promote uptake of nutrients (Wosten, 2019). To degrade polymers in lignocellulose and retrieve different sugar monomers as energy source for growth and reproduction, fungi need to secrete a broad spectrum and large number of enzymes, including hydrolytic and oxidative enzymes (Benocci et al., 2017; Meng et al., 2021). Filamentous fungi have been used as industrial cell factories to produce pharmaceuticals (e.g., penicillin and lovastatin), and organic acids (e.g., gluconic acid and citric acid) (Wosten, 2019; Lubeck and Lubeck, 2022). Moreover, due to the enormous protein secretion capacity and efficient post-translational modifications, filamentous fungi such as *Trichoderma reesei*, *Penicillium oxalicum*, and *Aspergillus* species are currently used in the production of various proteins, including cellulase and xylanase in industries (Meng et al., 2021; Liu et al., 2023; Zhang et al., 2024b). Still, it is crucial to improve the production levels of lignocellulose degrading enzymes and increase enzyme cocktails to produce fermentative sugars for further conversion of bioethanol and biochemicals.

Thermophilic fungi with optimal growth temperature between 45 and 55 ℃ have received considerable interest for the bioconversion of lignocellulosic biomass into

cellulosic ethanol since they are potentially important sources of industrially thermostable enzymes (Morgenstern et al., 2012; Basotra et al., 2016; Ajeje et al., 2021). Many thermophilic fungi have been shown to produce thermostable enzymes, such as endo-1,4-β-glucanase TeEgl5A. This gene was isolated from the thermophilic fungus *Talaromyces emersonii* and expressed in *Pichia pastoris* (Wang et al., 2014). The purified recombinant endo-1,4-β-glucanase exhibits optimal activity at 90°C, pH 4.5, and remains highly stable at 70°C over a broad pH range of 1.0 to 10.0 (Wang et al., 2014). Similarly, a highly thermostable xylanase TtXynA with a molecular weight of 82 kDa, was purified from *Thielavia terrestris* cultivated in carboxymethyl cellulose medium. This enzyme is optimally active at pH 5.5 and 85°C, while keeping most of its activity within a pH range of 4.5 to 10 (Garcia-Huante et al., 2017). The advantages of using thermostable enzymes at elevated temperatures include higher hydrolysis rates, less enzyme dosage, better substrate solubility and lower viscosity, and decreased risk of microbial contamination when compared with enzymes from mesophilic species (Morgenstern et al., 2012; Patel et al., 2019; Ajeje et al., 2021). Therefore, the application of thermostable cellulases and xylanase in the biorefinery processes would improve cost-effectiveness, as enzymes represent one of the major expenses in biofuel production (Akram et al., 2018; Ajeje et al., 2021).

Myceliophthora thermophila (synonym *Thermothelomyces thermophilus*, *Sporotrichum thermophile*) is a thermophilic filamentous fungus that grows optimally at temperatures between 45°C and 50°C and produces a complete array of enzymes required for the decomposition of plant cell wall polysaccharides (Karnaouri et al., 2014; Singh, 2016). In 2011, the genome of *M. thermophila* was sequenced, and sequence analysis revealed a rich repertoire of genes encoding plant biomass degrading enzymes (Berka et al., 2011). More than 380 CAZy-encoding genes were identified in *M. thermophila*, distributed across over the glycoside hydrolase (GH), glycosyl transferase (GT), polysaccharide lyase (PL), carbohydrate esterase (CE), auxiliary activity (AA), and carbohydrate-binding module (CBM) families (Drula et al., 2022). Particularly, there are at least 22 cellulases (7 endo-β-1,4-glucanases, 7 cellobiohydrolases, and 8 β-

glucosidases) and 18 xylanases (12 endo-1,4-β-xylanases and 6 β-xylosidases) in *M. thermophila* (Berka et al., 2011; Drula et al., 2022). This enzymatic profile is comparable to that of *P. oxalicum* HP7-1 in terms of both cellulases and xylanases but is higher than that of *T. reesei* QM6a with respect to xylanases (Zhao et al., 2024a). The majority of these cellulases and xylanases were characterised and showed optimum activities at temperatures between 60°C to 70 °C (Karnaouri et al., 2014; Basit et al., 2018). Moreover, *M. thermophila* distinguishes itself from *T. reesei* by possessing a relatively higher number of arabinofuranosidases and arabinases, which are important accessory enzymes in xylan degradation (Visser et al., 2011; Karnaouri et al., 2014). In addition, *M. thermophila* contains an extraordinarily higher number of LPMOs (22 in AA9 family, formerly GH61), compared with only three in *T. reesei* and nine in *Aspergillus nidulans* (Drula et al., 2022).

In addition to genomic insights, transcriptomic and exoproteomic analyses have further elucidated the lignocellulose degradation system of *M. thermophila*. Transcriptomic analysis of *M. thermophila* cultivated on different agricultural straws, including three monocot (barley, oat, triticale) and three dicot (alfalfa, canola, flax) plants showed that 59 CAZyme-encoding genes were up-regulated under both monocot and dicot straws conditions compared to glucose (Berka et al., 2011; Kolbusz et al., 2014). These genes encoded cellulolytic, hemicellulolytic, pectinolytic enzymes, and LPMOs. Subsequent exoproteome analysis under the same growth conditions was basically in agreement with the transcriptomic findings, but some notable discrepancies were observed. For example, three pectinolytic enzymes exhibited higher transcript levels under alfalfa straw conditions, which did not correlate with the lower protein levels (Kolbusz et al., 2014).

Another *M. thermophila* C1 strain was originally isolated from forest alkaline soil of eastern Russia. After its discovery, this strain underwent random mutagenesis by Dyadic International Inc., including two rounds of UV mutagenesis and one round of chemical mutagenesis, generating the *M. thermophila* mutant HC (high cellulase), which showed increased cellulase and extracellular protein production, as well as low-

viscosity phenotype in liquid culture. Such morphology is beneficial for commercial large-scale fermentation, as it boosts higher mass, oxygen and nutrient transfer and reduces energy input in large fermenters (Visser et al., 2011). Further strain improvement yielded a protease-deficient strain (HCprt^{-}) and a protease-deficient strain with the major protease gene *alp1* deleted (HCprt^{-}Δ*alp1*). There two mutants exhibited significantly reduced protease activity compared to the parental HC strain. In addition, another mutant LCprt^{-}, which displayed considerably lower cellulase activity and markedly reduced protease activity, was established as a protein expression platform for the production of various industrial enzymes (Visser et al., 2011).

Currently, *M. thermophila* has been engineered to produce bioethanol and various biochemicals, including fumaric acid (Gu et al., 2018; Li et al., 2020a). In addition, it has been employed as a model organism for studying basic fungal biology, such as sugar transporter signal transduction, protein secretion pathways, and asexual development (Li et al., 2022a; Gu et al., 2023; Drescher et al., 2025). However, the native production levels of lignocellulolytic enzymes in this fungus remain lower than those of mesophilic counterparts such as *Trichoderma* and *Aspergillus* species (Berka et al., 2011; Li et al., 2020c). Consequently, extensive research efforts have been devoted to improving lignocellulolytic enzyme production in *M. thermophila* (Li et al., 2020c; Li et al., 2023a; Zhao et al., 2023b).

1.4 Manipulation of transcription factors (TFs) in filamentous fungi for high-level enzyme production

To reduce the overall costs during the process of lignocellulose bioconversion, it is essential to increase lignocellulolytic enzyme production level (Kun et al., 2019; Yang et al., 2023). However, the wild-type fungal strains often do not produce enzymes at levels required for industry nor do they produce the appropriate cocktail of enzymes required for industrial applications. Therefore, engineering of fungal strains capable of producing miscellaneous enzymes at high levels is necessary (Kun et al., 2019; Liu and

Qu, 2019).

Filamentous fungi have evolved to express and secrete plant cell wall degrading enzymes for the degradation of lignocellulosic biomass in their habitats (Huberman et al., 2016). To utilize lignocellulose, fungi need to first recognize signal compounds derived from its complex polymers, such as monosaccharides or disaccharides. These low molecular weight compounds function as inducers, enabling fungi to detect the presence of specific polysaccharides (Benocci et al., 2017). Since these monosaccharides or disaccharides are rare in the environment, their presence is evidence that corresponding polysaccharides are available. Once one of these inducers is sensed by filamentous fungi, a signalling pathway is initiated, resulting in the activation of transcriptional activators, which translocate into the nucleus and trigger the expression of lignocellulolytic enzyme genes as well as genes involved in metabolic pathways required to use the resulting sugar monomers (Benocci et al., 2017; Meng et al., 2021).

For the deconstruction of lignocellulose, studies have revealed that various transcription factors (TFs) including transcriptional activators and transcriptional repressors, form a complex regulatory network, which regulates the production of lignocellulolytic enzymes and enzymes needed for the metabolism of the generated monosaccharides (Benocci et al., 2017; Meng et al., 2021; Mattam et al., 2022). The expression of lignocellulolytic enzyme encoding genes in filamentous fungi is strictly regulated at the transcriptional level by a set of transcriptional activators and repressors (Liu and Qu, 2019; Zhao et al., 2024a). Multiple TFs have been characterized, the majority of which belong to the Zn2Cys6 zinc binuclear cluster family of proteins, possessing Zn2Cys6-type DNA-binding domain and transcription or repression domain (Zhang et al., 2020; Meng et al., 2021). Therefore, engineering of these key regulators has been an efficient strategy to elevate the production of lignocellulolytic enzymes in several industrially relevant fungal species such as *Trichoderma reesei*, *Neurospora crassa*, *Penicillium oxalicum* and *Aspergillus* spp. (de Paula et al., 2019; Meng et al., 2021).

The Zn2Cys6 transcription factor Xyr1 plays an essential role in activation of the expression of major cellulolytic and xylanolytic enzyme genes in *T. reesei* (Stricker et al., 2006). The overexpression of *xyr1* through the strong constitutive *pdc* (pyruvate decarboxylase) promoter in *T. reesei* RUT C30 increased protein production and cellulase activity by 64 and 107%, respectively, compared to the parent strain during growth on cellulose (Wang et al., 2013). Similarly, the overexpression of *xlnR* , which encodes XlnR, a transcriptional activator of xylanase and cellulase genes in *Aspergillus oryzae*, under the control of the constitutive *tef1* (translation elongation factor 1-alpha) promoter, elevated both cellulase and xylanase activities when grown on xylose or xylan (Marui et al., 2002; Noguchi et al., 2009). XlnR in *P. oxalicum* is a positive transcription factor that control cellulase and xylanase expression, and overexpression of *xlnR* via the *Aspergillus nidulans gpdA* (glyceraldehyde-3-phosphate dehydrogenase A) promoter resulted in enhanced cellulase and xylanase activities cultivated in cellulose-containing medium (Li et al., 2015b). The *clr-2* gene encodes a Zn2Cys6 regulator that is crucial for cellulolytic gene expression in *N. crassa* (Coradetti et al., 2012). The overexpression of *clr-2* in *N. crassa* under the regulation of the constitutive *ccg-1* (clock-controlled gene 1) promoter improved cellulase production under inducing conditions and led to secretion levels under non-inducing conditions comparable to those of the wild type strain under Avicel induction (Coradetti et al., 2013). Also, overexpression of the transcriptional activator encoding gene *clrB*, the homologue of *clr-2*, using the *gpdA* promoter elevated the production of cellulase in *A. nidulans* under inducing conditions (Coradetti et al., 2013). Ace3 (the activator of cellulase expression 3) is considered a master regulator of cellulase and a modulator of xylanase genes in *T. reesei*. The overexpression of *ace3* increased cellulolytic and xylanolytic gene expression and enhanced subsequent corresponding enzyme production (Hakkinen et al., 2014). Recently, Ace4, which is a novel transcriptional activator of cellulase gene expression, has been characterized in *T. reesei*, the overexpression of this TF-encoding gene increased cellulase secretion by approximately 22% in comparison to the parental strain (Chen et al., 2021). These

results indicate that the overexpression of TFs is a feasible approach to elevate the production of plant biomass degrading enzymes.

Carbon catabolite repression (CCR) is a global regulatory system which prevents energy consumption for producing extracellular enzymes when the preferred carbon sources are available (Benocci et al., 2017). For lignocellulose degradation, when sufficient monosaccharide (such as glucose) is present in the environment, there is no need for fungal cells to express and secrete lignocellulolytic enzymes to release monosaccharides from plant cell wall polysaccharides, and thus the expression of CAZymes such as cellulase and xylanase is inhibited (Zhang et al., 2020; Meng et al., 2021). The Cys2His2-type transcriptional repressor CreA/Cre1, an ortholog of Mig1 from *Saccharomyces cerevisiae*, plays a pivotal role in mediating CCR in filamentous fungi, and is well conserved among the fungal kingdom (Benocci et al., 2017; Mattam et al., 2022). The suppression of (hemi)-cellulolytic gene transcription by CreA/Cre1 under both repressing and inducing conditions has been reported in several filamentous fungi (Sun and Glass, 2011; Antonieto et al., 2014). This repression was achieved by binding to two closely spaced consensus DNA motifs (5′-SYGGRG-3′) in the promoter regions of target genes, including cellulase and xylanase genes as well as genes encoding regulators of cellulolytic and xylanolytic gene expression (Benocci et al., 2017; Zhang et al., 2020). As CreA/Cre1 is a negative regulator for CAZyme expression, it represents an attractive target for improving the production of glycoside hydrolases associated with lignocellulose utilisation. For example, two *T. reesei* mutants were constructed where the *cre1* gene was completely deleted or replaced by a truncated form (*cre1-1*), isolated from the *T. reesei* Rut-C30 strain with elevated cellulase production capacity. These mutants were derepressed in cellulase and hemicellulase secretion during growth on glucose as the sole carbon source and produced pronouncedly enhanced levels of cellulase and xylanase under inducing conditions (Nakari-Setala et al., 2009). It has been demonstrated that the single-nucleotide mutation in the zinc finger DNA-binding domain of Cre1(a threonine-to-proline substitution) is responsible for the high cellulase production observed in the *T. reesei* PC-3-7 strain (Porciuncula

Jde et al., 2013). An *Aspergillus oryzae* mutant carrying deletion for *creA* displayed significantly improved xylanase and β-glucosidase production levels when grown in xylose-containing culture (Ichinose et al., 2018). In *Trichoderma orientalis* EU7-22 strain, the knockout of *creA* promoted cellulase and xylanase activities in both inducing and glucose repressing media (Long et al., 2018). Similarly, disruption of *cre-1* in *N. crassa* not only led to elevated expression of cellulolytic genes and cellulolytic activity, but also increased hemicellulase secretions when cultivated on crystalline cellulose (Sun and Glass, 2011). It has also been reported that the *P. oxalicum* mutant lacking *creA* exhibited enhanced cellulase and xylanases activities in comparison to the parental strain (Li et al., 2015b).

In addition to CreA/Cre1, there are other transcriptional repressors that affect the expression of genes encoding lignocellulose hydrolysing enzymes and thus are favoured targets for genetic manipulation. For instance, an essential regulatory gene, *PoxMBF1*, which encodes Multiprotein Bridging Factor 1, has been identified in *P. oxalicum*. Deletion of this gene resulted in substantially increased cellulolytic and xylanolytic enzyme production compared with the parental strain under both solid-state and submerged fermentation conditions (Zhao et al., 2019). In another study, a novel transcriptional repressor, CXRD (cellulolytic and xylanolytic regulator D), which also regulates cellulase and xylanase gene expression, has been characterised in this fungal species. Deletion of *cxrD* strongly improved (49.3 to 2,230%) cellulase and xylanase production during growth on solid media containing wheat bran and rice straw (Zhao et al., 2023a). In *N. crassa*, the hemicellulase regulator HCR-1 is involved in the regulation of hemicellulase gene expression in response to L-arabinose and xylan. Disruption of *hcr-1* led to increased protein secretion and xylanase production, but did not affect endoglucanase activity (Li et al., 2014). Disruption of *rce1*, which encodes a transcription repressor of cellulase expression in *T. reesei*, enhanced cellulase production when grown on cellulose, but had no effect on xylanase activity during cultivation on xylan (Cao et al., 2017). In contrast, a novel transcription factor, XTR1 (xylanase gene transcriptional repressor 1), was identified in *T. reesei* as a repressor

specifically controlling xylanase gene expression by binding to the *xyn1* promoter. Deletion of *xtr1* resulted in an approximately 50% increase in xylanase activity, without affecting cellulase activity (Xu et al., 2023).

Combinatorial manipulation of multiple TFs is also an efficient strategy that utilized in rational strain engineering to improve lignocellulolytic enzyme production levels. The *P. oxalicum* mutant possesses simultaneously overexpressed *clrB* and *xlnR* showed enhanced cellulase and xylanase activities compared to the mutant with single *clrB* overexpression in the presence of cellulose (Li et al., 2015b). Also, simultaneous deletion of *creA* and overexpression of *clrB* in *P. oxalicum* exerted considerable synergistic impacts on cellulase and xylanase gene expression, leading to a substantial increase in cellulolytic and xylanolytic production compared with that corresponding single gene mutants (Li et al., 2015b). The overexpression of *xyr1* combined with the silencing of *ace1*, which encodes a negative regulator of both cellulase and xylanase gene expression in *T. reesei*, resulted in increased cellulase and xylanase activity under cellulose-induced cultivation and higher endoglucanase activity under glucose-repressing conditions (Wang et al., 2013). Elevated production of cellulase and xylanase production, displaying 234% and 68% enhancements, respectively, was also obtained by simultaneous overexpression of *xyr1* and *ace3* in *T. orientalis* EU7-22 under inducing cultures (Xue et al., 2020). In another report, simultaneous overexpression of *ace3*, *xyr1*, and other three putative positive regulatory genes considerably elevated endoglucanase activity and extracellular protein production in *T. reesei* during growth on cellulose, compared with the parental strain (Sun et al., 2022). Additionally, it has recently been shown that a combination of deletion of *creA* and overexpression of *clbR*, which encodes a cellobiose-responsive transcriptional activator of cellulase expression in *Aspergillus aculeatus*, caused a 3.4- and 8.0-fold increase in cellulase and xylanase production, respectively, compared to the host strain (Tani et al., 2024). These findings support that the manipulation of transcriptional regulators is a very promising strategy for developing robust fungal strains capable of producing high yields of industrial enzymes.

1.5 Engineering of TFs in *M. thermophila* to improve lignocellulolytic enzyme production

Given the ability of *M. thermophila* to produce a complete set of thermostable cellulolytic and xylanolytic enzymes, it is of particular interest to engineer transcription factors (TFs) in this fungus to increase the production of industrially important enzymes. Overexpression of *Mtxyr1* resulted in improved xylanase production under both corncob-inducing and glucose-repressing conditions (Wang et al., 2015). RNA silencing of *Mtcre1* caused elevated transcription of cellulolytic genes and enhanced subsequent cellulase activity when grown on corncob powder-containing medium (Yang et al., 2015). Similarly, RNA silencing of *mhr1*, which encodes a transcription factor containing a fungal_TF_MHR (fungal transcription factor regulatory middle homology region), led to a 33% to 65% increase in cellulase activity and a 48% increase in xylanase activity relative to the WT strain during growth on wheat straw powder (Wang et al., 2018). MtCLR-4, a Zn(II)2Cys6 transcriptional activator involved in cellulase expression and intracellular cAMP regulation, can directly bind to the promoter regions of regulatory genes *Mtclr-2* and *Mtxyr-1*, and *Mtcr-1* gene, which encodes adenylyl cyclase, a crucial component of the cAMP signalling pathway. Overexpression of *Mtclr-4* enhanced cellulolytic activity and protein secretion under conditions of cellulose exposure (Liu et al., 2019c). Likewise, overexpression of *MtCol-26*, encoding a regulator of major amylase genes, resulted in elevated amylase activity by 30% when grown on starch (Xu et al., 2018). Another transcription factor, MtTRC-1 (transcriptional regulator of cellulases 1), was identified as an activator of cellulase production. It binds to the promoter regions of the key cellulase gene *Mtcbh1* and *Mthac-1*, which encodes the pivotal regulator of the unfolded protein response (UPR) pathway. It has been shown that overexpression of *Mttrc-1* markedly increased cellulase activity and secreted protein concentration (Li et al., 2022a). More recently, overexpression of *clr-5* from *N. crassa*, a gene encoding Zn2Cys6 transcription factor

orthologous to MtClr-5 in *M. thermophila*, under the regulation of the strong constitutive *MtgpdA* promoter, significantly elevated endoglucanase activity (~ 142%) and extracellular protein production (~ 187%) levels after 3 days of cultivation in cellulose medium (Xue et al., 2023). Collectively, these results demonstrate the feasibility of improving plant biomass degrading enzyme production in *M. thermophila* by modifying the expression of transcription factors.

In addition to RNA silencing and overexpression approaches, the CRISPR/Cas9 (clustered regularly interspaced short palindromic repeats/CRISPR associated 9) genome-editing system has been employed to manipulate the regulatory networks governing cellulolytic and xylanolytic enzyme production in *M. thermophila*. The CRISPR/Cas9 system consists of an endonuclease Cas9 and a synthetic single guide RNA (sgRNA), which comprises of CRISPR RNA (crRNA) that identifies the target DNA and trans-activating CRISPR RNA (tracrRNA) that interacts with Cas9 (Raheja et al., 2025) (Figure 1.3). The sgRNA is composed of a 20-bp protospacer sequence recognizing the target DNA by base paring and a sgRNA scaffold sequence that forms a complex with Cas9. Target recognition requires the presence of a 3-bp protospacer adjacent motif (PAM) immediately downstream of the target sequence. Once the mature sgRNA combines with Cas9 and guides to specific target site, Cas9 mediates a double-strand break (DSB) at the target loci upstream of the PAM. This disruption can be repaired by non-homologous end joining (NHEJ) that causes insertion or deletion mutagenesis, or by homology-directed repair (HDR) when an exogenous DNA fragment (donor DNA) is provided (Kun et al., 2019; Shen et al., 2024).

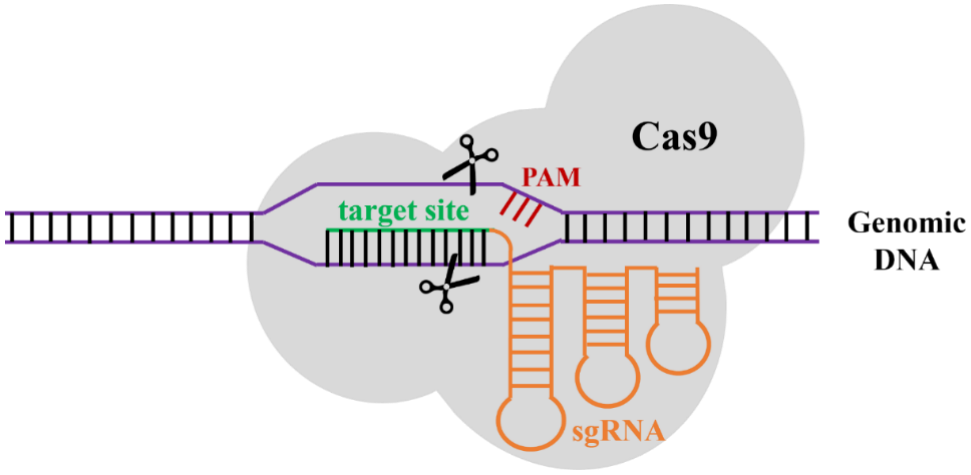

Figure 1.3. Schematic illustration of the CRISPR/Cas9 system. The single guide RNA (sgRNA) guides the Cas9 to the target locus, and Cas9 nuclease then performs a double-strand break (DSB) 3 bp upstream of the protospacer adjacent motif (PAM).

A functional CRISPR/Cas9 system was successfully established in *M. thermophila* in 2017 (Liu et al., 2017). The selected targets for deletion by using this system were the genes involved in the cellulase biosynthesis pathway, including a transcriptional repressor gene *cre1*, a putative endoplasmic reticulum stress regulator gene *res-1*, a β-glucosidase gene *gh1-1*, and an alkaline protease gene *alp-1*. Simultaneous deletions of up to four genes was achieved by neomycin selection marker replacement mediated by the CRISPR/Cas9 system in one transformation event. The efficiencies for single, double, triple, and quadruple deletions were 95%, 61–70%, 30%, and 22%, respectively. Using this highly efficient genome editing tool, multiple mutant strains containing one to four gene deletions showing substantially improved cellulase and xylanase production, which reached 3- to 13.3-fold higher activity compared to the parental strain (Liu et al., 2017). Moreover, deletion of *MtCol-26* by using CRISPR/Cas9 system increased expression of the major xylanase and cellulase genes and improved endoglucanase and xylanase activities approximately 3-fold in comparison to the *M. thermophila* WT strain in the presence of cellulose (Xu et al., 2018). Recently, deletion of *Mtara-1* in *M. thermophila*, which encodes a Zn(II)2Cys6 transcription factor, by

using the CRISPR/Cas9 tool, resulted in reduced protein secretion and arabinase activity when cultivated in arabinan-containing medium, highlighting its crucial role in the induction of arabinanolytic enzymes (Gu et al., 2023). Despite its success, the currently developed CRISPR/Cas9 system in *M. thermophila* requires three separate plasmids carrying the Cas9 nuclease, sgRNA sequence, and donor DNA fragment, making the gene editing process laborious and time-consuming. Therefore, the development of a rapid, and versatile genome-editing tool is still needed.

1.6 Research gaps and thesis aims

The *M. thermophila* genome comprises 9,097 protein-coding genes (https://www.ncbi.nlm.nih.gov/datasets/genome/GCF_000226095.1/), among which more than 500 are annotated as transcription factor genes in the DOE Joint Genome Institute-MycoCosm database (Home-*Myceliophthora thermophila* (*Sporotrichum thermophile*) v2.0) (Berka et al., 2011). Most of these transcription factors contain fungal Zn(2)-Cys(6) binuclear cluster domain (101 genes), fungal specific transcription factor domain (61 genes), or C2H2-type zinc finger domain (53 genes). In addition, putative transcription factors possessing helix-loop-helix DNA-binding domain (13 genes), basic leucine zipper domain (12 genes), and high mobility group box domain (10 genes) are also included. However, the functions of the majority of these TFs remain uncharacterized, offering great potential for the discovery of novel regulators involved in lignocellulose degradation.

The availability of genomics, transcriptomics, and secretomics data, together with recent advances in genome editing technologies, has paved the way for elucidating the molecular mechanisms underlying lignocellulose conversion in *M. thermophila*. (Berka et al., 2011; Karnaouri et al., 2014; Li et al., 2022a). These advances have promoted the identification of genes encoding cellulolytic and xylanolytic enzymes as well as putative transcriptional regulators. However, our understanding of the regulatory network controlling cellulase and xylanase expression in *M. thermophila* is limited, and

the key transcription factors involved remain largely unknown. A comprehensive understanding of cellulase and xylanase gene regulation necessitates further characterisation and functional analysis of these transcriptional factors, which would deepen our insights into enzyme expression at the molecular level and significantly facilitate rational strain engineering to enhance lignocellulolytic enzyme production.

Therefore, the overall aim of this thesis is to identify and characterise novel transcription factors involved in the regulation of cellulase and xylanase expression in *M. thermophila*. The specific aims are to:

1. Perform comparative transcriptomic analysis of *M. thermophila* grown in crystalline cellulose (Avicel) medium compared to glucose and identify potential transcription factor candidates.

2. Develop a CRISPR/Cas9-based gene editing system and construct transcription factor mutants through targeted gene deletion and overexpression.

3. Investigate the regulatory roles of selected transcription factors in cellulase and xylanase gene expression and enzyme production using molecular genetic approaches.

4. Conduct comparative transcriptomic analysis between TF-deletion mutants and the wild type strain of *M. thermophila* to comprehensively elucidate the regulatory functions of selected TFs at the transcriptome level.

1.7 Research framework

A comparative transcriptomic analysis of *M. thermophila* grown in liquid media containing either Avicel or glucose as the sole carbon source was first performed to identify potential transcription factor candidates. Subsequently, a CRISPR/Cas9-based gene editing system was developed, consisting of two plasmids that respectively carried the Cas9 nuclease and sgRNA sequence, and the donor DNA sequence. Using this system, the target genes were deleted in *M. thermophila*. Genes whose deletion resulted in significant changes in cellulase and/or xylanase production were also overexpressed using a newly established overexpression system.

After obtaining both deletion and overexpression mutants of the target genes, the *M. thermophila* wide type (WT) and deletion and overexpression strains were subjected to enzymatic activity analyses, including filter paper cellulase (FPase), endoglucanase (CMCase), β-glucosidase (pNPGase), and exoglucanase (pNPCase) activities, as well as xylanase activity, and extracellular protein concentration measurements.

Subsequently, molecular genetic analyses, including phenotypic observation, subcellular location of TFs, real-time quantitative PCR (RT-qPCR), electrophoretic mobility shift assays (EMSAs), and DNase I footprinting assays, were conducted to elucidate the regulatory mechanisms of target TFs involved in cellulase and xylanase expression. Finally, a comparative transcriptomic analysis between TF-disruption mutants and the WT strain was performed to comprehensively reveal the global regulatory roles of selected TFs at the transcriptome level. The overall research framework of this study is illustrated in Figure1.4.

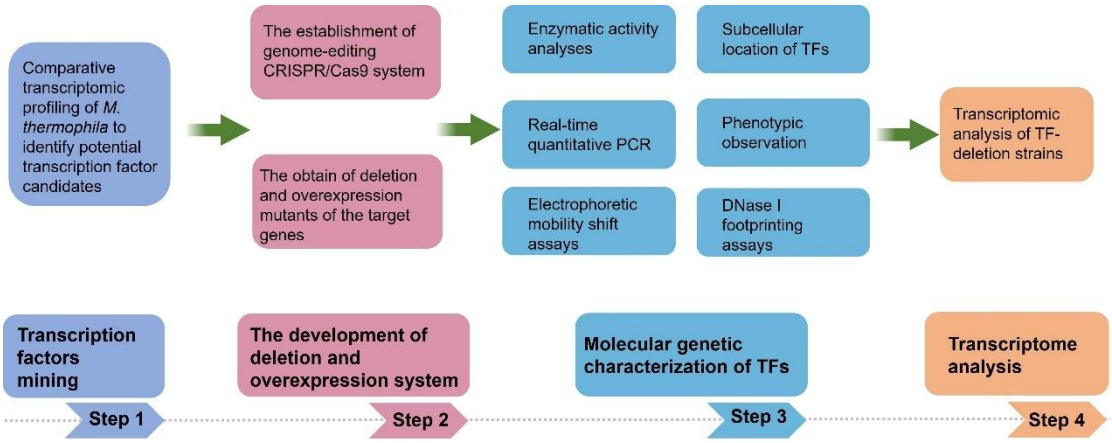

Figure 1.4. The overall research framework of this thesis.

1.8 Thesis structure

This thesis comprises of the following chapters:

Chapter 1: Introduction and literature review

Chapter 2: Identification of a novel forkhead transcription factor MtFKH1 for cellulase and xylanase gene expression in *Myceliophthora thermophila*

Chapter 3: Dual role of MtHAC-1 in regulating cellulase and xylanase production in *Myceliophthora thermophila*

Chapter 4: Transcription factor MtCLR-2 regulates cellulase production via direct modulation of *Mtegl2* and *Mtbgl1* expression in *Myceliophthora thermophila*

Chapter 5: General discussion and conclusions, provides the key findings, limitations, future directions and conclusions of this thesis.

1.9 Thesis significance

This thesis identified three novel transcription factors (TFs) through comparative transcriptomic analysis of *M. thermophila* cultivated in different carbon sources, including cellulase-inducing cellulose medium and cellulase-repressing medium. Differential expression profiling of putative TFs between these conditions proved to be a highly efficient strategy for identifying potential regulatory candidates in *M. thermophila* and provides a valuable reference for similar studies in other filamentous fungi.

A CRISPR/Cas9 gene editing system was also developed in this work. This versatile genome-editing tool can be applied not only for functional genomic studies and elucidating complex biological processes, but also for rational strain engineering to enhance the production of target proteins and biochemicals in *M. thermophila* and other filamentous fungi.

Among the transcription factors characterised, MtFKH1 is the first forkhead TF reported in *M. thermophila*, acting as a repressor of cellulase and xylanase gene expression. The identification of this novel regulator expands the repertoire of TFs that regulate lignocellulolytic enzyme genes, suggesting that TFs from other families besides zinc finger types in *M. thermophila* and other fungi may also play important regulatory roles in lignocellulose deconstruction. Furthermore, the bZIP TF MtHAC-1 was found to exert dual regulatory effects on the production of cellulase and xylanase, which was not previously reported, providing new insights into the regulatory

mechanisms underlying cellulase and xylanase gene expression. In addition, the Zn2Cys6-type TF MtCLR-2 identified in this study functions as a crucial transcriptional activator for cellulase expression and enzyme production, representing a promising target for rational engineering to elevate cellulolytic enzyme yields in filamentous fungi.

Overall, this thesis elucidates the molecular mechanisms underlying cellulase and xylanase gene expression, expands our knowledge on how these three TFs regulate lignocellulolytic enzyme gene expression, and provides potential targets for developing fungal cell factories applicable to biofuel and value-added biochemical production in biorefinery industries.

1.10 Research output arising from the thesis

1.10. 1 Peer-reviewed journal publications

Chapter 2

Yapeng Lai., Juan Wang., Ning Xie., Gang Liu., Donnabella Lacap-Bugler., **2025**. Identification of a novel forkhead transcription factor MtFKH1 for cellulase and xylanase gene expression in *Myceliophthora thermophila* (ATCC 42464). Microbiological Research, 294, 128097. This document can be found online at https://doi.org/10.1016/j.micres.2025.128097.

Chapter 3

Yapeng Lai., Juan Wang., Ning Xie., Gang Liu., Donnabella Lacap-Bugler., **2025**. Dual Role of MtHAC-1 in regulating cellulase and xylanase production in *Myceliophthora thermophila*. Microbial Biotechnology, 18(8), e70203. This document can be found online at https://doi.org/10.1111/1751-7915.70203.

Chapter 4

Yapeng Lai., Juan Wang., Ning Xie., Gang Liu., Donnabella Lacap-Bugler., 2026. Transcription factor MtCLR-2 regulates cellulase production via direct modulation

of *Mtegl2* and *Mtbgl1* expression in *Myceliophthora thermophila*. Microbial Cell Factories. This document can be found online at https://doi.org/10.1186/s12934-026-02976-1

1.10. 2 Conference presentations

Yapeng Lai., Juan Wang., Ning Xie., Gang Liu., Donnabella Lacap-Bugler. MtCLR-2 regulates cellulase production via *Mtegl2* and *Mtbgl1* in *Myceliophthora thermophila*. **2025**. Presented at the School of Science Research Showcase (October, 2025), Auckland University of Technology, New Zealand.

Yapeng Lai., Juan Wang., Ning Xie., Gang Liu., Donnabella Lacap-Bugler. MtCLR-2 regulates cellulase production via *Mtegl2* and *Mtbgl1* in *Myceliophthora thermophila*. **2025**. Presented at the New Zealand Microbiological Society Annual Conference (November 2025), Rotorua, New Zealand.

Chapter 2 Identification of a Novel Forkhead Transcription Factor MtFKH1 for Cellulase and Xylanase Gene Expression in *Myceliophthora Thermophila*

The content of this chapter has been published as

Yapeng Lai., Juan Wang., Ning Xie., Gang Liu., Donnabella Lacap-Bugler., **2025**. Identification of a novel forkhead transcription factor MtFKH1 for cellulase and xylanase gene expression in *Myceliophthora thermophila* (ATCC 42464). Microbiological Research, 294,128097. https://doi.org/10.1016/j.micres.2025.128097

2.1 Prelude

Myceliophthora thermophila is a thermophilic filamentous fungus that has become an important model organism for studying thermostable enzyme production due to its excellent capability to secrete lignocellulolytic enzymes. Despite over a decade of research on gene expression regulation, the transcriptional regulatory mechanisms underlying enzyme expression in this fungus remain unclear. This chapter focuses on the characterisation of novel transcription factors (TFs) involved in lignocellulose degradation. To address this, comparative transcriptomic analysis of *M. thermophila* grown on Avicel and glucose, combined with molecular genetic approaches, were employed to uncover TFs regulating cellulase and xylanase expression. Among several candidates identified through expression profiling, a previously uncharacterized forkhead transcription factor, MtFKH1, emerged as a crucial regulator. Using a newly established CRISPR/Cas9-mediated gene editing and overexpression system, we demonstrated that MtFKH1 acts as a negative regulator of cellulase and xylanase production. Intriguingly, disruption of *Mtfkh1* not only elevated cellulase and xylanase activities but also caused an impairment in sporulation, suggesting that MtFKH1 plays an additional role in fungal development. Subsequent analyses, including real-time quantitative reverse transcription PCR (RT-qPCR), electrophoretic mobility shift assays (EMSAs), and DNase I foot-printing, further confirmed that MtFKH1 directly binds to the promoter regions of genes encoding key cellulases and xylanase. In addition, transcriptomic analysis of the Δ*Mtfkh1* mutant followed by Gene Ontology (GO) enrichment further elucidated the genes and functional categories under MtFKH1 regulation. This study expands our knowledge on how forkhead transcription factors regulate lignocellulose degradation in *M. thermophila* and provides a novel target for engineering fungal cell factories with the hyperproduction of cellulase and xylanase.

2.2 Introduction

Lignocellulosic biomass has been regarded as a promising alternative raw material for biofuels and value-add biochemicals production (Rubin, 2008; Agrawal et al., 2021). The biological depolymerization of lignocellulose requires at least two main enzymes: cellulase and hemicellulase (Sanchez, 2009). Cellulase includes endo-β-1,4-glucanase (EGs; EC 3.2.1.4), cellobiohydrolase (CBHs; EC 3.2.1.91), and β-glucosidase (BGLs; EC 3.2.1.21). Hemicellulase mainly consists of endo-1,4-β-xylanase (EC 3.2.1.8), β-xylosidase (EC 3.2.1.37), along with other hydrolases and esterases (Gupta et al., 2016). The cellulase and xylanase act synergistically to hydrolyze lignocellulose into glucose and xylose, which are utilized to generate bioethanol and biochemicals by microbial fermentation (Gupta et al., 2016; Taha et al., 2016). These important enzymes have been applied in a variety of manufacturing processes in different industries including textile and detergent, paper pulp bleaching, food and feed, and pharmaceutical and nutraceutical industry (Juturu and Wu, 2014; Mendonca et al., 2023). The increased demand in the production of bioethanol and biochemicals from lignocellulosic biomass has placed cellulase and xylanase at the forefront of biorefinery processes, which necessitates exploring cost-efficiency in converting lignocellulosic biomass into fermentable sugars via enzymatic hydrolysis (Singhania et al., 2010; Bajaj and Mahajan, 2019; Liu et al., 2020). Nevertheless, the high cost of lignocellulose degrading enzymes is still a bottleneck for the commercial production of lignocellulosic biofuels to date (Liu et al., 2019a; Liu et al., 2019b; Sperandio and Filho, 2021).

Filamentous fungi are potent lignocellulolytic enzyme producers and have been utilized to produce a broad spectrum of enzymes mixes employed in diverse biotechnological applications (Berlin, 2013; Makela et al., 2014). Thermophilic fungi have been receiving considerable interest in the bioconversion of lignocellulosic biomass into cellulosic ethanol since they are a significant source of industrially thermostable enzymes (Morgenstern et al., 2012; Basotra et al., 2016). The advantages of using thermostable cellulases at elevated temperatures include higher hydrolysis

rates, better substrate solubility and lower viscosity, and decreased risk of microbial contamination when compared with enzymes from mesophilic species (Yeoman et al., 2010; Blumer-Schuette et al., 2014; Ajeje et al., 2021). *Myceliophthora thermophila* is a thermophilic filamentous fungus that grows optimally at temperatures between 45°C and 50°C and offers a complete array of carbohydrate-active enzymes (CAZymes) necessary for the decomposition of plant cell wall polysaccharides (Karnaouri et al., 2014). Currently, *M. thermophila* is attracting particular attention for its potential as an industrial factory for chemicals and biofuels production, since its genome, transcriptome and secretome are well annotated and accessible (Berka et al., 2011; Kolbusz et al., 2014). However, the production levels of biomass degrading enzymes from this fungal species are typically low compared with those regularly used mesophilic counterparts such as *Trichoderma* spp. and *Aspergillus* spp. (Berka et al., 2011; Singh, 2016). Therefore, extensive research has focused on improving the lignocellulolytic enzymes production in *M. thermophila* (Dos Santos Gomes et al., 2019; Li et al., 2020a; Li et al., 2020c).

In filamentous fungi, the expression of lignocellulolytic enzyme encoding genes is strictly regulated by a battery of transcriptional activators and repressors, and efficient manipulation of these key regulators will improve the production of the extracellular enzymes (Benocci et al., 2017; Adnan et al., 2022). XlnR is the first identified transcription factor involved in regulating the expression of xylanolytic and cellulolytic enzyme genes induced by xylose or xylan in *Aspergillus niger* (van Peij et al., 1998). Since then, several transcription regulators involved in lignocellulose degradation have been characterized, including the transcriptional activators CLR-1, CLR-2, CLR-4, Ace2, Ace3, Ace4, and Vib-1, and the transcriptional repressors Cre1, Ace1 (Alazi and Ram, 2018; Zhao et al., 2024a). All of which are engaged in the regulation of cellulolytic and/or hemicellulolytic enzyme production. The XlnR orthologs in *Trichoderma reesei* (Xyr1) and *Aspergillus oryzae* (XlnR) are essential for the synthesis of both cellulase and hemicellulase, while XLR-1 in *Neurospora crassa* and XlnR in *Aspergillus nidulans* are required only for hemicellulase gene expression

(Marui et al., 2002; Stricker et al., 2006; Sun et al., 2012; Klaubauf et al., 2014). In *N. crassa*, CLR-1, CLR-2 are indispensable regulators of cellulase expression, as CLR-2 homologs in *A. nidulans* (ClrB), and *Penicillium oxalicum* (ClrB) but not in *T. reesei* (Coradetti et al., 2012; Hakkinen et al., 2014; Craig et al., 2015; Li et al., 2015b). In *T. reesei*, Ace1 acts as a repressor of both cellulase and xylanase production, as the deletion of which led to an enhancement in the expression of all the major cellulase and two hemicellulase genes (Saloheimo et al., 2000; Aro et al., 2003). In contrast, the lack of Ace2 in *T. reesei* resulted in reduced expression of genes encoding for cellulases and xylanase when grown in cellulose media (Aro et al., 2001). Whilst Ace3 acts as positive regulator of cellulase and xylanase, which regulates the target genes directly and indirectly via modulating *xyr1* transcription in *T. reesei* (Hakkinen et al., 2014). The $Zn(II)_2Cys_6$ transcription factor CLR-4 plays a pivotal role in the regulation of cellulolytic gene expression and directly regulates the expression of CLR-1 by binding to the promoter regions of *clr-1* gene in *N. crassa* (Liu et al., 2019c). Furthermore, the newly reported Ace4 is identified as an activator involved in the regulation of genes responsible for encoding cellulase, and overexpression of *ace4* elevated cellulase production by 22% under cellulose-induced cultivation of *T. reesei* (Chen et al., 2021). The deletion of Cre1(encodes carbon catabolite repressor protein), which is a homolog of Mig1 in *Saccharomyces cerevisiae*, increased cellulolytic activity and upregulated the transcription of cellulolytic genes in the presence of cellulose in *N. crassa* (Sun and Glass, 2011). Moreover, overexpression of regulatory gene *vib-1* considerably improved cellulase production and protein secretion in *T. reesei* (Zhang et al., 2018).

In *M. thermophila*, a few transcription factors associated with lignocellulosic biomass degradation have also been identified. One transcriptional activator MtXyr1 and another transcriptional repressor MtCre1, which are involved in regulation of the expression of hemicellulolytic, or cellulolytic genes have been characterized in *M. thermophila* (Wang et al., 2015; Yang et al., 2015). Overexpression of MtXyr1 under the control of the strong constitutive *pdc* (pyruvate decarboxylase) promoter resulted in 9.0-fold higher xylanase activity in corncob-containing medium and exhibited less

effects on the cellulase activities while RNA interference of MtCre1 caused increased cellulolytic activity and expression level of cellulolytic genes under inducing conditions. In addition, MtXyr1 also controls the expression of genes engaged in pentose transport and catabolism (Dos Santos Gomes et al., 2019). Similar to its homolog CLR-4 in *N. crassa*, MtCLR-4 plays key role in the regulation of genes encoding (hemi-)cellulases through directly regulating the expression of the crucial transcription activators MtCLR-2 and MtXyr1, and *Mtcr-1* encoding adenylyl cyclase in the cAMP signaling pathway (Liu et al., 2019c). Recently, a novel transcriptional factor MtCLR-5 was found to be critical for cellulose depolymerization in *M. thermophila*, the deletion of this TF encoding gene decreased the endoglucanase activity and protein secretion when cultivated in cellulose media (Xue et al., 2023). However, to-date our understanding of the gene expression system of lignocellulolytic enzymes is limited in *M. thermophila*, and more transcription factors involved in the regulatory network controlling plant biomass degradation remains to be elucidated.

The forkhead transcription factors, which contain the typical forkhead box (Fox) or winged helix DNA-binding domain (Korver et al., 1997), are crucial regulators that control development, cell cycle, signal transduction, morphogenesis, and metabolism regulation (Carlsson and Mahlapuu, 2002). Forkhead proteins are conserved in yeast, filamentous fungi as well as in mammals. Some members from this protein family have been characterized, including ScFKH1 and ScFKH2 in *S. cerevisiae* (Hollenhorst et al., 2000; Zhu et al., 2000), HcFKH1 in *Hapsidospora chrysogena* (formerly *Acremonium chrysogenum*) (Schmitt et al., 2004), PrFKH1 in *Penicillium rubens* (formerly *Penicillium chrysogenum*) (Dominguez-Santos et al., 2015), PoX08522 in *Penicillium oxalicum* (Zhao et al., 2016), AnFKHB in *Aspergillus nidulans* (Jang et al., 2023), and FOXOs in humans (Bach et al., 2018; Laissue, 2019). However, the regulatory role of forkhead proteins in lignocellulose degrading enzymes production in *M. thermophila* remains largely unknown.

In the current study, a novel transcriptional factor in *M. thermophila* was identified through comparative transcriptomic and molecular genetics analyses. Here, the key

regulator gene, *Mtfkh1* in *M. thermophila* ATCC 42464, encoding a forkhead protein that negatively regulates the expression of major cellulase and xylanase genes by directly binding to their promoter regions was described. To the best of our knowledge, MtFKH1 is the first characterized member of the forkhead protein family in *M. thermophila*, which enriches our understanding of the regulation of lignocellulose degradation in filamentous fungi.

2.3 Materials and Methods

2.3.1 Strains and culture conditions

Myceliophthora thermophila (ATCC 42464) was used as the parental strain throughout this study. The *M. thermophila* strains were cultured on potato dextrose agar (PDA) plates at 45°C for 7 days to obtain asexual spores (conidia), which were suspended with 0.2% (v/v) Tween-80 solution to prepare spore suspensions. For mycelial growth (for DNA extraction), the fungi were cultured in Mandels medium (Wang et al., 2015) [(g/L) $(NH_4)_2SO_4$, 1.4; Urea, 0.3; KH_2PO_4, 2.0; $MgSO_4 \cdot 7H_2O$, 0.3; $CaCl_2 \cdot 2H_2O$, 0.4; $FeSO_4 \cdot 7H_2O$, 0.005; $ZnSO_4 \cdot 7H_2O$, 0.0017; $CoCl_2 \cdot 6H_2O$, 0.0037; $MnSO_4 \cdot H_2O$, 0.0016; tryptone, 1.0; Tween-80, 0.15% (v/v); and 50 mL citrate buffer containing citric acid and NaOH (pH 4.5)] containing 2% (w/v) glucose, incubated at 45°C for 36 h. For enzymatic activity, RT-qPCR, and comparative transcriptomic analyses, approximately 5×10^7 fresh spores (final concentration, 1×10^6 spores mL^{-1}) of *M. thermophila* strains were pre-grown in 50 mL Mandels medium containing 2% (w/v) glucose at 45°C with shaking at 150 rpm for 36 h. Subsequently, mycelia of *M. thermophila* strains were collected and washed with the Mandels medium (without carbon source) and aliquots of wet mycelia (0.55 g) were transferred into 50 mL Mandels medium containing 2% (w/v) Avicel (Sigma-Aldrich, St. Louis, MO, USA), incubated at 45°C with shaking at 150 rpm for 48-96 h. For fungal colony morphology assay, spore suspensions of *M. thermophila* strains (1.5 μL, 1×10^7 mL^{-1}) were dropped onto PDA, solid Mandels medium supplemented with 2% (w/v) glucose or 1% (w/v) Avicel as the sole carbon source, and cultivated at 45°C for 3 or 4 days. For growth observation in liquid culture,

spores from *M. thermophila* strains were inoculated at a concentration of 1×10^6 spores mL^{-1} in 50 mL Mandels medium with 2% (w/v) glucose or 2 % (w/v) Avicel and grown at 45°C for 36 h.

Escherichia coli DH5α was used for plasmid construction and propagation, cultivated at 37℃ in Luria-Bertani (LB) medium supplemented with ampicillin (100 μg mL^{-1}).

2.3.2 Plasmid construction

All primer sequences used in this study are listed in Table S2.1. All PCR products were amplified using Phanta Max Super-Fidelity DNA Polymerase (Vazyme Biotech, Nanjing, China). pFC332, a AMA1 plasmid contains *A. nidulans* optimized Cas9 with attached SV40 nuclear localization signal (PKKKRKV) and hygromycin B resistance gene (*hph*) selection marker, was a gift from Uffe Mortensen (Addgene plasmid # 87845) (Nodvig et al., 2015). The sgRNA (guide RNA) scaffold with the *BsrG*I site was synthesized by IGE Biotechnology (Guangzhou, China) and the double-stranded sgRNA scaffold was gained using the primers sgRNA scaffold-F/R with the aid of annealing buffer for DNA oligos (5×) (Beyotime Biotech, Shanghai, China). The U6 promoter of *M. thermophila* was amplified from genomic DNA using the primers U6p-F/R (Liu et al., 2017). The U6 promoter and sgRNA scaffold fragments were cloned into the *Pac*I site of pFC332 via the ClonExpress® Ultra One Step Cloning Kit (Vazyme Biotech, Nanjing, China) to create the plasmid pFC332-Cas9-U6p-sgRNA scaffold following the manufacturer's instructions.

For the disruption of target genes using the CRISPR/Cas9 system, the Cas9-U6p target gene-sgRNA scaffold expression cassettes were constructed. The protospacer sequences targeting MYCTH_2310243, MYCTH_2302011, MYCTH_2082522, MYCTH_2306976, MYCTH_2297579, MYCTH_2307931, MYCTH_2308823, and MYCTH_2129372, were selected using the sgRNACas9 tool (Xie et al., 2014) with minimized off-target effects. All protospacer sequences that fused with sgRNA scaffold aimed at the eight different genes, and U6 promoters were amplified from pFC332-

Cas9-U6p-sgRNA scaffold vector and ligated and cloned into pFC332 vector, which generated the corresponding plasmids Cas9-U6p-*MYCTH_2310243*-sgRNA, Cas9-U6p-*MYCTH_2302011*-sgRNA, Cas9-U6p-*MYCTH_2082522*-sgRNA, Cas9-U6p-*MYCTH_2306976*-sgRNA, Cas9-U6p-*MYCTH_2297579*-sgRNA, Cas9-U6p-*MYCTH_2307931*-sgRNA, Cas9-U6p-*MYCTH_2308823*-sgRNA, and Cas9-U6p-*MYCTH_2129372*-sgRNA. The donor DNA vectors were constructed using selectable maker cassette P*gpd-neo* amplified from plasmid pBC-*neo* (Li et al., 2020d). The 5′ and 3′ flanking fragments of *MYCTH_2310243*, *MYCTH_2302011*, *MYCTH_2082522*, *MYCTH_2306976*, *MYCTH_2297579*, *MYCTH_2307931*, *MYCTH_2308823,* and *MYCTH_2129372* were separately amplified from *M. thermophila* genomic DNA. The resultant 5′, 3′, and P*gpd-neo* fragments were assembled and inserted into pUC19 plasmid digested by *Hin*dIII/*Eco*RI using One Step Cloning Kit (Vazyme Biotech, Nanjing, China) to generate the eight corresponding donor DNA sequences.

For gene overexpression, the strong constitutive promoter of *Mtpdc* (MYCTH_112121, pyruvate decarboxylase), P*gpdA-hph* , and T*tef1* fragment were obtained by separately amplifying from pUC19-P*pdc*-T*pdc* (Wang et al., 2015), PAN7-1(GenBank: Z32698.1), and pFC332 vectors. They were then ligated into the *Hin*dIII and *Eco*RI sites of pUC19 plasmid, generating the plasmid pUC19-P*pdc-hph*. To establish a universal overexpression system in *M. thermophila*, the *MtgpdA* (MYCTH_2311855, glyceraldehyde-3-phosphate dehydrogenase) terminator was amplified from *M. thermophila* gDNA with T*gpdA*-F/T*gpdA*-R primer set. The *Ppdc* and *hph* cassette were amplified in the pUC19- P*pdc-hph* plasmid. The *Ppdc*, *TgpdA,* and *hph* cassette were assembled and inserted into pUC19 plasmid to yield the overexpression plasmid pUC19-P*pdc*-T*gpdA-hph*. The *MYCTH_2307931* overexpressing vector was constructed by amplifying *MYCTH_2307931* using *MYCTH_2307931*-F/R primer set which was then ligated into the *Not*I and *Xba*I sites of universal overexpression pUC19-P*pdc*-T*gpdA-hph* plasmid, creating the pUC19-P*pdc-MYCTH_2307931*-T*gpdA-hph* vector. The One Step Cloning Kit (Vazyme Biotech, Nanjing, China) was utilized to construct MYCTH_2307931-eGFP expression

vector (pUC19-P*pdc-MYCTH_2307931-eGFP*-T*gpdA-hph* vector) with enhanced GFP (*eGFP*) fused to *MYCTH_2307931*as a reporter gene.

2.3.3 Transformation of *Myceliophthora thermophila* protoplasts

Protoplast preparation and transformation of *M. thermophila* was described in (Wang et al., 2015) with the following modifications. For the deletion of genes, approximately 20 μg Cas9-U6p-target genes-sgRNA cassette and 20 μg target genes-donor vector were mixed and added to 200 μL protoplasts suspension of *M. thermophila* wild-type strain. After incubating in protoplast regeneration medium at 30°C for 16 h, the pellet of transformants were maintained in PDA medium contains hygromycin B (75 μg mL^{-1}) and G418(100 μg mL^{-1}) at 45°C for 4-5 days to screen for positive clones. Similarly, for gene overexpression, 20 μg pUC19-P*pdc-MYCTH_2307931*-T*gpdA-hph* vector was transformed into the *M. thermophila* protoplasts and transformants were screened for *hph* resistance with hygromycin B (75 μg mL^{-1}). The pure positive deletion and overexpression transformants were obtained and verified through streaking onto selection plates with corresponding antibiotics for three successive rounds, followed by genomic PCR identification and sequencing with different specific paired primers (Table S2.1).

2.3.4 Total DNA and RNA extraction

Total fungal DNA and RNA were extracted from fresh mycelia harvested from respective liquid medium through vacuum filtration. The DNA and RNA were extracted and purified using fungal DNA extraction kit (Sangon Biotech, Shanghai, China) and RNA extraction kit TransZol Up (TransGen Biotech, Beijing, China), respectively, following the manufacturer's protocols. The DNA and RNA were visualized and assessed by electrophoresis and quantified using the NanoDrop 2000 Spectrophotometer (Thermo Scientific, Waltham, MA, USA).

2.3.5 RNA sequencing and transcriptome analysis

Fresh spores (final concentration, 1×10^6 spores mL^{-1}) of *M. thermophila* WT strain were inoculated into 50 mL Mandels medium with 2% (w/v) glucose or 2% (w/v) Avicel as the sole carbon source at 45°C for 36 h. RNA of *M. thermophila* strain cultured on different media were obtained and designated as GRNA (Glucose) and ARNA (Avicel). The *MtFKH1*-specific transcriptomes were analysed by growing the wild type (WT) and Δ*MtFKH1* strain of *M. thermophila* in Mandels medium supplemented with 2% (w/v) glucose, and after optimum growth, washed mycelia were transferred into Mandels medium containing 2% (w/v) Avicel incubated for 48 h followed by RNA extraction. The mRNA was enriched by Oligo (dT) beads and reverse transcribed into cDNA using Illumina NEBNext Ultra RNA Library Prep Kit (New England Biolabs, Ipswich, MA, USA). The cDNA libraries were constructed and sequenced using Illumina Novaseq6000 by Gene Denovo Biotechnology Co. (Guangzhou, China). The quality reads were mapped against the *M. thermophila* ATCC 42464 genome using HISAT2. v2.4 (Kim et al., 2015). The RSEM software was used to analyse the gene expression levels (fragment per kilobase of transcript per million mapped reads, FPKM) (Li and Dewey, 2011). The differentially expressed genes (DEGs) were identified by DESeq2 (Love et al., 2014), with absolute fold change > 2 ($\log_2$ fold change > 1 or < −1) and adjusted Pvalue (padj) < 0.05 as thresholds. Gene Ontology (GO) enrichment analysis was implemented using the OmicShare tools (https://www.omicshare.com/tools). All DEGs were mapped against GO terms in the Gene Ontology database (http://www.geneontology.org/). Significantly enriched GO terms in DEGs compared with the *M. thermophila* ATCC 42464 genome background were calculated by hypergeometric test. GO terms with Pvalue < 0.05 were considered significantly enriched. The raw reads of transcriptomic data are available at the Gene Expression Omnibus (GEO) under accession number #GSE274481 and #GSE274798.

2.3.6 Subcellular localization of MYCTH_2307931-GFP in *M. thermophila*

MYCTH_2307931-GFP positive transformants were inoculated into Mandels medium

containing 2% (w/v) glucose and incubated at 45°C for 36 h. Mycelia were harvested and stained with 5 mg L^{-1} DAPI (4',6-diamidino-2-phenylindole) solution for 15 min under darkness and then washed with PBS solution three times. Fungal cells were observed using an Olympus BX53 fluorescence microscopy system, with the Olympus cellSens Standard software used for image processing.

2.3.7 Protein and enzyme activity measurements

Samples of the fermentation cultures (2 mL) from different time points were collected by centrifugation at 4°C, 12,000 rpm for 10 min to remove mycelia and other solid materials. 20 μL unconcentrated culture supernatant was loaded on a 10% polyacrylamide gel (PAGE Gel Quick Preparation Kit, Yeasen Biotech, Nanjing, China) and ran at 120 V for 80 min in Tris-Glycine-SDS running buffer. The protein bands were stained with Coomassie Brilliant Blue R-250 (Sangon Biotech, Shanghai, China). The concentration of extracellular protein in culture supernatants was determined with a Modified Bradford Protein Assay Kit (Sangon Biotech, Shanghai, China) based on absorbance at 595 nm, using bovine serum albumin (BSA) as the standard. The filter paper cellulase (FPase), endoglucanase (CMCase) and xylanase activities were measured by the method reported previously (Eveleigh et al., 2009; Ma et al., 2016) with some modifications. Briefly, 150, 150, and 100 μL of appropriately diluted crude enzyme solution was added to 600 μL of 50 mM citrate buffer (pH 4.8) containing Whatman No. 1 filter paper (25 mg, 1.0 cm × 3.0 cm; GE Healthcare Limited, Little Chalfont, United Kingdom), 500 μL of 50 mM citrate buffer containing 1% sodium carboxymethyl cellulose (CMC-Na; Sangon Biotech, Shanghai, China), 100 μL of 50 mM citrate buffer containing 1% beechwood xylan (Sigma-Aldrich, Darmstadt, Germany), and incubated at 50 °C for 60, 30 and 10 min, respectively. The reducing sugars generated were determined by the 3,5-dinitrosalicylic acid method described earlier (Ghose, 1987) at 540 nm.

The β-glucosidase (pNPGase) and exoglucanase (pNPCase) activities were assayed using *p*-nitrophenyl-β-D-glucopyranoside (pNPG) and *p*-nitrophenyl-β-D-

cellobioside (pNPC) (both from Aladdin Biochemical Technology, Shanghai, China) as substrates, respectively, according to the method previously described (Zou et al., 2012; Mansour et al., 2016) with some modifications. In brief, 100 µL of properly diluted culture supernatant was incubated with 100 µL of 1 mg mL^{-1} substrates dissolved in 50 mM citrate buffer (pH 4.8) at 50°C for 30 min. The reaction was terminated by adding 500 µL of 2% (w/v) Na_2CO_3 and the absorbance was measured at 405 nm on the Synergy™ HTX multi-mode reader (BioTek, winooski, VT, USA). One unit of enzymatic activity (U) was defined as the amount of 1 µmol glucose or *p*-nitrophenol produced by 1 mL enzyme from the substrate per minute under standard assay conditions.

2.3.8 Real-time quantitative reverse transcription-PCR (RT-qPCR) analysis

The cDNA was synthesized from RNA using HiScript® III RT SuperMix (+gDNA wiper) (Vazyme Biotech, Nanjing, China) following the manufacturer's protocol. Each 20 µL PCR reaction mixture was composed of 10 µL of Hieff UNICON® Universal Blue qPCR SYBR Green Master Mix (Yeasen Biotech, Shanghai, China), 0.4 µL of each primer (10 uM), 2.0 µL of diluted cDNA and 7.2 µL of sterile water. The thermocycler protocol was as follows: initial denaturation for 2 min at 95 °C, followed by 40 cycles of 5 s at 95 °C and 20 s at 63 °C. Melt curves assays were performed after each run to confirm specific amplification of all primers. The primers used for the genes are shown in Table S2.1. The *actin* gene (*MYCTH_2314852*) of *M. thermophila* was used as an endogenous control and expression levels of the genes were calculated by the comparative CT method $2^{-\Delta\Delta CT}$ (Livak and Schmittgen, 2001). The expression of each tested gene in the WT was set as 100%. All the experiments were performed in triplicates.

2.3.9 Expression and purification of the MtFKH1 DNA-binding domain

The DNA fragments encoding the putative DNA-binding domain $MtFKH1_{237\text{-}356}$ were amplified from *M. thermophila* genomic DNA. The purified PCR products were

inserted into the *Hin*dIII site of pET-51b vector to construct a fusion plasmid pET-51b-MtFKH1$_{237\text{-}356}$ and was subsequently introduced into *E. coli* BL21(DE3) for protein expression. The resulting recombinant strain was cultured in LB medium until OD600 was 0.6 and induced with 1.0 mM isopropyl-β-D-thiogalactopyranoside (IPTG) at 28°C for 24 h to produce the Strep II-tagged fusion protein. The recombinant protein was purified using a Strep-Tactin Sepharose High Performance Affinity column (Cytiva, Shanghai, China) according to the supplier's guidelines. The purified protein was verified by sodium dodecyl sulfate-polyacrylamide gel electrophoresis (SDS-PAGE) analysis, and the protein band was excised and identified using LC-MS/MS with PEAKS Studio 8.5 (Bioinformatics Solutions Inc., Waterloo, Canada) analysis system.

2.3.10 Electrophoretic mobility shift assays

Different DNA fragments were used as probes in the gel-shift assays. For MtFKH1-binding experiments, the promoter regions of *bgl1* (MYCTH_66804) (P1, − 350 to − 1; P2, − 650 to − 300; P3, − 1000 to − 600), *cbh1* (MYCTH_109566) (P1, − 350 to − 1), *xyn1* (MYCTH_112050) (P3, − 1000 to − 650) and *xyr1* (MYCTH_2310145) (P1, − 350 to − 1) were obtained by PCR from the genomic DNA of *M. thermophila* using the primers listed in Table S2.1. The PCR products were purified using PCR Product Purification Kit (Sangon Biotech, Shanghai, China) and quantified using a NanoDrop 2000 Spectrophotometer (Thermo Scientific, Waltham, MA, USA). The subsequent binding experiments were performed based on a modified gel mobility shift assay reported previously (Wang et al., 2011). In each EMSA reaction, constant amount (100 ng) of the DNA probes were incubated with gradual quantities (0-0.2 μg) of recombinant proteins individually at 25°C for 30 min in solution containing Gel-Shift Binding Buffer (Beyotime Biotech, Shanghai, China). After incubation, the protein-DNA complexes and free DNA were separated by electrophoresis on native 6% polyacrylamide gels with 0.5 × TBE running buffer (44.5 mM Tris-boric, 1 mM EDTA, pH 8.2) at 110 V for 70 min at 4°C. Finally, gels were visualized with the Bio-Rad Gel-Doc^{TM} Imaging System (Bio-Rad Laboratories Inc., Hercules, CA, USA). Purified

Strep II-His-tagged protein from *E. coli* BL21(DE3) cells transformed with the vector pET-51b-MtCLR-$2_{30\text{-}89}$ was used as the negative control.

2.3.11 DNase I footprinting assays

DNase I footprinting assays were implemented according to a previously reported protocol (Wang et al., 2012). For preparing fluorescent 6-carboxyfluorescein (FAM)-labeled probe, *bgl1* promoter region (P1, − 350 to − 1) was amplified from *M. thermophila* genomic DNA using the primers *bgl1*-p1-F/R. The FAM-labeled probe was subsequently purified and quantified with NanoDrop 2000 Spectrophotometer. For each assay, 400 ng probe was incubated with various quantities of purified MtFKH1$_{237\text{-}356}$ in a total mixture of 40 μL in the same binding buffer as described in EMSAs. After incubation at 25°C for 30 min, 10 μL solution containing 0.015-unit DNase I (Promega, Madison, WI, USA) and 100 nmol $CaCl_2$ were added and further incubated at 25°C for 1 min. The reaction was stopped by adding 140 μL DNase I stop solution (200 mM unbuffered sodium acetate, 30 mM EDTA, and 0.15% SDS). After enzymatic digestion, the protein was removed by phenol-chloroform extraction, and the DNA was precipitated with ethanol and resuspended in Milli-Q water. The DNA sequencing analysis was performed as previously described (Wang et al., 2012).

2.4 Results

2.4.1 Comparative transcriptomic analysis of *M. thermophila*

Carbon Catabolite Repression (CCR) is a global regulatory system which ensures preferential utilisation of glucose or other readily available carbon sources over less-favored carbohydrates such as cellulose (Adnan et al., 2017; Benocci et al., 2017). Thus, glucose and lignocellulose are the most widely used repressor and inducer for lignocellulolytic enzymes production, respectively. In the current study, the cellulase and xylanase production was evaluated in inducing and repressing carbon sources. As expected, all the enzymatic activities of *M. thermophila*, including filter-paper cellulase

(FPase), endo-glucanase (CMCase), and xylanase, were increased by 128%, 292%, and 417%, respectively, when grown on Avicel compared with that of glucose after 48 h (Figure 2.1A). Transcription factors (TFs) play a pivotal regulatory role in fugal lignocellulolytic enzymes synthesis. We speculated that TFs may be responsible for the significant improvements in cellulase and xylanase activities observed under Avicel conditions. Therefore, the transcriptomes of *M. thermophila* wild type (WT) cultured on Avicel and glucose were screened for potential regulators of cellulolytic and xylanolytic genes expression.

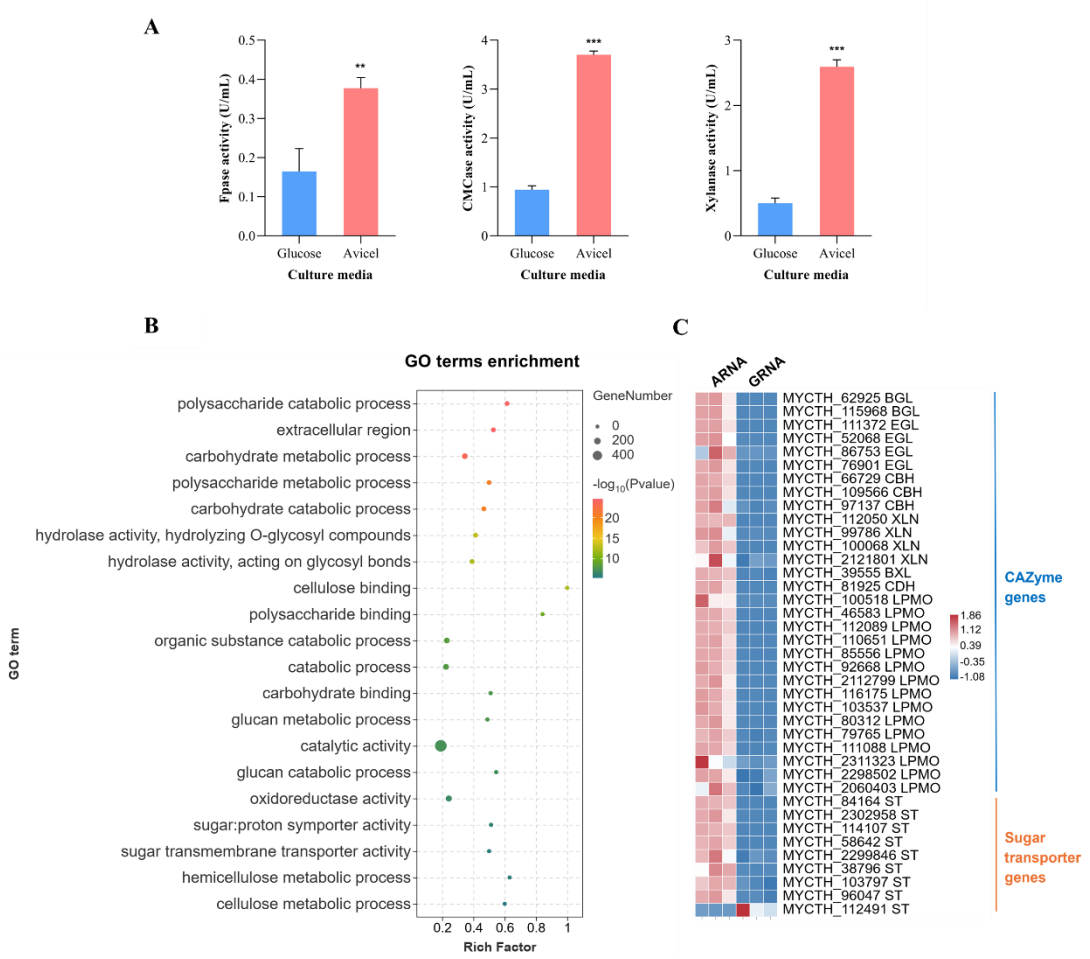

Figure 2.1. Comparative transcriptomic analysis of *M. thermophila* grown on Avicel (ARNA) and Glucose (GRNA). (A) Enzymatic activities of filter-paper cellulase, endo-glucanase, and xylanase of *M. thermophila* cultured for 48 h in 2% (w/v) Avicel or 2% (w/v) glucose culture media after a shift from liquid Mandels medium containing 2% (w/v) glucose. **p < 0.01 and ***p < 0.001 indicate significant differences in enzyme activities detected in *M. thermophila* between Avicel and glucose cultures (Student's t tests). Error bars indicate the SD from three replicates. (B) Gene Ontology (GO) enrichment analysis of 1558 differentially expressed genes (DEGs) in the Biological Process (BP), Cellular Component (CC), and Molecular Function (MF) categories for *M. thermophila* under Avicel and Glucose conditions. The screening criteria for DEGs are |log2 fold change| > 1 and padj < 0.05. (C) Heatmap analysis of expression profiles for the cellulase genes, xylanase genes, xylosidase gene, cellobiose dehydrogenase gene, LPMO (AA9) encoding genes, and putative sugar transporter encoding genes when |log2 fold change| > 2 and padj < 0.05 as thresholds in M. thermophila cultured on Avicel compared with that on glucose. BGL, β-glucosidase; EGL, endoglucanase; CBH, cellobiohydrolase; XLN, xylanase; BXL, β-xylosidase; CDH, cellobiose dehydrogenase; LPMO, lytic polysaccharide monooxygenase; ST, sugar transporter.

The total RNAs obtained from the mycelia of *M. thermophila* grown on Aviel or glucose for 36 h were sequenced. There were 24-34 million quality reads generated > 92% were mapped onto the *M. thermophila* genome (Table S2.2).

Compared to glucose as the carbon source, 1558 differentially expressed genes (DEGs) were identified in *M. thermophila* when grown in Avicel, comprising 752 upregulated and 806 downregulated genes. Gene Ontology (GO) enrichment analysis revealed that these DEGs were significantly enriched in polysaccharide catabolic process, carbohydrate metabolic process, and polysaccharide metabolic process (Biological Process) or hydrolase activity acting on glycosyl bonds, and cellulose or polysaccharide binding (Molecular Function) (Figure 2.1B).

The comparative transcriptome analysis also uncovered substantial differences in the expression of 10 genes encoding putative transcription factors when |log2 fold change | > 2 and padj < 0.05 were used as thresholds, of which, four genes were upregulated and six were downregulated when cultivated on Avicel (Table 2.1). Based on the DNA-binding domain or transcriptional activation domain predicted by bioinformatics, these TFs were classified into seven types: High Mobility Group (HMG), Helix-loop-helix (HLH), Fungal_TF, Zinc finger (Zn2Cys6, C2H2), Forkhead, basic-leucine zipper (bZIP), and CP2 transcription factor (Table 2.1). It is noteworthy that MYCTH_38704 (MtCLR-2) and MYCTH_2310995 (MtHAC-1) were found to regulate cellulase secretion in *M. thermophila* (Li et al., 2022a; Zhang et al., 2022).

Furthermore, nine key cellulase genes including two β-glucosidase genes *MYCTH_62925* and *MYCTH_115968*, four endoglucanase genes (*MYCTH_111372*, *MYCTH_52068*, *MYCTH_86753*, and *MYCTH_76901*), and three cellobiohydrolase genes (*MYCTH_66729*, *MYCTH_109566*, and *MYCTH_97137*), five crucial xylanolytic genes including four crucial xylanase genes (*MYCTH_112050*, *MYCTH_99786*, *MYCTH_100068*, and *MYCTH_2121801*), and a xylosidase gene *MYCTH_39555*, were substantially upregulated on Avicel relative to those on glucose (Figure 2.1C), demonstrating that considerably improved lignocellulolytic enzyme activities detected in cellulose culture (Figure 2.1A).

Additionally, 15 LPMOs (AA9) encoding genes were strongly induced under Avicel cultivation conditions (Figure 2.1C). Lytic polysaccharide monooxygenases (LPMOs) are copper-dependent enzymes that split glycosidic linkages on the surface of cellulose in an oxidative manner, thus promoting cellulase access to the glycosidic bonds within the polysaccharides (Kjaergaard et al., 2014). Moreover, a gene encoding cellobiose dehydrogenase gene (*MYCTH_81925*, MtCDH-2), which is deemed the primary redox partner of LPMOs being expressed and secreted in the presence of cellulose (Phillips et al., 2011), was also upregulated by the presence of Avicel (Figure 2.1C).

Table 2.1. Candidate TFs from transcriptomic analysis of *M. thermophila* on Avicel and glucose.

Gene symbol	**InterPro annotation[a]**	**Domain description**	**Log2FoldChange[b]**
MYCTH_2129372	IPR009071	High Mobility Group (HMG)-box	7.22
MYCTH_2310243	IPR011598	Helix-loop-helix (HLH)	4.86
MYCTH_38704	IPR007219	Fungal_TF	3.62
MYCTH_2308823	IPR001138	Zinc finger, Zn2Cys6	2.11
MYCTH_2306976	IPR001138	Zinc finger, Zn2Cys6	-7.04
MYCTH_2307931	IPR001766	Forkhead domain	-4.25
MYCTH_2310995	IPR004827	basic-leucine zipper (bZIP)	-2.69
MYCTH_2297579	IPR013087	Zinc finger, C2H2	-2.20
MYCTH_2082522	IPR007604	CP2 transcription factor	-2.12
MYCTH_2302011	IPR001138	Zinc finger, Zn2Cys6	-2.06

[a] (https://www.ebi.ac.uk/interpro/)

[b] Gene expression levels of *M. thermophila* cultivated on Avicel compared to glucose.

In addition to these CAZyme genes, eight putative sugar transporter encoding

genes including *MYCTH_84164* (cellodextrin transporter-like protein1, CLp1 ortholog) (Cai et al., 2015), *MYCTH_2302958* (ortholog of CLp1), *MYCTH_114107* (cellodextrin transport-2, CDT-2 ortholog) (Znameroski et al., 2014), *MYCTH_58642*, *MYCTH_2299846*, *MYCTH_38796*, *MYCTH_103797*, and *MYCTH_96047* were highly induced in *M. thermophila* strain during growth in Avicel, except for *MYCTH_112491* (Figure 2.1C). These observations were consistent with the findings that numerous sugar transporter-encoding genes were upregulated in the presence of sugarcane bagasse or wheat straw but repressed by glucose (de Souza et al., 2011; Ries et al., 2013), suggesting that these genes were required for better utilisation of diverse sugars generated form complex biomass degradation.

Expression pattern analyses also identified a few genes linked to carbon metabolism pathways. With regards to gluconeogenesis, one upregulated and three downregulated genes were detected when cells were grown in Avicel. The DEGs included triosephosphate isomerase gene *MYCTH_2304931*, fructose-bisphosphatase gene *MYCTH_2306943*, phosphoenolpyruvate synthase gene *MYCTH_2311072*, and phosphoenolpyruvate carboxykinase gene *MYCTH_2315623*. Similarly, four genes involved in the tricarboxylic acid (TCA) cycle were characterized, including one upregulated (succinyl-CoA ligase *MYCTH_2296474*), and three downregulated genes (isocitrate lyase *MYCTH_110871*, aconitate hydratase *MYCTH_2309261*, and 2-oxoglutarate dehydrogenase *MYCTH_2312383*) on Avicel compared with those on glucose. The varied expression of these genes involved in anabolic and catabolic metabolism may be beneficial to efficient utilisation of cellulose as the carbon source under carbon starvation conditions.

2.4.2 Novel regulatory gene potentially regulating cellulase and xylanase production

To identify novel TFs controlling cellulase and xylanase production in *M. thermophila*, a CRISPR/Cas9 system was established to create deletion strains of eight potential regulatory genes (Figure S2.1). Protospacer sequences containing 20-nucleotide targets

for the eight candidate genes were designed for gene editing (Table 2.2). The resultant disruption mutants were confirmed by PCR using three specific primer sets (Table S2.1), and five candidate genes were successfully deleted (Figure S2.1). Measurements of enzymatic activities in the deletion mutants (Δ*MYCTH_2310243*, Δ*MYCTH_2306976*, Δ*MYCTH_2307931*, Δ*MYCTH_2308823*, and Δ*MYCTH_2129372*) compared with WT under Avicel conditions revealed that Δ*MYCTH_2307931* showed 31% and 34% enhancement in Fpase and xylanase activity, respectively (Figure S2.1). Hence, the TF encoding gene *MYCTH_2307931* was considered for all downstream analysis.

Table 2.2. List of protospacer and protospacer adjacent motif (PAM) sequences of each target gene used in this chapter.

Gene symbol	Protospacer sequence	PAM
MYCTH_2129372	TTCTGCGAGGCACATGCGCC	CGG
MYCTH_2310243	TCTCACGGTCCATTAGTCGA	TGG
MYCTH_2308823	GCGCTACGATGCACAACACC	GGG
MYCTH_2306976	TATGGGCGCCTGACTGTTCA	AGG
MYCTH_2307931	CTGTGCCTCTCCTGCACAAC	AGG
MYCTH_2297579	GTCGCAACGCACTATGCGCC	TGG
MYCTH_2082522	GCTACTATACGCCCACTTCG	GGG
MYCTH_2302011	CAATGACGTTCCCGTTCCAG	AGG

2.4.3 MYCTH_2307931 acts as a forkhead transcription factor

The *MYCTH_2307931* gene contains two exons encoding a 724 amino acids (aa) protein. The InterPro analysis (https://www.ebi.ac.uk/interpro/) and tertiary structure assessment showed the presence of a forkhead DNA-binding domain (IPR001766) between the residue positions 237 and 356 (Figure 2.2A-B). Additionally, protein alignment using BLASTP indicated that MYCTH_2307931 shares 28% to 44% identity

with its close homologs from different organisms including *S. cerevisiae* (ScFKH1, GenBank: DAA08422.1; ScFKH2, GenBank: DAA10477.1), *H. chrysogena* (HcFKH1, GenBank: AAP35674.1), *A. nidulans* (AnFKHB, GenBank: CBF83869.1), and *P. oxalicum* (PoX08522, GenBank: AOP12492.1) with high similarity confined in the DNA-binding forkhead domain (Figure 2.2A). All matching proteins have been characterized as members of the forkhead TFs family with diverse roles in microbial development and metabolism. MYCTH_2307931 is subsequently re-designated as MtFKH1(where Mt represents *M. thermophila* and FKH represents forkhead) since it is the first forkhead protein functionally characterized in *M. thermophila*.

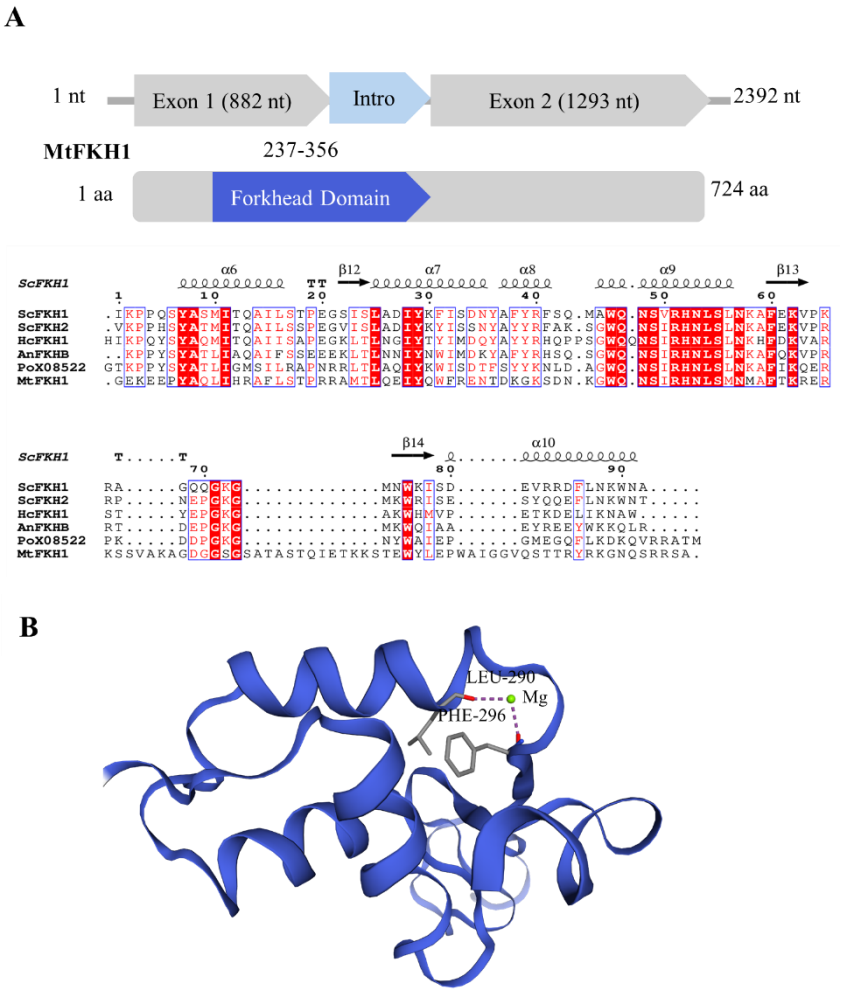

Figure 2.2. Characterisation of the MYCTH_2307931 as a forkhead protein. (A) Analysis of conserved domain in the MtFKH1 protein and protein sequence alignment. The MtFKH1 gene possesses two exons, and the predicted Forkhead DNA-binding domain (DBD) is highlighted. Protein alignment of the DBD between MtFKH1 and previously reported forkhead proteins in Saccharomyces cerevisiae S288C (ScFKH1, GenBank: DAA08422.1; ScFKH2, GenBank: DAA10477.1), *Hapsidospora chrysogena* (HcFKH1, GenBank: AAP35674.1), *Aspergillus nidulans* FGSC A4 (AnFKHB, GenBank: CBF83869.1), and *Penicillium oxalicum* HP7-1 (PoX08522, GenBank: AOP12492.1) confirmed the presence of conserved amino acids (aa) within the DBD. The identical aa are highlighted in red boxes, and aa in red characters with blue frames indicate similar amino acid residues across different proteins. α, β, and TT represent α-helices, β-strands, and β-turns, respectively, in DBD of ScFKH1, which was obtained from SWISS-MODEL (P40466). (B) The tertiary structure of the DBD of MtFKH1 was gained by homology modelling using SWISS-MODEL. The green ball represents magnesium ion.

2.4.4 MtFKH1 plays a key role in cellulase and xylanase production

To further explore the regulatory roles of *Mtfkh1*, *M. thermophila* Δ*Mtfkh1* strain and the WT parental strain were cultivated in liquid Mandels medium containing 2% (w/v) Avicel for 48-96 h after a shift from glucose. The results revealed that cellulase activities corresponding to FPase, pNPCase, and pNPGase activities, as well as xylanase production of Δ*Mtfkh1* were increased by 25% to 42%, 36% to 57%, 17% to 62%, and 34% to 86% respectively, compared with the WT (Figure 2.3A-D). Additionally, Δ*Mtfkh1* secreted approximately 141% to 158% higher protein than the WT when grown on Avicel (Figure 2.3E). These results were validated by the SDS-PAGE analysis of the extracellular protein (Figure 2.3F).

To further verify the alterations in cellulase and xylanase production in the mutant Δ*Mtfkh1* caused by the specific disruption of the *Mtfkh1* gene, the overexpression strain OE-*Mtfkh1* was generated, in which *Mtfkh1* was driven by a strong constitutive promoter P*pdc* (MYCTH_112121, pyruvate decarboxylase). The positive overexpression mutant was confirmed by PCR with specific primers (Table S2.1 and Figure S2.1). Evaluation of the enzyme production showed a 26% to 55% decrease in FPase, pNPCase, pNPGase, and xylanase yields, as well as extracellular protein content, by OE-*Mtfkh1* strain, during the presence of Avicel relative to the activities detected in the WT (Figure 2.3A-E). These findings indicate that MtFKH1 is a repressor of cellulase and xylanase production.

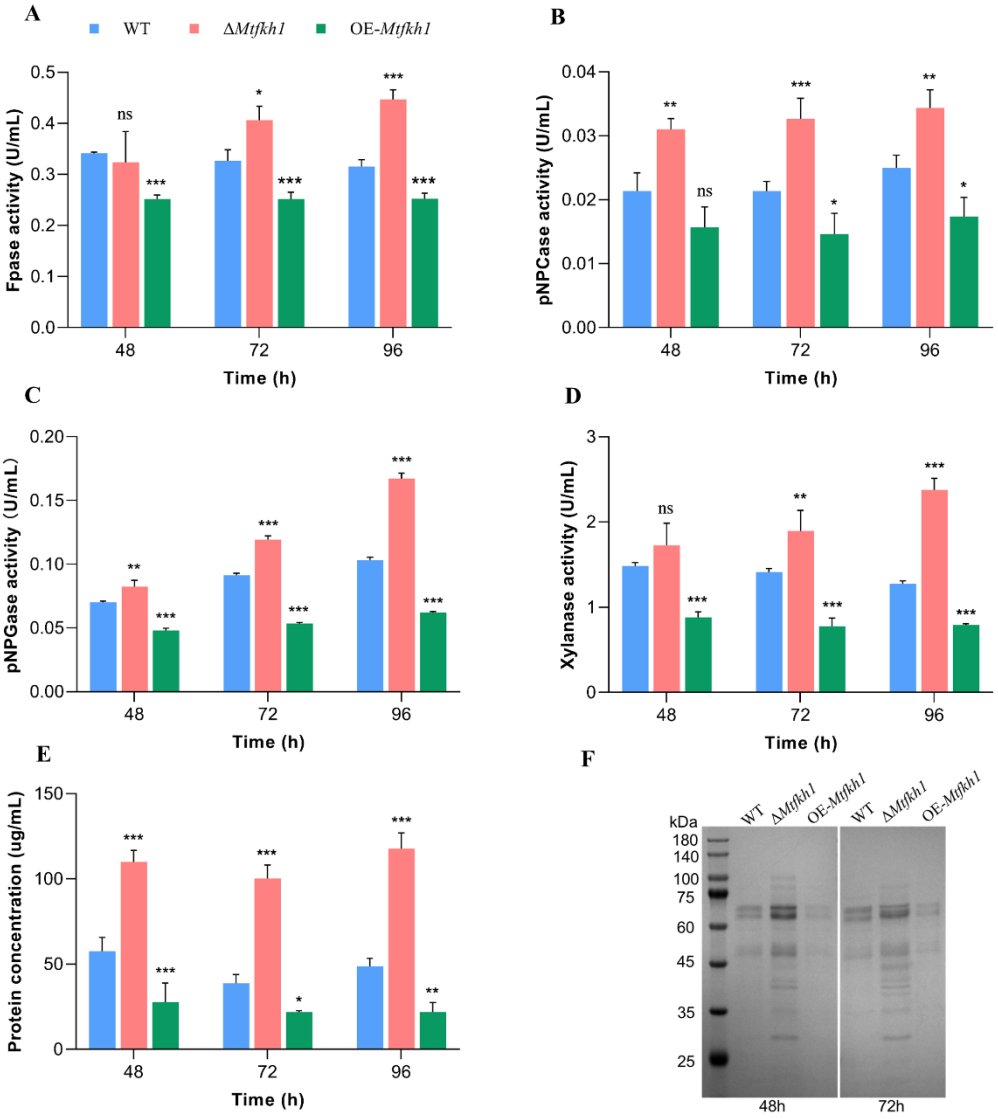

Figure 2.3. Enzyme activities and protein production of *M. thermophila* WT strain, ΔMtfkh1 deletion mutant, and OE-Mtfkh1 overexpression strain. Culture supernatants were collected from fungal strains cultivated on Avicel for 48-96 h at 45 °C after shifting from glucose. (A) Filter paper cellulase (FPase) activity. (B) Cellobiohydrolase (pNPCase) activity. (C) β-glucosidase (pNPGase) activity. (D) Xylanase activity. (E) Extracellular protein concentration. (F) SDS-PAGE analysis of the secreted proteins at 48 and 72 h. M, 10-180 kDa protein marker. *p < 0.05, **p < 0.01, and ***p < 0.001 indicate remarkable differences in enzyme activities and secreted protein detected between WT and Δ*Mtfkh1* or OE-*Mtfkh1* strains (Two-way ANOVA), ns indicates not significant. Error bars represent the SD from three replicates.

2.4.5 MtFKH1 controls sporulation in *M. thermophila*

To evaluate the role of MtFKH1 in growth phenotype, *M. thermophila* WT, Δ*Mtfkh1*, and OE-*Mtfkh1* strains were cultivated on solid plates containing glucose or Avicel as the sole carbon source, and PDA plates. None of these *M. thermophila* strains displayed considerable differences in colony phenotype on all tested culture media (Figure 2.4A). The quantitative assessment of the asexual spores produced by strains WT, Δ*Mtfkh1*, and OE-*Mtfkh1* on Avicel plates was also carried out. Surprisingly, Δ*Mtfkh1* produced only 38% of the spores generated from the WT after 7 days, whereas OE-*Mtfkh1* presented similar level of conidia formation with the WT (Figure 2.4B). The hyphal growth observed in Δ*Mtfkh1* mutant incubated in liquid shake flasks containing glucose or Avicel as the sole carbon source was consistent with its growth on glucose or cellulose solid plates, exhibiting no noticeable differences relative to that detected in both WT and OE-*Mtfkh1* strains (Figure 2.4C and Figure S2.2), which was also confirmed by microscopic investigation (Figure S2.2). Taken together, these results suggest that MtFKH1 regulates sporulation not fungal growth.

2.4.6 Subcellular localization of MtFKH1 in *M. thermophila*

To determine whether MtFKH1is a nuclear protein, the *Mtfkh1* gene was fused to a *gfp* (green fluorescent protein) gene under the control of the powerful constitutive promoter P*pdc*. The expression vector was introduced to the WT strain to generate the overexpression strain expressing the MtFKH1-GFP fusion protein. The green fluorescence signal was observed in the intracellular nuclei across the fungal cells, which merged well with the nucleic acid-specific blue dye DAPI (Figure 2.4D), demonstrating that MtFKH1 is located in the *M. thermophila* nucleus.

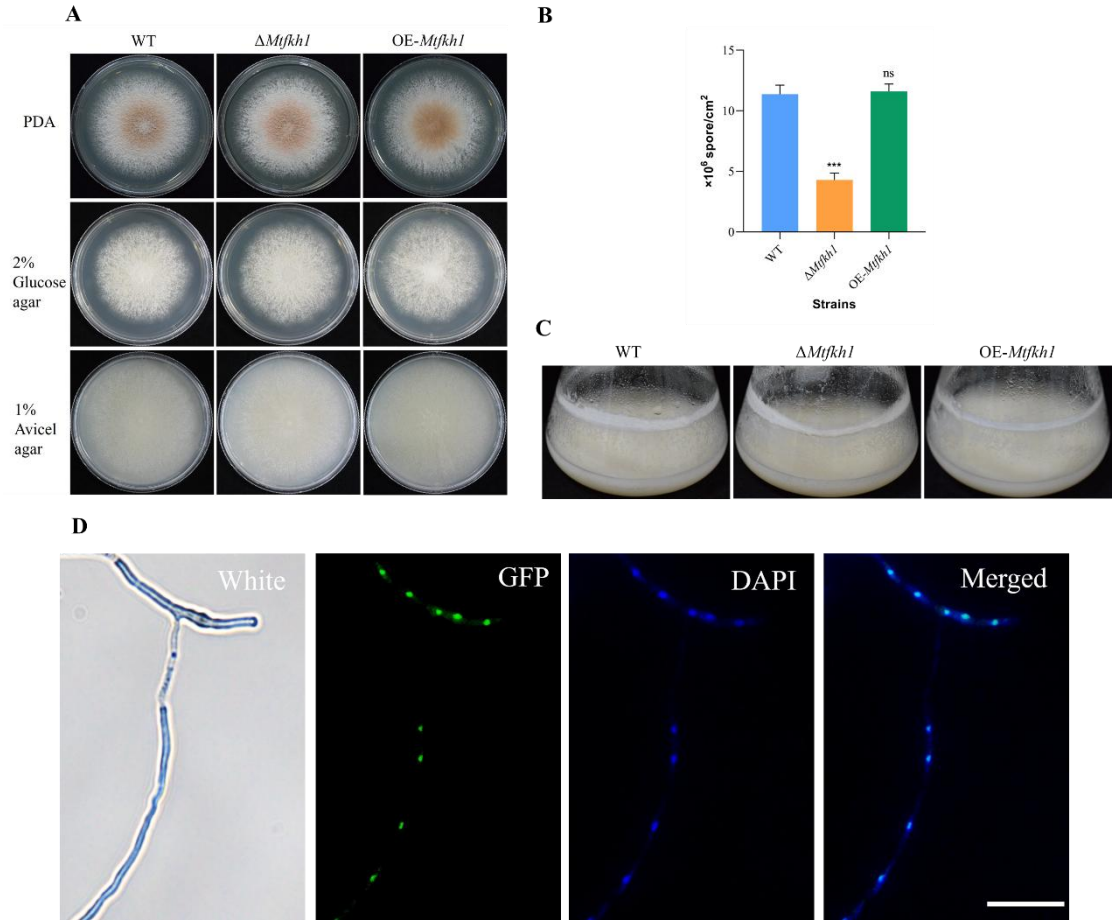

Figure 2.4. Phenotypic analyses of *M. thermophila* WT, Δ*Mtfkh1* and OE-*Mtfkh1* strains, and subcellular localization of MtFKH1 protein. (A) Colony phenotype on PDA, solid plates containing 2% (w/v) glucose or 1% (w/v) Avicel as the sole carbon source after 3 (PDA) or 4 days (glucose and Avicel) of growth at 45 °C. (B) Quantitative evaluation of conidiation on plates containing 1% (w/v) Avicel incubated at 45 °C for 7 days. ***$p < 0.001$ demonstrates significant differences in sporulation between WT and Δ*Mtfkh1* strains (Student's t tests), ns represents no remarkable differences between WT and OE-*Mtfkh1* strains. Error bars indicate the SD from three replicates. (C) Growth observation in liquid shake cultures containing 2 % (w/v) Avicel grown at 45 °C for 36 h. (D) Subcellular location of MtFKH1 in *M. thermophila*. MtFKH1-GFP strain was grown in liquid Mandels medium with 2% (w/v) glucose as sole carbon source at 45 °C for 36 h. Location of MtFKH1 was monitored by merging EGFP signal and blue florescence signal which was from nuclei-specific dye DAPI. Samples were observed using an Olympus BX53 fluorescence microscope. Scale bar = 20 µm.

2.4.7 MtFKH1 regulates the expression of major cellulase and xylanase genes

To investigate whether MtFKH1 transcriptionally controls the expression of cellulase and xylanase genes in *M. thermophila* grown on cellulose, real-time quantitative reverse transcription PCR (RT-qPCR) was performed, with the WT as the control. The transcription levels of key cellulase and xylanase genes as well as genes encoding two crucial regulators Cre1 and Xyr1 in *M. thermophila*, including β-glucosidase gene *bgl1*(*MYCTH_66804*), cellobiohydrolase gene *cbh1* (*MYCTH_109566*), xylanase gene *xyn1* (*MYCTH*_112050), *cre1* (*MYCTH_2310085*), and *xyr1* (*MYCTH_2310145*) were measured at 48 and 72 h after transferring from glucose to Avicel. The results indicated that *cbh1* showed 1.6- and 6.6-fold enhancements in transcription levels in Δ*Mtfkh1* at 48 and 72 h, respectively. Likewise, *bgl1* exhibited 1.0-fold elevation in transcript level at 48 h and slight increase (62%) at 72 h due to the deletion of *Mtfkh1* in *M. thermophila*. In addition, the expression of *xyn1* in Δ*Mtfkh1* was increased by 63% to 94% during the overall period, whereas no change was observed in the transcript levels of *cre1* and *xyr1* at both 48 and 72 h (Figure 2.5). These data suggest that the expression of the major cellulase and xylanase genes was significantly improved in Δ*Mtfkh1* compared with WT at certain periods during the presence of Avicel, although with varied degrees.

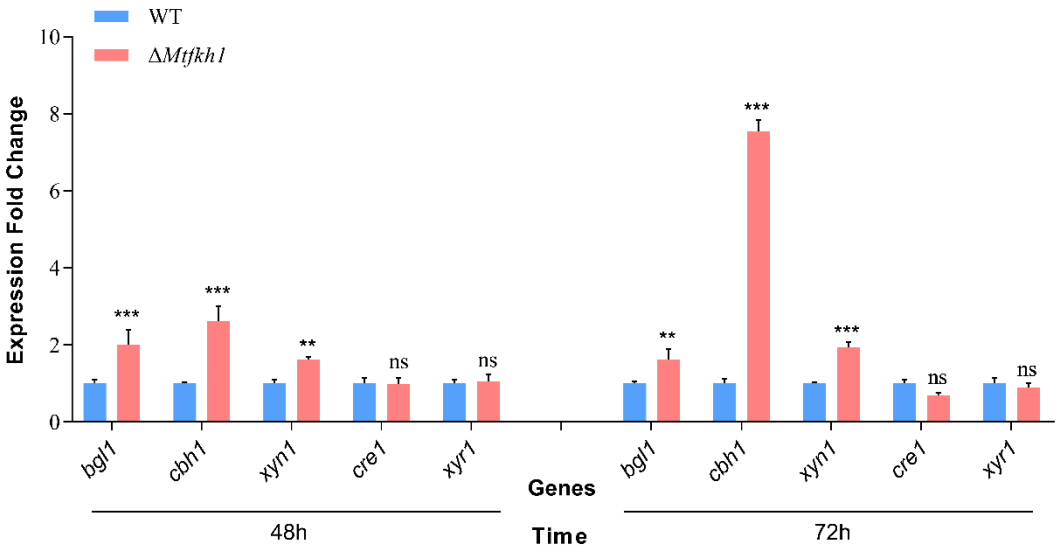

Figure 2.5. Relative transcription levels of genes associated with lignocellulose degradation in *M. thermophila* WT and Δ*Mtfkh1* strains. Strains were pre-cultured in glucose for 36 h, washed and shifted to 2% (w/v) Avicel medium and cultivated for 48 and 72 h. Expression levels of the detected genes in Δ*Mtfkh1* were normalized against WT. Asterisks on bars represent notable differences from unmarked bars in each group (Two-way ANOVA, **p < 0.01, and ***p < 0.001), ns indicate no remarkable differences. Error bars represent the SD from three replicates.

2.4.8 MtFKH1 binds to the promoter regions of crucial cellulase and xylanase genes

The above findings revealed that MtFKH1 regulates cellulase and xylanase production in *M. thermophila* by controlling transcript levels of cellulolytic and xylanolytic genes. To confirm whether MtFKH1 directly regulates targeted genes expression, electrophoretic mobility shift assays (EMSAs) were performed. Strep II-fused DNA binding domain of MtFKH1 ($MtFKH1_{237\text{-}356}$) was expressed and purified from *E. coli* BL21(DE3) (Figure S2.3). Probes covering the promoter regions of *bgl1*(− 1 to − 1000), *cbh1*(− 350 to − 1), *xyn1*(− 1000 to − 650), and *xyr1*(− 350 to − 1) were amplified by PCR. Significant binding was observed for promoter regions of both *bgl1*, *cbh1*, and *xyn1* with different amount of the recombinant $MtFKH1_{237\text{-}356}$, and the size of each

shifted band increased along with increasing quantity of MtFKH1$_{237-356}$ (0-0.2 μg) (Figure 2.6). In contrast, no retardation was detected between MtFKH1$_{237-356}$ and the *xyr1* promoter, which was used as the negative control. Additionally, purified Strep II-fused MtCLR-2$_{30-89}$ was also utilized as a negative control to exclude the possibility that Strep II-His tag protein bound to the target genes (Data not shown). Taken together, the EMSAs results indicate that MtFKH1 specifically binds to the promoter regions of key cellulase and xylanase genes *bgl1*, *cbh1*, and *xyn1in vitro*.

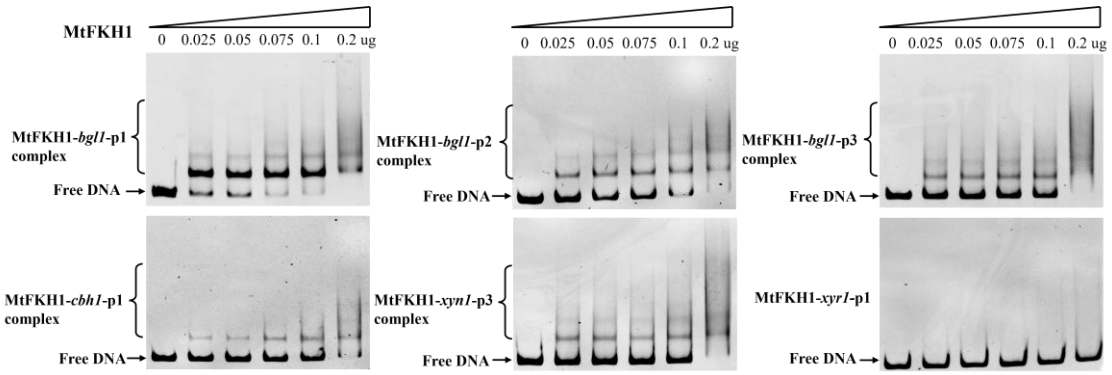

Figure 2.6. Electrophoretic mobility shift (EMSA) analysis of the interactions between MtFKH1 and the promoter regions of key genes encoding cellulase and xylanase. Each experiment contains 100 ng probe and indicated quantities of purified MtFKH1 binding domain. The promoter of *xyr1* was used as negative control.

2.4.9 Identification of MtFKH1 binding sites in the upstream region of *Mtbgl1*

To confirm the precise DNA region bound by MtFKH1 in the promoter of *bgl1*, a DNase I footprinting assay was performed using purified MtFKH1$_{237-356}$ and the FAM-labeled promoter fragment of *bgl1*(P1, − 350 to − 1), which exhibited the strongest specific shift (Figure 2.6). As the abundance of MtFKH1 protein increased to 2 μg, one apparently protected region was observed in *bgl1*-P1(5′-CGGGAAGGCAAACATTGT-3′) (Figure 2.7A), matching the consensus 5′-G/A T/C C/A A A T/C A-3′ (underlined) characterized from 17 different promoter sequences bound by other various forkhead proteins (Kaufmann et al., 1995). It was speculated that 5′-RYMAAYA-3′ might be a conserved motif that MtFKH1 binds to in *M.*

thermophila. Therefore, the binding site in the *bgl1*-p2, *bgl1*-p3, *cbh1*-p1, and *xyn1*-p3 were tested. The results identified at least one similar motif in the upstream region of each target gene (5′-RYMANYA-3′), with the "ANYA" sequence highly conserved (Figure 2.7B). As expected, no 5′-RYMANYA-3′ site was found in *xyr1*-p1.

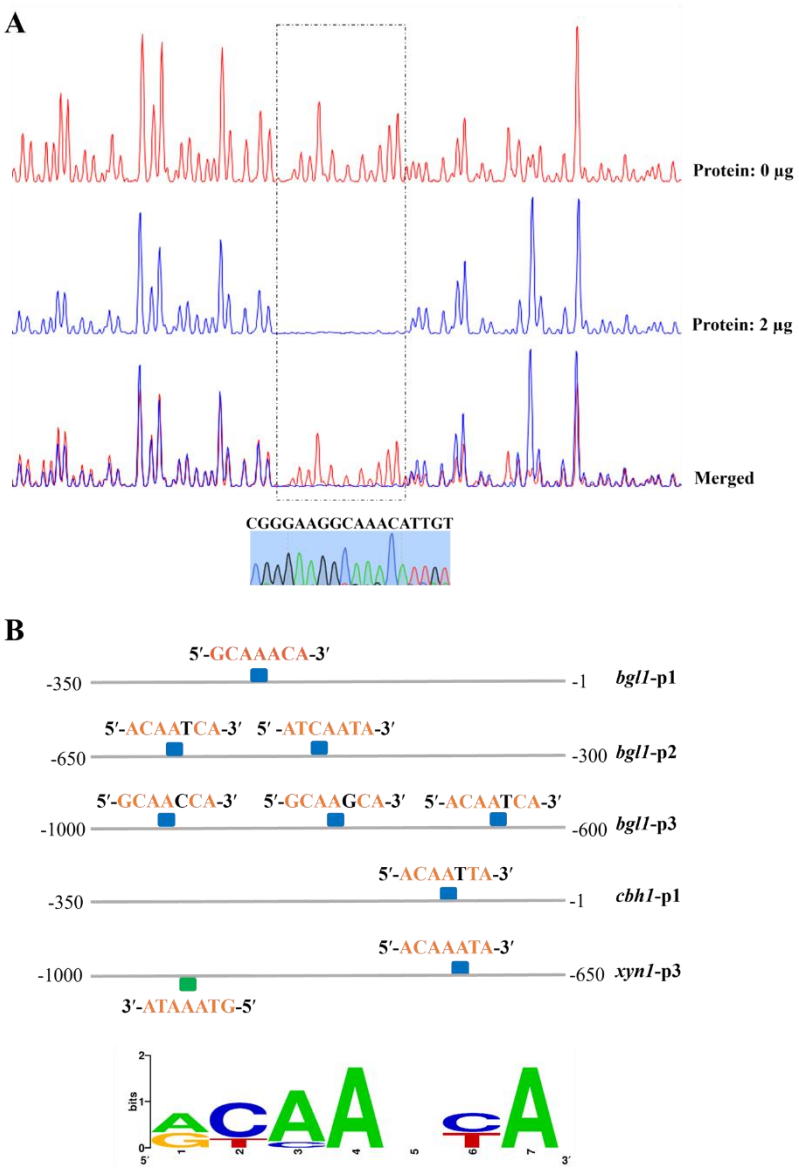

Figure 2.7. Identification of the sequence bound by MtFKH1 in the promoter regions of crucial cellulase and xylanase genes. (A) Identification of the MtFKH1-protected sequence in the bgl1 upstream region (bgl1-P1) by performing DNase I footprinting assay. The upper two-colored lines indicate the different amounts of MtFKH1 used: red, 0 μg; blue, 2 μg. The merged red and blue lines identify the DNA sequence protected from DNase I degradation, which is presented in dashed box. (B) Schematic diagram of the putatively conserved MtFKH1 binding motif in the promoter regions of *bgl1*, *cbh1*, and *xyn1*. Nucleotides in orange represent the identical, whereas that in black indicate the altered compared to the consensus 5′-RYMAAYA-3′. blue box, sense strand; green box, antisense strand.

2.4.10 Transcriptome analysis of the *Mtfkh1* deletion mutant

To comprehensively characterize the regulation of MtFKH1, transcriptional profiling analysis of the WT and Δ*Mtfkh1* strains cultured on Avicel for 48 h after transferring from glucose was conducted. Compared to the WT strain, Δ*Mtfkh1* displayed significantly changed transcription levels of 734 genes, with 221 genes being substantially upregulated and 513 genes being substantially downregulated. The GO analysis of the DEGs in Δ*Mtfkh1* showed that hydrolase activity (acting on glycosyl bonds), polysaccharide binding, and carbohydrate metabolic process were significantly enriched functional categories (Figure 2.8A), which was in accordance with the phenotypes detected in Δ*Mtfkh1* during the presence of cellulose. Comparative transcriptomic analysis revealed that 17 CAZyme-encoding genes exhibited significantly altered transcription levels in Δ*Mtfkh1* (Figure 2.8B), among which, two cellobiohydrolase genes including *cbh1*(*MYCTH_109566*) and *MYCTH_66729* were upregulated in Δ*Mtfkh1* compared with WT strain, which could explain the enhanced cellobiohydrolase activity in *Mtfkh1* deletion mutant. However, *MYCTH_42937* and *MYCTH_51545*, which also encode cellobiohydrolase, were downregulated in Δ*Mtfkh1*, indicating that the two cellobiohydrolase encoding genes might contribute less to the secreted enzyme. Similarly, the high expression of the three xylanase genes (*MYCTH_100068*, *MYCTH_52904*, *MYCTH_49824*) and low transcription of xylanase gene *MYCTH_99786* could be responsible for the improved xylanase production observed in Δ*Mtfkh1*. Moreover, three LPMO (AA9) encoding genes (*MYCTH_80312*, *MYCTH_46583*, and *MYCTH_100518*) showed higher transcript levels in Δ*Mtfkh1* than in the WT strain.

Besides CAZyme genes, expression levels of genes encoding putative transcription factors were also remarkably altered, with four genes being increased and fourteen genes being decreased in Δ*Mtfkh1*, the majority of which belong to Fungal Zn(II)2Cys6 and Zinc finger (C2H2) families (Figure 2.8C). All these TF-encoding genes are unidentified except for *MYCTH_2301920*, encoding an essential regulator AmyR for starch utilisation in *M. thermophila*, overexpression of which exhibited 30%

elevation in amylase activity (Xu et al., 2018).

Seven genes encoding sugar transporters were also observed showing markedly increased expression levels in Δ*Mtfkh1* relative to WT (Figure 2.8D). Among them, *MYCTH_2308157* and *MYCTH_112491* encode orthologs of high-affinity (HGT-1) and low-affinity glucose transporter (GLT-1), respectively (Wang et al., 2017). In *N. crassa*, individual deletion of *hgt-1* or *glt-1* showed less effect on cellulase expression (Wang et al., 2017). In contrast, a putative cellodextrin transporter protein CLP1-encoding gene *MYCTH_2302958* was downregulated in Δ*Mtfkh1*. CLP1 represses cellulase induction on both cellobiose and Avicel in *N. crassa*, although it cannot transport cellodextrin (Cai et al., 2015), suggesting that MtCLP-1 might also affect cellulase induction pathway.

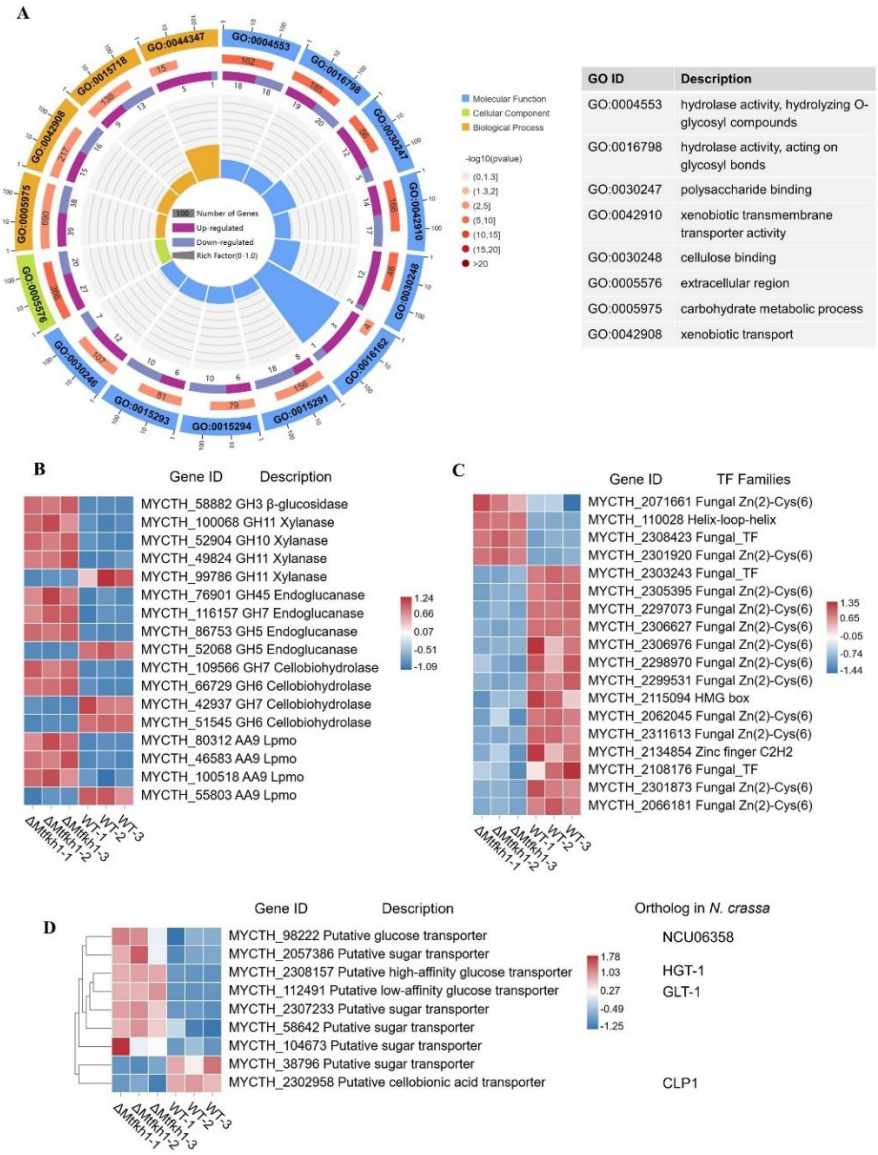

Figure 2.8. Transcriptional profiling analysis between WT and Δ*Mtfkh1* cultivated on Avicel for 48 h after a shift from glucose. (A) Functional enrichment of 734 DEGs in Δ*Mtfkh1* strain within the Molecular Function (MF), Cellular Component (CC), and Biological Process (BP) categories in GO analysis. The left circle diagram represents GO enrichment, from periphery to inner circle, the first circle, ID of GO term; the second circle, the number of genes of specific GO term in *M. thermophila* genome background, and p value; the third circle, the number of upregulated and downregulated genes of the given GO term in Δ*Mtfkh1* compared to that in WT strain; the innermost layer, rich factor, which corresponds of the proportion of DEGs in all background genes in a specific GO term. The right table lists the major enriched GO terms and corresponding descriptions. (B-D) Heatmap analysis of transcript levels for genes encoding CAZymes, putative TFs, and putative sugar transporters, respectively, between Δ*Mtfkh1* and WT during the presence of Avicel.

2.5 Discussion

In the present study, a novel transcription factor (MtFKH1) that negatively regulates cellulase and xylanase genes expression in *M. thermophila* was functionally characterized via comparative transcriptome and genetic analyses. These two approaches are regarded as highly-efficient approaches in screening novel TFs, as described in the characterisation of regulators HCR-1 in *N. crassa* (Li et al., 2014), PoxMBF1 in *P. oxalicum* (Zhao et al., 2019), TpRfx1 in *Talaromyces pinophilus* (Liao et al., 2018), and ACE4 in *T. reesei* (Chen et al., 2021). *M. thermophila* is a thermophilic fungus with significant potential for application in the conversion of plant biomass in biorefineries (Visser et al., 2011; Gu et al., 2023). In this study, transcriptional profiling was implemented on *M. thermophila* grown under different conditions (Avicel and glucose), and transcript levels of genes encoding transcription factors, CAZymes, sugar transporters and those involved in gluconeogenesis and TCA cycle were found to vary. Many CAZyme genes, including key cellulase, xylanase, and LPMO (AA9) genes, were highly induced by Avicel, indicating complex synergy between various enzymes involved in lignocellulose degradation. Specifically, eight novel candidate TFs showed remarkably different transcription levels between Avicel and glucose media and five of them were successfully deleted by the newly established CRISPR/Cas9 system, which led to the identification of a forkhead TF. Notably, the deletion of this nuclear localized transcription factor MtFKH1 dramatically increased cellulase and xylanase production, whereas the overexpression of MtFKH1 decreased cellulase and xylanase secretion under Avicel induction. This suggests that MtFKH1 is a repressor of cellulase and xylanase biosynthesis. Intriguingly, the endoglucanase activity was unaffected by the disruption of *Mtfkh1* (Figure S2.4), consistent with the expression level of the major endoglucanase genes. The transcription of three endoglucanase genes (*MYCTH_76901*, *MYCTH_116157* and *MYCTH_86753*) was elevated in Δ*Mtfkh1* compared to WT, whereas *MYCTH_52068*, that also encodes endoglucanase, was reduced, implying a self-equilibrating mechanism that tunes biosynthesis of cellulase. Overall, this study

provides a candidate target for fungal strain engineering to enhance cellulase and xylanase yields.

The forkhead regulator has been shown to participate in the regulation of cellulase and xylanase gene expression. In *P. oxalicum*, Δ*Pox08522* mutant showed an 81% increase in xylanase activity but a 72% decrease in β-glucosidase activity compared with the parent strain (Zhao et al., 2016). In this study, the regulatory roles of the forkhead proteins in cellulase and xylanase production in the filamentous fungus *M. thermophila* was further explained. Compared with the forkhead regulator Pox08522, the loss of *Mtfkh1* resulted in an enhancement in both cellulase and xylanase production, indicating the overlapping and divergent functions of forkhead regulators involved in lignocellulose degradation. Comparative transcriptomic analysis showed the pronounced upregulated expression of the cellobiohydrolase and xylanase genes in the Δ*Mtfkh1* mutant when cultivated in Avicel. Conversely, *cre1* and *xyr1*, which encode the major regulator of cellulase and/or xylanase, expressed no significant differences between the Δ*Mtfkh1* mutant and the WT strain, which was also confirmed by the RT-qPCR assay. Of note, the expression of β-glucosidase gene *bgl1* (*MYCTH_66804*) exhibited a 62 %-100 % increase in expression in Δ*Mtfkh*1 compared to WT according to RT-qPCR analysis. This observation was seen in the transcriptomic data, demonstrating a 41 % elevation (log2 fold change = 0.5), although not statistical significant. Comparative transcriptome profiling revealed upregulation of *bgl3* (*MYCTH_58882*), another gene encoding β-glucosidase, in the Δ*Mtfkh1* mutant

In addition, several sugar transporter-encoding genes exhibited altered expression levels (seven upregulated and two downregulated) in Δ*Mtfkh1*. In fungi, sugar transporters are closely associated with nutrient uptake and sense of molecular signals to suppress or activate lignocellulolytic enzyme induction, such as CDT-1/2 and CLP1 in *N. crassa* (Znameroski et al., 2014; Cai et al., 2015), and arabinose transporter MtLat-1 from *M. thermophila* (Gu et al., 2023). Whether the changed transcript levels of these sugar transporters are responsible for the high cellulase and xylanase activities in Δ*Mtfkh1* mutant remains to be further investigated. Moreover, eighteen genes

encoding transcription factors were also observed displaying markedly altered expression levels in Δ*Mtfkh1* compared to WT, the majority of which possess unknown functions. Consequently, the increased production of cellulase and xylanase by mutant Δ*Mtfkh1* may also be the result of the combined effects of these putative transcriptional regulators. Based on our current knowledge, Pox08522 and MtFKH1 are, to date, the only two forkhead transcription factors known to regulate cellulase and xylanase biosynthesis in filamentous fungi. This implies that other uncharacterized proteins from the forkhead family in different fungal species may also play similar roles, warranting further exploitation.

MtFKH1 belongs to the forkhead protein family, which is evolutionarily conserved based on its forkhead box DNA-binding domain (DBD), and it exists widely from fungi to mammals. Like other classic transcription factors of lignocellulolytic enzyme gene expression, our EMSA analysis indicated that MtFKH1 could bind to the promoter regions of the main cellulase and xylanase genes. Previous study revealed that forkhead regulatory proteins shared the consensus motif 5′-G/A T/C C/A A A T/C A-3′ in the promoter regions of target genes (Kaufmann et al., 1995). For instance, StFKH1 of *S. cerevisiae* was found to bind to 5′-RYAAACAWW-3′ (Zhu et al., 2000), and Trident in mouse (FoxM1 in human) was capable of binding to TAAACA site (Korver et al., 1997; Laoukili et al., 2007). The DNase I footprinting assay demonstrated that MtFKH1 bound to 5′-CGGGAAGGCAAACATTGT-3′ in *bgl1*-p1, which displayed highest binding capacity with MtFKH1 during EMSA analyses, sharing the core motif recognized by other forkhead family members. Comparisons of different promoter regions of major cellulolytic and xylanolytic genes contributed to the discovery that AANYA is highly conserved in the promoter regions of target genes except for one of the assumptive binding sites ATCAATA of *bgl1*-p2. Additionally, the binding motifs in the *bgl1*-p3 showed one nucleotide variation compared to that in *bgl1*-p1, although increased predicted binding sites were observed in the *bgl1*-p3, which may help to explain that higher binding affinity detected between MtFKH1 and *bgl1*-p1. Similarly, the potential binding sequence of MtFKH1 in *cbh1*-p1 exhibited a nucleotide alteration

relative to that in the *xyn1*-p3, which was consistent with the EMSA analysis that MtFKH1 prefer to bind to the promoter region of *xyn1*. These findings suggest that MtFKH1 directly regulates cellulase and xylanase production at the transcriptional level.

It has also been documented that forkhead proteins control cell development and morphogenesis. Knock-down of *Prfkh1* by RNAi (RNA interference) caused a 2.5-fold reduction in the number of spores compared with the control strain in *P. rubens*, although the hyphal morphology was unaffected (Dominguez-Santos et al., 2015). Likewise, deletion of *AnfkhB* displayed an impairment in conidiation under both light and dark conditions in *A. nidulans* (Jang et al., 2023). In *Magnaporthe oryzae*, loss of *Mofkh1* showed less effect on the number of conidia but resulted in decreased conidial germination compared to that of wild-type strain (Park et al., 2014). Also, deletion of both *fkh1* and *fkh2* exhibited pseudohyphal growth which was different from the nutritionally induced pseudohyphal phenotype in *S. cerevisiae* (Hollenhorst et al., 2000). The present study revealed that the Δ*Mtfkh1* mutant exhibited a 62% reduction in spore production compared with the WT, further supporting the involvement of forkhead regulators in controlling fungal strain development. In filamentous fungi, the fungal development is tightly correlated with the activity of fungal velvet family proteins and the secondary metabolism regulator LaeA (Yu et al., 2024). Our transcriptomic data reflected that two important genes *MYCTH_113912* and *MYCTH_2294559*, which are predicted to be involved in cellular spore formation process, were downregulated (log_2 fold change = -1.26 and -1.04, respectively) in Δ*Mtfkh1* mutant compared to the WT. MYCTH_113912 is the *M. thermophila* ortholog of the velvet family proteins velB in *A. nidulans* and vel2 in *T. reesei*. It was reported that velB in *A. nidulans* acts as a positive regulator of conidiation and deletion of *velB* caused decreased number of conidia, and reduced and delayed transcript levels of several crucial asexual regulatory genes (Park et al., 2012). Similarly, in *T. reesei*, loss of *vel2* (the velB ortholog) resulted in sharp reduction of sporulation as well as downregulated expression of two key conidiation genes (Karimi Aghcheh et al., 2013; Liu et al., 2016). In addition,

MYCTH_2294559 is orthologous to methyltransferase LaeA in *A. nidulans* and Lae1 in *T. reesei*. LaeA is a global regulator of secondary metabolism and participating in regulating growth, as well as sexual and asexual development in fungi (Bok and Keller, 2004; Karimi Aghcheh et al., 2013). The disruption of *lae1* substantially reduced sporulation, while overexpression of *lae1* resulted in increased sporulation in *T. reesei* (Seiboth et al., 2012). Likewise, LaeA is essential for the normal conidiation in *P. oxalicum*, as loss of which led to decreased levels of conidiation (Zhang et al., 2016). We, therefore, inferred that the decreased expression of genes encoding MtvelB and MtLaeA may cause sporulation defect in Δ*Mtfkh1* mutant.

The CRISPR/Cas9 genome editing is a powerful technique for accelerating in the manipulation of genes and pathways in fungal strains for manufacturing commodity chemicals and fuels with better yield (Pant et al., 2022; Shen et al., 2024). A CRISPR/Cas9 system was previously established in *M. thermophila*, generating multiple mutants with elevated lignocellulolytic enzymes production (Liu et al., 2017). In this study, we updated this system by integrating Cas9 protein and u6 promoter driven sgRNA in one expression vector, attempting to enhance the editing efficiency and make it labor-saving. We indeed obtained deletion strains for five potential regulatory genes, but the number of positive transformants differed. For example, two mutants for *MYCTH_2310243* were attained while only one stable mutant for MtFKH1 was gained. Moreover, three candidate TF genes failed to be disrupted by the CRISPR/Cas9 system, which was possibly due to the existence of lethal genes or inappropriate selection for protospacer sequences of target genes and/or low deletion efficacy of this CRISPR/Cas9 tool, indicating the genome editing system need to be further optimized to elevate the editing efficiency. Recently, new CRISPR/Cas12a and Base-Editing systems have been developed in *M. thermophila* (Liu et al., 2019d; Zhang et al., 2022), which should pave the way for identifying crucial regulators involved in plant biomass degradation and extend the toolkit for this fungal strain improvement.

Transcription factors play important roles in the regulation of cellulase and xylanase gene expression in filamentous fungi. In this study, we identified a novel

forkhead transcription factor, MtFKH1, for the first time, which represses the cellulase and xylanase gene expression in *M. thermophila*. The deletion of regulatory repressor genes is a common genetic manipulation strategy to improve the production of extracellular enzymes. For example, simultaneous disruption of *cre1* and *res-1* resulted in higher secreted protein production and increased cellulase and xylanase activities in *M. thermophila* (Liu et al., 2017). The novel regulator MtFKH1 adds to the growing list of transcription factors that regulate cellulolytic and xylanolytic gene expression in *M. thermophila*, and offers a potential target for fungal genetic engineering. In *M. thermophila*, nearly all identified transcription factors involved in regulating cellulase and/or hemicellulase production belong to either the zinc finger Zn2Cys6 type (Xyr1, Clr-2, Clr-4, Clr-5, Ara-1, AmyR) (Dos Santos Gomes et al., 2019; Gu et al., 2023) or the zinc finger C2H2 type (Cre1,TRC-1, Res-1) (Liu et al., 2017; Li et al., 2022a) except for Hac-1, which is a basic-leucine zipper (bZIP) DNA-binding protein (Li et al., 2022a). Thus, the characterisation of MtFKH1 suggests that transcriptional regulators from other families besides zinc finger types in this fungus may also merit attention in the context of lignocellulose deconstruction.

2.6 Conclusion

In summary, the data of this study revealed that a new forkhead transcription factor MtFKH1 negatively regulates the expression of key cellulase and xylanase genes by directly binding to their promoter regions and is involved in controlling sporulation. This work expands the novel functions of the forkhead proteins in the regulation of genes encoding lignocellulosic biomass-degrading enzymes including cellulase and xylanase in *M. thermophila*, and could be useful for engineering of fungal strains with elevated cellulase and xylanase production capacity.

2.7 Supplementary information

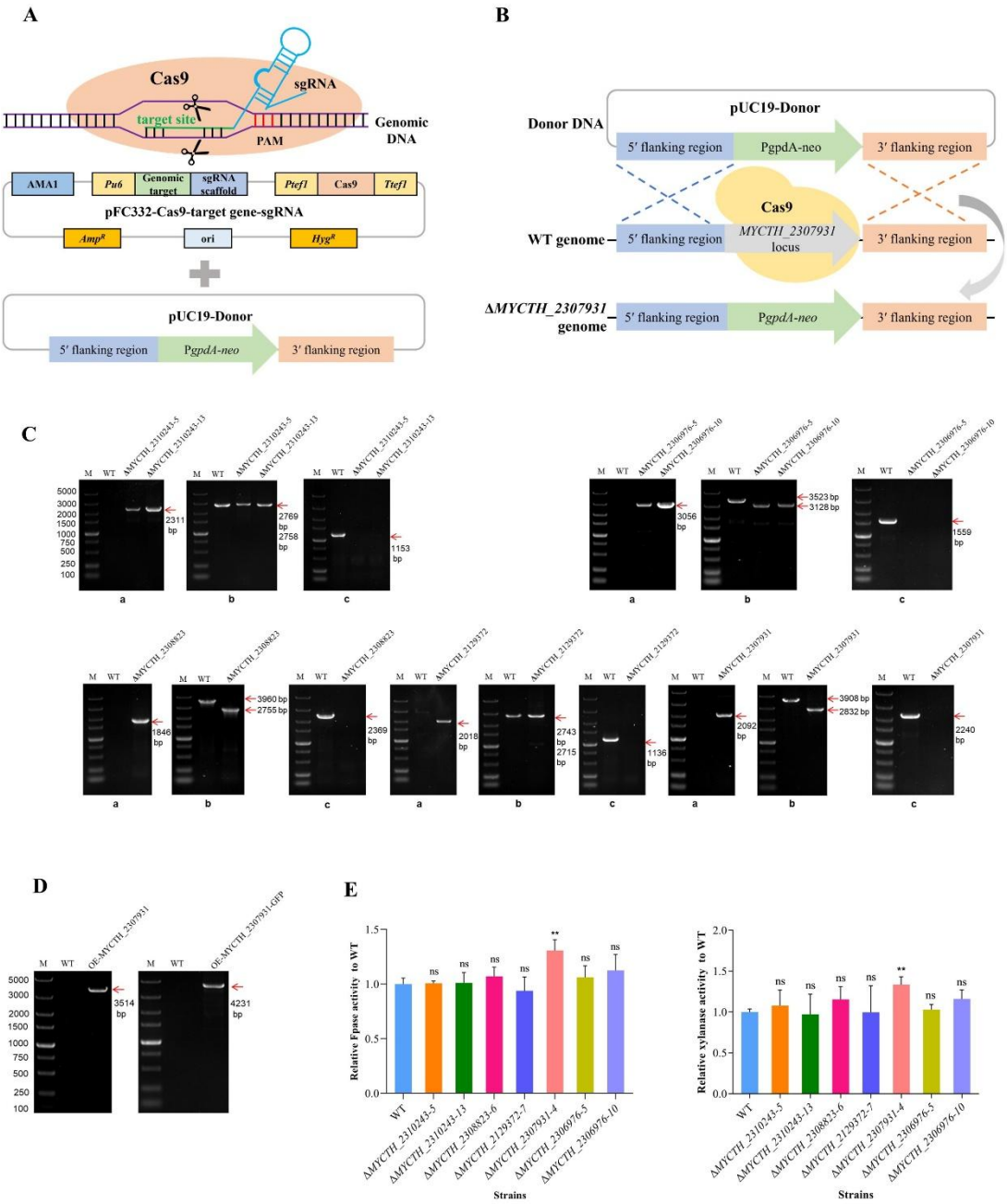

Figure S2.1. Characterisation of the MYCTH_2307931 regulator involved in cellulase and xylanase production in *M. thermophila*. (A) Establishment of the CRISPR/Cas9 system. The target site, 20 bp protospacer sequence; sgRNA, single chimeric guide RNA; PAM, protospacer adjacent motif. hyg, hygromycin B resistance gene; neo, G418 resistance gene. (B) Schematic of the deletion of MYCTH_2307931 through homologous recombination mediated by the CRISPR/Cas9 system. (C) PCR analysis for deletion strains of candidate regulatory genes. Primer 1-F locates in PgpdA-neo,

and Primer 1-R locates out of 3′ flanking region of target genes; Primer 2-F locates out of 5′ flanking region of target genes, and Primer 2-R is in 3′ flanking region; The primer pair 3 is used to amplify target genes. a, the primer pair 1; b, the primer pair 2; c, the primer pair 3; M, DL 5000 Marker; WT, *M. thermophila* wild type strain. (D) PCR analysis for MYCTH_2307931 overexpression and MYCTH_2307931-GFP fused expression strains. M, DL 5000 Marker; WT, *M. thermophila* wild type strain. (E) Filter-paper cellulase and xylanase activities of deletion strains of the candidate regulatory genes cultured on Avicel for 48 h after transferring from glucose. **$p < 0.01$ indicate significant differences between deletion strain and *M. thermophila* wild type (WT) strain (Student's t tests), ns indicate not significant. Error bars represent the SD from three replicates.

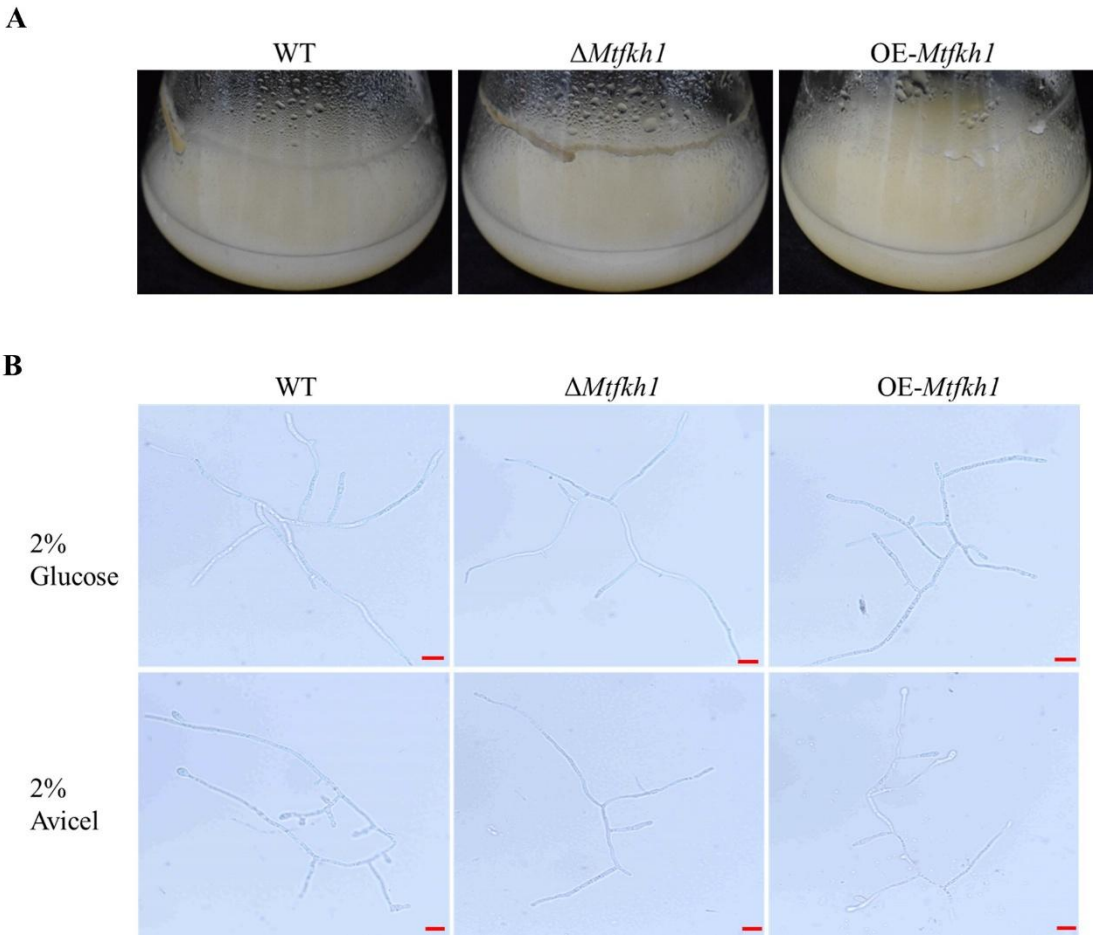

Figure S2.2. Growth observation and microscopic assessment of *M. thermophila* WT, Δ*Mtfkh1* and OE-*Mtfkh1* strains in liquid shake media. (A) Growth observation in liquid shake cultures containing 2% (w/v) glucose grown at 45°C for 36 h. (B) Microscopic investigation of mycelia collected from liquid media with 2% (w/v) glucose or 2% (w/v) Avicel cultivated at 45°C for 36 h. Scale bars = 10 μm

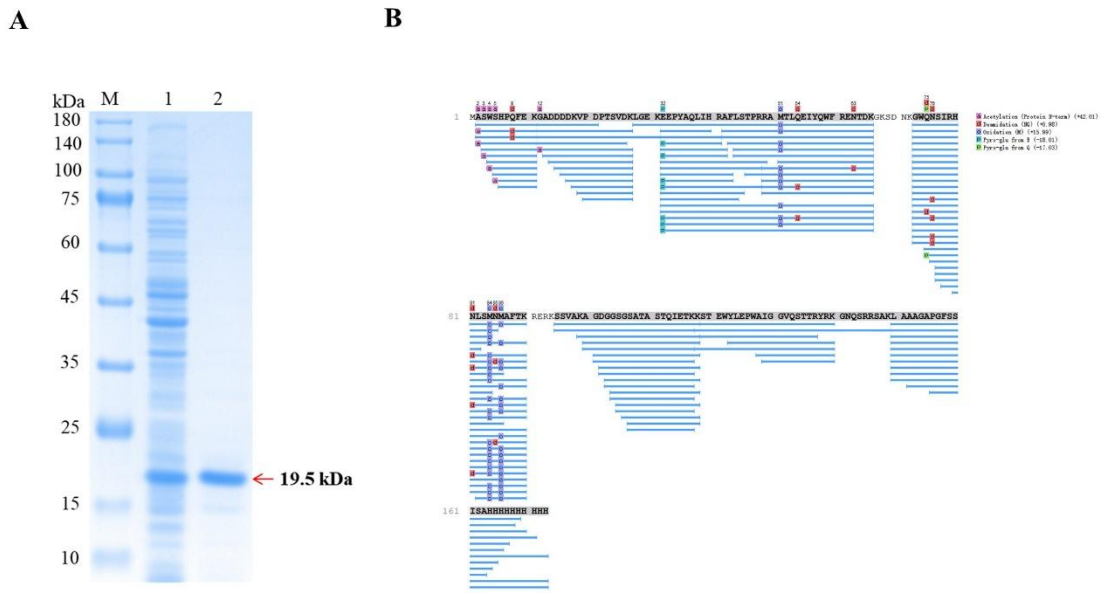

Figure S2.3. SDS-PAGE and LC-MS/MS analysis of purified MtFKH1$_{237-356}$ protein.(A) SDS-PAGE verification of purified MtFKH1$_{237-356}$. The samples were run on a 10% polyacrylamide gel. M, 10-180 kDa protein marker; Lane 1, crude protein; Lane 2, purified MtFKH1$_{237-356}$. (B) LC-MS/MS identification of target MtFKH1$_{237-356}$ protein. The target protein band on the gel was excited and subjected to LC-MS/MS with PEAKS Studio 8.5 system. The 94% of identified amino acids of target protein were mapped to theoretical amino acid residues of Strep II-MtFKH1$_{237-356}$ fused protein.

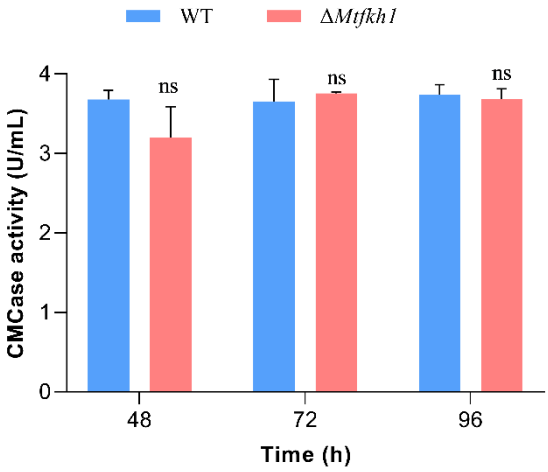

Figure S2.4. Endoglucanase (CMCase) activities of *M. thermophila* WT and Δ*Mtfkh1* strains. Culture supernatants were collected from fungal strains cultivated on Avicel for 48-96 h at 45°C after a shift from glucose. Ns indicates not significant between WT and Δ*Mtfkh1*(Two-way ANOVA). Error bars represent the SD from three replicates.

Table S2.1. List of PCR primers used in this study.

Construction of pFC332-Cas9-U6p-sgRNA scaffold vector		
synthesis of sgRNA scaffold	sgRNA scaffold-F	cctcTGTACAGTTTTAGAGCTAGAAATAGCAAGTTAAAATAAGGCTAGTCCGTTATCAACTTGAAAAAGTGGCACCGAGTCGGTGCTTTTTTT
	sgRNA scaffold-R	gtctcggctgaggtcttaattaaAAAAAAAGCACCGACTCGGTGCCACTTTTTCAAGTTGATAACGGACTAGCCTTATTTTAACTTGCTATTTCTAGCTCTAAAACTGTACA
Cloning of U6 promoter	U6p-F	gtttccgctgagggtttaattaaAGGATCGGTGGAGTGAAGTTCG
	U6p-R	gctctaaaactgtacaGAGGAAAGAAAGAAAAGAAGAGGAGG
Construction of pFC332-Cas9-U6p-target genes-sgRNA vectors		
Cloning of U6 promoter	U6p-F	gtttccgctgagggtttaattaaAGGATCGGTGGAGTGAAGTTCG
	U6p-MYCTH_2129372-R	GGCGCATGTGCCTCGCAGAAGAGGAAAGAAAGAAAAGAAGAGGAGG
	U6p-MYCTH_2310243-R	TCGACTAATGGACCGTGAGAGAGGAAAGAAAGAAAAGAAGAGGAGG
	U6p-MYCTH_2308823-R	GGTGTTGTGCATCGTAGCGCGAGGAAAGAAAGAAAAGAAGAGGAGG
	U6p-MYCTH_2306976-R	TGAACAGTCAGGCGCCCATAGAGGAAAGAAAGAAAAGAAGAGGAGG
	U6p-MYCTH_2307931-R	GTTGTGCAGGAGAGGCACAGGAGGAAAGAAAGAAAAGAAGAGGAGG
	U6p-MYCTH_2297579-R	GGCGCATAGTGCGTTGCGACGAGGAAAGAAAGAAAAGAAGAGGAGG
	U6p-MYCTH_2082522-R	CGAAGTGGGCGTATAGTAGCGAGGAAAGAAAGAAAAGAAGAGGAGG
	U6p-MYCTH_2302011-R	CTGGAACGGGAACGTCATTGGAGGAAAGAAAGAAAAGAAGAGGAGG
Cloning of target genes-sgRNA	g-MYCTH_2129372-F	TTCTGCGAGGCACATGCGCCGTTTTAGAGCTAGAAATAGCAAGTTAAAATAA
	g-MYCTH_2310243-F	TCTCACGGTCCATTAGTCGAGTTTTAGAGCTAGAAATAGCAAGTTAAAATAA
	g-MYCTH_2308823-F	GCGCTACGATGCACAACACCGTTTTAGAGCTAGAAATAGCAAGTTAAAATAA
	g-MYCTH_2306976-F	TATGGGCGCCTGACTGTTCAGTTTTAGAGCTAGAAATAGCAAGTTAAAATAA
	g-MYCTH_2307931-F	CTGTGCCTCTCCTGCACAACGTTTTAGAGCTAGAAATAGCAAGTTAAAATAA

	g-MYCTH_2297579-F	GTCGCAACGCACTATGCGCCGTTTTAGAGCTAGAAATAGCAAGTTAAAATAA
	g-MYCTH_2082522-F	GCTACTATACGCCCACTTCGGTTTTAGAGCTAGAAATAGCAAGTTAAAATAA
	g-MYCTH_2302011-F	CAATGACGTTCCCGTTCCAGGTTTTAGAGCTAGAAATAGCAAGTTAAAATAA
	gRNA-R	gtctcggctgaggtcttaattaaAAAAAAAGCACCGACTCGGTG
Construction of Donor DNA vectors		
MYCTH_2129372-upstream	MYCTH_2129372-up-F	tgcctgcaggtcgactctagaGTGCCTGGACCTGGAGCTG
	MYCTH_2129372-up-R	acgattcgaagccgcgCATTGCGGTGGTCTTCCG
Cloning of Pgpd-neo	MYCTH_2129372-neo-F	aatgCGCGGCTTCGAATCGTGG
	MYCTH_2129372-neo-R	aggctgagcTCAGAAGAACTCGTCAAGAAGGC
MYCTH_2129372-downstream	MYCTH_2129372-down-F	agttcttctgaGCTCAGCCTGCAGAGGGTATC
	MYCTH_2129372-down-R	ggtacccggggatcctctagaACGCAAGGCATAATGCCG
MYCTH_2310243-upsreeam	MYCTH_2310243-up-F	gaccatgattacgccaagcttGGAGTAGCAAGACGACATGTCCC
	MYCTH_2310243-up-R	attcgaagccgcgGTCTGATCCGCTTATCGCAGC
Cloning of Pgpd-neo	MYCTH_2310243-neo-F	atcagacCGCGGCTTCGAATCGTGG
	MYCTH_2310243-neo-R	ccgtgttgctcatacTCAGAAGAACTCGTCAAGAAGGC
MYCTH_2310243-downstream	MYCTH_2310243-down-F	tctgaGTATGAGCAACACGGCATTTGG
	MYCTH_2310243-down-R	aaaacgacggccagtgaattcCAGCGGCTAATGGTTGGCT
MYCTH_2308823-upstream	MYCTH_2308823-up-F	gaccatgattacgccaagcttTGCACCAGCTTGCACGGT
	MYCTH_2308823-up-R	attcgaagccgcgTGCGACTGACCGAGCGTC
Cloning of Pgpd-neo	MYCTH_2308823-neo-F	agtcgcaCGCGGCTTCGAATCGTGG
	MYCTH_2308823-neo-R	ggacaccttTCAGAAGAACTCGTCAAGAAGGC

MYCTH_2308823-downstream	MYCTH_2308823-down-F	gttcttctgaAAGGGTGTCCCAAGGATGAAG
	MYCTH_2308823-down-R	aaaacgacggccagtgaattcTATATGATTCGGTACCCCCGG
MYCTH_2306976-upstream	MYCTH_2306976-up-F	gaccatgattacgccaagcttCCGGAGGGTGGTCGGGTT
	MYCTH_2306976-up-R	aagccgcgGGCTTGGGATGTGGATGCG
Cloning of Pgpd-neo	MYCTH_2306976-neo-F	acatcccaagccCGCGGCTTCGAATCGTGG
	MYCTH_2306976-neo-R	acttccggcaTCAGAAGAACTCGTCAAGAAGGC
MYCTH_2306976-downstream	MYCTH_2306976-down-F	gttcttctgaTGCCGGAAGTGAAATGAAGTG
	MYCTH_2306976-down-R	aaaacgacggccagtgaattcGGCCATTCCTGTTGCGGG
MYCTH_2307931-upstream	MYCTH_2307931-up-F	gaccatgattacgccaagcttCACAGCGACCGCCGATGA
	MYCTH_2307931-up-R	acgattcgaagccgcgCTCCGCGGCGGCTTTCGC
Cloning of Pgpd-neo	MYCTH_2307931-neo-F	ggagCGCGGCTTCGAATCGTGG
	MYCTH_2307931-neo-R	ctccaccacaTCAGAAGAACTCGTCAAGAAGGC
MYCTH_2307931-downstream	MYCTH_2307931-down-F	gttcttctgaTGTGGTGGAGTTGGCCGTT
	MYCTH_2307931-down-R	aaaacgacggccagtgaattcCAGAGTGCCGAAAACGTCCG
MYCTH_2297579-upstream	MYCTH_2297579-up-F	gaccatgattacgccaagcttACGAGTGTGCAAGAAATTCCG
	MYCTH_2297579-up-R	attcgaagccgcgGCTTGCTGGGGGATGATGG
Cloning of Pgpd-neo	MYCTH_2297579-neo-F	agcaagcCGCGGCTTCGAATCGTGG
	MYCTH_2297579-neo-R	ggaagcctcaagcttcaaTCAGAAGAACTCGTCAAGAAGGC
MYCTH_2297579-downstream	MYCTH_2297579-down-F	gaTTGAAGCTTGAGGCTTCCTCG

	MYCTH_2297579-down-R	aaaacgacggccagtgaattcTTTAACGAGCAGCGTTGC
MYCTH_2082522-upstream	MYCTH_2082522-up-F	gaccatgattacgccaagcttCGTTTCAAGCCTGACTACCTTACC
	MYCTH_2082522-up-R	gGATTGCGACAACGTTGTCTAGG
Cloning of Pgpd-neo	MYCTH_2082522-neo-F	agacaacgttgtcgcaatcCGCGGCTTCGAATCGTGG
	MYCTH_2082522-neo-R	gaactctTCAGAAGAACTCGTCAAGAAGGC
MYCTH_2082522-downstream	MYCTH_2082522-down-F	cgagttcttctgaAGAGTTCTCAAATAGGTGCTGGAGG
	MYCTH_2082522-down-R	aaaacgacggccagtgaattcGCACCACCACAGGCCCAA
MYCTH_2302011-upstream	MYCTH_2302011-up-F	gaccatgattacgccaagcttGGCGCTGTGGGTCGTGGG
	MYCTH_2302011-up-R	aagccgcgGATTACGAACAAGTAGCGAAAGTAGAA
Cloning of Pgpd-neo	MYCTH_2302011-neo-F	ttgttcgtaatcCGCGGCTTCGAATCGTGG
	MYCTH_2302011-neo-R	tagtgcgcagTCAGAAGAACTCGTCAAGAAGGC
MYCTH_2302011-downstream	MYCTH_2302011-down-F	gttcttctgaCTGCGCACTATTTCGCCTTT
	MYCTH_2302011-down-R	aaaacgacggccagtgaattcAATGGTCTTAATGTTCAAGCCAGA
Construction of pUC19-Ppdc-hph plasmid		
Cloning of Ppdc	Ppdc-F	gaccatgattacgccaagcttCCGAGTGTACTCCGTAAGGAGG
	Ppdc-R	aagggaattcTCTAGAGCGGCTGTATACCGC
Cloning of PgpdA-hph	PgpdA-hph-F	ccgctctagaGAATTCCCTTGTATCTCTACACACAGG
	PgpdA-hph-R	cgaatgtccgcCTATTCCTTTGCCCTCGGACG
Cloning of Ttef1	Ttef1-F	aaggaatagGCGGACATTCGATTTATGCC
	Ttef1-R	aaaacgacggccagtgaattcGTATTGGGATGAATTTTGTATGCAC
Construction of pUC19-Ppdc-TgpdA-hph plasmid		
Cloning of Ppdc	Ppdc-F	gaccatgattacgccaagcttCCGAGTGTACTCCGTAAGGAGG

	Ppdc-R	cgatTCTAGAGCGGCTGTATACCGC
Cloning of TgpdA	TgpdA-F	atacagccgctctagaATCGGTCGGCCCCCCCCT
	TgpdA-R	gatacaagggaattcGGCCAATTAATTAATTCATCAGGG
Cloning of hph cassette	hph-F	tggccGAATTCCCTTGTATCTCTACACACAGG
	hph-R	aaaacgacggccagtgaattcGTGCATACAAAATTCATCCCAATAC
Construction of MYCTH_2307931 overexpression vector		
Cloning of MYCTH_2307931	MYCTH_2307931-F	tcgccaacaacagacgcggccgcATGGCGGTCATATCCACCATG
	MYCTH_2307931-R	ggggggccgaccgattctagaTCAGTACCCCTGTGCTTGCC
Construction of MYCTH_2307931-GFP expression vector		
Cloning of MYCTH_2307931	MYCTH_2307931-F	tcgccaacaacagacgcggccgcATGGCGGTCATATCCACCATG
	MYCTH_2307931-R	ttgctcaccatGTACCCCTGTGCTTGCCCA
Cloning of GFP	MYCTH_2307931-GFP-F	caggggtacATGGTGAGCAAGGGCGAGG
	GFP-R	ggggggccgaccgattctagaTCACTTGTACAGCTCGTCCATGCC
PCR analysis of gene deletion and overexpression in *M. thermophila* strains		
PCR detecting MYCTH_2129372 deletion	neo-in-F	CAGCCCGATTTCCATTCCT
	MYCTH_2129372-out-R	GCTCTGCGTCGCTTCTTGT
	MYCTH_2129372-out-F	GGCATCCCATAATAACCCTCA
	MYCTH_2129372-in-R	CGCCTACCTCGGAATCACCTA
	MYCTH_2129372-F	CGGAAAGTGGTGCTATTGGG
	MYCTH_2129372-R	GGAGGGAATCTGCCATCGT
PCR detecting MYCTH_2310243 deletion	neo-in-F	TCACTGAAGCGGGAAGGGACT
	MYCTH_2310243-out-R	CGGATGAAAGCGTTAAGTAAGC

	MYCTH_2310243-out-F	TTTTGACTGAAAGTCGAGGCG
	MYCTH_2310243-in-R	AAGGGCACTGGTAAGAATGAAG
	MYCTH_2310243-F	CTTTCCCGAACGGCACCTC
	MYCTH_2310243-R	CTGGCACGCTTCCAACTCC
PCR detecting MYCTH_2308823 deletion	neo-in-F	ACTGGGCACAACAGACAATC
	MYCTH_2308823-out-R	CTACGGGAGAAGGAAGAAGAG
	MYCTH_2308823-out-F	CAGGGCCGTGTCGTCGATCAGT
	MYCTH_2308823-in-R	CCGTAGCCGCCGAGAAGGTAT
	MYCTH_2308823-F	GCTCCTTCGCCCTTCGCTAC
	MYCTH_2308823-R	GGATTCCGCTCGGTTGTCG
PCR detecting MYCTH_2306976 deletion	neo-in-F	TTGGCCGAGGTTGCGATTTCT
	MYCTH_2306976-out-R	GCGACAGCAGGGTGCGATACA
	MYCTH_2306976-out-F	CGACCAAGTACCCGAGCCAGTT
	MYCTH_2306976-in-R	TTCCGTTACCGAGTTGATCCTTTA
	MYCTH_2306976-F	ATGGGAACTGCGTCATCGC
	MYCTH_2306976-R	TCAACCAGCTCCGCACCG
PCR detecting MYCTH_2307931 deletion	neo-in-F	TTACCACCTGCTCATCACCTTT
	MYCTH_2307931-out-R	GCTCCGTTGCTGATCCTACAC
	MYCTH_2307931-out-F	CGGCGGGAAATGACAATAGCA
	MYCTH_2307931-in-R	CCGGAGCAAGACCAAGGAAAA
	MYCTH_2307931-F	ATGGCGGTCATATCCACCATG
	MYCTH_2307931-R	TCAGTACCCCTGTGCTTGCC

PCR detecting MYCTH_2307931 overexpression and MYCTH_2307931-GFP fused expression	Ppdc-F	CGGTTACGGAAACGGAAAG
	PgpdA-R	CAGCCAACTGCAAACAGAATA
RT-qPCR analysis		
RT-qPCR of bgl1	RT-q-bgl1-F	AGCCAGGAGAATGGTAACGC
	RT-q-bgl1-R	TGACAGCCCAAACCCAAACT
RT-qPCR of cbh1	RT-q-cbh1-F	GCGGTAACTCCCTGAACCTC
	RT-q-cbh1-R	AAGTAGAGGGCGCCATTGAG
RT-qPCR of xyn1	RT-q-xyn1-F	CATGAAGTGGGATGCTACTGAGCC
	RT-q-xyn1-R	CGATGACCGAGGTGAGCGAGT
RT-qPCR of cre1	RT-q-cre1-F	GAATCTTCCCCCGCCGCTCAG
	RT-q-cre1-R	CTCGCCAACATTGCCACATCC
RT-qPCR of xyr1	RT-q-xyr1-F	ATGGATGATACCGATTACCAGAACG
	RT-q-xyr1-R	TGGGAGGAAGTAGCCAAAGATGC
RT-qPCR of actin	RT-q-actin-F	AACGCTCCTGCCTTCTAC
	RT-q-actin-R	GTAACACCATCACCAGAGTC
Construction of pET-51b-MtFKH1237-356 plasmid		
Cloning of MtFKH1237-356 encoding gene	MtFKH1237-356-F1	ccgacgtcggtcgacaagcttGGGGAAAAGGAGGAGCCG
	MtFKH1237-356-R1	tggtgaaggcCATGTTCATGCTTAGATTATGCCG
	MtFKH1237-356-F2	catgaacatgGCCTTCACCAAGCGGGAG
	MtFKH1237-356-R2	agctcctgcggccgcaagcttGGCGCTGCGCCGGGATTG
The obtain of probes for EMSAs		

PCR amplification of bgl1-P1	bgl1-P1-F	CACCCCAGCTTCCTAGCCTC
	bgl1-P1-R	GATGGGCGACGTCTCGTATC
PCR amplification of bgl1-P2	bgl1-P2-F	CGCTCAGCGTGACATCCG
	bgl1-P2-R	GTGGGAAAATCTTCTTGCGCG
PCR amplification of bgl1-P3	bgl1-P3-F	CACAGTTTGTTGTGTTTCATGGG
	bgl1-P3-R	TCTTGTGATTGTCGGGTTCGG
PCR amplification of cbh1-P1	cbh1-P1-F	ATCATTCGATGGCTGACTGGC
	cbh1-P1-R	GGCGGAAGAGGATCAGCAC
PCR amplification of xyn1-P3	xyn1-P3-F	CTGGGTTAACCAGCCCGTATT
	xyn1-P3-R	ACAGACGGATTGATGCCATGC
PCR amplification of xyr1-P1	xyr1-P1-F	ATGCTATTCTCGCATCTCCCTAA
	xyr1-P1-R	CTTGGACCGGAGATGGAGATATG

Note: The lowercase nucleotides represent homologous arm fragments for constructing corresponding vectors.

Table S2.2. The clean reads and mapping rate for RNA sequencing when *M. thermophila* grown on Avicel (A-RNA) and Glucose (G-RNA).

Sample	Clean reads	Clean rate (%)	Mapping rate
A-RNA-1	33631674	89.87	92.59%
A-RNA-2	34501063	97.28	93.94%
A-RNA-3	23410147	96.21	92.06%
G-RNA-1	24558453	96.12	92.83%
G-RNA-2	29388637	97.39	93.82%
G-RNA-3	27789873	95.95	92.47%

Chapter 3 Dual Role of MtHAC-1 in Regulating Cellulase and Xylanase Production in *Myceliophthora thermophila*

The content of this chapter has been published as

Yapeng Lai., Juan Wang., Ning Xie., Gang Liu., Donnabella Lacap-Bugler., **2025**. Dual Role of MtHAC-1 in regulating cellulase and xylanase production in *Myceliophthora thermophila*. Microbial Biotechnology, 18(8), e70203. https://doi.org/10.1111/1751-7915.70203

3.1 Prelude

In Chapter 2, a CRISPR/Cas9-mediated gene deletion system was developed in *M. thermophila*, providing a versatile tool for functional genomics, which enabled the elucidation of the regulatory role of the forkhead transcription factor MtFKH1. In addition, comparative transcriptomic analysis of *M. thermophila* cultivated on Avicel and glucose revealed that the gene encoding the bZIP TF MtHAC-1 (MYCTH_2310995) exhibited a significantly decreased expression on Avicel, indicating its potential involvement in lignocellulose utilisation. In this chapter, the same gene manipulation and molecular genetic approaches were used showing MtHAC-1 exhibiting dual regulatory effects on the production of cellulase and xylanase in *M. thermophila*, which was not previously reported. Moreover, MtHAC-1 was found to directly bind to the promoter regions of key cellulase and xylanase genes, as well as one important regulatory gene (*Mtxyr1*). MtHAC-1 also participates in the regulation of 26S proteasome-encoding genes under cellulolytic conditions. This is the first study of the dual role of MtHAC-1 in cellulolytic and xylanolytic enzyme production, providing novel insights into the regulatory mechanisms underlying cellulase and xylanase gene expression. Findings from this study offer potential strategies for fungal strain engineering in biorefinery applications.

3.2 Introduction

Lignocellulosic biomass is mainly composed of cellulose (40-50%), hemicellulose (25-30%) and lignin (15-20%), represents the most abundant renewable resource on Earth that can be transformed into biofuels and value-added biochemicals (Gupta et al., 2016). Cellulose is frequently found intermingled with xylan, the primary component of hemicellulose, to form a heterogenous complex of carbohydrate polymers (Taha et al., 2016; Xu et al., 2023). Therefore, the decomposition of xylan is considered to significantly enhance the accessibility of cellulose to cellulases, thereby boosting the overall efficiency of lignocellulose degradation (Bajaj and Mahajan, 2019; Xu et al., 2023). The degradation of cellulose needs a synergistic manner of complex cellulase components, which depolymerize cellulose into glucose that can be fermented by microbes to generate biofuels such as bioethanol (Bhardwaj et al., 2021; Zhao et al., 2024b). Like cellulose, hydrolysis of xylan requires a cooperative action of multiple xylanolytic enzymes (Bernardi et al., 2021). Generally, endo-1,4-β-D-xylanase (EC 3.2.1.8) is recognized as the key enzyme that acts on xylan backbone to release xylo-oligosaccharides and xylose, which possess potential industrial applications (Mendonca et al., 2023).

Filamentous fungi are the primary contributors to the depolymerization of lignocellulose by producing an assortment of extracellular hydrolases, including cellulase and xylanase (Mattam et al., 2022). Several well-studied fungi, such as *Trichoderma reesei*, *Penicillium oxalicum*, *Neurospora crassa*, and *Myceliophthora thermophila*, have been utilized as cell factories to produce lignocellulolytic enzymes (Liu and Qu, 2019; Zhang et al., 2020). Among these, the thermophilic fungus *M. thermophila* is receiving attention due to its capability to secrete large amounts of thermostable carbohydrate-active enzymes (CAZymes) involved in the breakdown of lignocellulosic biomass (Berka et al., 2011; Singh, 2016). The *M. thermophila* C1 strain has been developed as a platform to produce diverse industrially important enzymes for cost-efficient applications (Visser et al., 2011). Recently, *M. thermophila* was

genetically engineered to generate valuable enzymes and chemicals, such as cellulase, malic acid and succinic acid, based on the multi-omics analysis and genome-editing technique (Liu et al., 2019d; Li et al., 2020b; Gu et al., 2023). However, the production levels of lignocellulose degrading enzymes in this fungus are much lower as compared to the more commonly used mesophilic counterparts such as species of *Trichoderma* and *Aspergillus* (Berka et al., 2011).

Biosynthesis of cellulase and xylanase in filamentous fungi is regulated by a variety of transcription factors (TFs) (Benocci et al., 2017; Zhao et al., 2024a). A few transcriptional regulators have been identified to be involved in controlling cellulase and/or xylanase gene expression in *M. thermophila*. MtXyr1 is the principal activator of genes encoding xylan-degrading enzymes, as well as those related to pentose transport and catabolism (Dos Santos Gomes et al., 2019). Overexpression of MtXyr1 elevated xylanase production in both glucose and corncob-containing media but showed less impact on cellulase activity (Wang et al., 2015). In contrast to MtXyr1, MtCre1 serves as an essential repressor of cellulolytic enzyme biosynthesis. RNA interference of *Mtcre1* resulted in improved cellulase production and upregulated transcript levels of cellulase genes when cultured in inducing medium (Yang et al., 2015). It was previously documented that MtClr-4 acts as a pivotal regulator for (hemi-)cellulase gene expression through regulating the expression of the crucial transcriptional activators MtClr-2 and MtXyr1 (Liu et al., 2019c). In addition, a Zn2Cys6 transcription factor MtClr-5 was found to be important for cellulose degradation, as the *MtClr-5* disruption mutant exhibited reduced protein secretion and endoglucanase activity, compared to *M. thermophila* parental strain during growth on Avicel (microcrystalline cellulose) (Xue et al., 2023). However, despite *M. thermophila* possessing a relatively higher number of xylanase-encoding genes (Karnaouri et al., 2014), the number of identified transcription factors associated with the xylanolytic enzyme system remains lower than that in the well-known lignocellulolytic fungus *T. reesei*. This implies a substantial potential to uncover additional regulators involved in xylan degradation. Moreover, the regulatory mechanisms of the expression of

cellulolytic and xylanolytic genes in *M. thermophila* remain largely unknown (Dos Santos Gomes et al., 2019; Li et al., 2022a). Understanding these regulatory mechanisms would facilitate fungal strain engineering for the hyperproduction of cellulase and xylanase in *M. thermophila*.

A special feature of filamentous fungi is the highly efficient enzyme secretion capacity, which enables them to degrade plant derived polymers in their natural habitat to support cellular growth (Pakula et al., 2003; Sakekar et al., 2021). During the lignocellulolytic response, newly synthesized glycoside hydrolases are sent to the endoplasmic reticulum (ER) to be folded and modified for secretion (Huberman et al., 2016). When misfolded proteins accumulate in the ER, a condition termed as ER stress, which activates the unfolded protein response (UPR) pathway, triggering a gene expression program that coordinates the protein-folding machinery to mitigate the stress (Hetz and Papa, 2018; Yao et al., 2023). In filamentous fungi, such as *T. reesei*, *Aspergillus nidulans*, *Aspergillus niger*, and *N. crassa*, the UPR pathway is mediated by the transcription factor HacA/Hac1/Hac-1 (Saloheimo et al., 2003; Mulder and Nikolaev, 2009; Montenegro-Montero et al., 2015). It was reported that growth of *N. crassa* on Avicel imposed high demands on ER function (Montenegro-Montero et al., 2015), and lack of *hac-1* caused a reduction in cellulase secretion capacity (Fan et al., 2015). Also, the Δ*hac-A* strain of *Aspergillus oryzae* showed markedly downregulated expression of amylolytic enzymes in response to ER stress (Zhou et al., 2016). Additionally, the expression of *hac-1*/*hacA* is highly induced in *N. crassa* and *A. nidulans*, respectively, during growth on cellulose (Brown et al., 2013; Fan et al., 2015). However, transcriptome profiling of *M. thermophila* cultivated in Avicel and glucose media revealed that the transcript level of *Mthac-1* (MYCTH_2310995, an ortholog of HacA/Hac-1) was down-regulated in response to Avicel (Lai et al., 2025), suggesting that Mthac-1 may play a distinct role in lignocellulose deconstruction. Therefore, we decided to investigate the role of MtHac-1 in the expression of lignocellulolytic enzyme genes of *M. thermophila* in more detail to provide the basic knowledge required for targeted strain improvement.

In this study, we investigated the function of MtHac-1 by gene deletion and overexpression, growth phenotype analysis, electrophoretic mobility shift assays (EMSAs), and comparative transcriptomic analysis. We demonstrate that MtHac-1 positively regulates cellulase and xylanase activity in the early stage of cultivation under cellulose but inhibits their production during the middle and late culture phases. This TF modulates the expression of major cellulase and xylanase genes, as well as the regulatory gene *Mtxyr1*, by directly binding to their promoter regions. We also show that MtHac-1 is essential for normal hyphal development and sporulation. In addition, MtHac-1 is involved in mediating the proteasome degradation system.

3.3 Materials and Methods

3.3.1 Strains and culture conditions

Myceliophthora thermophila (ATCC 42464) and its mutants were grown on potato dextrose agar (PDA) plates at 45℃ for 7 days to produce mature conidia. For DNA extraction, mature conidia of *M. thermophila* strains were inoculated in 50 mL Mandels medium containing 2% (w/v) glucose as the carbon source as previously described (Lai et al., 2025) and cultured at 45°C for 36 h. For enzymatic activity, RT-qPCR, and RNA-seq analyses, the spores (approximately 5×10^7) of *M. thermophila* strains were initially grown in 50 mL Mandels medium containing 2% (w/v) glucose at 45°C with shaking at 150 rpm. After 36 h of incubation, the mycelia were washed with the Mandels medium (without carbon source) and an equal amount of wet mycelia (0.55 g) was transferred to 50 mL Mandels medium with 2% (w/v) Avicel (Sigma-Aldrich, St. Louis, MO, USA) for continued culture for 48-96 h (Lai et al., 2025). The investigation of colony morphology and conidiation on solid plates, as well as growth observation in liquid culture, were performed as previously described (Lai et al., 2025). The number of spores was counted using hemocytometer after 7 days of incubation. The fungal mycelia in liquid culture were either used for shake-flask study or harvested and subjected to a light microscope.

Escherichia coli DH5α cells were used for plasmid manipulation and propagation and were cultivated at 37℃ in Luria-Bertani (LB) medium containing ampicillin (100 μg mL^{-1}).

3.3.2 Plasmid construction

All primer sequences used in this study are listed in Table S3.1. For the deletion of *Mthac-1* using the CRISPR/Cas9 system, the Cas9-U6p-*Mthac-1*-sgRNA expression cassette was constructed as previously reported (Lai et al., 2025). In brief, the *M. thermophila* U6 promoter, and the protospacer sequence that fused with sgRNA scaffold were amplified from pFC332-Cas9-U6p-sgRNA scaffold vector and cloned into pFC332 vector, which generated the corresponding plasmid Cas9-U6p-*Mthac-1*-sgRNA. Approximately 1 kb of 5′ and 1.5 kb of 3′ flanking fragments of *Mthac-1* were amplified from *M. thermophila* genomic DNA. The two resultant PCR sequences were fused with the G418-resistance cassette P*gpd-neo* amplified from plasmid pBC-*neo* (Li et al., 2020d), and inserted into the HindIII and EcoRI sites of pUC19 plasmid using One Step Cloning Kit (Vazyme Biotech, Nanjing, China) to generate donor-*Mthac-1-neo* vector.

For overexpression of *Mthac-1*, the *Mthac-1* coding region (unspliced form) was amplified from genomic DNA using *Mthac-1*-F/R primer set, which was then ligated into the NotI and XbaI sites of pUC19-P*pdc*-T*gpdA-hph* plasmid (Lai et al., 2025), under the control of the strong constitutive *Mtpdc* (MYCTH_112121, pyruvate decarboxylase) promoter.

3.3.3 *Myceliophthora thermophila* transformation

Protoplast preparation and transformation of *M. thermophila* was performed as previously described (Lai et al., 2025). Positive transformants were selected based on resistance to neomycin and hygromycin B (75 μg mL^{-1} hygromycin B combined with 100 μg mL^{-1} G418) or solely hygromycin B (75 μg mL^{-1}) after 4-5 days of culture. Successful transformants were further confirmed through genomic PCR analysis and

sequencing using different specific primer pairs (Table S3.1).

3.3.4 Total DNA and RNA extraction

Total fungal DNA and RNA were extracted from fresh mycelia collected from corresponding liquid culture via vacuum filtration. The harvested mycelia were mechanically ground into fine power in liquid nitrogen for the subsequent use. The DNA and RNA were extracted using fungal DNA extraction kit (Sangon Biotech, Shanghai, China) and RNA extraction kit TransZol Up (TransGen Biotech, Beijing, China), respectively, according to the manufacturer's instructions. Agarose gel electrophoresis and a NanoDrop 2000 Spectrophotometer (Thermo Scientific, Waltham, MA, USA) were used to evaluate the quality and quantity of the DNA and RNA.

3.3.5 Real-time quantitative PCR

The HiScript III RT SuperMix kit (Vazyme Biotech, Nanjing, China) was employed to synthesize cDNA from RNA following the manufacturer's protocols. Each PCR was performed in a 20 μL reaction mixture containing 10 μL of Hieff UNICON Universal Blue qPCR SYBR Green Master Mix (Yeasen Biotech, Shanghai, China), 0.4 μL of 10 μM forward primer, 0.4 μL of 10 μM reverse primer (Table S3.1), 2.0 μL of diluted cDNA, and 7.2 μL of sterile water. The thermocycler was as follows: initial denaturation for 2 min at 95 °C, followed by 40 cycles of 5 s at 95 °C and 20 s at 63 °C. The relative expression level of each gene was calculated by the comparative $2^{-\Delta\Delta CT}$ method (Livak and Schmittgen, 2001) with the *actin* gene (*MYCTH_2314852*) of *M. thermophila* as an endogenous control.

3.3.6. Transcriptome analysis

The total RNA isolated from the wild type and Δ*Mthac-1* strains of *M. thermophila* cultured on 2% (w/v) Avicel for 48 h after shift from glucose was utilized for RNA-seq on the Illumina Novaseq6000 platform by Gene Denovo Biotechnology Corporation (Guangzhou, China). The generated high-quality reads were mapped to the genome

sequence of *M. thermophila* ATCC 42464 using HISAT2. v2.4 (Kim et al., 2015). The expression abundance (FPKM, fragment per kilobase of transcript per million mapped reads) of each gene was calculated by the RSEM software (Li and Dewey, 2011). DESeq2 was employed for analysis of differential gene expression with thresholds of absolute fold change > 2 and adjusted *p*-value (padj) < 0.05 (Love et al., 2014). Gene Ontology (GO) enrichment assay was performed using the OmicShare tools (https://www.omicshare.com/tools). All differentially expressed genes (DEGs) were mapped against GO terms in the Gene Ontology database (http://www.geneontology.org/). GO terms with *p*-value < 0.05 were considered significantly enriched compared with the *M. thermophila* genome background using hypergeometric test. The raw reads of transcriptome data have been deposited in the Gene Expression Omnibus (accession number: GSE290641) at the National Center for Biotechnology Information (NCBI).

3.3.7 Protein and enzyme activity assays

Samples of crude enzyme were collected at the indicated time for the analyses of extracellular enzyme activity. The protein concentration in culture supernatant was measured using a Modified Bradford Protein Assay Kit (Sangon Biotech, Shanghai, China) with bovine serum albumin (BSA) as the standard. The absorbance of the reaction mixture was determined at 595 nm. For sodium dodecyl sulfate-polyacrylamide gel electrophoresis (SDS-PAGE) analysis, 20 μL of unconcentrated culture supernatant was subjected to a 10% polyacrylamide gel with the aid of the PAGE Gel Quick Preparation Kit (Yeasen Biotech, Nanjing, China). Cellulase activities including filter paper cellulase (FPase), endoglucanase (CMCase), β-glucosidase (pNPGase), and exoglucanase (pNPCase) activities, as well as xylanase activity were measured as previously described (Lai et al., 2025). One unit (U) for FPase, CMCase, and xylanase activity was defined as the amount of 1 μmol glucose or 1 μmol xylose produced by 1 mL enzyme from the substrate per minute under standard assay conditions. One unit (U) for pNPGase and pNPCase activity was the amount of 1 μmol

p-nitrophenol (pNP) released by 1 mL enzyme per minute from the appropriate substrate. Triplicate independent biological experiments were conducted for each sample.

3.3.8 Electrophoretic mobility shift assays

The DNA sequence encoding the putative DNA-binding domain MtHAC-1$_{126\text{-}190}$ was amplified from *M. thermophila* genomic DNA using the primer set shown in Table S3.1. The purified PCR fragments were ligated into the HindIII stie of pET-51b to form a Strep II-tagged protein expression plasmid, which was then introduced into *E. coli* BL21(DE3) for protein expression. The expression and purification of recombinant protein was performed as previously reported (Lai et al., 2025).

EMSAs were conducted as described previously (Wang et al., 2012; Lai et al., 2025). In brief, promoter regions of *bgl1* (MYCTH_66804) (P2, − 650 to − 300), *cbh1* (MYCTH_109566) (P1, − 350 to − 1), *egl2* (MYCTH_86753) (P2, − 650 to − 300), *xyn1* (MYCTH_112050) (P2, − 650 to − 300; P3, − 1000 to − 650), and *xyr1* (MYCTH_2310145) (P2, − 650 to − 300) were amplified from *M. thermophila* genomic DNA using specific primers (Table S3.1) and used as probes. In each EMSA reaction, various amounts (0-0.8 μg) of MtHAC-1$_{126\text{-}190}$ were incubated with a constant quantity (100 ng) of the DNA probes at 25°C for 30 min in binding buffer. Purified Strep II-tagged protein from *E. coli* BL21 (DE3) cells harbored with the vector pET-51b-MtCLR-2$_{30\text{-}89}$ was used as the negative control.

3.4 Results

3.4.1 Identification of MtHAC-1 as a bZIP-type protein

The *M. thermophila Mthac-1* gene (MYCTH_2310995) is 1774 bp in length, and contains a traditional intron of 58 nt, the removal of which creates the *Mthac-1* mRNA of 1716 nucleotides (Figure 3.1A). A previous study demonstrated that growth of *M. thermophila* in cellulose-containing medium induces endoplasmic reticulum (ER)

stress, resulting in the unconventional splicing of a 23-nt intron from the *Mthac-1* mRNA, thereby producing a mature transcript of 1347 nucleotides (Figure 3.1A) (Li et al., 2022a). The MtHac-1 protein consists of 571 amino acids and contains a typical basic leucine-zipper (bZIP) domain (Figure 3.1B). However, removal of the 23-nt intron would alter the open reading frame of the *M. thermophila hac-1* mRNA, resulting in the production of a 448-amino-acid protein that shares an identical N-terminus but has a distinct C-terminus compared to the conventional MtHAC-1 protein (Figure 3.1B) (Li et al., 2022a). The bZIP domain is a contiguous α-helix that is composed of a basic region mediating DNA binding and a leucine zipper motif needed for dimerization (Maldonado-Bonilla, 2020). The Hac-1 orthologs from *Saccharomyces cerevisiae*, *N. crassa*, *T. reesei*, *A. niger*, *A. nidulans*, *A. oryzae*, and *Aspergillus flavus* have been characterized (Kaufman, 1999; Saloheimo et al., 2003; Mulder and Nikolaev, 2009; Montenegro-Montero et al., 2015). The alignment of these proteins from different fungal species with MtHac-1 revealed that the basic motif is highly conserved, whereas the leucine zipper is more variable (Figure 3.1C).

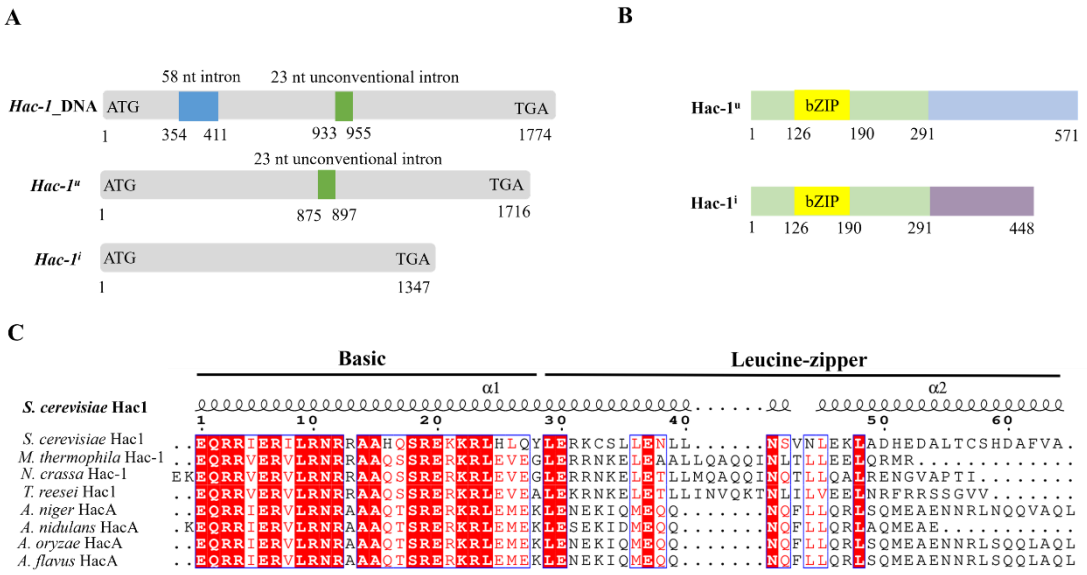

Figure 3.1. MtHAC-1 is a putative bZIP-type protein. (A) The gene structure of *Mthac-1* DNA and mRNA. *Hac-1*^{u}, unspliced form of *Mthac-1* mRNA; *Hac-1*^{i}, noncanonical spliced form of *Mthac-1* mRNA. (B) Schematic representation of Mthac-1 amino acids. Yellow box, bZIP domain; Blue box, unique C-terminus of MtHac-1^{u}; Purple box, unique C-terminus of MtHac-1^{i}; Green box, shared N-terminus of both MtHac-1^{u} and MtHac-1^{i}. (C) Alignment of protein sequences of the conserved bZIP domain in selected fungal MtHAC-1 homologs. The *α* represents α-helix, which is based on *S. cerevisiae* Hac1, obtained from SWISS-MODEL. The identical amino acids are presented as white letters in a red background, and amino acids in red letters within blue frames indicate similar physical and chemical properties.

3.4.2 Dual effects of MtHAC-1 on cellulase and xylanase induction in *M. thermophila*

To investigate the role of Mthac-1 in cellulase and xylanase production, the *Mthac-1* deletion mutants were generated by using CRISPR/Cas9 system (Figure S3.1). A 20-nucleotide protospacer sequence targeting *Mthac-1* was designed for gene editing (Table S3.1). The Cas9-U6p-sgRNA expression cassette targeting *Mthac-1* was co-transformed into *M. thermophila* wild-type (WT) protoplasts along with a donor DNA vector containing the P*gpd-neo* selection marker and the 5′ and 3′ homologous arms of *Mthac-1*. Deletion of the *Mthac-1* gene was accomplished through homology-directed

repair (HDR) mediated by the CRISPR/Cas9 system. Finally, two independent Δ*Mthac-1* mutants, designated Δ*Mthac-1*-1 and Δ*Mthac-1*-2, were successfully obtained and subsequently used for further analysis. Moreover, the encoding sequence of *Mthac-1* driven by the strong constitutive promoter P*pdc* (pyruvate decarboxylase, MYCTH_112121) was integrated ectopically into the genome of *M. thermophila* wild-type (WT) to create the *Mthac-1*-overexpression (OE-*Mthac-1*) strain. The correct deletion and integration events in the obtained mutants were verified by genomic PCR with several specific primers (Table S3.1 and Figure S3.2). After growth in Avicel medium for 48 h, the FPase, CMCase, xylanase, pNPCase, and pNPGase activities, and secreted protein of *Mthac-1* deletion mutants decreased by 41% to 49%, 50% to 65%, 58% to 70%, 51% to 63%, 38% to 47%, and 25% to 41% respectively, compared with those of the WT (Figure 3.2 A-F). However, compared to the WT, Δ*Mthac-1* strains showed a significant elevation in FPase activity (49% to 100%), CMCase activity (16% to 27%), xylanase activity (185% to 440%), pNPCase activity (107% to 260%), and pNPGase activity (58% to 390%) after cultivation in Avicel medium for 72 and 96 h (Figure 3.2A-E). Additionally, Δ*Mthac-1* mutants secreted 97% to 124% higher protein than WT on Avicel at 72 and 96 h (Figure 3.2F), which was confirmed by extracellular secretome profiling through SDS-PAGE (Figure S3.3). In contrast to Δ*Mthac-1* mutants, improved FPase activity (25%) and extracellular protein production (68%) were observed in the OE-*Mthac-1* strain when grown on Avicel for 48 h, although a low increase in the CMCase activity (12%) was also detected (Figure 3.2A, B, and F). As expected, after 72 and 96 h of cultivation, the OE-*Mthac-1* strain exhibited a noticeable reduction in FPase activity (28% to 52%), CMCase activity (19% to 81%), xylanase activity (22% to 47%), and pNPCase activity (54% to 90%), in comparison to those of the WT strain (Figure 3.2A to D). Furthermore, while the pNPGase activity and secreted protein of the OE-*Mthac-1* strain increased by 40% and 12%, respectively, relative to the WT during the presence of Avicel at 72 h, their production decreased by 40% and 35%, correspondingly, after 96 h of growth (Figure 3.2E and F). Notably, although Δ*Mthac-1*-1 and Δ*Mthac-1*-2 exhibited minor differences in enzymatic activities, both

strains displayed consistent phenotypic trends, supporting the reliability and robustness of the Δ*Mthac-1* phenotype. Such variation is expected and may result from differences in homologous recombination events that mediated by the CRISPR/Cas9 system (Huang and Cook, 2022). Taken together, these results indicate that Mthac-1 plays a positive role in regulating cellulase and xylanase activities during the early phase of growth on Avicel but acts as a repressor in the middle and later stages.

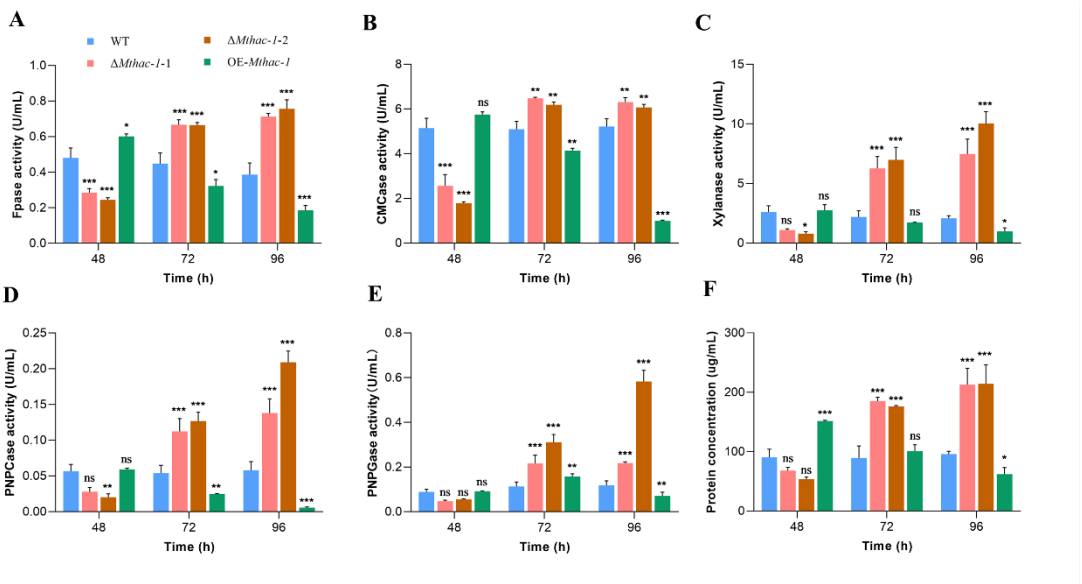

Figure 3.2. Cellulase and xylanase activities (A to E), and total protein (F) in supernatants from cultures of *M. thermophila* WT strain, Δ*Mthac-1* mutants, and OE-*Mthac-1* strain. (A**)** Filter paper cellulase (FPase) activity. (B) Endoglucanase (CMCase) activity. (C) Xylanase activity. (D) Cellobiohydrolase (pNPCase) activity. (E) β-glucosidase (pNPGase) activity. (F) Extracellular protein production. These *M. thermophila* strains were grown on glucose for 36 h and subsequently transferred to 2% Avicel medium and cultivated for 48-96 h. *$p < 0.05$, **$p < 0.01$, and ***$p < 0.001$ indicate significant differences between the WT and Δ*Mthac-1* mutants or OE-*Mthac-1* strain (Two-way ANOVA), ns indicates not significant. Error bars represent the SD from three replicates. Δ*Mthac-1*-1 and Δ*Mthac-1*-2, represent two independently constructed Δ*Mthac-1* mutant strains.

3.4.3 The *Mthac-1* gene is required for normal radial growth and conidiation on solid media

To investigate the effects of MtHac-1 on the growth of *M. thermophila*, we compared the colony phenotypes of the WT, Δ*Mthac-1* mutant, and OE-*Mthac-1* strains on PDA medium and solid agar plates containing glucose or Avicel. The Δ*Mthac-1* mutant formed smaller and more compact colonies in comparison to the WT on all tested carbon sources (Figure 3.3A). As shown in Figure 3.3B, after 48 h of inoculation, the Δ*Mthac-1* mutant developed few hyphae branching with no developing conidia, compared with the normal conidiogenesis of the WT. After 72 h of incubation, the *Mthac-1* deletion strain produced only a few conidia (Figure 3.3B). This observation was quantitatively confirmed, as the Δ*Mthac-1* strain generated only 15% of the spores produced by the WT when cultivated on Avicel for 7 days (Figure 3.3C).

Given the impairment in radial growth, we further examined the mycelial growth of the Δ*Mthac-1* mutant, along with the WT and OE-*Mthac-1* strains, in liquid shake flasks containing glucose or Avicel. Microscopic examination revealed that the Δ*Mthac-1* strain developed aberrant mycelia with no hyphal branching after 36 h of growth in liquid Avicel medium (Figure 3.3D). However, the Δ*Mthac-1* strain gradually developed normal mycelia at 72 and 96 h, similar to that formed by the WT after 36 h (Data not shown). This was consistent with the extracellular protein production pattern observed in the *Mthac-1* deletion mutant (Figure 3.2F). To utilize lignocellulose, filamentous fungi need to secrete numerous enzymes to degrade this complex polymer into monosaccharides and/or oligosaccharides, which can then be absorbed by the cells to support growth (Benocci et al., 2017; Gu et al., 2023). Since efficient cellulase production is vital for mycelial growth on cellulose, we reasoned that the growth defects of the Δ*Mthac-1* mutant in liquid Avicel culture during the early phase may be due to a reduced cellulase secretion capacity on this carbon source. Interestingly, growth on glucose was unaffected in the Δ*Mthac-1* strain (Figure 3.3D), indicating a specific defect correlated with cellulose utilisation, which supports our hypothesis. This is similar to *N. crassa*, where the growth of the corresponding mutant in *N. crassa* was

impaired under liquid cellulose culture but was comparable to that of the WT in liquid media containing sucrose or xylan (Montenegro-Montero et al., 2015). Notably, the OE-*Mthac-1* strain displayed indistinguishable growth from the WT on media containing different carbon sources, both under solid and liquid culture conditions (Figure 3.3A-D). Collectively, these findings suggest that MtHac-1 is essential for normal radial growth, conidiation on solid media, and mycelial development in liquid cellulose culture during the early stage.

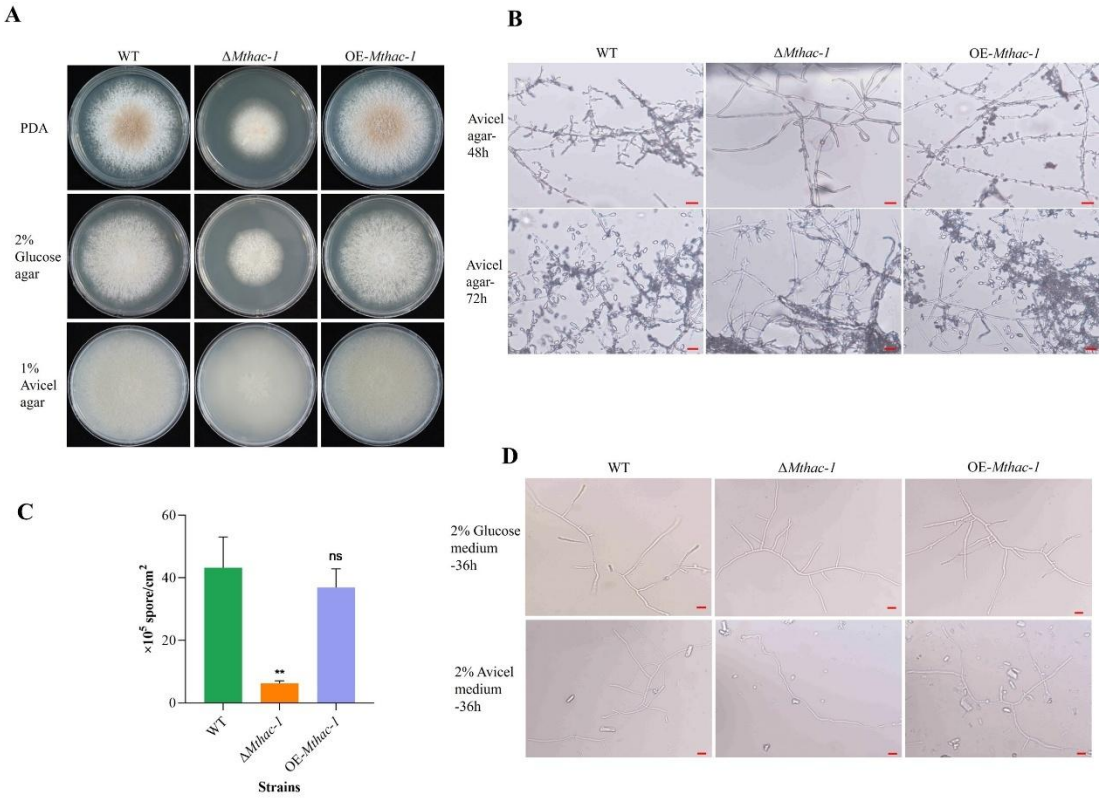

Figure 3.3. Growth phenotype analyses of *M. thermophila* WT, Δ*Mthac-1*, and OE-*Mthac-1* strains. (A) Fungal colonies on PDA, agar plates containing 2% (w/v) glucose or 1% (w/v) Avicel for 3 (PDA) or 4 days (glucose and Avicel) at 45°C. (B) Microscopic investigation of fungal hypha and conidiation. Fungal strains were grown on 1% (w/v) solid Avicel medium for 48 and 72 h. Scale bar = 10 µm. (C) Quantitative determination of fungal sporulation when cultured in 1% (w/v) solid Avicel medium for 7 days at 45°C. $^{**}p < 0.01$ represents a significant difference in conidiation between WT and Δ*Mthac-1* strains (Student's t-tests), ns indicates no significant difference between WT and OE-*Mthac-1* strains. Error bars indicate the SD from three replicates. (D) Microscopic observation of fungal mycelia grown in liquid glucose or Avicel media at 45°C for 36 h. Scale bar = 10 µm.

3.4.4 MtHAC-1 regulates the expression of major cellulase and xylanase genes and the regulatory gene *xyr1*

The findings suggest that MtHac-1 is involved in regulating cellulase and xylanase production in *M. thermophila*, possibly by modulating cellulase and xylanase genes and/or vital transcription factor genes at the mRNA level. To investigate this further, RT-qPCR was employed to analyse the expression of the β-glucosidase gene *bgl1* (*MYCTH_66804*), cellobiohydrolase gene *cbh1* (*MYCTH_109566*), endoglucanase gene *egl2* (*MYCTH_86753*), xylanase gene *xyn1* (*MYCTH_112050*), and the regulatory genes including *cre1* (*MYCTH_2310085*) and *xyr1* (*MYCTH_2310145*). Expression levels were measured in *M. thermophila* WT and Δ*Mthac-1* strains grown in Avicel medium for 24, 48, and 72 h following transfer from glucose. The transcript levels of *cbh1* and *egl2* decreased by 50% to 56% in Δ*Mthac-1* compared with the WT after 24 h of growth on Avicel, however, their expression exhibited 12.0- to 34.7-fold elevations at 48 and 72 h (Figure 3.4). Similarly, *bgl1* expression was reduced by 61% to 80% in the *Mthac-1* disruption strain at 24 and 48 h but displayed a 4.8-fold enhancement at 72 h (Figure 3.4). In addition, *xyn1* showed consistently elevated expression ranging from 3.0- to 15.7-fold in Δ*Mthac-1* compared with the WT during the entire cultivation period (24-72 h) (Figure 3.4). Furthermore, the transcript levels of *xyr1* were substantially increased (approximately 4.0-fold) at 48 and 72 h in strain Δ*Mthac-1*, whereas *cre1* expression remained unchanged (Figure 3.4). These expression patterns, except for the abnormal upregulation of *xyn1* at 24 h, agreed with the trends in protein secretion and enzymatic activities observed in the Δ*Mthac-1* strain during the presence of Avicel.

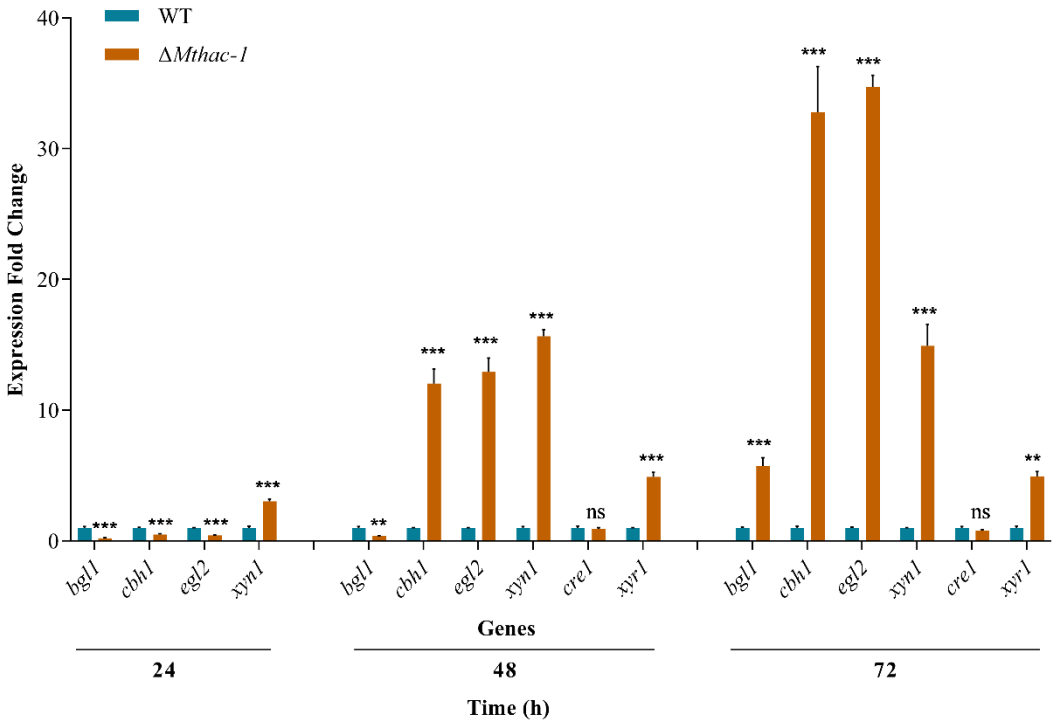

Figure 3.4. The transcription levels of major cellulase and xylanase genes and the regulatory genes *cre1* and *xyr1* in the *M. thermophila* Δ*Mthac-1* mutant compared to the WT strain. Strains were pre-grown in glucose for 36 h, washed and transferred to 2% (w/v) Avicel medium and cultivated for 24, 48, and 72 h. The transcript level of each gene in Δ*Mthac-1* was normalized to the level of the corresponding gene in WT. $^{**}p < 0.01$, and $^{***}p < 0.001$ represent significant differences between the Δ*Mthac-1* and WT strains (Two-way ANOVA), ns indicate no significant difference. Error bars represent the SD from three replicates.

3.4.5 MtHAC-1 can bind to the promoter regions of major cellulase and xylanase genes and the regulatory gene *xyr1*

The RT-qPCR data revealed that MtHAC-1 controls the transcription levels of key cellulase and xylanase genes and the crucial regulatory gene *xyr1*. To confirm whether MtHAC-1 directly or indirectly regulates the expression of these target genes, electrophoretic mobility shift assays (EMSAs) were conducted, involving the DNA-binding domain of MtHAC-1 and the promoter regions of tasted genes. It is generally challenging to accomplish recombinant expression of full-length regulatory proteins in *E. coli*. Therefore, MtHAC-$1_{126\text{-}190}$, containing the putative bZIP domain, was expressed in *E. coli* BL21(DE3) and purified to generate the fusion protein MtHAC-$1_{126\text{-}190}$ with Strep II-His tag (Figure S3.4). Probes covering the promoter regions of *bgl1* (P2, − 650 to − 300), *cbh1* (P1, − 350 to − 1), *egl2* (P2, − 650 to − 300), *xyn1* (P2, − 650 to – 300; P3, − 1000 to − 650), and *xyr1* (P2, − 650 to − 300) were amplified by PCR using specific primer pairs. In the EMSAs, the recombinant MtHAC-$1_{126\text{-}190}$ bound to the promoter regions of both *bgl1*, *cbh1*, *egl2*, *xyn1*, and *xyr1* in a protein concentration-dependent pattern (Figure 3.5A). The binding complex bands occurred upon the addition of 0.1 µg MtHAC-$1_{126\text{-}190}$. This binding was specific since no retardation was observed in the promoter of *xyn1*-P3 (Figure 3.5A). Additionally, MtHAC-$1_{126\text{-}190}$ displayed a high affinity for the probe fragments of the *xyn1*-P2 and *xyr1*-P2 promoter regions, while weak binding capacity was detected with the *bgl1*, *cbh1*, *egl2* promoter regions (Figure 3.5A). Purified Strep II-fused MtCLR-$2_{30–89}$ was used as a negative control to exclude nonspecific binding (Data not shown). These findings illustrate that MtHac-1 regulates cellulase and xylanase gene expression through two pathways: direct binding, and through essential TF gene *Mtxyr1*.

In *S. cerevisiae*, 5′-CAGCGTG-3′, a partly palindromic sequence (underlined) around a spacer of one nucleotide, which is termed the UPRE-1(unfolded protein response element), was demonstrated to be essential for Hac1 binding (Mori et al., 1998). Subsequent studies revealed that a large set of Hac1-regulated genes, although lacking the UPRE-1 sequence, contain the UPRE-2 motif (5′-TACGTG-3′) (Patil et al.,

2004). In addition, bioinformatic analysis found that UPRE-2-like motif (5′-ACGTG(T/G)(C/A)-3′) exhibited strong binding interactions with ScHac1 (Fordyce et al., 2012). To determine the MtHAC-1 binding sequence in the promoter regions of target genes, these identified ScHac1-binding motifs were used to search the corresponding promoter regions of *bgl1*, *cbh1*, *egl2*, *xyn1*, and *xyr1*. The results identified binding sites that are consistent with these conventional sequences in the upstream regions of *bgl1* (UPRE-1), *xyn1* (UPRE-2-like), and *xyr1* (UPRE-2-like) (Figure 3.5B). This is in line with the observation in *A. niger*, where the sequence 5′-AC<u>ACGTGTC</u>CT-3′, resembles the UPRE-2-like motif (underlined), exhibiting much stronger binding capacity with HacA (Mulder et al., 2006). Moreover, one similar binding motif was also detected in the promoter regions of *bgl1* and *egl2*, which was referred to as UPRE-1-like motif (Figure 3.5B). However, no sequences matching any known binding consensus were found in the *cbh1* promoter, indicating that additional, yet unrecognized, oligonucleotide sequences may be required for binding of MtHAC-1 to genes lacking canonical motifs.

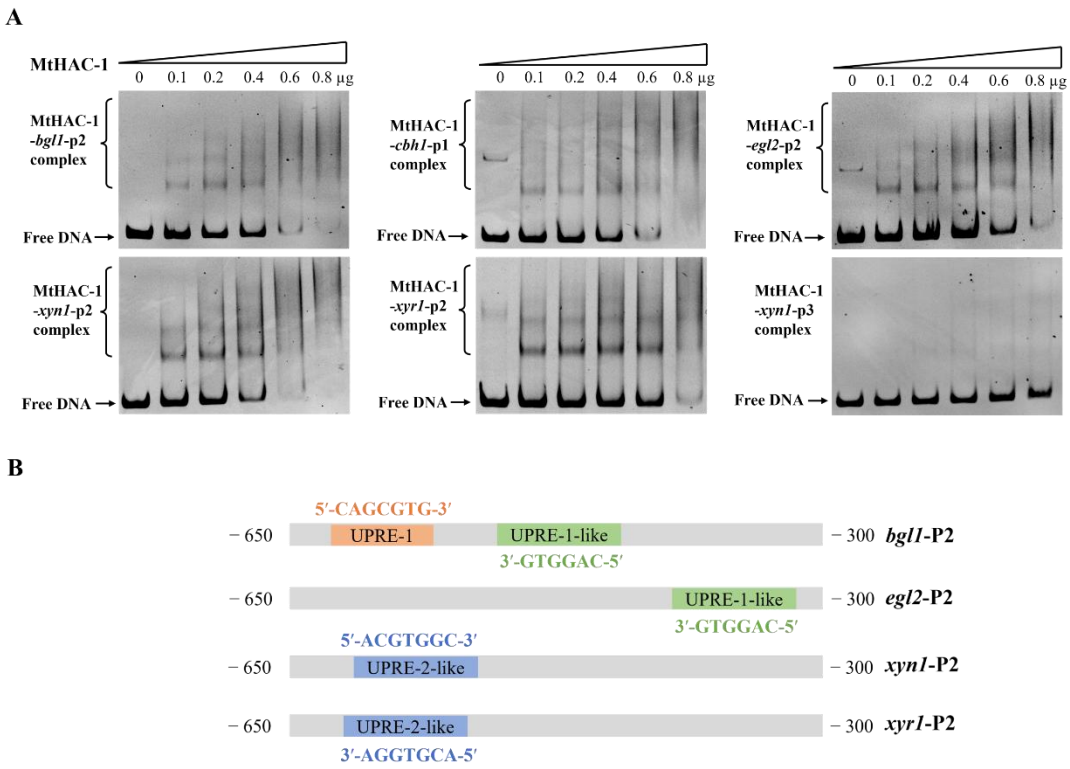

Figure 3.5. Identification of MtHAC-1 binding motifs in the promoter regions of target genes. (A) Electrophoretic mobility shift assays (EMSA) of the binding between MtHAC-1 and the promoter regions of genes encoding cellulase and xylanase, and regulatory gene *xyr1*. Each reaction system contains 100 ng of candidate probe and indicated amounts of purified MtHAC-1 binding domain. The promoter of *xyn1*(*xyn1*-p3) was employed as negative control. (B) Schematic demonstration of the putative MtHAC-1binding motifs in the promoter regions of experimentally confirmed target genes (*bgl1*, *egl2*, *xyn1*, and *xyr1*). Box in orange indicates UPRE-1 motif, boxes in green represent UPRE-1-like motif, while boxes in blue stand for UPRE-2-like motif.

3.4.6 Transcriptomic analysis of the *Mthac-1* deletion mutant on Avicel

To comprehensively understand the function of MtHac-1, comparative transcriptomics of the WT and Δ*Mthac-1* strains grown in Avicel medium for 48 h after switching from glucose, were assayed by RNA-Seq. Analysis of differential gene expression uncovered that 3488 genes showed altered transcription levels between the WT and Δ*Mthac-1* strains, of which 2473 genes were significantly upregulated and 1015 genes were markedly downregulated in the Δ*Mthac-1* strain (Figure 3.6A). Gene Ontology (GO) analysis of the differentially expressed genes (DEGs) in the Δ*Mthac-1* mutant indicated that proteasome complex, extracellular region, polysaccharide catabolic process, hydrolase activity (acting on glycosyl bonds), transmembrane transporter activity and so on, were significantly enriched functional categories (Figure 3.6B), consistent with the phenotypes observed in Δ*Mthac-1* under cellulose induction conditions.

Expression pattern analyses of CAZyme genes revealed that those involved in cellulose and xylan degradation were expressed at considerably altered levels (Figure 3.6C). Two endoglucanase genes were highly induced, and three endoglucanase genes were downregulated in Δ*Mthac-1*, indicating that *egl2* and *MYCTH_116157* might contribute more to the increased endoglucanase activity. Similarly, the expression of two genes encoding cellobiohydrolase (*cbh1* and *MYCTH_2303045*) was increased and other two cellobiohydrolase genes was reduced by the absence of *Mthac-1*. In contrast, transcript levels of five β-glucosidase genes were significantly decreased in Δ*Mthac-1* compared to the WT, which was consistent with RT-qPCR detection showing that *bgl1* displayed lower expression level in Δ*Mthac-1* after 48 h of cultivation on Avicel. As expected, many genes encoding xylan-degrading enzymes exhibited elevated expression levels in Δ*Mthac-1* relative to the WT on Avicel, including four endo-xylanases (xyn1, GH11, and GH30), one GH43 β-xylosidase, and eight xylanolytic accessory enzymes (GH43, GH62, CE1, and CE15), in accordance with the elevated xylanase production in the Δ*Mthac-1* mutant during the middle and late stages of growth. The increase in expression levels of four LPMO (AA9) genes which are commonly considered to play an oxidative role in cellulose depolymerization, was also

observed in Δ*Mthac-1* during 48 h of growth on Avicel (Figure S3.5). One of these AA9 genes, encoding MtLPMO9C (MYCTH_100518), was reported to be active toward cellulose, implying that the other three LPMO genes regulated by MtHac-1 might also be associated with the oxidative split of Avicel.

Apart from these CAZyme genes, the genes that encode putative transcription factors also had changed expression levels, which include fourteen upregulated and eleven downregulated genes in Δ*Mthac-1* (Figure 3.6D). Most of these TFs are classified into Fungal Zn(II)2Cys6 and Fungal_TF families. Among these transcriptional regulators, the forkhead protein MtFKH1 (MYCTH_2307931) which was newly identified as a repressor of cellulase and xylanase gene expression (Lai et al., 2025), showed a noticeably lower expression level ($\log_2$ fold change = −7.2) by the deletion of *Mthac-1*. This may partly contribute to the enhanced cellulase and xylanase activities. It is worth noting that Mtxyr1, which is a pivotal transcriptional activator of xylanolytic genes, exhibited a 53% increase in the transcript level in the Δ*Mthac-1*. Despite not meeting the statistical threshold, it still partially agreed with the RT-qPCR results.

The expression of genes encoding putative sugar transporters was also analysed by comparative transcriptomic analysis. A total of 21 genes, annotated as xylose, glucose, hexose, cellodextrin, cellobionic acid or other putative sugar transporters, showed varying degrees of differential expression (Figure 3.6E). Twelve of these genes unregulated their transcription in Δ*Mthac-1* and others reduced compared to the WT. In particular, the transcript level of gene encoding L-arabinose transporter MtLat-1 (MYCTH_95427), which has been recently shown to be involved in the repression of xylanase activity in *M. thermophila* on arabinan but not on xylan (Gu et al., 2023), was decreased ($\log_2$ fold change = −1.98), indicating that it may also play a role during the presence of cellulose.

A crucial response was also detected in the expression of genes that encode 26S proteasome (Figure 3.6F). All the 13 genes encoding 20S proteasome core complex, including seven α-type subunits (MYCTH_112442, MYCTH_2133968,

MYCTH_2299195, MYCTH_2301275, MYCTH_2302907, MYCTH_2306141, and MYCTH_2313535), and six β-type subunits (MYCTH_2055659, MYCTH_2136659, MYCTH_2296370, MYCTH_2296573, MYCTH_2301064, and MYCTH_2308969) showed elevated transcript levels in the Δ*Mthac-1* mutant (Figure 3.6F). In addition, 14 out of a total of 18 genes encoding 19S proteasome regulatory particle, including ten Regulatory Particle Non-ATPase (RPN) subunits (MYCTH_109876, Sem1; MYCTH_2298906, Rpn1; MYCTH_2308377, Rpn2; MYCTH_2313931, Rpn5; MYCTH_2312284, Rpn6; MYCTH_2084627, Rpn8; MYCTH_2309273, Rpn9; MYCTH_2313806, Rpn10; MYCTH_2050660, Rpn11; and MYCTH_2294698, Rpn13), and four Regulatory Particle ATPase (RPT) subunits (MYCTH_2295098, Rpt1; MYCTH_2095260, Rpt3; MYCTH_2076503, Rpt4; and MYCTH_2084256, Rpt6) were also expressed at higher levels in Δ*Mthac-1* compared with the WT during growth in Avicel medium (Figure 3.6F). These data illustrated that MtHac-1 is closely associated with the protein degradation system, implying its involvement in a complex regulatory network.

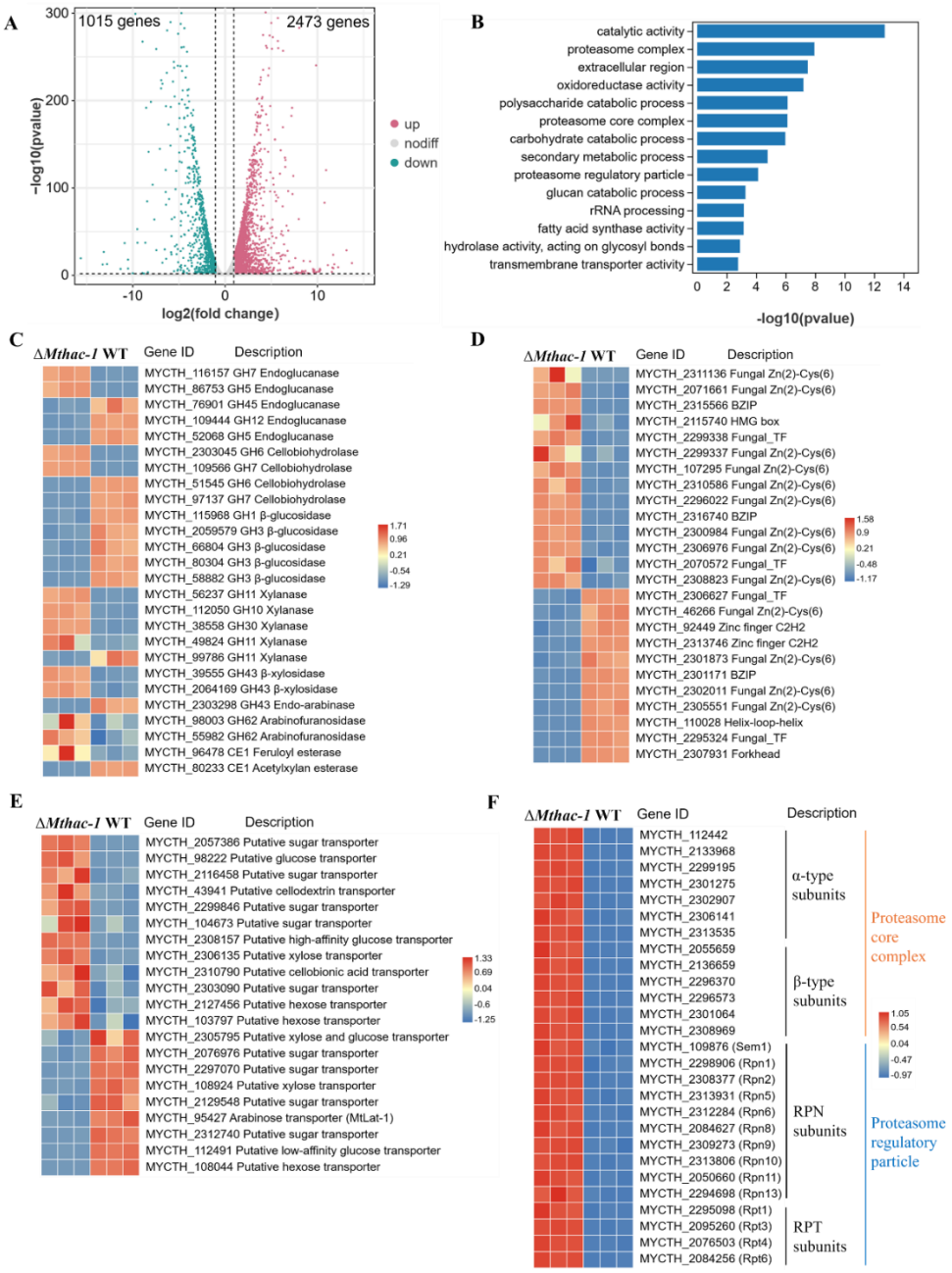

Figure 3.6. Comparative transcriptomic analysis of strains Δ*Mthac-1* and WT cultivated in Avicel medium for 48 h after transfer from glucose medium. (A) Volcano plots illustrating differentially expressed genes (DEGs) between Δ*Mthac-1* and WT. The significantly upregulated and downregulated genes in the Δ*Mthac-1* strain are plotted in red and green, respectively. (B) Gene Ontology (GO) enrichment analysis of DEGs in the biological process, cellular component, and molecular function categories. (C to F) Heatmap analysis of expression profiles for genes encoding cellulases and xylan-degrading enzymes (C), putative transcription factors (D), putative sugar transporters (E), and 26S proteasome (F), respectively, between Δ*Mthac-1* and WT strains.

3.5 Discussion

Filamentous fungi are known to secrete numerous enzymes in their natural settings to degrade the complex polymetric substances for nutrients uptake (Jadhav et al., 2024). During the cellulolytic response, the nascent lignocellulolytic enzyme polypeptides are translocated into the ER to be folded and processed for secretion (Huberman et al., 2016). This process can result in considerable ER stress and trigger the UPR, which aims to maintain ER homeostasis (Li et al., 2022a). In *S. cerevisiae*, the UPR pathway depends on the transcription factor Hac1, which undergoes an unconventional splicing reaction in its mRNA, where a 252-nucleotide (nt) noncanonical intron is cleaved to generate a translationally active form (Xia, 2019). In contrast, in filamentous fungi, such as *T. reesei*, *A. nidulans*, *A. niger* and *N. crassa*, the loss of a 20 or 23-nt unconventional intron from the mRNA of HacA/Hac1/Hac-1 is responsible for mediating the UPR signaling pathway (Saloheimo et al., 2003; Mulder and Nikolaev, 2009; Montenegro-Montero et al., 2015). A similar phenomenon was also observed in *M. thermophila*, where the *Mthac-1* mRNA undergoes a noncanonical splicing via removing a 23-nt intron when grown on cellulose, although the amount of unspliced mRNA is more than spliced form (Li et al., 2022a). This indicates that the growth of *M. thermophila* on cellulose solely could trigger the ER stress, which is in line with the *N. crassa* phenotypes in previous study (Montenegro-Montero et al., 2015). Structure analysis showed that the *Mthac-1*^{u} (unspliced) mRNA contains an ORF encoding for 571 amino acids, while the *Mthac-1*^{i} (unconventional spliced) mRNA encodes a protein of 448 amino acids (Figure 3.1), which is caused by the removal of this 23-nt intron, leading to the frameshift in the *M. thermophila hac-1* mRNA. Furthermore, it has been suggested that the UPR is involved in regulating lignocellulolytic enzyme production (Huberman et al., 2016). For example, a transcriptional down-regulation mechanism was found in *T. reesei*, where the transcript levels of genes encoding secreted proteins, such as cellulases and xylanases, were reduced in response to ER stress (Pakula et al., 2003). Similarly, the selective transcriptional down-regulation of the glucoamylase

gene has also been observed in *A. niger* upon UPR activation (Al-Sheikh et al., 2004). In addition, the growth of *N. crassa* on cellulose was severely impaired and no secreted protein was detected in the absence of *hac-1* (Montenegro-Montero et al., 2015). Here, we carry out this study to elucidate the role of MtHac-1 in *M. thermophila*, particularly focusing on its role in lignocellulose degradation. Through a combination of transcriptomic analyses and molecular genetic assays, we showed that MtHac-1 exerts a dual regulatory effect on cellulase and xylanase production. It directly regulates the expression of key cellulase and xylanase genes while also modulating the transcription of the crucial xylanolytic activator *Mtxyr1*. Transcriptome profiling further revealed that the majority of genes encoding components of the 26S proteasome exhibited increased transcript levels in the Δ*Mthac-1* mutant, highlighting a tight association between MtHac-1 and the protein degradation machinery in *M. thermophila*.

It was reported that constitutively activated HacA (the spliced form of *hacA* that lacks the 20-nt untraditional intron) in *A. niger* triggered the UPR signaling and had a negative effect on the expression of genes encoding starch-degrading and xylanolytic enzymes, sugar transporters as well as AmyR, a key transcriptional activator involved in starch degradation (Carvalho et al., 2012). In *N. crassa*, however, the loss of *hac-1* impaired cellulase secretion without affecting transcription levels of cellulase genes in the presence of cellulose (Fan et al., 2015). These findings indicate that MtHac-1 homologs may play divergent roles in different fungi during the lignocellulolytic response. In this study, the disruption of *Mthac-1* elevated cellulase, xylanase, and extracellular protein production after 72 and 96 h of growth in Avicel medium, whereas the overexpression of *Mthac-1* decreased both enzymatic activities, and protein secretion at the late phase (Figure 3.2). In contrast, Δ*Mthac-1* mutants showed reduced cellulase and xylanase activities, as well as decreased protein secretion following 48 h of cultivation on Avicel, contrary to the enhanced levels displayed by the OE-*Mthac-1* strain (Figure 3.2). The discrepancy observed in Δ*Mthac-1* mutant regarding enzymatic activities and overall protein secretion in the early and middle/late stages of incubation was supported by the RT-qPCR analysis. These data revealed that the expression levels

of key cellulase and xylanase genes in Δ*Mthac-1* were substantially elevated after 48 and 72 h of induction with Avicel but were strongly down-regulated after 24 h (except for *xyn1* at 24 h and *bgl1* at 48 h, which will be discussed below) (Figure 3.4). It appears that MtHAC-1 may act in a similar manner to that of its ortholog *N. crassa* HAC-1 in the early cultivation period, promoting cellulolytic and xylanolytic enzymes secretion. However, during the middle and later stages, it functions similarly to *A. niger* hacA, exerting a negative effect on cellulase and xylanase production. We propose the dual role of MtHAC-1 plays in response to cellulose induction: (1) During the early phase of growth on cellulose, the *M. thermophila* needs to express and secrete large quantities of enzymes to depolymerize this complex substance for supporting cellular growth (Gu et al., 2023; Liu et al., 2024). This increased demand for protein secretion imposes higher folding and processing requirements, necessitating a fully active and functional UPR to accommodate these enzymes in large amounts (Montenegro-Montero et al., 2015). In this context, MtHAC-1 therefore positively regulates lignocellulolytic enzyme secretion. (2) In the middle and late stages of growth, secreted enzymes are sufficient for nutrient acquisition. As a result, the accumulation of large amounts of unfolded or misfolded proteins may occur, triggering a feedback repression mechanism of the UPR signaling, which downregulates the transcription of extracellular enzymes, thereby reducing ER load and preventing excessive energy depletion (Pakula et al., 2003; Al-Sheikh et al., 2004; Carvalho et al., 2012; Zhang et al., 2021). During this process, MtHAC-1 represses the secretion of cellulase and xylanase. This dual regulatory behavior potentially reflects the dynamic role of MtHAC-1 as a key transcription factor that maintains the balance between enhanced protein secretion and ER processing capacity, ensuring basal growth and cellular homeostasis of *M. thermophila* across different growth phases during the lignocellulolytic response (Montenegro-Montero et al., 2015; Huberman et al., 2016).

In eukaryotic cells, the 26S proteasome is comprising the 20S core complex and the 19S proteasome regulatory particle, which serves to remove proteins that are misfolded or dysfunctional as well as no longer needed, and plays fundamentally

essential roles in regulating almost all major cellular processes (Mao, 2021; Sakata et al., 2021). The expression patten analysis done in this study showed that the vast majority of genes encoding 20S proteasome core complex and 19S proteasome regulatory particle displayed higher transcript levels by the deletion of *Mthac-1* (Figure 3.6). Since Mthac-1 mediates the UPR signaling pathway in *M. thermophila* (Li et al., 2022a), it is likely that the deletion of *Mthac-1* disrupted ER homeostasis, impacted the accurate protein folding and the removal of unfolded proteins. The disruption of *Mthac-1* may trigger the cell′s demand for proper degradation of accumulated misfolded proteins, especially during the middle and late cultivation phases in cellulose medium, when cellulase and xylanase secretion is strongly elevated in the Δ*Mthac-1* mutant. This helps to explain why the enhanced expression levels of genes encoding the 26S proteasome was observed in Δ*Mthac-1*.

Interestingly, the RT-qPCR results showed a 3.0-fold upregulation of *xyn1* in Δ*Mthac-1* at 24 h under cellulose induction, which conflicted with the reduced xylanase activity detected during the early period. The *M. thermophila* genome encodes at least ten xylanases, classified into GH10 and GH11 families (Karnaouri et al., 2014). Among these, *xyn1* (*MYCTH_112050*) has been reported to exhibit the highest transcript abundance and relatively high secretion levels when grown on various lignocellulosic substrates compared to glucose (Kolbusz et al., 2014; Lai et al., 2025). However, other xylanase genes also show considerable transcript levels and/or secretion capacity in response to lignocellulose induction, such as *xyn2* (*MYCTH_100068*), *xyn3* (*MYCTH_116553*), and *xyn4* (*MYCTH_89603*) (Berka et al., 2011; Kolbusz et al., 2014). The reduced xylanase activity observed in the Δ*Mthac-1* mutant after 48 h of growth in Avicel medium may be attributed to the downregulation of these other xylanase genes at 24 h, despite the upregulation of *xyn1* at that time point. Likewise, RT-qPCR analysis revealed that *bgl1* was downregulated by 61% in Δ*Mthac-1* after 48 h of growth in Avicel medium, consistent with transcriptomic data showing reduced transcription of *bgl1* and four other β-glucosidase genes but was contradictory to the increased β-glucosidase activity observed at 72 h (Figure 3.2, 3.4, and 3.6). In Δ*Mthac-1*, the

transcript levels of cellulase and xylanase genes after 24, 48, and 72 h of growth on Avicel generally corresponded to the production levels of cellulolytic and xylanolytic enzymes at 48, 72, and 96 h, respectively (Figure 3.2, 3.4, and 3.6). These findings relate with previous observations in the *xpp1* deletion mutant of *T. reesei*, which exhibited higher xylanolytic activity than the parent strain after 72 h, matched the enhanced *xyn2* level after 48 h but not the lower expression at 24 h (Derntl et al., 2015). It appears that the transcript levels of *bgl1* in Δ*Mthac-1* at 48 and 72 h of cellulose induction correlated with the corresponding β-glucosidase secretion levels at the same time points. This temporal discrepancy between the transcription and secretion patterns of β-glucosidase and those of endoglucanase, cellobiohydrolase, and xylanase was probably because of the higher translation/secretion efficiency of β-glucosidase enzymes, leading to a shorter lag between transcription and secretion. This phenomenon warrants further investigation.

In addition to the major cellulase and xylanase genes, the RT-qPCR and transcriptomic data presented here also reflected the upregulated expression of regulatory gene *Mtxyr1* in Δ*Mthac-1* after 48 and 72 h of growth on Avicel (Figure 3.4). Since MtXyr1 is the pivotal activator of xylanase gene expression, MtHac-1 was tested if it can regulate the expression of xylanase gene directly or indirectly. The EMSA results indicated that MtHac-1 was capable of binding to the promoter regions of both *Mtxyn1* and *Mtxyr1* (Figure 3.5), showing a strong preference for the upstream regions of these genes compared to the crucial cellulase genes *Mtbgl1*, *Mtcbh1*, and *Mtegl2*. This study confirmed *in vitro* interaction between MtHac-1 and its target genes. However, considering that MtHAC-1 exhibits distinct temporal roles, possibly due to interactions with co-regulators, whether such interactions occur *in vivo* would require further investigation.

Earlier research has shown that Hac1/HacA is necessary for normal growth and development in fungi. In *A. niger*, deletion of *hac-A* resulted in severe growth defects and almost abolished sporulation on rich media (Mulder and Nikolaev, 2009). Also, disruption of *Hac1* has been found to impact hyphal morphology with reduced

polarized growth in *Candida albicans* (Wimalasena et al., 2008). Deletion mutants of *hac-1* in *N. crassa* and *hacA* in *Aspergillus fumigatus* on the other hand, displayed normal growth in rich solid media, although decreased conidiation was observed in *A. fumigatus* (Richie et al., 2009; Montenegro-Montero et al., 2015), indicating different roles of MtHac-1 orthologs in fungal development. In this study, the Δ*Mthac-1* mutant displayed stunted mycelial growth, produced less conidia on all tested solid media compared to the WT (Figure 3.3). Similar growth phenotype was also reported in *A. flavus*, where the loss of *hacA* led to retarded mycelial growth and inhibited conidiation on PDA medium (Yu et al., 2024). The transcriptomic data in the current study revealed that the deletion of *Mthac-1* downregulated the expression level of *MYCTH_2293942* ($\log_2$ fold change = −4.5), which encodes the *M. thermophila* ortholog of the membrane flavoprotein TmpA found in *A. nidulans*. Earlier study has reported that TmpA to be involved in regulation of asexual reproduction, as loss of which caused decreased number of conidia (Soid-Raggi et al., 2006). Moreover, a forkhead regulatory gene *Mtfkh1*, which controls sporulation in *M. thermophila* (Lai et al., 2025), also showed reduced transcript level in Δ*Mthac-1* ($\log_2$ fold change = −7.2). Therefore, the downregulation of genes encoding MtTmpA and MtFKH1 may contribute to conidiation defect displayed by the Δ*Mthac-1* mutant grown on solid media.

3.6 Conclusion

In summary, the current study demonstrates that MtHac-1 plays a dual regulatory role in cellulase and xylanase production, likely maintaining a balance between extracellular enzyme secretion and ER processing capacity. Moreover, MtHac-1 regulates cellulase and xylanase gene expression through two mechanisms: by directly binding to the promoter regions of major cellulase and xylanase genes with different motifs and modulating the xylanolytic gene activator Mtxyr1. Finally, MtHac-1 is associated with the 26S proteasome degradation system, and the upregulation of 26S proteasome-encoding genes in the Δ*Mthac-1* mutant during the middle stage upon cellulose

induction likely represents a compensatory response to the loss of *Mthac-1*. These findings provide novel insights into the regulatory mechanism of MtHac-1 in controlling the expression of fungal cellulolytic and xylanolytic genes.

3.7 Supplementary information

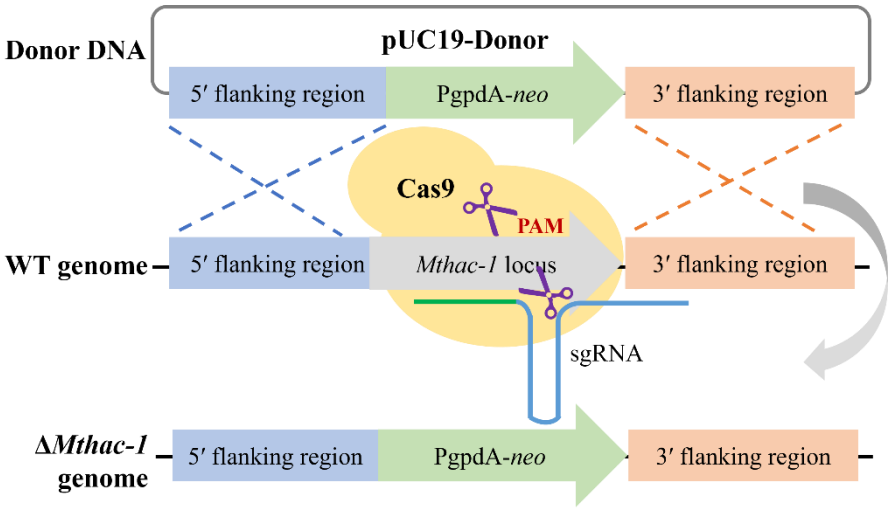

Figure S3.1. Schematic representation of the deletion of *Mthac-1* in *M. thermophila* using the CRISPR-Cas9 system. sgRNA, single chimeric guide RNA; PAM, protospacer adjacent motif; *neo*, G418 resistance gene.

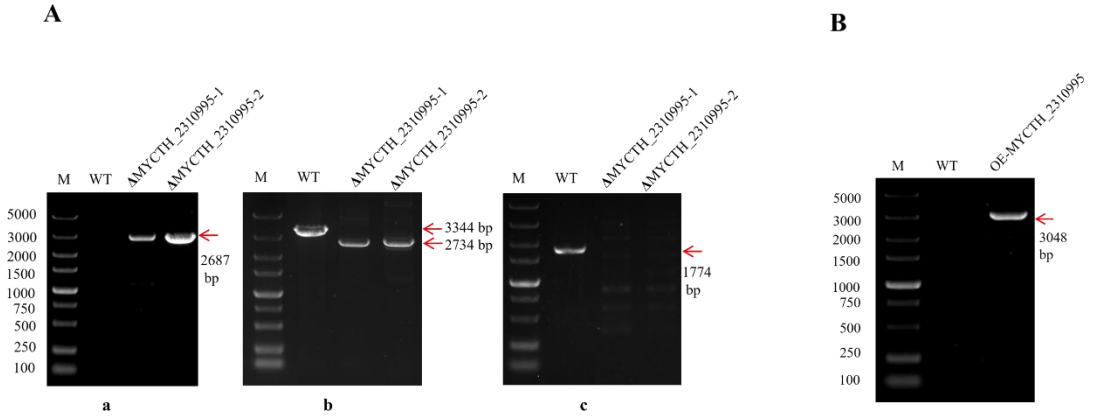

Figure S3.2. Genomic PCR verification of the deletion and overexpression of *Mthac-1* in *M. thermophila*.(A) PCR analysis for deletion strains of *Mthac-1*. Primer 1-F locates in PgpdA-neo, and Primer 1-R locates out of 3′ flanking region of *Mthac-1*; Primer 2-F locates out of 5′ flanking region of *Mthac-1*, and Primer 2-R is in 3′ flanking region; The primer pair 3 is used to amplify *Mthac-1*. a, the primer pair 1; b, the primer pair 2; c, the primer pair 3; M, DL 5000 Marker; WT, *M. thermophila* wild type strain. (B) PCR analysis for *Mthac-1*overexpression strain. M, DL 5000 Marker; WT, *M. thermophila* wild type strain.

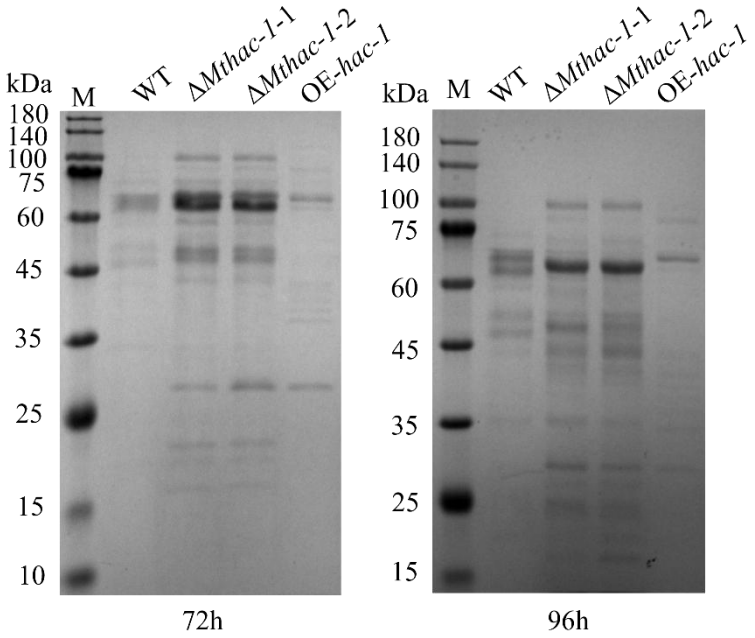

Figure S3.3. SDS-PAGE analysis of the secreted proteins in *M. thermophila* WT, Δ*Mthac-1*, and OE-*Mthac-1* strains grown for 72 and 96 h on Avicel after a shift from glucose medium. M, 10-180 kDa protein marker; WT, *M. thermophila* wild type strain.

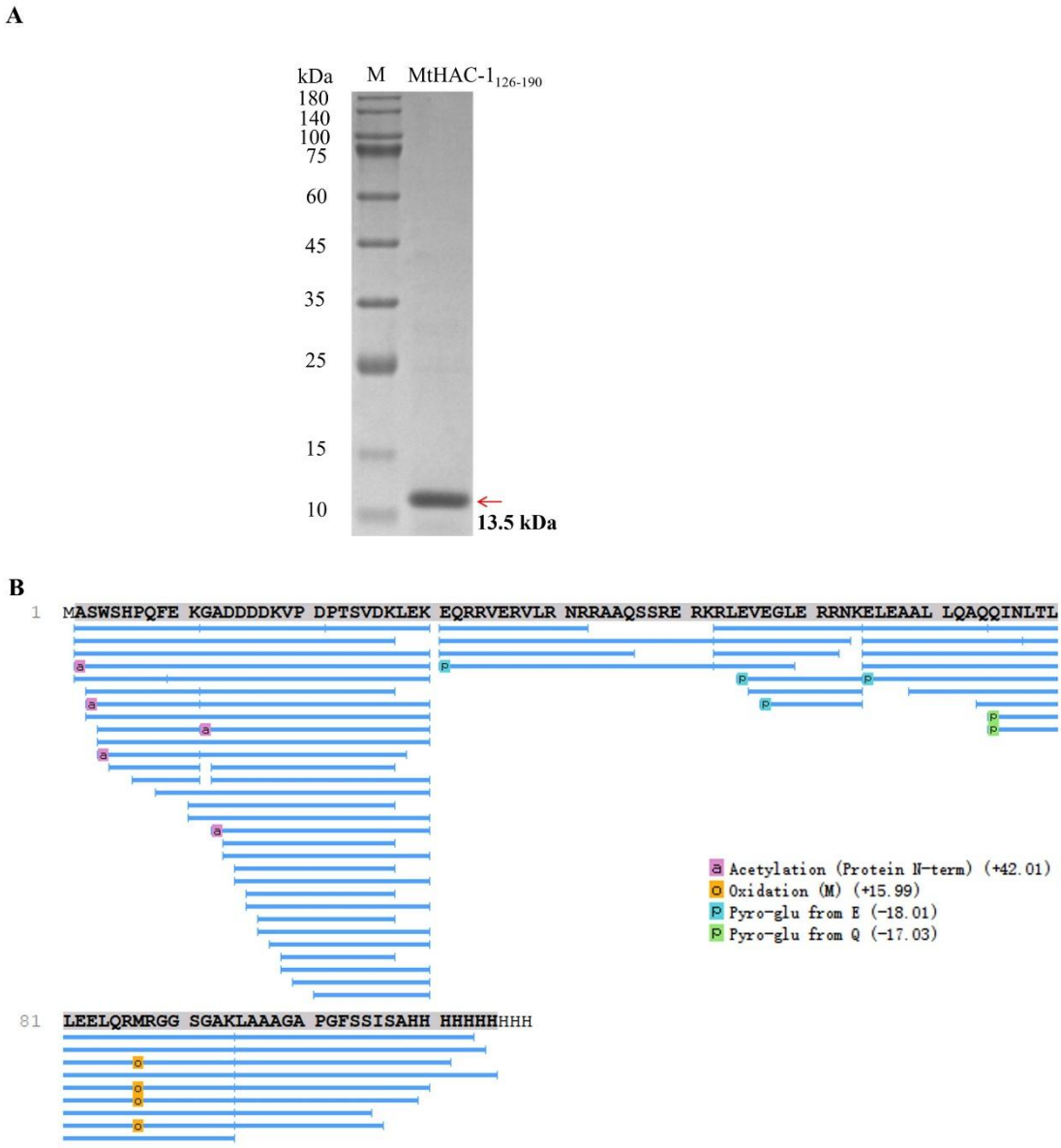

Figure S3.4. SDS-PAGE and LC-MS/MS analysis of purified MtHAC-1$_{126-190}$ protein. (A) SDS-PAGE verification of purified MtHAC-1$_{126-190}$. The sample was loaded onto a 12.5 % polyacrylamide gel. The concentration of the purified MtHAC-1$_{126-190}$ is 398 µg mL^{-1}. M, 10-180 kDa. (B) LC-MS/MS characterisation of MtHAC-1$_{126-190}$ protein. The target protein band was excised from the gel and analysed using LC-MS/MS assays with the PEAKS Studio 8.5 system. Approximately 97% of the amino acids of the target protein matched the theoretical amino acid sequence of the Strep II-MtHAC$_{126-190}$-His tag fusion protein.

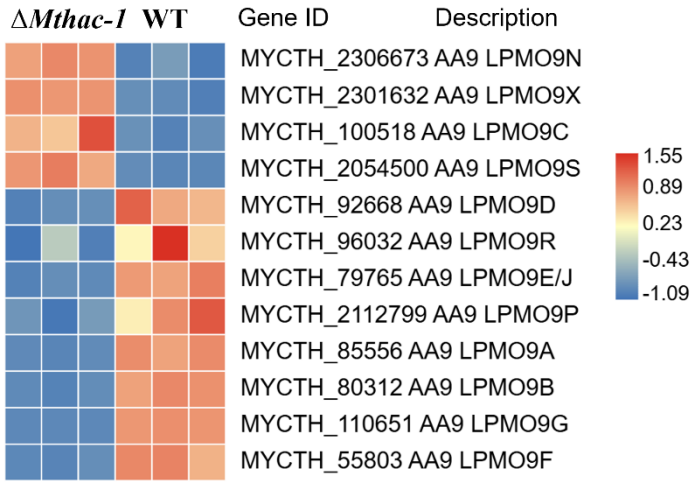

Figure S3.5. Heatmap analysis of expression profiles for genes encoding lytic polysaccharide monooxygenases (LPMOs) (AA9) between *M. thermophila* Δ*Mthac-1* and WT strains grown in Avicel medium for 48 h after a shift from glucose medium.

Table S3.1. List of PCR primers used in this study.

Construction of pFC332-Cas9-U6p-MYCTH_2310995-sgRNA vector		
Cloning of U6 promoter	U6p-F	gtttccgctgagggtttaattaaAGGATCGGTGGAGTGAAGTTCG
	U6p-MYCTH_2310995-R	GGAGTGCATTTCAGACATCTGAGGAAAGAAAGAAAAGAAGAGGAGG
Cloning of target gene-sgRNA	g-MYCTH_2310995-F	AGATGTCTGAAATGCACTCCGTTTTAGAGCTAGAAATAGCAAGTTAAAATAA
	gRNA-R	gtctcggctgaggtcttaattaaAAAAAAAGCACCGACTCGGTG
Construction of Donor DNA vectors		
MYCTH_2310995-upstream	MYCTH_2310995-up-F	gaccatgattacgccaagcttAAGACGATCGAGATCAGTGCTGT
	MYCTH_2310995-up-R	attcgaagccgcgCTCGGGACTCGCACGACG
Cloning of Pgpd-neo	MYCTH_2310995-neo-F	tcccgagCGCGGCTTCGAATCGTGG
	MYCTH_2310995-neo-R	cagatcgtTCAGAAGAACTCGTCAAGAAGGC
MYCTH_2310995-downstream	MYCTH_2310995-down-F	gagttcttctgaACGATCTGTATGAATCAATTTTTTTGG
	MYCTH_2310995-down-R	aaaacgacggccagtgaattcAAGCACACCGGAAATGTAATCC
Construction of MYCTH_2310995 overexpression vector		
Cloning of MYCTH_2310995	MYCTH_2310995-F	tcgccaacaacagacgcggccgcATGTCTGAAATGCACTCCTGGG
	MYCTH_2310995-R	gggggggccgaccgattctagaTCATTGAAAGCGCCGCCT
PCR analysis of gene MYCTH_2310995 deletion and overexpression in *M. thermophila* strains		
PCR detecting MYCTH_2310995 deletion	neo-in-F	TTACCACCTGCTCATCACCTTT
	MYCTH_2310995-out-R	CCTCCTCGTGTCTCAGAACCT
	MYCTH_2310995-out-F	CCTGATTGCCGCACCTGGAGA
	MYCTH_2310995-in-R	TACGGACAGCCCGGTAGAACG

	MYCTH_2310995-F	TCCCAAAGCCCGACCTCAC
	MYCTH_2310995-R	GCTCCGTTCAGCCATCCACT
PCR detecting MYCTH_2310995 overexpression	Ppdc-F	CGGTTACGGAAACGGAAAG
	PgpdA-R	CAGCCAACTGCAAACAGAATA
RT-qPCR analysis		
RT-qPCR of bgl1	RT-q-bgl1-F	AGCCAGGAGAATGGTAACGC
	RT-q-bgl1-R	TGACAGCCCAAACCCAAACT
RT-qPCR of cbh1	RT-q-cbh1-F	GCGGTAACTCCCTGAACCTC
	RT-q-cbh1-R	AAGTAGAGGGCGCCATTGAG
RT-qPCR of egl2	RT-q-egl2-F	GACTTCTCGATGGAGCGTCTGGT
	RT-q-egl2-R	TTCGTGTCCGTGATGATGTTGC
RT-qPCR of xyn1	RT-q-xyn1-F	CATGAAGTGGGATGCTACTGAGCC
	RT-q-xyn1-R	CGATGACCGAGGTGAGCGAGT
RT-qPCR of cre1	RT-q-cre1-F	GAATCTTCCCCCGCCGCTCAG
	RT-q-cre1-R	CTCGCCAACATTGCCACATCC
RT-qPCR of xyr1	RT-q-xyr1-F	ATGGATGATACCGATTACCAGAACG
	RT-q-xyr1-R	TGGGAGGAAGTAGCCAAAGATGC
RT-qPCR of actin	RT-q-actin-F	AACGCTCCTGCCTTCTAC
	RT-q-actin-R	GTAACACCATCACCAGAGTC
Construction of pET-51b-MtHAC-1$_{126\text{-}190}$ plasmid		
Cloning of MtHAC-1$_{126\text{-}190}$ encoding gene	MtHAC-1$_{126\text{-}190}$-F	ccgacgtcggtcgacaagcttGAGAAGGAACAGCGGCGAG
	MtHAC-1$_{126\text{-}190}$-R	agctcctgcggccgcaagcttGGCACCGCTGCCACCCCG
The obtain of probes for EMSAs		

PCR amplification of bgl1-P2	bgl1-P2-F	CGCTCAGCGTGACATCCG
	bgl1-P2-R	GTGGGAAAATCTTCTTGCGCG
PCR amplification of cbh1-P1	cbh1-P1-F	ATCATTCGATGGCTGACTGGC
	cbh1-P1-R	GGCGGAAGAGGATCAGCAC
PCR amplification of egl2-P2	egl2-P2-F	ACTTGGCGAACGGAGATTTCC
	egl2-P2-R	CTGTGCCCGGAGCGGCAT
PCR amplification of xyn1-P2	xyn1-P2-F	TTCTTCTCGATGGCTTGCACC
	xyn1-P2-R	GACCGTCCTGGAATCTTCGAG
PCR amplification of xyn1-P3	xyn1-P3-F	CTGGGTTAACCAGCCCGTATT
	xyn1-P3-R	ACAGACGGATTGATGCCATGC
PCR amplification of xyr1-P2	xyr1-P2-F	GAGGACTGGCCAAGCGCT
	xyr1-P2-R	GGGGTAAGGTCAGTAGCAGGC

Note: The green capital nucleotides indicate the protospacer sequence of MYCTH_2310995 gene. The lowercase nucleotides represent homologous arm fragments for constructing corresponding vectors.

Chapter 4 Transcription factor MtCLR-2 regulates cellulase production via direct modulation of *Mtegl2* and *Mtbgl1* expression in *Myceliophthora thermophila*

The content of this chapter has been published as

Yapeng Lai., Juan Wang., Ning Xie., Gang Liu., Donnabella Lacap-Bugler., **2026**. Transcription factor MtCLR-2 regulates cellulase production via direct modulation of *Mtegl2* and *Mtbgl1* expression in *Myceliophthora thermophila*. https://doi.org/10.1186/s12934-026-02976-1

4.1 Prelude

In Chapter 2, comparative transcriptomic analysis of *M. thermophila* grown on Avicel and glucose identified a gene, *MYCTH_38704*, encoding a transcription factor homologous to the well-studied cellulase regulator CLR-2 from *Neurospora crassa*. This gene exhibited significantly higher expression level under cellulose-inducing conditions, suggesting that MtCLR-2 may be involved in cellulose degradation. However, the specific function and underlying molecular mechanism of MtCLR-2 in regulating cellulase gene expression remains unclear. In this chapter, the regulatory role of MtCLR-2 in cellulose deconstruction was investigated. Using gene manipulation, enzymatic activity assay, and transcriptomic analyses described in Chapters 2 and 3, revealed that MtCLR-2 acts as a pivotal activator of cellulase gene expression. Enzymatic activity assays showed that deletion of *Mtclr-2* substantially reduced cellulase activities, with the most pronounced effect observed in endoglucanase production. In contrast, overexpression of *Mtclr-2* enhanced cellulase secretion when the fungus was cultivated on Avicel. Fluorescence microscopy confirmed that MtCLR-2 localizes in the nucleus, consistent with its regulatory role as a transcriptional regulator. Moreover, subsequent DNA and protein interaction analyses demonstrated that MtCLR-2 directly binds to the promoter regions of key cellulase genes in a zinc-dependent manner. Interestingly, transcriptomic profiling indicated that MtCLR-2 also influences the expression of ribosomal protein genes under cellulosic conditions, which was not previously reported for CLR-2 homologs in other fungal species. These findings contribute to a better understanding of the regulatory network governing cellulase production in *M. thermophila* and identify MtCLR-2 as a promising target for engineering strains with improved cellulase biosynthesis.

4.2 Introduction

Lignocellulose, the most abundant renewable energy source on earth, can be converted into fermentable sugars for the production of biofuels and value-added biochemicals in biorefineries (Li et al., 2022c). The primary components of lignocellulosic material are cellulose, hemicellulose, and lignin, with cellulose accounting for the highest proportion (40-50%) (Gupta et al., 2016). The complete hydrolysis of cellulose requires the concerted activities of three complementary cellulase enzymes, which are endo-1,4-β-glucanase (EC 3.2.1.4), cellobiohydrolase (EC 3.2.1.91), and β-glucosidase (EC 3.2.1.21). These three cellulases act synergistically to decompose cellulose to release glucose as the final product that can be subsequently fermented into ethanol (Taha et al., 2016). In addition, lytic polysaccharide monooxygenases (LPMOs; AA9) have been shown to work in synergy with cellulolytic enzymes during the decomposition of the recalcitrant cellulose (Frommhagen et al., 2018a). These copper-dependent enzymes oxidatively cleave glycosidic bonds of the cellulose when reducing agents are present, thus improving the efficiency of cellulases and promoting the enzymatic conversion of cellulose (Andlar et al., 2018).

Filamentous fungi are highly efficient decomposers of lignocellulose in the terrestrial biosphere due to their ability to secrete a broad spectrum and large amounts of extracellular enzymes associated with the deconstruction of plant-derived biomass (Makela et al., 2014; Mattam et al., 2022). Among others, *Myceliophthora thermophila* is known for the production of a wide array of thermostable carbohydrate-active enzymes (CAZymes) involved in lignocellulose degradation (Berka et al., 2011; Singh, 2016). Recently, this fungus has been genetically modified to produce cellulases and xylanases, as well as biochemicals and biofuels, such as fumaric acid, malic acid, and ethanol (Liu et al., 2017; Gu et al., 2018; Li et al., 2019; Li et al., 2020a), based on the current omics technologies and fungal genome editing tools (Liu et al., 2017; Liu et al., 2019d). The *M. thermophila* genome encodes at least eight β-glucosidases (BGLs), seven endoglucanases (EGLs), and seven cellobiohydrolases (CBHs) (Karnaouri et al.,

2014). Among them, *egl2* (MYCTH_86753), *cbh1* (MYCTH_109566) and *cbh2* (MYCTH_66729), and *bgl1* (MYCTH_66804), which encode endoglucanase, cellobiohydrolases, and β-glucosidase, respectively, exhibit high transcript levels and secretion quantities when grown on various sources of lignocellulosic biomass compared to glucose (Berka et al., 2011; Kolbusz et al., 2014; Lai et al., 2025). These extracellular enzymes thus represent the major cellulases of *M. thermophila*. Therefore, a better understanding of the regulatory mechanism governing the expression of these cellulase genes would facilitate fungal strain engineering and elevate cellulase production in *M. thermophila*.

The transcriptional induction of cellulases or xylanases is strictly controlled by transcription factors (Huberman et al., 2016; Benocci et al., 2017). In *M. thermophila*, a couple of regulators that are involved in the lignocellulose depolymerization were identified, including MtXyr1, MtCre1, MtCLR-4, and MtTRC-1. MtXyr1 not only regulates the expression of genes encoding xylanolytic enzymes but also controls genes associated with pentose transport and catabolism, while having no noticeable effect on cellulase secretion (Wang et al., 2015; Dos Santos Gomes et al., 2019). MtCre1 acts as the primary transcriptional repressor of cellulolytic genes, and its silencing or disruption upregulates the transcription of cellulase genes and enhances cellulase production under inducing conditions (Yang et al., 2015; Liu et al., 2017). Analogous to its homolog CLR-4 in *Neurospora crassa*, MtCLR-4 plays a positive role in regulating cellulase gene expression by modulating its downstream targets, MtCLR-2 and MtXyr1, and the cAMP signaling pathway (Liu et al., 2019c). MtTRC-1 functions as a transcriptional activator, regulating cellulase production via modulating the expression of the transcription factor gene *Mthac-1* and the cellobiohydrolase gene *Mtcbh-1* (Li et al., 2022a). Recently, the Zn(II)2Cys6 transcription factor MtClr-5 was reported to be crucial for cellulose decomposition, as its deletion reduced endoglucanase activity and protein secretion under cellulolytic conditions (Xue et al., 2023). In addition, our recent study demonstrated that the forkhead regulator MtFkh1 represses major cellulase and xylanase gene expression by directly binding to their

promoter regions (Lai et al., 2025).

The transcription factor CLR-2 was first identified in *N. crassa* which is an essential regulator of cellulase, but not hemicellulase gene expression (Coradetti et al., 2012). The deletion of *clr-2* caused severe growth defects and completely abolished cellulase activity on Avicel, but not on xylan (Coradetti et al., 2012). Since then, orthologs of NcCLR-2 were fully characterized in other filamentous ascomycete fungi. The *Aspergillus nidulans* mutant carrying a disruption of *clrB*, the ortholog of *clr2*, failed to elicit cellulase gene expression and lost cellulolytic activity during growth on cellulose (Coradetti et al., 2012). Similarly, the ClrB (homolog of CLR-2) is indispensable for the production of cellobiohydrolases and endoglucanases in *Aspergillus niger* (Raulo et al., 2016; Kun et al., 2021). A recent study further showed the involvement of *A. niger* ClrB in the utilisation of xyloglucan and galactomannan (Kun et al., 2023). Also, ClrB acts as an activator of the cellulolytic gene expression in *Penicillium oxalicum* (Li et al., 2015b; Zhao et al., 2016). In *Aspergillus oryzae*, the CLR-2 ortholog (ManR) was reported as a regulator of both mannanolytic and cellulolytic enzyme genes (Ogawa et al., 2012,2013). However, the ortholog of CLR-2 was described in *Trichoderma reesei* and *Talaromyces cellulolyticus* but had only a minor impact on cellulase activity (Hakkinen et al., 2014; Fujii et al., 2015; Fujii et al., 2021). These results indicate both similarities and differences in the functions of NcCLR-2 orthologs. In our previous analysis of the *M. thermophila* transcriptome profiling data, we noted that *Mtclr-2* (*MYCTH_38704*), the ortholog of *N. crassa clr-2*, was highly upregulated under cellulosic conditions (Lai et al., 2025), implying that this gene may play roles in cellulose degradation. Indeed, the regulator MtCLR-2 has been found to be important for cellulase expression (Zhang et al., 2022). However, the detailed molecular basis of its role in the cellulase expression has still not been fully revealed.

In the present study, we further characterised the function of MtCLR-2 in cellulose utilisation in *M. thermophila*. By a combination of molecular genetic approaches and comparative transcriptomic analyses, we found that MtCLR-2 positively regulates

cellulase production by regulating the expression of the major endoglucanase gene (*egl2*) and β-glucosidase gene (*bgl1*) through directly binding to their promoter regions. In addition, we also demonstrated that MtCLR-2 is involved in ribosome biosynthesis, suggesting it regulates cellulase expression at both the transcriptional and translational levels.

4.3 Materials and methods

4.3.1 Strains and culture conditions

Myceliophthora thermophila (ATCC 42464) was used as parental strain throughout this work. Conidial suspensions of *M. thermophila* strains were prepared by culturing them on potato dextrose agar (PDA) plates at 45°C for 7 days. The spores were harvested and suspended in 0.2% (v/v) Tween-80 solution and counted using a hemocytometer. Regarding mycelial growth (for DNA extraction), the fungi were grown in Mandels medium containing 2% (w/v) glucose as carbon source, incubated at 45°C with shaking at 150 rpm for 36 h (Lai et al., 2025). For enzymatic activity assays, RT-qPCR, and comparative transcriptome analyses, mycelia were first pre-cultured from conidia in Mandels medium containing 2% (w/v) glucose for 36 h (final concentration, 1×10^6 spores mL^{-1}). The mycelia were then washed with carbon-free Mandels medium, and an equal amount (0.55 g) of wet mycelia was transferred into 50 mL of Mandels medium supplemented with 2% (w/v) Avicel (Sigma-Aldrich, Darmstadt, Germany), and incubated at 45°C with shaking at 150 rpm for 48–96 h. For fungal colony morphology and conidiation assays, 1.5 μL of spore suspensions (1×10^7 mL^{-1}) from *M. thermophila* strains were inoculated onto the center of PDA and solid plates containing 1% (w/v) Avicel and cultivated at 45°C for 3–7 days. For growth observation in liquid culture, conidia of fungal strains were added to 50 mL Mandels medium supplemented with 2% (w/v) glucose or 2 % (w/v) Avicel (final concentration, 1×10^6 conidia mL^{-1}), and grown at 45°C for 36 h. Mycelia from the liquid shaking cultures were then harvested for microscopic analysis using light microscopy.

Escherichia coli DH5α was used for plasmid construction and propagation, cultured at 37℃ in Luria-Bertani (LB) medium supplemented with ampicillin (100 μg mL^{-1}).

4.3.2 Plasmid construction

All the primer sequences used in this study are listed in Table S4.1. For the knockout of *Mtclr-2* (MYCTH_38704) using the CRISPR/Cas9 system, the Cas9-U6p-*Mtclr-2*-sgRNA expression cassette was constructed as described previously (Lai et al., 2025). Specific sgRNA target site for *Mtclr-2* was identified using the sgRNACas9 tool with minimum off-target effects (Xie et al., 2014). The DNA fragments, including the U6 promoter of *M. thermophila*, and the target DNA sequence that fused with sgRNA scaffold were obtained by PCR using the pFC332-Cas9-U6p-sgRNA scaffold vector as the template (Lai et al., 2025) and cloned into the pFC332 vector to create the plasmid Cas9-U6p-*Mtclr-2*-sgRNA. To construct donor DNA vector, the 5′ and 3′ flanking segments of *Mtclr-2* were separately amplified from *M. thermophila* genomic DNA by PCR, fused with the selectable marker cassette P*gpd-neo* from a pBC-*neo* plasmid (Li et al., 2020d), and inserted into the HindIII and EcoRI sites of pUC19 plasmid to generate Donor-*Mtclr-2-neo* using One Step Cloning Kit (Vazyme Biotech, Nanjing, China).

To generate *Mtclr-2* overexpression vector, the gene-coding region of *Mtclr-2* was amplified from genomic DNA and ligated into pUC19-P*pdc*-T*gpdA-hph* plasmid at the NotI and XbaI sites, under the control of the strong constitutive *Mtpdc* (MYCTH_112121, pyruvate decarboxylase) promoter of *M. thermophila*. Similarly, for intracellular localization analysis of MtCLR-2, the PCR-amplified *Mtclr-2* coding region without the stop codon and the *gfp* (green fluorescent protein) gene were assembled and cloned into the NotI and XbaI sites of pUC19-P*pdc*-T*gpdA-hph* plasmid to generate the *Mtclr-2-gfp* cassette.

4.3.3 Transformation of *Myceliophthora thermophila* protoplasts

Protoplast preparation and transformation of *M. thermophila* was conducted in line with a previously reported procedure (Lai et al., 2025). Possible transformants for gene deletion or overexpression in *M. thermophila* were screened for resistance to neomycin and hygromycin B (75 μg mL^{-1} hygromycin B combined with 100 μg mL^{-1} G418) or to hygromycin B alone (75 μg mL^{-1}) after 4-5 days of culture on PDA plates. Positive transformants were verified by PCR analysis with different specific primer pairs (Table S4.1), followed by sequencing.

4.3.4 Protein and enzyme activity assays

The extracellular protein concentration in the culture supernatant was measured using a Modified Bradford Protein Assay kit (Sangon Biotech, Shanghai, China) based on absorbance at 595 nm. A 20 μL aliquot of culture supernatant was loaded on a 10% polyacrylamide gel (PAGE Gel Quick Preparation Kit, Yeasen Biotech, Nanjing, China) to analyse the proteins by SDS-PAGE. Cellulase activities, including filter paper cellulase (FPase), endoglucanase (CMCase), β-glucosidase (pNPGase), and cellobiohydrolase (pNPCase), were determined as previously described (Lai et al., 2025). One unit (U) of enzymatic activity was defined as the amount of enzyme that releases 1 μmol of either glucose or *p*-nitrophenol (*p*NP) from the substrate per minute under standard assay conditions.

4.3.5 Fluorescence microscopy examination

To determine subcellular localization of MtCLR-2 in *M. thermophila*, MtCLR-2-GFP positive transformants were inoculated into Mandels medium containing 2% (w/v) glucose or 2% (w/v) Avicel as the sole carbon source and cultivated for 36 h at 45 °C. The mycelia were collected and incubated in darkness with 5 mg L^{-1} 4′,6-diamidino-2-phenylindole (DAPI) solution for 15 min, and then washed with PBS solution three times. Fungal mycelia were observed under an Olympus BX53 fluorescence microscope, and the images were processed using Olympus cellSens Standard software.

4.3.6 Real-time quantitative PCR

Total RNA was extracted from frozen mycelia using an RNA extraction kit TransZol Up (TransGen Biotech, Beijing, China) according to the manufacturer's instructions. Reverse transcription was performed using the HiScript III RT SuperMix kit with gRNA wiper (Vazyme Biotech, Nanjing, China) following the manufacturer's protocols. Quantitative PCR was performed with Hieff UNICON Universal Blue qPCR SYBR Green Master Mix (Yeasen Biotech, Shanghai, China), as described in our previous study (Lai et al., 2025). The transcript level of each gene was estimated by the $2^{-\Delta\Delta CT}$ method (Livak and Schmittgen, 2001) with the *actin* gene (MYCTH_2314852) as an internal control. The relative transcript level was determined by calculating the radio of the transcript level in the *Mtclr-2* deletion mutant to that in the WT control, which was set as 100 %. Each reaction was conducted in triplicate.

4.3.7 Expression and purification of the MtCLR-2 DNA-binding domain

The three exon-coding sequences of *Mtclr-2* were first obtained by amplifying from *M. thermophila* genomic DNA using the primer sets shown in Table S4.1. These fragments were then assembled and inserted into the HindIII stie of pET-51b to generate pET-51b-MtCLR-$2_{1\text{-}798}$ plasmid. Due to the short length and limited expression of the MtCLR-2 DNA-binding domain (amino acids 44 to 75), an extended fragment comprising amino acids 30 to 89, which includes the core domain and 14 additional residues on both the N- and C-terminal sides, was selected for expression. To express the MtCLR-2 DNA-binding domain, the sequence encoding the amino acids 30 to 89 was amplified by PCR from the pET-51b-MtCLR-$2_{1\text{-}798}$ plasmid and was ligated into the pET-51b to create the pET-51b-MtCLR-$2_{30\text{-}89}$ recombinant plasmid. The codon optimized pUC57-MtCLR-$2_{1\text{-}272}$ vector, containing DNA sequence that encodes amino acids 1 to 272, was synthesized by IGE Biotechnology (Guangzhou, China). This plasmid includes an additional 14 amino acids that were absent in the MtCLR-2 DBD compared to the NcCLR-2 DBD. For the expression of the MtCLR-2 DBD that restores the missing 14

amino acids (residues 30 to 103), the corresponding DNA sequence was amplified by PCR using the pUC57-MtCLR-$2_{1\text{-}272}$ plasmid as the template and was inserted into HindIII-digested pET-51b to obtain the recombinant vector pET-51b-MtCLR-$2_{30\text{-}103}$. The recombinant plasmids were subsequently introduced into *E. coli* BL21(DE3) for protein expression, and the Strep II-tagged proteins were purified and verified as described previously (Lai et al., 2025).

4.3.8 Electrophoretic mobility shift assays

EMSAs were carried out as previously reported (Lai et al., 2025). Briefly, promoter regions of *bgl1* (MYCTH_66804, P2, − 650 to − 300), *egl2* (MYCTH_86753, P2, − 650 to – 300; P3, − 1000 to − 600) were amplified from *M. thermophila* genomic DNA using specific primers shown in Table S4.1. For each EMSA reaction, varying amounts of purified recombinant MtCLR-$2_{30\text{-}89}$ (0-0.04 μg) or MtCLR-$2_{30\text{-}103}$ (0-0.1 μg) were incubated with a fixed amount (100 ng) of the corresponding DNA probe in binding buffer, with or without $ZnSO_4$ at a final concentration of 12.5 mM, at 25°C for 30 min

4.3.9 Analysis of transcriptomic data

The quality and quantity of total RNA extracted from *M. thermophila* wild-type strain and its mutant were assessed using agarose gel electrophoresis and a NanoDrop 2000 Spectrophotometer (Thermo Scientific, Waltham, MA, USA). High-quality purified RNA was used for RNA sequencing (RNA-seq) on the Illumina NovaSeq 6000 platform, performed by Gene Denovo Biotechnology Corporation (Guangzhou, China). Clean reads were generated and mapped to the *M. thermophila* ATCC 42464 genome using HISAT2 v2.4 (Kim et al., 2015). Gene expression levels were calculated using RSEM software (Li and Dewey, 2011), with transcript abundance represented as fragments per kilobase of transcript per million mapped reads (FPKM). Differential gene expression analysis was conducted using DESeq2 (Love et al., 2014), with criteria set at an absolute fold change > 2 and an adjusted *P*-value (padj) < 0.05. The detailed data are shown in Additional file 10: Table S2. Gene Ontology (GO) enrichment analysis was

performed using OmicShare tools (https://www.omicshare.com/tools). All differentially expressed genes (DEGs) were mapped to GO terms in the Gene Ontology database (http://www.geneontology.org/), and significantly enriched GO terms (*P*-value < 0.05) were identified via a hypergeometric test against the *M. thermophila* genome background. The raw transcriptome sequencing data have been deposited in the Gene Expression Omnibus (GEO) database under the accession number GSE305312 at the National Center for Biotechnology Information (NCBI).

4.4 Results

4.4.1 Identification of the MtCLR-2 protein

The *M. thermophila Mtclr-2* (MYCTH_38704) is 2570 bp in length and contains three exons encoding a protein composed of 798 amino acids (aa) (Figure 4.1). A BLASTP search of the *M. thermophila* genome, using the *N. crassa* CLR-2 (NCU08042, NcCLR-2) protein sequence as a query, revealed MYCTH_38704 as a putative ortholog of NcCLR-2, sharing 81% sequence identity with this close ortholog. In addition, the InterPro analysis (https://www.ebi.ac.uk/interpro/) showed the presence of a typical fungal transcription factor domain (IPR007219) between residues 259 and 434 of MtCLR-2 (Fig. 1). However, compared to NcCLR-2, MtCLR-2 lacks 14 aa in its Zn(II)2Cys6 fungal-type DNA-binding domain (DBD), between residues 44 and 75, which may explain why InterPro analysis did not detect this domain in MtCLR-2.

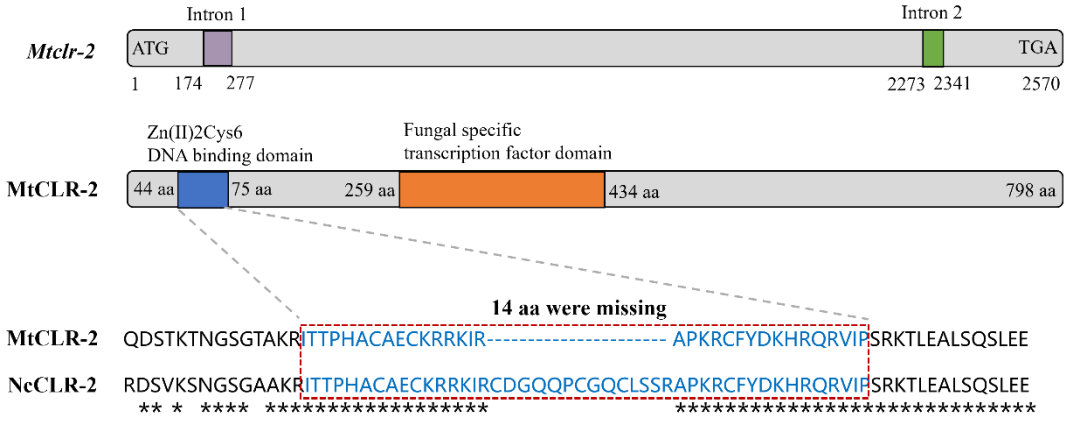

Figure 4.1. Schematic representation of the *Mtclr-2* gene structure and the predicted functional domains of the MtCLR-2 protein. MtCLR-2 lacks 14 aa in its putative Zn(II)2Cys6 fungal-type DNA-binding domain compared to NcCLR-2. NcCLR-2, *N. crassa* CLR-2.

4.4.2 Positive effect of MtCLR-2 on the production of cellulase in *M. thermophila*

To confirm the influence of MtCLR-2 on cellulase induction, we constructed *Mtclr-2* deletion mutants by using CRISPR/Cas9 system (Figure S4.1). The protospacer sequence targeting *Mtclr-2* was designed for gene editing (Table S4.1). The Cas9-U6p-*Mtclr-2*-sgRNA plasmid was co-transformed into *M. thermophila* wild-type (WT) protoplasts along with a donor DNA vector carrying the neomycin resistance gene cassette (P*gpd-neo*) flanked by the 5′ and 3′ homologous arms of *Mtclr-2*. Deletion of the *Mtclr-2* gene was accomplished via homologous recombination mediated by the CRISPR/Cas9 system. The obtained disruption strains were verified by genomic PCR with three specific primer pairs (Figure S4.2). After 48-96 h growth in Avicel medium, the Δ*Mtclr-2* mutants displayed a marked reduction in filter paper enzyme activity (by 56% to 60%) and β-glucosidase activity (by 26% to 40%), while endoglucanase activity was almost abolished (reduced by 90% to 92%) compared with those of the WT (Figure 4.2A-C). Moreover, Δ*Mtclr-2* secreted 48% to 64% less protein than the WT under cellulosic conditions (Figure 4.2D), as confirmed by SDS-PAGE analysis of extracellular proteins (Figure S4.3).

Meanwhile, the *Mtclr-2* overexpression strain OE-*Mtclr-2* was created, in which *Mtclr-2* was driven by the strong constitutive pyruvate decarboxylase (MYCTH_112121) promoter P*pdc*. The positive overexpression mutant was validated by genomic PCR using specific primer set (Figure S4.2). As expected, OE-*Mtclr-2* strain exhibited a significant elevation in filter paper enzyme activity (83% to 216%), β-glucosidase activity (132% to 143%), endoglucanase activity (138% to 190%), and secreted protein (150% to 293%), compared to those of the WT when cultivated on Avicel (Figure 4.2A-D). These results demonstrate that MtCLR-2 is an activator of cellulase production under cellulose induction in *M. thermophila*.

Furthermore, the role of MtCLR-2 in fungal development was explored. As shown in Figure 4.3A, the Δ*Mtclr-2* mutant showed similar colony phenotype to that of the WT and OE-*Mtclr-2* strains when grown on PDA and solid Avicel media. In addition, both the *Mtclr-2* disruption and overexpression strains produced comparable numbers of asexual spores to the WT after 7 days of growth on Avicel plates (Figure 4.3B). These observations suggest that MtCLR-2 is dispensable for hyphal radial growth or sporulation on solid cellulose medium. However, the Δ*Mtclr-2* mutant grew poorly in liquid cellulose culture, characterized by aberrant mycelial morphology with few hyphal branches after 36 h (Figure 4.3C), but exhibited normal growth in liquid glucose medium (Figure S4.4), which was similar to *N. crassa* Δ*clr-2* and *A. nidulans* Δ*clrB* mutants (Coradetti et al., 2012). This growth impairment implies a specific defect associated with cellulose utilisation, which is in accordance with the substantially decreased cellulase production observed in the mutant Δ*Mtclr-2*.

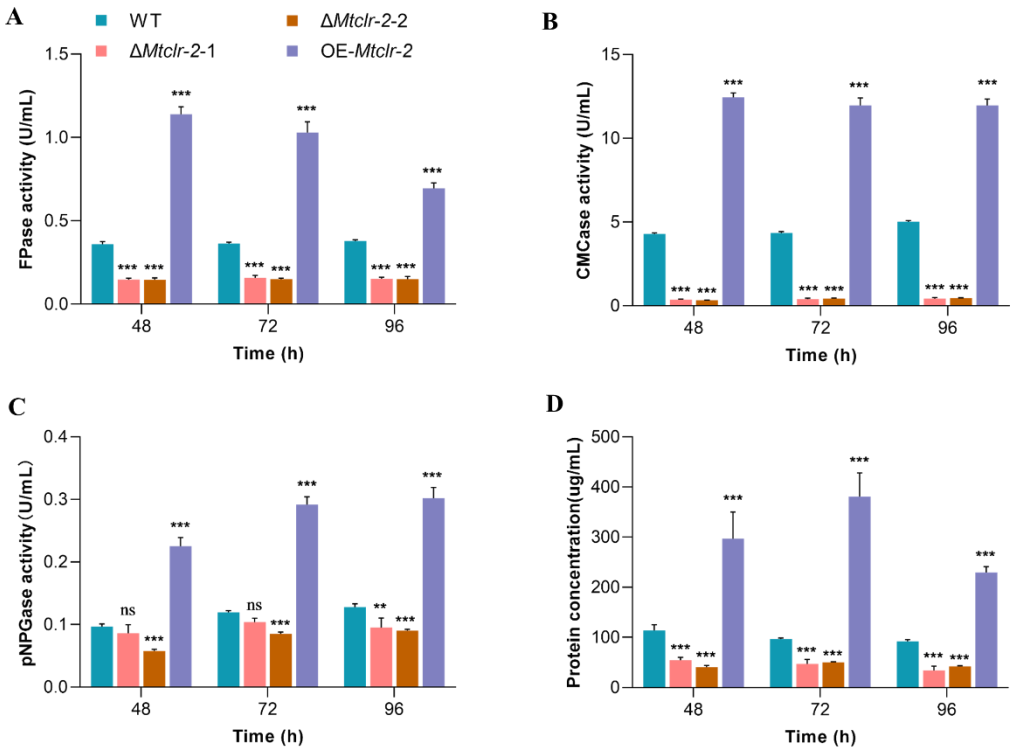

Figure 4.2. Cellulase activities and protein production of *M. thermophila* WT strain, Δ*Mtclr-2* mutants, and OE-*Mtclr-2* strain. (A) Filter paper cellulase (FPase) activity. (B) Endoglucanase (CMCase) activity. (C) β-glucosidase (pNPGase) activity. (D) Extracellular protein concentration. These *M. thermophila* strains were pre-grown in glucose for 36 h and then transferred to 2% (w/v) Avicel medium and cultured for 48-96 h. $^{**}p < 0.01$, and $^{***}p < 0.001$ indicate significant differences between the WT and Δ*Mtclr-2* mutants or OE-*Mtclr-2* strain (Two-way ANOVA), ns indicates not significant. Error bars represent the SD from three replicates.

4.4.3 Subcellular localization of MtCLR-2 in *M. thermophila*

To assess the subcellular localization of MtCLR-2, the *Mtclr-2* open reading frame was fused to the *gfp* (green fluorescent protein encoding gene) under the control of the *Mtpdc* promoter (Figure S4.2). This expression cassette was introduced into the WT strain, generating a strain expressing MtCLR-2-GFP. After growth in both glucose and Avicel media for 36 h, the MtCLR-2-GFP signal was found to be accumulated in the nuclei across the fungal hyphae. This signal overlapped with the blue fluorescence of the nucleic acid-specific dye DAPI (Figure 4.3D), confirming that MtCLR-2 localizes

in the *M. thermophila* nucleus under both glucose-repressing and cellulose-inducing conditions (Figure S4.5).

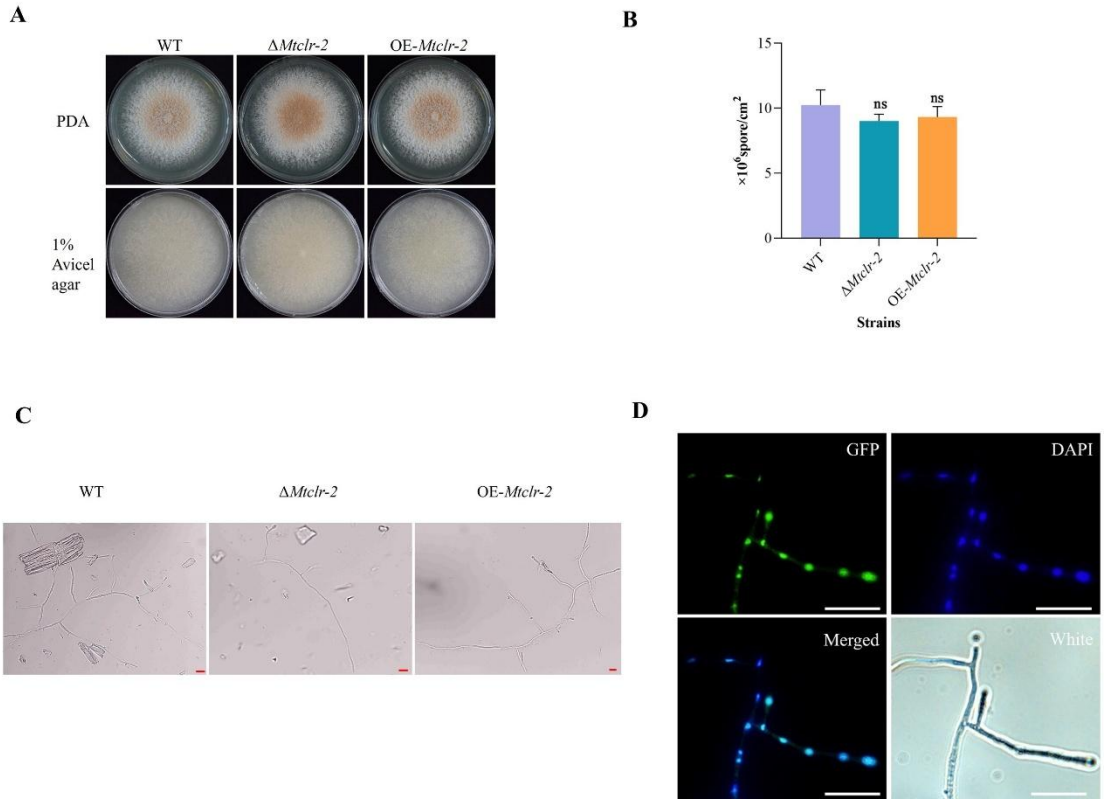

Figure 4.3. Phenotypic analyses of *M. thermophila* WT, Δ*Mtclr-2*, and OE-*Mtclr-2* strains and subcellular localization of MtCLR-2 protein. (A) Colony phenotype on PDA and 1% (w/v) Avicel solid plates after 3 (PDA) or 4 days (Avicel) of growth at 45°C. (B) Quantitative determination of conidiation on plates containing 1% (w/v) Avicel cultivated at 45°C after 7 days. ns indicates no noticeable differences between WT and Δ*Mtclr-2*, or OE-*Mtclr-2* strains (Student's t tests). Error bars represent the SD from three replicates. (C) Microscopic observation of fungal mycelia after 36 h of cultivation in liquid shaking flasks containing 2% (w/v) Avicel as the sole carbon source. Scale bar = 10 μm. (D) Subcellular location of MtCLR-2 in *M. thermophila*. MtCLR-2-GFP strain was cultivated in liquid medium containing 2% (w/v) glucose as the sole carbon source at 45°C for 36 h. Scale bar = 20 μm.

4.4.4 MtCLR-2 regulates the expression of major cellulase genes

To test whether MtCLR-2 exerts its impact on cellulase production at the transcriptional level, we analysed the expression of cellulase genes in the WT strain and Δ*Mtclr-2* mutant using real-time quantitative reverse transcription PCR (RT-qPCR). As shown in Figure 4.4, the β-glucosidase gene *bgl1* (*MYCTH_66804*) exhibited 29% to 32% reductions in transcription levels in the *Mtclr-2* deletion strain compared with the WT during the entire induction period (24-72 h) on Avicel. Similarly, transcript level of the endoglucanase gene *egl2* (*MYCTH_86753*) was substantially decreased (by 32-fold) in Δ*Mtclr-2* mutant after 24 h of growth in Avicel medium, and was reduced by 47% to 80% at 48 and 72 h. These results are in agreement with the observed reduction in cellulase activity in the Δ*Mtclr-2* strain. Additionally, the effects of MtCLR-2 on the transcriptional levels of key regulatory genes, including *cre1* (*MYCTH_2310085*) and *xyr1* (*MYCTH_2310145*), were examined. The transcription of *cre1* and *xyr1* was not significantly altered by the deletion of *Mtclr-2* throughout the cultivation period under cellulose-inducing conditions (Figure 4.4). These observations imply that MtCLR-2 influences cellulase production primarily through regulating cellulase gene transcription.

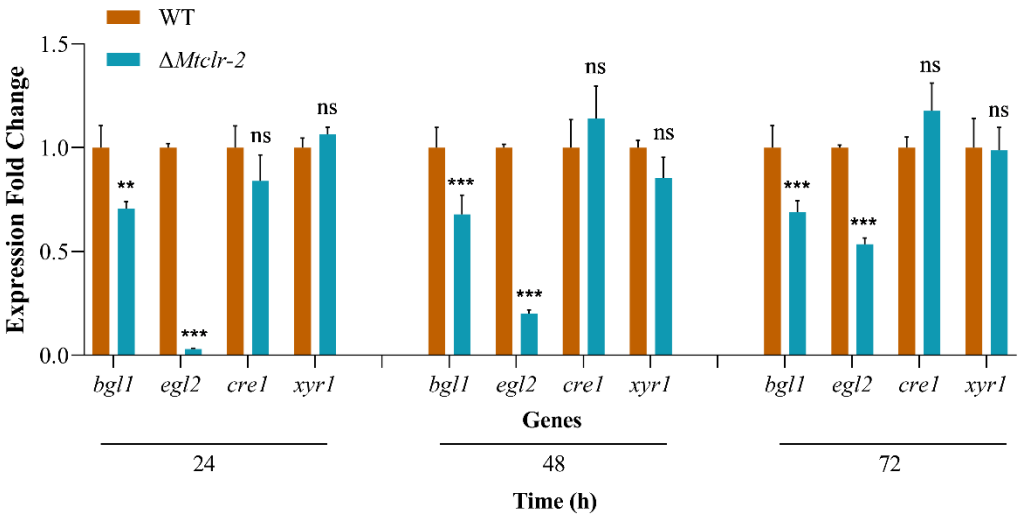

Figure 4.4. Relative transcription levels of major cellulase genes *bgl1* and *egl2* as well as the regulatory genes *cre1* and *xyr1* in *M. thermophila* WT and Δ*Mtclr-2* strains. Strains were pre-grown in glucose for 36 h, washed and transferred to 2% (w/v) Avicel medium and cultivated for 24, 48, and 72 h. The expression level of each gene in Δ*Mtclr-2* was normalized to the level of the corresponding gene in WT. $^{**}p < 0.01$, and $^{***}p < 0.001$ represent significant differences between the Δ*Mtclr-2* and WT strains (Two-way ANOVA), ns indicate no significant difference. Error bars represent the SD from three replicates.

4.4.5 MtCLR-2 binds to the promoter regions of *Mtbgl1* and *Mtegl2* in a zinc-dependent manner

To determine whether MtCLR-2 directly regulates the expression of *bgl1* and *egl2*, electrophoretic mobility shift assays (EMSAs) were performed. Given that MtCLR-2 lacks 14 aa within its DBD compared to NcCLR-2, we wondered whether this loss affects its DNA-binging capability. To answer this question, Strep II-fused DNA binding domain of MtCLR-2 (MtCLR-$2_{30\text{-}89}$) and MtCLR-$2_{30\text{-}103}$, which restores the missing 14 aa, were expressed and purified from *E. coli* BL21(DE3) (Figure S4.6). DNA Probes corresponding to the promoter regions of *bgl1* (P2, − 650 to − 300) and *egl2* (P2, − 650 to – 300; P3, − 1000 to − 600) were obtained by PCR. In the initial EMSAs, neither MtCLR-$2_{30\text{-}89}$ nor MtCLR-$2_{30\text{-}103}$ exhibited detectable binding to the

upstream regions of *bgl1* or *egl2* (Figure 4.5A-B). Considering that MtCLR-2 is a predicted Zn(2)-C6-type TF, we hypothesized that zinc ions may be required for its DNA-binding activity. To test this, zinc ions were supplemented in the EMSA reaction buffer. Under these conditions, both MtCLR-$2_{30\text{-}89}$ and MtCLR-$2_{30\text{-}103}$ bound to the promoter regions of *bgl1* and *egl2* and the size of protein-DNA complex increased along with increasing amounts of MtCLR-$2_{30\text{-}89}$ and MtCLR-$2_{30\text{-}103}$ (Figure 4.5A-B). These findings suggest that MtCLR-2 binds its target genes in the presence of zinc ions and the absence of the 14 aa in its DBD has no impact on its ability to recognize and bind target promoters.

Previous ChIP-seq (chromatin immunoprecipitation and next-generation sequencing) analysis revealed a conserved $CGG_{N11}CCG$ motif in the upstream regions of NcCLR-2-bound genes, which is nearly identical to the DNA-binding motif of its closest paralog, Gal4p, in *Saccharomyces cerevisiae* (Craig et al., 2015). To determine whether MtCLR-2 recognizes a similar motif, we searched for the promoter regions *bgl1*-P2, *egl2*-P2, and *egl2*-P3. The conserved $CGG_{N11}CCG$ sequences were found in all these promoters, with *egl2*-P2 and *egl2*-P3 sharing identical motif fragments within their overlapping region (Figure 4.5C). Thus, MtCLR-2 may identify and bind the $CGG_{N11}CCG$ motif in the promoter regions of its target genes, analogous to its homolog NcCLR-2.

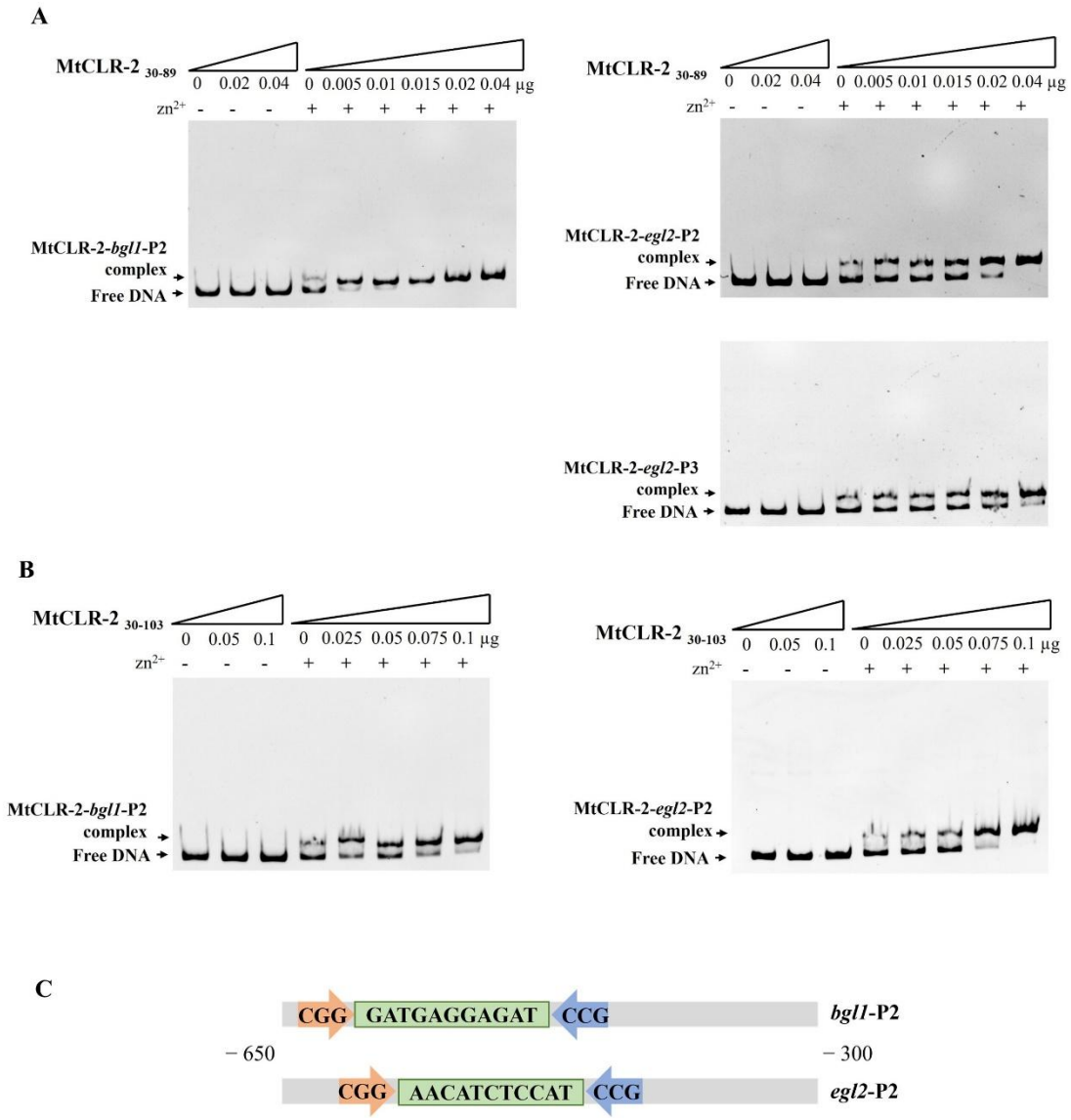

Figure 4.5. Electrophoretic mobility shift assays (EMSAs) of the interactions between MtCLR-2 and the promoter regions of major genes encoding cellulases. (A) EMSAs of the binding between MtCLR-$2_{30\text{-}89}$ and the promoter regions of *bgl1* and *egl2* in the presence or absence of zinc ions. (B) EMSAs of the binding between MtCLR-$2_{30\text{-}103}$ and the promoter regions of *bgl1* and *egl2* in the presence or absence of zinc ions. The concentration of zinc ions in the reaction buffer was 25 mM. (C) Schematic diagram of the putatively conserved MtCLR-2 binding motif in the promoter regions of *bgl1* and *egl2*. MtCLR-2 may identify and bind the $CGG_{N11}CCG$ motif in the promoter regions of its target genes, box in green indicates variable N_{11} nucleotides.

4.4.6 Transcriptomic analysis of the *Mtclr-2* deletion mutant on Avicel

To obtain a genome-wide understanding of the molecular mechanism by which MtCLR-2 regulates cellulase production, transcriptional profile analysis was performed using the Δ*Mtclr-2* mutant grown on Avicel with the WT as comparison strain. When compared to WT, transcript levels of 2228 genes were markedly altered in mutant Δ*Mtclr-2* after 48 h of growth, with 1323 genes showing significantly decreased transcription and 905 genes displaying substantial upregulation (Figure 4.6A). A Gene Ontology (GO) analysis revealed that these differentially expressed genes (DEGs) in Δ*Mtclr-2* were enriched in the functional categories of cytosolic ribosome, polysaccharide metabolic process, and cellulose binding (Figure 4.6B), in accordance with the phenotypes observed in Δ*Mtclr-2* in response to cellulose.

Comparative transcriptomic analysis revealed that three endoglucanase genes including *egl2*, *MYCTH_52068*, and *MYCTH_111372*, were remarkably downregulated in Δ*Mtclr-2* in comparison to WT, except for *MYCTH_116157* (Figure 4.6C), which was in line with the endoglucanase secretion phenotype when exposed to Avicel. Three intracellular β-glucosidase genes (*MYCTH_115968*, *MYCTH_62925*, and *MYCTH_38200*) showed lower expression levels by the deletion of *Mtclr-2*. Likewise, the transcript levels of two extracellular β-glucosidase genes, *bgl1* and *MYCTH_58882*, were reduced by approximately 25% ($\log_2$ fold change = – 0.42 and – 0.41, respectively) in the Δ*Mtclr-2* mutant, which was consistent with RT-qPCR results showing lower transcript of *bgl1* in the mutant strain, although the expression changes did not reach the strict differential analysis criteria. In addition, nine genes encoding LPMOs (AA9 family) exhibited lower transcription levels in the Δ*Mtclr-2* mutant than in the WT, with the exception of *MYCTH_2311323* (Figure 4.6C). Among these, MtLPMO9B (MYCTH_80312), MtLPMO9C (MYCTH_100518), MtLPMO9D (MYCTH_92668), and MtLPMO9J (MYCTH_79765), were found to be active against cellulose (Frommhagen et al., 2016; Frommhagen et al., 2018b; Kadowaki et al., 2018), and MtLPMO9I (MYCTH_46583) was shown to have strong synergistic effects with endoglucanase, resulting in elevated enzymatic hydrolysis yields toward cellulose

(Karnaouri et al., 2017). Similar observation was reported in *N. crassa*, where disruption of *Ncclr-2* led to decreased expression of several secreted endoglucanase genes and one predicted intracellular β-glucosidase gene as well as one extracellular β-glucosidase gene (Coradetti et al., 2012; Coradetti et al., 2013), while its constitutive expression caused the upregulation of several LPMO-encoding genes (Craig et al., 2015), confirming the conserved role of CLR-2 orthologs in regulating genes involved in cellulose decomposition.

Besides these cellulose degrading genes, 56 genes encoding putative transcription factors (TFs) were also observed showing altered expression levels, with 19 genes being downregulated and 37 genes being upregulated in the Δ*Mtclr-2* mutant (Figure 4.6C). The majority of these TFs can be classified into Fungal Zn(II)2Cys6, Fungal_TF, and Zinc finger C2H2 families. Of these, the gene encoding CLR-4 (MYCTH_2296492), which positively regulates cellulase gene expression (Liu et al., 2019c), was downregulated (log2 fold change = – 1.02) in the absence of *Mtclr-2*. In contrast, one gene encoding MtCOL-26 (MYCTH_2301920), a repressor of cellulase production (Xu et al., 2018), was highly induced in strain Δ*Mtclr-2* (log_2 fold change = 1.83). Therefore, the downregulation of *Mtclr-4* and upregulation of *Mtcol-26* may partially account for the reduced cellulase production seen in the Δ*Mtclr-2* mutant. Consistent with the RT-qPCR analysis above, the essential regulatory genes *Mtcre1* and *Mtxyr1* displayed no differential expression between Δ*Mtclr-2* and WT strains.

Genes encoding predicted sugar transporters were also differentially expressed in the *Mtclr-2* disruption strain (Figure S4.7). Among 15 genes annotated as transporters for glucose, xylose, cellodextrin, cellobionic acid, or other sugars, two genes increased their transcription in Δ*Mtclr-2*, whereas the remaining genes decreased. Notably, *MYCTH_2302958* and *MYCTH_84164*, showed transcriptional changes, with the former downregulated (log_2 fold change = − 4.7) and the latter upregulated (log_2 fold change = 2.3). These two genes encode proteins that share 55% and 54% sequence similarity, respectively, with cellobionic acid transporter CBT-1 in *N. crassa*, which suppresses cellulase induction on both cellobiose and Avicel (Cai et al., 2015; Li et al.,

2015a). Whether the altered expression of these putative *cbt-1* homologs contributes to the decreased cellulase induction observed in the Δ*Mtclr-2* mutant remains to be elucidated.

Intriguingly, a set of ribosomal protein genes exhibited reduced transcript abundance in the mutant Δ*Mtclr-2*, including 25 potential genes encoding 40S small ribosomal subunit proteins and 36 encoding 60S large ribosomal subunit proteins (Figure 4.6D). Additionally, seven genes encoding putative mitochondrial ribosomal proteins, including three small ribosomal protein genes and four large ribosomal protein genes, were also downregulated upon *Mtclr-2* disruption (Figure 4.6D). Noteworthily, such transcriptional repression of ribosomal protein genes has not been reported in other fungal species where the roles of MtCLR-2 homologs have been explored. These findings suggest that MtCLR-2 may regulate the production of cellulase not only at the transcriptional level but potentially also at the translational level.

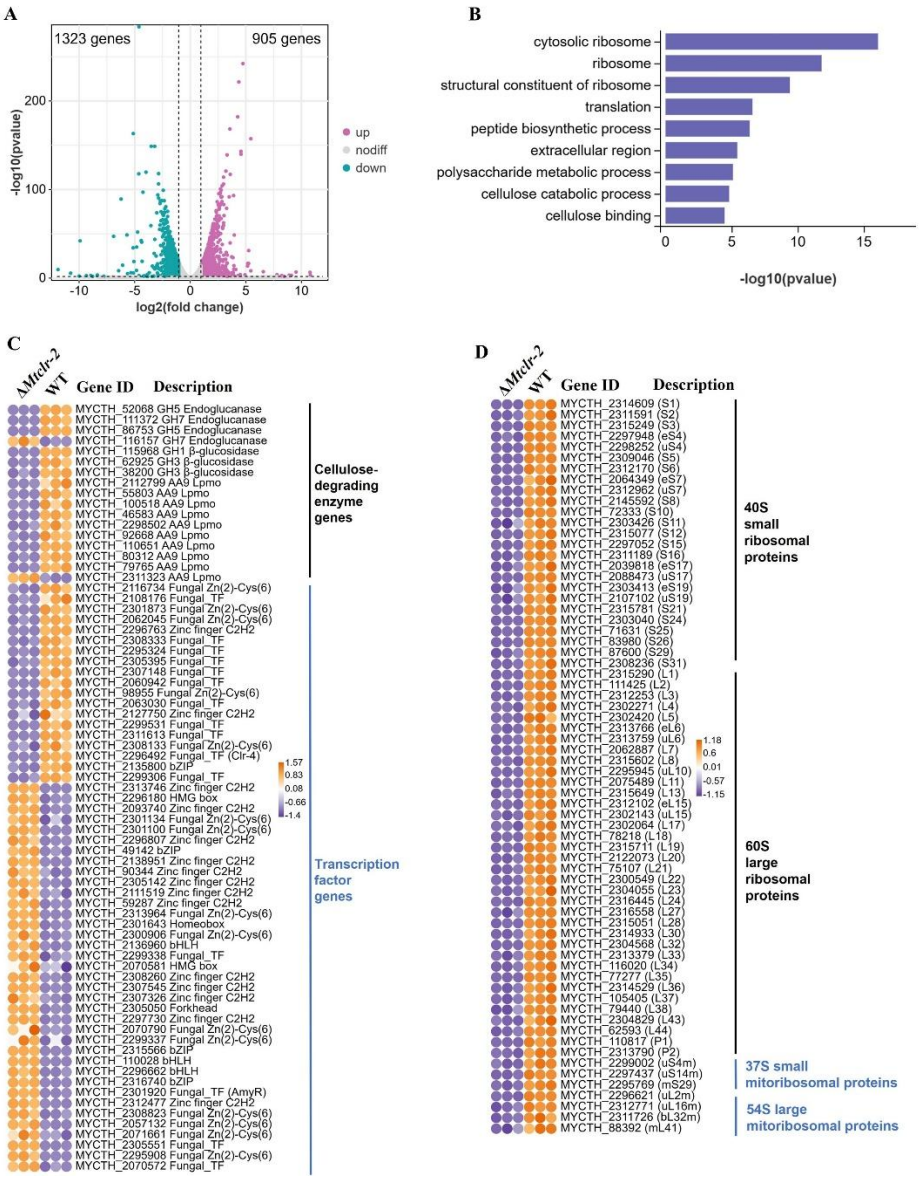

Figure 4.6. Comparative transcriptomic analysis of strains Δ*Mtclr-2* and WT cultivated in 2% (w/v) Avicel medium for 48 h after a shift from glucose. (A) Volcano plots demonstrating differentially expressed genes (DEGs) between Δ*Mtclr-2* and WT strains. Genes that were significantly upregulated and downregulated in the Δ*Mtclr-2* mutant compared to the WT are plotted in red and green, respectively. (B) Gene Ontology (GO) enrichment of 2228 DEGs in the biological process, cellular component, and molecular function categories. (C) Heatmap analysis of expression profiles for genes encoding cellulases, LPMOs, and putative transcription factors between Δ*Mtclr-2* and WT strains. **(D)** Heatmap analysis of expression profiles for genes encoding putative ribosomal proteins between Δ*Mtclr-2* and WT strains.

4.5 Discussion

M. thermophila is a thermophilic fungus able to secrete a complete set of thermostable enzymes involved in plant biomass degradation, including cellulases and xylanases. In recent years, this fungus has been developed into a platform to produce industrially relevant enzymes (Visser et al., 2011; Zhu et al., 2023) and used as a model system for exploring basic fungal cell biology, such as the mechanism of expression and secretion of lignocellulolytic enzymes (Li et al., 2022a; Gu et al., 2023; Zhao et al., 2023b). A few transcription regulators related to lignocellulose deconstruction have been identified in this fungus, including MtFkh1, MtXyr1, MtCre1, MtClr-4, and MtTrc-1 (Yang et al., 2015; Dos Santos Gomes et al., 2019; Liu et al., 2019c; Li et al., 2022a; Lai et al., 2025). However, more transcription factors involved in inducing the expression of lignocellulolytic enzyme-encoding genes in *M. thermophila* remain to be elucidated. In this paper, we illuminated the molecular basis underlying cellulase expression regulated by MtCLR-2, which is the ortholog of NcCLR-2 in *N. crassa*. The assay of cellulase production of *Mtclr-2* deletion and overexpression strains indicated that MtCLR-2 serves as an activator of cellulase production. The disruption of this nuclear localized transcription factor MtCLR-2 drastically decreased cellulolytic enzyme production, whereas the overexpression of MtCLR-2 resulted in cellulase enzyme activities that were elevated approximately two-fold compared with the WT when *M. thermophila* was grown on cellulose. This role was supported by our RT-qPCR and transcriptomic analyses, which uncovered downregulated expression of the major endoglucanase and β-glucosidase genes and several genes encoding crucial LPMOs (AA9 family) in the Δ*Mtclr-2* strain. In addition, the severely affected growth of Δ*Mtclr-2* in liquid cellulose medium but normal growth in glucose culture suggested that MtCLR-2 is specifically involved in cellulose catabolism. However, no obvious difference was observed in the cellobiohydrolase activity between the Δ*Mtclr-2* and WT strains for growth on Avicel (Figure S4.8), despite transcriptomic data revealed the downregulation of five cellobiohydrolase genes and upregulation of one

cellobiohydrolase gene in the Δ*Mtclr-2* mutant (Figure S4.7), indicating a self-equilibrating mechanism that modulates production of cellulase. Overall, herein, we provide a potential target for rational fungal strain engineering for hyperproduction of cellulase.

Previous studies showed that the absence of *Ncclr-2* resulted in no detectable endoglucanase activity and almost abolished secreted protein production when *N. crassa* was grown on cellulose (Coradetti et al., 2012). Our research also demonstrated that MtCLR-2 has a similar role in the regulation of endoglucanase and total protein secretion in cellulose-induced cultures. Also, the considerably reduced endoglucanase activity was reported on *A. nidulans* Δ*clrB* (Coradetti et al., 2012) and *P. oxalicum* Δ*clrB* mutants (Li et al., 2015b). Accordingly, significant decrease in expression levels of the major endoglucanase genes was observed in the Δ*Mtclr-2* strain, which was in accordance with findings from *N. crassa*, *A. nidulans*, *A. niger*, *P. oxalicum*, and *A. oryzae*, where the deletion of *Mtclr-2* orthologs caused the downregulation of the essential endoglucanase genes under cellulosic conditions (Coradetti et al., 2012; Coradetti et al., 2013; Ogawa et al., 2013; Li et al., 2015b; Raulo et al., 2016; Kun et al., 2021). These observations clearly indicate the conserved role of CLR-2 orthologs in endoglucanase gene regulation. Similar to *N. crassa* CLR-2 and *A. nidulans* ClrB, several important LPMO-encoding genes were downregulated by the deletion of *Mtclr-2* in response to Avicel, the majority of which have been found to exert oxidative roles toward cellulose (Coradetti et al., 2013). Regarding β-glucosidase and cellobiohydrolase gene expression, however, differences in function of CLR-2 homologs have been reported. For example, the Δ*clrB* mutant of *P. oxalicum* exhibited reduced cellobiohydrolase activity (Li et al., 2015b) and enhanced β-glucosidase activity when exposed to Avicel (Zhao et al., 2016), which was consistent with the downregulation of the main cellobiohydrolase genes and upregulation of the major β-glucosidase genes. In contrast, the present study showed that the disruption of *Mtclr-2* decreased β-glucosidase activity while having no impact on cellobiohydrolase production, highlighting the complex regulatory networks in which CLR-2 orthologs

are involved in regulating the expression of different cellulase enzymes. In addition, overexpression of *TRIREDRAFT_26163*, the *T. reesei* ortholog of *Ncclr-2*, resulted in only a slight elevation in cellulase production (Hakkinen et al., 2014). Similarly, in *T. cellulolyticus*, the loss of *tclB2*, which is the ortholog of *Ncclr-2*, exhibited minor effects on cellulase activity when cultivated on cellulose (Fujii et al., 2015). Therefore, the role of CLR-2 orthologs in cellulose utilisation appears to be partially conserved among filamentous fungi.

The production of cellulolytic enzymes in fungi is tightly regulated by transcription factors (Huberman et al., 2016; Benocci et al., 2017). According to our transcriptomic data analysis, transcription factors involved in the regulation of cellulase gene expression, including *Mtclr-4* (Liu et al., 2019c) and *MtCol-26* (Xu et al., 2018), showed altered expression levels by the deletion of *Mtclr-2*, implying that MtCLR-2 regulates cellulase production by modulating transcript levels of regulatory proteins. These targeted transcription factors could function as secondary regulators, enabling more fine-tuned gene expression (Craig et al., 2015). In *N. crassa*, *xlr-1*, which encodes a key transcription factor that regulates the expression of hemicellulolytic enzyme genes and is necessary for utilisation of hemicellulose, was downregulated in the Δ*clr-2* strain (Coradetti et al., 2012). However, this is not the case for *M. thermophila*, where the transcription of *Mtxyr1*, the ortholog of *xlr-1*, remained unchanged in the mutant Δ*Mtclr-2* under conditions of cellulose exposure. In addition, CLR-1, another predominant regulator of cellulolytic enzymes in *N. crassa*, is essential for *clr-2* expression, since the expression of *clr-2* was abolished in the Δ*clr-1* mutant, while that of *clr-1* was not influenced by the disruption of *clr-2* during growth on Avicel (Coradetti et al., 2012). Further DNA motif analysis of the bound genes revealed that CLR-1 binds to the promoter region of *clr-2* under cellulosic conditions (Craig et al., 2015). Similar to *N. crassa clr-2*, *Mtclr-2* is not required for the expression of *Mtclr-1* (*MYCTH_2298863*), the *Ncclr-1* ortholog in *M. thermophila*, revealed by the transcriptome data showing the unaffected expression level of *Mtclr-1* in the Δ*Mtclr-2* mutant. Whether *Mtclr-2* is bound and regulated by MtCLR-1 needs to be further

investigated. Unlike the results observed with *Ncclr-2* and *Mtclr-2*, the expression of *clrA*, the ortholog of *clr-1*, which is involved in cellulose degradation, was reported to be (partially) dependent on ClrB in *A. niger* (Kun et al., 2023), suggesting divergences between the regulatory networks coordinating lignocellulose deconstruction and utilisation among different filamentous fungi.

In *N. crassa*, CLR-2 binds to 5′-CGGN$_{11}$CCG-3′ motifs in the promoter regions of its regulon (Craig et al., 2015). Combined ChIPseq and RNAseq analyses identified that 54 genes were both bound by CLR-2 and dependent on it for their expression (Craig et al., 2015). Our data showed that *egl2* and *bgl1* were consistently downregulated at all examined time points in the *Mtclr-2* disruptant, indicating the high dependence of MtCLR-2 for activation of their expression. Further EMSA analysis demonstrated that MtCLR-2 can directly bind to the promoter regions of *egl2* and *bgl1* in a zinc-dependent manner, although the lack of 14 aa in its DNA-binding domain compared to NcCLR-2. Similar to NcCLR-2, the 5′-CGGN$_{11}$CCG-3′ sequence was found in the upstream regions of both *egl2* and *bgl1*, indicating that MtCLR-2 might also bind this motif to regulate its target genes. In addition, the 5′-CGGN$_{11}$CCG-3′ motif was identified in the promoter regions of *Mtlpmo9B*, *Mtlpmo9C*, and *Mtlpmo9D*, but was absent in those of *Mtcre1* and *Mtxyr1*. This observation is consistent with the expression patterns of these genes in the Δ*Mtclr-2* mutant revealed by both RT-qPCR and/or transcriptomic analyses, further supporting the regulatory importance of this motif. It has been shown that ClrB in *A. nidulans* can bind to 5′-CGGN$_8$CCG-3′ motifs in the promoter region of the β-mannosidase gene *mndB* in the presence of zinc ions, and loss of either one of the CGG or CCG triplet completely abolished protein–DNA interaction (Li et al., 2016). Likewise, *eglA* and *bgl4* were downregulated in the *A. niger* Δ*clrB* strain when grown in soybean hull or guar gum liquid media, and both gene possess predicted ClrB consensus binding sites (5′-CGGN$_8$CCG-3′) in their upstream regions (Kun et al., 2023). These experimentally confirmed or putative binding sequences of ClrB in *A. nidulans* and *A. niger* are highly similar to the predicted binding site of MtCLR-2 identified in this study. Nevertheless, *A. nidulans* ClrB does not bind directly to the *eglB* promoter,

which contains one 5′-CGGN$_8$CCG-3′ site. Instead, it is recruited to a CeRE-like (cellulose-responsive element-like) sequence upstream of *eglB*, which also contains a CCG triplet, through the assistance of McmA, a SRF (serum response factor)-type MADS box protein that regulates both cellulase production and asexual/sexual development (Li et al., 2016). This implies a different type of ClrB-mediated regulatory system. Whether MtCLR-2 interacts with unknown cofactors to facilitate its binding and regulatory functions remains to be determined.

An unexpected finding of this study is that 68 genes encoding ribosomal proteins were downregulated in the absence of *Mtclr-2*, which may explain dramatically decreased protein secretion in the cultures of strain Δ*Mtclr-2* cultivated on cellulose. Studies in yeast indicate the activation of ribosomal protein genes (RPGs) transcription is accomplished by several partly specialized regulatory factors that are not unique to RPG promoters (Petibon et al., 2021). The most prominent transcription factors are Rap1 (Repressor/activator protein 1), Fhl1 (Forkhead-like 1), and Ifh1 (Interacts with forkhead 1), which form a regulatory complex at the majority of RPG promoters (Hogues et al., 2008). In addition, the high mobility group (HMG)-box protein Hmo1 binds to around half of the promoters of RPGs bound by Rap1-Fhl1-Ifh1 complex (Shore et al., 2021). However, the orthologs of these identified transcription factors regulating RPGs are absent in *M. thermophila*. On the other hand, the TOR (target of rapamycin) pathway has been demonstrated to be essential for the transcription of RPGs in *S. cerevisiae*, in which the key genes are *Tor1* and *Tor2* (Powers and Walter, 1999). When the TOR pathway is inactivated by nutrient starvation or by treatment of cells with rapamycin, the transcript level of RPGs is downregulated (Powers and Walter, 1999; Marion et al., 2004). It has also been proposed that the transcription factor Sfp1, which acts downstream of the TOR pathway, modulates the transcription of RPGs in response to changes in nutrient availability (Marion et al., 2004; Lempiainen et al., 2009). While orthologs of Tor1/Tor2 (*MYCTH_2307294*) and Sfp1 (*MYCTH_2294631*) are present in *M. thermophila*, their expression levels did not differ significantly between the Δ*Mtclr-2* and WT strains ($\log_2$ fold change = − 0.58 and 0.03, respectively).

In *N. crassa*, it has been reported that the disruption of *cpc-1*, which encodes a bZIP transcription factor known as the cross pathway control-1(CPC1), resulted in elevated expression of 37 ribosomal protein genes, suggesting that CPC1 acts as a repressor of ribosomal protein gene expression (Tian et al., 2007). In our transcriptomic analysis, *MYCTH_2315566*, the ortholog of *cpc-1* in *M. thermophila*, was upregulated in the Δ*Mtclr-2* mutant (log_2 fold change = 1.63), which may partially be responsible for the observed downregulation of genes involved in ribosome biogenesis. It is also possible that, in the loss of *Mtclr-2*, fungal cells reduced the transcription of ribosomal protein genes as an adaptive response to nutrient limitation during cultivation on cellulose. Since the Δ*Mtclr-2* mutant is unable to secrete sufficient cellulases to efficiently degrade cellulose into monosaccharides and/or oligosaccharides, it likely experiences carbon scarcity. In such scenario, the downregulation of ribosome biogenesis may serve as a strategy to conserve energy for basic cellular functions, given that ribosome synthesis is one of the most energy-consuming processes in the cell (Powers and Walter, 1999; Lempiainen et al., 2009). The growth defect of Δ*Mtclr-2* on cellulose, but not on glucose, suggests that the downregulation of ribosomal protein genes and the resulting secretion impairment, may be specifically associated with cellulose utilisation. It has been shown that ribosomal protein gene expression is strongly induced when yeast cells are transferred from unfavorable carbon source to glucose-containing medium (Griffioen et al., 1994; Griffioen et al., 1996; Powers and Walter, 1999). Moreover, in *N. crassa*, the rate of ribosomal protein synthesis increased considerably after a nutritional upshift from acetate to glucose, but was severely repressed upon a shift from glucose to glycerol (Shi and Tyler, 1991). Similar observation was reported in *S. cerevisiae*, where transcript levels of 90 ribosomal proteins were reduced in response to amino deficiency (Natarajan et al., 2001). Likewise, in *N. crassa*, 67 genes encoding predicted ribosomal proteins were downregulated under amino acid starvation (Tian et al., 2007). These studies indicate that the altered expression of ribosomal protein genes represents a common response to nutritional changes. However, the precise mechanism by which MtCLR-2 mediates the regulation of ribosomal protein gene expression under

cellulolytic conditions merits further investigation.

4.6 Conclusion

This study identified MtCLR-2 as a positive regulator of cellulase production. Deletion of *Mtclr-2* markedly reduced cellulase production, whereas its overexpression significantly enhanced cellulase activity in *M. thermophila* under Avicel conditions. RT-qPCR analysis and *in vitro* binding assays demonstrated that MtCLR-2 regulates cellulase gene expression by directly binding to the promoter regions of *egl2* and *bgl1*, thereby modulating their production. Furthermore, comparative transcriptomic analysis revealed that MtCLR-2 is also involved in ribosomal protein biosynthesis. Our results from this study not only provide insights into the regulatory network for cellulase gene expression but also highlight MtCLR-2 as a promising target for rational genetic engineering to enhance cellulolytic enzyme production in *M. thermophila*.

4.7 Supplementary information

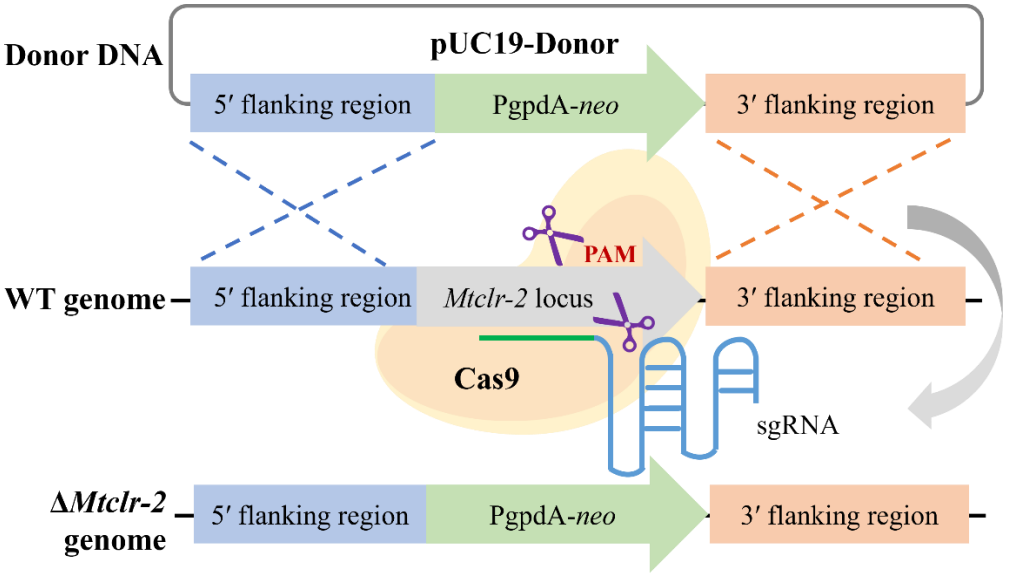

Figure S4.1. Schematic diagram of the deletion of *Mtclr-2* in *M. thermophila* using the CRISPR-Cas9 system. sgRNA, single chimeric guide RNA; PAM, protospacer adjacent motif; *neo*, G418 resistance gene.

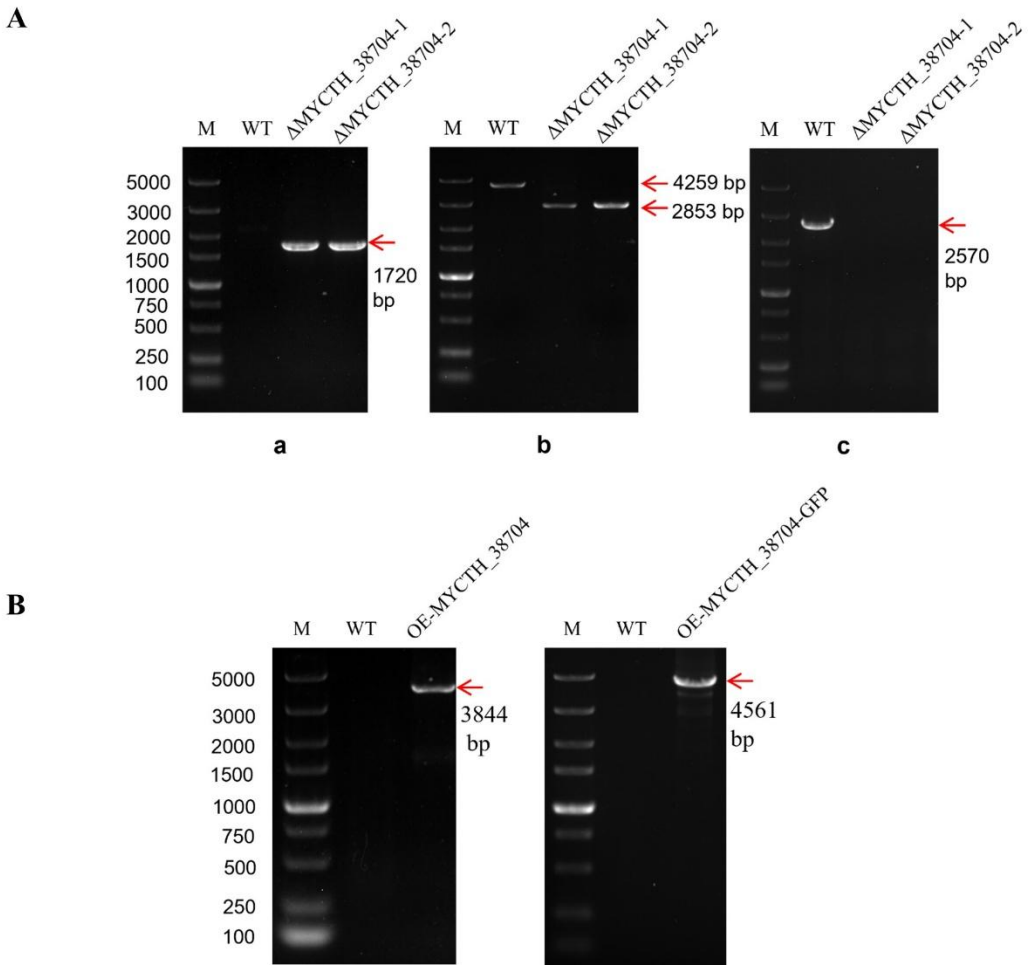

Figure S4.2. Genomic PCR verification of the deletion and overexpression of *Mtclr-2* in *M. thermophila*. (A) PCR analysis for deletion strains of *Mtclr-2*. Primer 1-F locates in P*gpdA-neo*, and Primer 1-R locates out of 3′ flanking region of *Mtclr-2*; Primer 2-F locates out of 5′ flanking region of *Mtclr-2*, and Primer 2-R is in 3′ flanking region; The primer pair 3 is used to amplify *Mtclr-2*. a, the primer pair 1; b, the primer pair 2; c, the primer pair 3; M, DL 5000 Marker; WT, *M. thermophila* wild type strain. (B) PCR analysis of the *Mtclr-2* overexpression strain and the *Mtclr-2-gfp* fusion strain. M, DL 5000 Marker; WT, *M. thermophila* wild type strain.

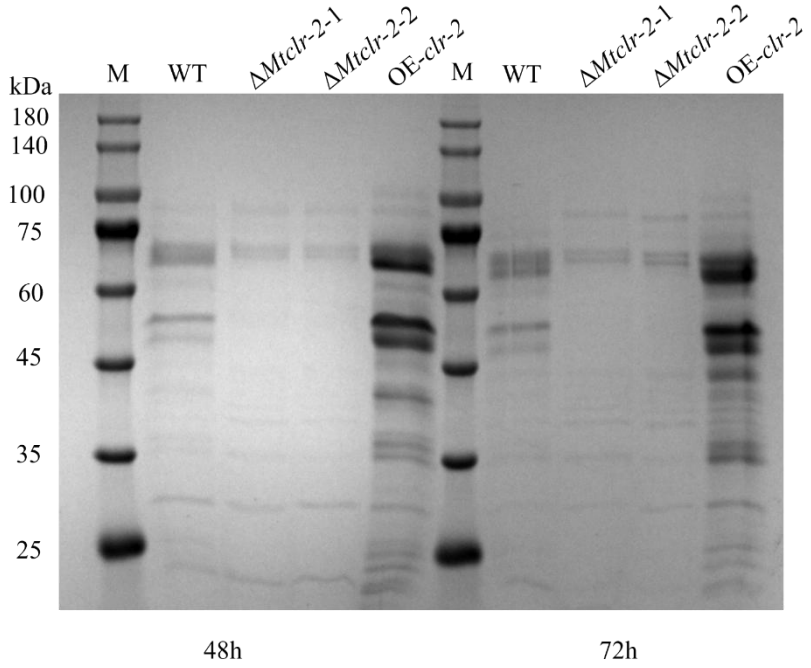

Figure S4.3. SDS-PAGE analysis of the secreted proteins in *M. thermophila* WT, Δ*Mtclr-2*, and OE-*Mtclr-2* strains. These strains were grown in glucose medium for 36 h and subsequently transferred to liquid Avicel medium for 48 and 72 h. M, 10-180 kDa protein marker; WT, *M. thermophila* wild type strain.

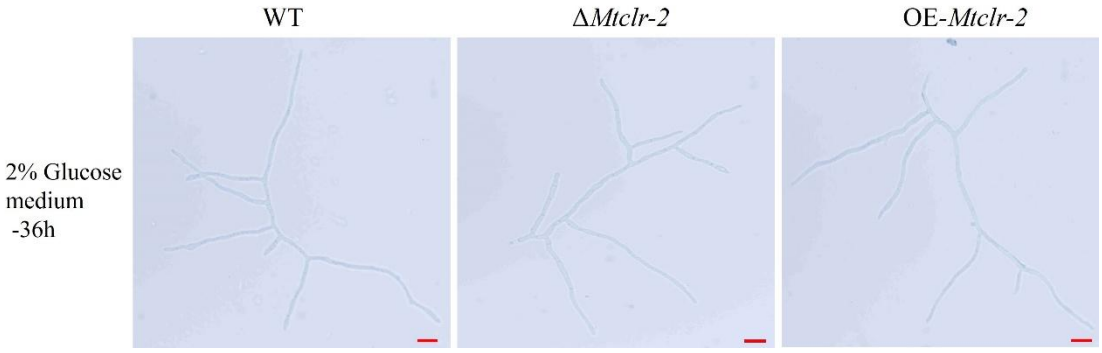

Figure S4.4. Microscopic observation of fungal growth of *M. thermophila* WT, Δ*Mtclr-2* and OE-*Mtclr-2* strains cultured in shaken liquid medium. The mycelia were harvested from liquid media containing 2% (w/v) glucose as the sole carbon source after cultivation at 45°C for 36 h. Scale bars = 10 μm.

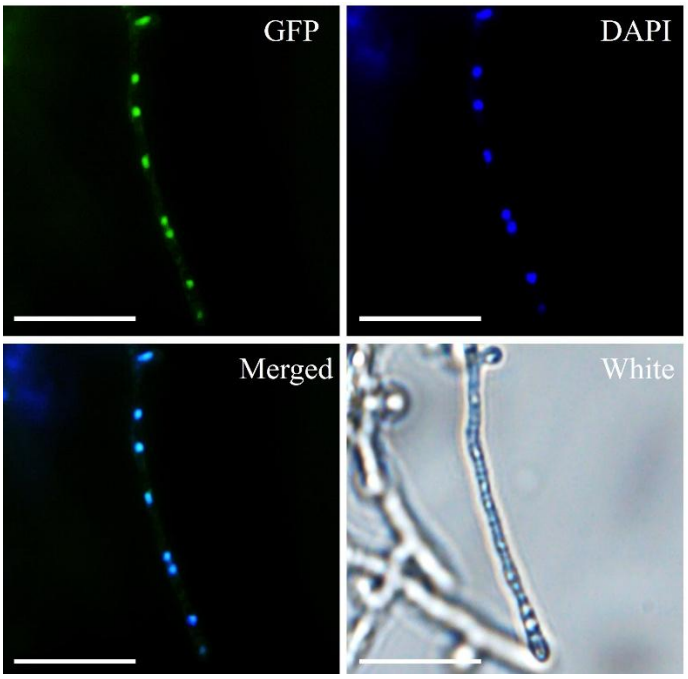

Figure S4.5. Subcellular location of MtCLR-2 in *M. thermophila*. MtCLR-2-GFP strain was cultivated in liquid medium containing 2% (w/v) Avicel as the sole carbon source at 45°C for 36 h. Scale bar = 20 μm.

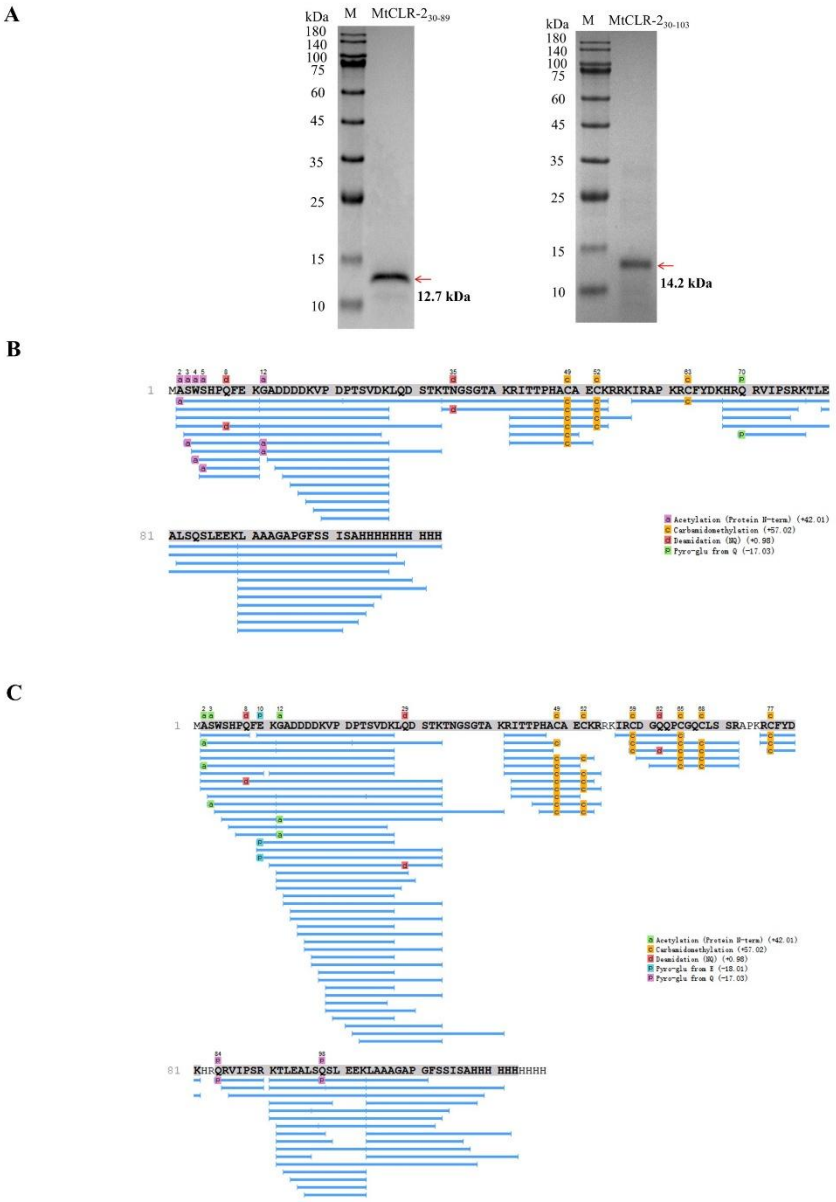

Figure S4.6. SDS-PAGE and LC-MS/MS analysis of purified MtCLR-2$_{30-89}$ and MtCLR-2$_{30-103}$ proteins. (A) SDS-PAGE verification of purified MtCLR-2$_{30-89}$ and MtCLR-2$_{30-103}$. The sample was loaded onto a 12.5% polyacrylamide gel. M, 10-180 kDa. (B-C) LC-MS/MS characterisation of MtCLR-2$_{30-89}$ (B) and MtCLR-2$_{30-103}$ (C) proteins. The target protein band was excised from the gel and analysed using LC-MS/MS assays with the PEAKS Studio 8.5 system. Approximately 99% and 91% of the amino acids of the target protein matched the theoretical amino acid sequence of the Strep II-MtCLR-2$_{30-89}$-His tag fusion protein, and Strep II-MtCLR-2$_{30-103}$-His tag fusion protein, respectively.

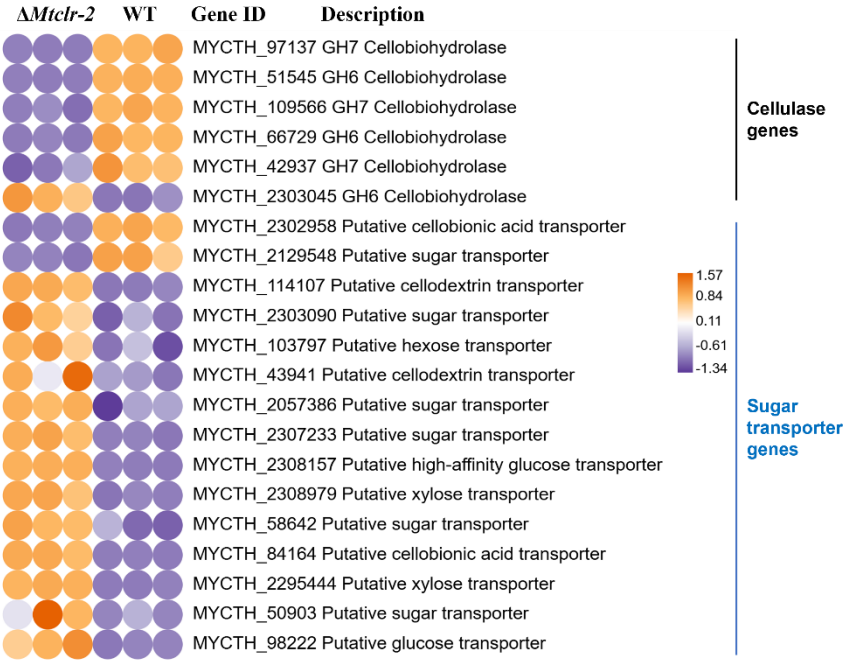

Figure S4.7. Heatmap analysis of expression profiles for genes encoding cellobiohydrolases and putative sugar transporters between Δ*Mtclr-2* and WT strains grown in 2% (w/v) Avicel medium for 48 h after a shift from glucose medium.

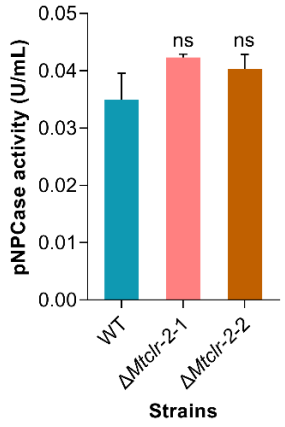

Figure S4.8. Cellobiohydrolase (pNPCase) activity of *M. thermophila* WT and Δ*Mtclr-2* strains. Culture supernatants were collected from fungal strains cultivated on 2% (w/v) Avicel for 72 h at 45°C after a shift from glucose. Ns indicate not significant (Student's t tests). Error bars represent the SD from three replicates.

Table S4.1. List of PCR primers used in this study.

Construction of pFC332-Cas9-U6p-MYCTH_38704-sgRNA vector		
Cloning of U6 promoter	U6p-F	gtttccgctgagggtttaattaaAGGATCGGTGGAGTGAAGTTCG
	U6p-MYCTH_38704-R	GTGCTTGTCATAGAAACACCGAGGAAAGAAAGAAAAGAAGAGGAGG
Cloning of target gene-sgRNA	g-MYCTH_38704-F	GGTGTTTCTATGACAAGCACGTTTTAGAGCTAGAAATAGCAAGTTAAAATAA
	gRNA-R	gtctcggctgaggtcttaattaaAAAAAAAGCACCGACTCGGTG
Construction of Donor DNA vectors		
MYCTH_38704-upstream	MYCTH_38704-up-F	gaccatgattacgccaagcttTCTGCATCTGCTCCCCATGT
	MYCTH_38704-up-R	attcgaagccgcgTTGGGTGCCCTGCTGGAG
Cloning of Pgpd-neo	MYCTH_38704-neo-F	cacccaaCGCGGCTTCGAATCGTGG
	MYCTH_38704-neo-R	ccaggatgctTCAGAAGAACTCGTCAAGAAGGC
MYCTH_38704-downstream	MYCTH_38704-down-F	gttcttctgaAGCATCCTGGAGCAGCTTCC
	MYCTH_38704-down-R	aaaacgacggccagtgaattcGTAGTGGAGGTAGTAGCCGCCG
Construction of MYCTH_38704 overexpression vector		
Cloning of MYCTH_38704	MYCTH_38704-F	tcgccaacaacagacgcggccgcATGGCACCAACCATCCCAG
	MYCTH_38704-R	ggggggccgaccgattctagaTCACTGGACGTAGCCAAACTCC
Construction of MYCTH_38704-GFP expression vector		
Cloning of MYCTH_38704	MYCTH_38704-F	tcgccaacaacagacgcggccgcATGGCACCAACCATCCCAG
	MYCTH_38704-R	ttgctcaccatCTGGACGTAGCCAAACTCCATG
Cloning of GFP	MYCTH_38704-GFP-F	tacgtccagATGGTGAGCAAGGGCGAGG
	GFP-R	gggggccgaccgattctagaTCACTTGTACAGCTCGTCCATGCC
PCR analysis of gene MYCTH_38704 deletion and overexpression in *M. thermophila* strains		

PCR detecting MYCTH_38704 deletion	neo-in-F	TGTCATCTCACCTTGCTCCTG
	MYCTH_38704-out-R	CGCCGTTACGCTAGAACTCTT
	MYCTH_38704-out-F	CGCCTGTTACACTACTTTCACG
	MYCTH_38704-in-R	AGTCCTATTCCCAAGACTACTACCC
	MYCTH_38704-F	ATGGCACCAACCATCCCAG
	MYCTH_38704-R	TCACTGGACGTAGCCAAACTCC
PCR detecting MYCTH_38704 overexpression and MYCTH_38704-GFP fused expression	Ppdc-F	CGGTTACGGAAACGGAAAG
	PgpdA-R	CAGCCAACTGCAAACAGAATA
RT-qPCR analysis		
RT-qPCR of bgl1	RT-q-bgl1-F	AGCCAGGAGAATGGTAACGC
	RT-q-bgl1-R	TGACAGCCCAAACCCAAACT
RT-qPCR of egl2	RT-q-egl2-F	GACTTCTCGATGGAGCGTCTGGT
	RT-q-egl2-R	TTCGTGTCCGTGATGATGTTGC
RT-qPCR of cre1	RT-q-cre1-F	GAATCTTCCCCCGCCGCTCAG
	RT-q-cre1-R	CTCGCCAACATTGCCACATCC
RT-qPCR of xyr1	RT-q-xyr1-F	ATGGATGATACCGATTACCAGAACG
	RT-q-xyr1-R	TGGGAGGAAGTAGCCAAAGATGC
RT-qPCR of actin	RT-q-actin-F	AACGCTCCTGCCTTCTAC
	RT-q-actin-R	GTAACACCATCACCAGAGTC
Construction of pET-51b-MYCTH_387041-798 plasmid		
Cloning of MYCTH_387041-798 encoding gene	MYCTH_387041-798-exon1-F	ccgacgtcggtcgacaagcttGCACCAACCATCCCAGTGC

	MYCTH_387041-798-exon1-R	ttgggtgccctgATCTTGCGCCGCTTGCAC
	MYCTH_387041-798-exon2-F	cgcaagatCAGGGCACCCAAGCGGTG
	MYCTH_387041-798-exon2-R	atccacggggctgccgaggGGTGCGGGAGGGGGGGAT
	MYCTH_387041-798-exon3-F	cCCTCGGCAGCCCCGTGGA
	MYCTH_387041-798-exon3-R	agctcctgcggccgcaagcttCTGGACGTAGCCAAACTCCATG
Construction of pET-51b-MYCTH_3870430-89 plasmid		
Cloning of MYCTH_3870430-89 encoding gene	MYCTH_3870430-89-F	ccgacgtcggtcgacaagcttCAGGACAGCACCAAGACCAAC
	MYCTH_3870430-89-R	agctcctgcggccgcaagcttTTCTTCGAGTGACTGCGACAGG
Construction of pET-51b-MYCTH_3870430-103 plasmid		
Cloning of MYCTH_3870430-103 encoding gene	MYCTH_3870430-103-F	ccgacgtcggtcgacaagcttCAAGACAGCACTAAAACCAACGG
	MYCTH_3870430-103-R	agctcctgcggccgcaagcttTTCTTCCAGAGACTGAGACAGCG
The obtain of probes for EMSAs		
PCR amplification of bgl1-P2	bgl1-P2-F	CGCTCAGCGTGACATCCG
	bgl1-P2-R	GTGGGAAAATCTTCTTGCGCG
PCR amplification of egl2-P2	egl2-P2-F	ACTTGGCGAACGGAGATTTCC
	egl2-P2-R	CTGTGCCCGGAGCGGCAT
PCR amplification of egl2-P3	egl2-P3-F	TATTGTCGCAGACCGCCAG
	egl2-P3-R	CGCGGATGGAGATGTTCCG

Note: The green bold capital nucleotides indicate the protospacer sequence of MYCTH_38704 gene. The lowercase nucleotides represent homologous arm fragments for constructing corresponding vectors.

Chapter 5 General Discussion and Conclusions

5.1 Discussion of key findings

Lignocellulosic biomass is the most abundant renewable resource on Earth and can be converted into fermentable sugars for the production of biofuels and high-value biochemicals. It is therefore considered a potential alternative to fossil fuels (Gupta and Verma, 2015; Xu et al., 2023; Joyia et al., 2024). Filamentous fungi are highly efficient decomposers of lignocellulosic residues in nature because they can express and secrete a broad variety and large amounts of lignocellulolytic enzymes that decompose lignocellulose into sugar monomers, which serves as energy for supporting growth and reproduction (Makela et al., 2014; Meng et al., 2021; Mattam et al., 2022). Among these fungi, *M. thermophila* is well known to produce a wide array of thermostable CAZymes involved in lignocellulose degradation (Berka et al., 2011; Singh, 2016). The thermostability of its enzyme sets has a distant advantage under the elevated temperatures of industrial processes (Morgenstern et al., 2012; Patel et al., 2019; Ajeje et al., 2021). However, the native production levels of cellulolytic and xylanolytic enzymes in this fungus are typically lower than those of mesophilic fungi such as *Trichoderma* and *Aspergillus* species (Berka et al., 2011; Li et al., 2020c)

During lignocellulose bioconversion for cellulosic bioethanol production, the production of enzymes is a critical bottleneck, representing one of the major expenses in the overall process (Akram et al., 2018; Ajeje et al., 2021; Sperandio and Filho, 2021; Meng et al., 2025).To reduce the total cost of lignocellulose bioconversion, improving lignocellulolytic enzyme production is a feasible and effective strategy (Kun et al., 2019; Yang et al., 2023).

In filamentous fungi, the expression of plant polysaccharide degrading enzymes is tightly controlled at the transcriptional level through a complex regulatory network composed of multiple transcriptional activators and transcriptional repressors (Benocci et al., 2017; Meng et al., 2021; Mattam et al., 2022). It has been demonstrated that engineering of theses crucial regulators is an efficient and promising strategy to elevate the yields of lignocellulolytic enzymes, including overexpression of transcriptional

activators, deletion of repressors, or a combination of both approaches (de Paula et al., 2019; Liu and Qu, 2019; Meng et al., 2021; Madhavan et al., 2022). In *M. thermophila*, several transcription factors have been identified to regulate cellulase and/or hemicellulase production (Liu et al., 2017; Dos Santos Gomes et al., 2019; Li et al., 2022a; Gu et al., 2023). Nevertheless, given the large number of putative TF genes that could possibly be associated with lignocellulose degradation in *M. thermophila*, including Zn(II)2Cys6-type (101 genes), fungal-specific (61 genes), C2H2-type (53 genes), helix-loop-helix (13 genes), basic leucine zipper (12 genes), and high mobility group (10 genes) and other types, the number of functionally characterised TFs remains very limited. Therefore, the overall aim of this thesis was to identify and characterise novel transcription factors involved in the regulation of cellulase and xylanase expression in *M. thermophila*, and to elucidate the molecular mechanism underlying their regulation.

In Chapter 2, comparative transcriptomic analysis of *M. thermophila* grown in Avicel and glucose was performed to identify potential transcription factor candidates. A CRISPR/Cas9-based gene editing system and a constitutive promoter (P*pdc*)-driven overexpression system were developed to manipulate target genes. Using these approaches, a novel forkhead transcription factor, MtFKH1, was identified as a negative regulator of cellulase and xylanase production, and its molecular mechanism of regulation was elucidated. In Chapter 3 and 4, using the same gene manipulation and molecular genetic analyses, the functions of two additional transcription factors, the bZIP-type MtHAC-1 and the Zn(II)2Cys6-type MtCLR-2, were characterised. Their roles in lignocellulose degradation and the molecular mechanisms by which they regulate cellulase and xylanase expression were investigated.

5.2 Chapter 2: MtFKH1 is a novel forkhead transcription factor

Comparative transcriptomic analysis combined with molecular genetic approaches is an efficient strategy for identifying novel TFs, as demonstrated in studies of *N. crassa*

(Li et al., 2014), *P. oxalicum* (Zhao et al., 2019), *T. pinophilus* (Liao et al., 2018), and *T. reesei* (Chen et al., 2021). Glucose and lignocellulose are commonly used as repressive and inductive carbon sources, respectively, for the production of lignocellulolytic enzymes. In this study, cellulase and xylanase production in *M. thermophila* was examined under both inducing and repressing conditions. As expected, the cellulolytic and xylanolytic activities of *M. thermophila* were markedly increased when grown on crystalline cellulose compared with glucose. To identify potential TFs contributing to the enhanced cellulase and xylanase production observed under Avicel-inducing conditions, a comparative transcriptomic analysis was performed using the WT strain of *M. thermophila* cultivated in media containing either crystalline cellulose or glucose as the sole carbon source. This analysis uncovered eight novel TF candidates from different transcription factor families that were differentially expressed under inducing conditions.

Gene deletion and overexpression are widely used strategies to study gene function. Although CRISPR/Cas9-mediated gene editing tool and constitutive promoter-driven overexpression system have been established in *M. thermophila*, these approaches typically require multiple plasmids, making the gene manipulation process laborious and time-consuming (Wang et al., 2015; Yang et al., 2015; Liu et al., 2017). To efficiently investigate the regulatory roles of the putative TFs identified in this study, a versatile and rapid system was developed that integrated CRISPR/Cas9-based gene editing with a constitutive promoter (P*pdc*)-driven platform. Using this system, a novel forkhead transcription factor, designated MtFkh1, was identified.

Enzymatic activity evaluation of the *Mtfkh1* deletion and overexpression mutants revealed that MtFkh1 is a repressor of cellulase and xylanase biosynthesis. This finding is consistent with observations in *P. oxalicum*, where deletion of the forkhead regulatory gene *Pox08522* led to an increased xylanase activity (Zhao et al., 2016). Interestingly, the *P. oxalicum* mutant lacking *Pox08522* also exhibited a decrease in β-glucosidase activity, indicating that forkhead regulators may possess both overlapping and divergent roles in lignocellulose degradation among different filamentous fungi. To date,

MtFKH1 and Pox08522 are the only two known forkhead transcription factors involved in the regulation of cellulase and xylanase biosynthesis in filamentous fungi, implying that other unknown members of this family may exert similar regulatory roles in different fungal species.

Subsequent EMSA assay and DNase I footprinting analysis demonstrated that MtFKH1 specifically binds to the consensus motif within the promoter regions of major cellulase and xylanase genes, similar to forkhead family members characterized from *S. cerevisiae* and mammals (Kaufmann et al., 1995; Korver et al., 1997; Zhu et al., 2000; Laoukili et al., 2007). This finding provides insight into the regulatory mechanism of MtFKH1 from the molecular level and offers a potential strategy for promoter engineering in improving enzyme production. Replacing repressor-binding site in cellulase promoters with activator-binding site is a common practice to improve target gene expression. For instance, substitution of the binding site of the repressor Ace1 in the *cbh1* promoter with that of activators Ace2 and Xyr1 largely improved transcription efficiency of target gene in *T. reesei*, and this engineered promoter further enhanced *A. niger* mannanase production in *T. reesei* (Sun et al., 2020). These results suggest that a similar strategy could be applied to replace the binding site of MtFKH1 in the cellulase and xylanase promoters with those of transcriptional activators, thereby increasing their expression and enzyme yields in *M. thermophila*.

5.3 Chapter 3: The dual role of MtHAC-1

Filamentous fungi have a strong ability to secrete numerous proteins into their habitats to decompose the complex lignocellulosic substances for nutrient absorption (Jadhav et al., 2024). During the lignocellulolytic response, nascent cellulase and xylanase polypeptides are translocated into the ER for folding and processing (Huberman et al., 2016). This process can lead to ER stress and subsequently activate the UPR pathway, aiming to alleviate the stress and restore ER homeostasis (Li et al., 2022a). In filamentous fungi, the UPR pathway is mediated by the bZIP transcription factor HacA/Hac1/Hac-1 (Saloheimo et al., 2003; Mulder and Nikolaev, 2009; Montenegro-Montero et al., 2015). The loss of a 20 or 23-nt unconventional intron from the mRNA

of hacA/hac1/hac-1 is responsible for mediating the UPR signalling pathway. Notably, in *M. thermophila*, the mRNA of Mthac-1 (the homolog of hacA/hac1/hac-1) undergoes a noncanonical splicing to remove a 23-nt intron when grown on cellulose, indicating that the growth of this fungus on cellulose induces ER stress (Li et al., 2022a).

In Chapter 2, transcriptome profiling of *M. thermophila* cultivated on Avicel and glucose revealed that the gene encoding the bZIP transcription factor MtHac-1 showed significantly reduced expression on Avicel, indicating its potential involvement in lignocellulose utilisation, which motivated the investigation of its regulatory function. Through a combination of gene deletion, overexpression, and enzymatic activity assays, results showed that MtHac-1 positively regulates cellulase and xylanase activities during the early phase of cellulose cultivation but suppresses their production during the middle and late stages. This dual regulatory pattern likely reflects the dynamic role of MtHac-1 in balancing protein secretion capacity with ER processing load, thereby maintaining cellular homeostasis of *M. thermophila* across different stages of cellulose-induced growth (Montenegro-Montero et al., 2015; Huberman et al., 2016). This phenomenon has not been previously reported for MtHac-1 homologues, highlighting both similar and distinct roles of HacA/Hac1/Hac-1 in filamentous fungi. Importantly, both deletion and overexpression of *Mthac-1* improved cellulase and xylanase production, underscoring its potential application in fungal strain engineering.

Further DNA and protein interaction experiments demonstrated that MtHac-1 binds to not only the promoter regions of major cellulase and xylanase genes but also the promoter of *Mtxyr1* gene, which encodes a crucial transcriptional activator of xylanolytic enzyme genes. These findings indicate that MtHac-1 regulates cellulase and xylanase gene expression through two mechanisms: direct binding, and indirect regulation via binding to the master regulator *Mtxyr1*. However, given that 25 putative transcription factor genes showed changed expression levels in the *Mthac-1* deletion mutant, further work is needed to determine whether MtHac-1 directly targets these promoters and whether MtHac-1 interacts with other co-regulators *in vivo*.

As a transcription factor, nuclear localization is essential for exerting its regulatory roles in gene expression. In *A. niger*, a GFP-HacA fusion, in which the *hacA* ORF (spliced form of *hacA*) was fused to the 3′ end of the *gfp* encoding region, has shown

to be located in the nucleus (Mulder et al., 2004). Similarly, a HacA-eGFP strain of *A. oryzae*, where the *hacA* ORF (lacking the 20-nt intron) was placed within the 5′ end of the eGFP mRNA, was also found to localize to the nucleus (Zhou et al., 2016). These studies imply that removal of the untraditional intron may facilitate the translocation of HacA to the nucleus. To investigate the subcellular localization of MtHac-1 in response to cellulose induction, the ORF of *Mthac-1*^{u} was fused to the *gfp* gene under control of the *pdc* promoter, and the *Mthac-1*^{u}*-gfp* construct was introduced into the *M. thermophila*. Since the unconventional splicing event, that is, the removal of 23-nt intron in the *Mthac-1* mRNA would cause a frameshift resulting in the disruption of the posterior GFP. Only the unspliced *Mthac-1*^{u}*-gfp* form could generate active GFP for monitoring. The fluorescence microscopy analysis revealed that the fused MtHac1^{u}-GFP protein failed to localize to the nucleus (data not shown), supporting that the noncanonical splicing of the Hac1/HacA is a prerequisite for nuclear localization. To conclusively determine the subcellular location of MtHac1, further experiments using a construct in which the spliced *Mthac-1* transcript is fused to *gfp* encoding region will be required.

5.4 Chapter 4: MtCLR-2 directly regulates expression of *Mtegl2* and *Mtbgl1*

The transcription factor Clr-2 (cellulose degradation regulator 2) was initially identified in *N. crassa* as an activator of cellulase activity, but not hemicellulase gene expression (Coradetti et al., 2012). In the same study, the function of ClrB in *A. nidulans*, which is orthologous to Clr-2, was also shown to be essential for activating cellulase gene expression and activity, indicating a conserved function between *N. crassa* and *A. nidulans*. In Chapter 2, comparative transcriptome profiling of *M. thermophila* grown on cellulose and glucose uncovered that *Mtclr-2* (*MYCTH_38704*), the ortholog of *N. crassa clr-2*, was significantly upregulated under cellulosic conditions (log2 fold change = 3.62), suggesting its involvement in cellulose degradation. Although previous work reported that MtClr-2 contributes to cellulase production (Zhang et al., 2022), the underlying molecular mechanism has remained unclear, encouraging further

investigation.

Using the CRISPR/Cas9-based gene editing tool and the P*pdc*-driven overexpression system developed in Chapter 2, *Mtclr-2* was deleted and overexpressed. Enzymatic activity assays showed that the Δ*Mtclr-2* mutants displayed substantially reduced cellulase activities, especially endoglucanase activity, while overexpression of *Mtclr-2* markedly elevated cellulase production, indicating that MtClr-2 acts as a positive regulator of cellulase biosynthesis. To elucidate the regulatory mechanism, EMSAs revealed that MtClr-2 directly binds to the promoters of β-glucosidase gene *bgl1* and the endoglucanase gene *egl2* in a zinc-dependent manner, suggesting that MtClr-2 directly controls cellulase production from the transcriptional level. The EMSA results further confirmed that the lack of 14 aa within the DNA-binding domain of MtCLR-2, relative to NcCLR-2, does not compromise its binding capacity and regulatory function.

Unexpectedly, transcriptomic analysis revealed that 68 ribosomal protein genes were downregulated in the Δ*Mtclr-2* mutant, consistent with the considerably reduced protein secretion observed during growth on cellulose. Such an effect has not been reported for MtClr-2 orthologs in other fungal strains, suggesting a fungus-specific role for MtClr-2, and a possible involvement in translational regulation.

Ribosome biogenesis is closely associated with nutrient availability to adjust protein biosynthetic capacity. For example, when cells are cultivated under optimal growth conditions, high ribosome abundance is required to sustain rapid protein biosynthesis (Griffioen et al., 1994; Griffioen et al., 1996; Powers and Walter, 1999). On the other hand, ribosome biogenesis is one of the most energy-consuming processes in cells (Powers and Walter, 1999; Bosio et al., 2011). The ribosome biogenesis involves hundreds of genes, requires the coordinated activity of all three nuclear RNA polymerases and represents a large fraction of total transcriptional output (Lempiainen et al., 2009; Bosio et al., 2011). Therefore, to conserve energy for basic cellular functions, cells must restrict the generation of new ribosomes under conditions where the requirement of protein synthesis is decreased, such as nutrient deprivation (Powers

and Walter, 1999). The substantial reduction in cellulase production in Δ*Mtclr-2* mutant grown on cellulose may impose a carbon-limiting environment, thereby triggering a global downregulation of ribosome biogenesis genes as a strategy to conserve energy. Additionally, fungal homeostatic mechanism may further reduce the global abundance of mRNA transcripts, including those encoding cellulases and cellulose-degrading enzymes, to match the diminished translational capacity (Rudra et al., 2005), further reducing the cellulase production. However, the downregulation of ribosomal protein genes was observed at the transcript level, whether this leads to reduced translation of these ribosomal protein mRNAs or decreased ribosome abundance in the Δ*Mtclr-2* mutant under cellulolytic conditions remains unknown and merits further investigation.

5.5 Potential interactions between key transcription factors

Biosynthesis of cellulases and xylanases in filamentous fungi is tightly regulated by a complicated regulatory network mediated by multiple transcription factors (Zhao et al., 2023a). These TFs not only bind to the promoters of and control the expression of genes encoding cellulolytic and hemicellulolytic enzymes, but also of genes encoding numerous additional transcription factors. These secondary transcription factors could function as drivers of second-tier transcriptional responses, enabling a more fine-tuned and dynamic regulation of gene expression under different carbon sources (Craig et al., 2015). For example, in *N. crassa*, the cellulase activator CLR-1 binds to upstream of *clr-2*, which encodes anther essential activator of cellulase production, thereby modulating its expression (Craig et al., 2015). Similarly, ACE4 from *T. reesei* binds not only to cellulase gene promoters but also to the promoter region of *ace3*, activating its expression to further regulate cellulase expression (Chen et al., 2021). In *P. oxalicum*, three TFs PoxCxrA, PoxCxrB, and PoxNsdD have been shown to be crucial for the regulation of cellulase and xylanase gene expression, and these TFs bind to the promoter regions of one another and regulate their expression (Yan et al., 2017). These findings imply the complex regulatory network that governs lignocellulose degradation.

In this study, we observed substantially lowered expression of the forkhead TF gene *Mtfkh1* in the Δ*Mthac-1* mutant, indicating that MtHAC-1 positively regulates the expression of *Mtfkh1* to regulate the production of cellulase and xylanase. We also demonstrated that MtHAC-1 binds to the promoter of *Mtxyr1*, an essential activator of xylanolytic genes, and regulates its expression. Regarding MtCLR-2, the genes encoding the cellulase activator MtCLR-4 and the repressor MtAmyR, showed downregulated and upregulated expression levels in the mutant Δ*Mtclr-2*, respectively, suggesting that MtCLR-2 modulates these two regulatory proteins. Interestingly, MtCLR-4 has been reported to bind to the promoter of *Mtclr-2* in *M. thermophila*, further illustrating the intricate regulatory interactions among TFs that coordinate cellulase gene expression. Whether MtHAC-1 directly binds to the promoter of *Mtfkh1*, and whether MtCLR-2 directly targets the upstream regions of *Mtclr-4* and *MtamyR*, requires further investigation.

5.6 Strengths and limitations of the study

5.6.1 Strengths

The overall aim of this study was to identify and characterise novel transcription factors involved in the regulation of cellulase and xylanase expression in the thermophilic filamentous fungus *M. thermophila*. Through comparative transcriptomic analysis of *M. thermophila* grown in liquid media containing either Avicel or glucose as the sole carbon source, major CAZyme genes, including crucial cellulases, hemicellulases, and LPMOs (AA9), were found to be differentially expressed, implying complex synergy between various enzymes involved in lignocellulose degradation. Importantly, this analysis revealed eight novel TF candidates and two previously reported regulators showed markedly altered transcription levels between Avicel and glucose media, including *Mtfkh1*, *Mthac-1*, and *Mtclr-2*. This approach proved highly effective and precise for discovering potential regulatory proteins in *M. thermophila* and provides a valuable reference for similar studies in other filamentous fungi.

A major strength of this study is the development of a versatile and rapid gene

manipulation platform that integrates CRISPR/Cas9-based gene editing tool with a constitutive promoter (P*pdc*)-driven overexpression system. This new platform requires fewer plasmids than previously established system, significantly simplifying genetic manipulation processes and improving efficiency. Using this platform, the regulatory roles of MtFKH1, MtHAC-1, and MtCLR-2 in cellulase and xylanase production were systematically elucidated. Moreover, both CRISPR/Cas9-mediated deletion or P*pdc*-driven overexpression were applied to elevate cellulase and xylanase production in *M. thermophila* and could be used for genetic engineering to improve the production of target proteins and biochemicals in other filamentous fungi.

This thesis identified and characterised the first forkhead transcription factor in *M. thermophila*, MtFKH1, which acts as a repressor of cellulase and xylanase gene expression. Through comparative transcriptomic analysis and molecular genetic approaches, MtFKH1 was shown to directly bind to the promoter regions of key cellulase and xylanase genes. This finding suggests that transcriptional regulators beyond the extensively studied zinc finger families may also play important regulatory roles in lignocellulose deconstruction in filamentous fungi. In addition, the bZIP TF MtHAC-1 was found to exert dual regulatory effects on the production of cellulase and xylanase at different growth stages, likely maintaining a balance between enzyme secretion and ER processing capacity. This regulatory pattern has not been previously reported for HAC-1 homologs, providing new insights into the regulatory mechanisms underlying cellulase and xylanase gene expression. Furthermore, illustrating that the Zn2Cys6-type regulator MtCLR-2 functions as a key transcriptional activator of cellulase gene expression and enzyme production, and that the absence of a 14 aa in its DNA-binding domain does not compromise its regulatory function. MtCLR-2 was also found to influence the expression of ribosomal protein genes, which has not been observed for CLR-2 homologs in other fungi, indicating a specific role for MtCLR-2 in *M. thermophila*, and a possible involvement in translational regulation.

Collectively, the identification and characterisation of MtFKH1, MtHAC-1, and MtCLR-2 elucidate the molecular mechanisms underlying cellulase and xylanase gene

expression, expand our understanding of how these three TFs regulate lignocellulolytic enzyme gene expression. These findings also expand the repertoire of known transcription factors that regulate cellulolytic and xylanolytic gene expression in *M. thermophila* and underscore the potential for mining TF families beyond the commonly studied zinc finger groups. In addition, this thesis offers promising genetic engineering targets such as the simultaneous deletion of *Mtfkh1* and *Mthac-1* combined with overexpression of *Mtclr-2*, which may be exploited to enhance lignocellulolytic enzyme production for biorefinery applications.

5.6.2 Limitations

Through transcriptomic analysis of *M. thermophila* cultured on Avicel and glucose, 10 genes encoding putative transcription factors showed substantially altered expression levels when using a threshold of |log2 fold change | > 2. However, when applying the more commonly used threshold of |log2 fold change | > 1, an additional 28 genes exhibited significant transcriptional changes. These genes may also participate in lignocellulose degradation, and their regulatory roles require further investigation.

In this study, the CRISPR/Cas9 genome editing system was optimised by integrating the Cas9 protein and the *u6* promoter-driven sgRNA cassette into a single expression vector. Although seven potential regulatory genes were successfully deleted, the number of positive transformants varied across targets. For instance, two deletion mutants were obtained for *Mthac-1* and *Mtclr-2*, while only one stable mutant strain was generated for *Mtfkh1*. Additionally, three candidate regulatory genes failed to be deleted by this system, indicating that the gene editing system still requires further optimisation to increase editing efficiency and reliability.

To determine the precise DNA motif recognized by MtFKH1 in the promoter regions of its target genes, a DNase I footprinting assay was performed, which is a standard approach to identify specific protein binding motif in the promoter regions of genes (Gao and Kunos, 2000). This method identified the sequence that MtFKH1 binds (5′-CGGGAAGGCAAACATTGT-3′) in the promoter of *bgl1*, consistent with the

consensus motifs described for other forkhead proteins. However, attempts to apply this approach to determine the binding motifs for MtHAC-1, and MtCLR-2 did not yield satisfactory results, suggesting that further optimisation or the use of other methods is necessary to define their binding sites.

To elucidate the regulatory roles of MtFKH1, MtHAC-1, and MtCLR-2, transcriptomic analyses were performed using the *M. thermophila* WT strain and the corresponding deletion mutants after 48 h of growth on cellulose following a shift from glucose. Although the transcriptomic data were generally consistent with the phenotypes of the deletion mutans, cellulase and xylanase production is dynamic and continuous process. This is particularly relevant for MtHAC-1, which exerts distinct regulatory effects at early, middle and late stages of cultivation. Therefore, a single time point may not fully reflect the temporal complexity of transcriptional regulation. Additional transcriptome analyses at multiple time points such as 24 and 72 h may be required to more comprehensively understand the regulatory process.

With respect to the role of MtHAC-1 in ER stress and the unfolded protein response, previous studies have primarily focused on the mRNA level of HacA/Hac1/Hac-1, especially the conventional and unconventional splicing of *HacA/Hac1/Hac-1* mRNA in filamentous fungi. To date, there have been no studies investigating the corresponding unspliced or spliced protein forms. While this study confirms the regulatory role of MtHAC-1, experiments specifically addressing the biological functions of the two MtHAC-1 protein isoforms were not performed. Previous research has shown that overexpression of *Mthac-1* (the conventional coding region, representing the unspliced version) results in two distinct transcript forms, corresponding to the spliced and unspliced *Mthac-1* mRNAs, each accounting for approximately half of total transcripts under Avicel induction (Li et al., 2022a). It can be speculated that these two mRNAs are translated into two distinct MtHAC-1 proteins, but whether the unspliced MtHAC-1 protein has any biological function, and what specific roles the spliced MtHAC-1 protein plays, remains to be understood.

For industrial application of filamentous fugus in biorefinery processes, large-

scale fermentation performance is the prerequisite. For instance, the *M. thermophila* HC-type C1 strain can produce 50–70 g/L total secreted protein in laboratory-scale fed-batch fermentations, and further strain modification and processing engineering have elevated yields to more than 100 g/L in large-scale fermentations (Visser et al., 2011). In contrast, strains in this study were cultivated in 50 mL shake-flask cultures, which differ greatly from fed-batch and commercial-scale conditions. Whether the deletion and overexpression strains generated in this work maintain their performance in larger fermenters remains to be determined.

5.7 Future Directions

Although CRISPR/Cas12a and Base-Editing systems have been established in *M. thermophila* (Liu et al., 2019d; Zhang et al., 2022), the CRISPR/Cas9-based gene editing system is still the most widely used tool for gene manipulation and strain improvement. To overcome the low editing efficiency observed in the current CRISPR/Cas9 system, multiple strategies could be considered. Designing at least two sgRNAs for one target gene has been applied in other fungal strains. For example, two sgRNAs targeting distinct loci of *cbh1* and *cbh2* were constructed to disrupt these genes in *T. reesei* QM53 strain (Zhang et al., 2024a). Moreover, tRNA-gRNA array based on endogenous tRNA processing system has been successfully applied in *T. reesei* and *A. niger*, which can generate multiple sgRNAs from a single transcript and allow efficient multiple genome editing (Li et al., 2023b; Zhang et al., 2024a). A similar multiple sgRNA processing platform can be developed for *M. thermophila*. It is also worth noting that a variety of RNA polymerase III-based promoter, including 5S rRNA, U3 snRNA promoters, have been used to drive multiple sgRNAs in filamentous fungi (Li et al., 2023b; Shen et al., 2024). However, to date, only the U6 snRNA promoter has been applied in *M. thermophila*. Future optimisation and technological advancement of CRISPR systems are expected to further promote functional genomics, regulatory studies, and strain engineering in this thermophilic fungus.

In this study, EMSA method confirmed that MtFKH1, MtHAC-1, and MtCLR-2 can directly bind to the promoter regions of their respective target genes. However, these results represent *in vitro* interaction confirmation. Given the complexity of the

transcriptional regulatory network regulating cellulase and xylanase gene expression, future work should investigate whether these TFs bind their targets *in vivo*, and whether they physically or functionally interact with other known or yet unidentified regulators. A genome-wide integration of ChIP-seq and RNA-seq has been used to reveal relationships between transcription factor binding and target gene expression dependence (Craig et al., 2015). This combined analysis will be essential to define conserved DNA-binding motifs and global regulatory networks for MtFKH1, MtHAC-1, MtCLR-2, and other TFs.

Transcriptomic profiling of *M. thermophila* cultured on Avicel and glucose identified an additional 28 potential TF-encoding genes that warrant further investigation. Moreover, many putative TFs showed altered expression in the Δ*Mtfkh1*, Δ*Mthac-1*, and Δ*Mtclr-2* mutants when cultivated on Avicel. For instance, in the Δ*Mtfkh1* mutant, four regulatory genes were upregulated and fourteen were downregulated compared to WT. These secondary transcription factors may also contribute to lignocellulose degradation and should be functionally characterised. Considering the large number of unidentified TFs in *M. thermophila*, the development of high-throughput screening or functional genomics platforms will be critical for boosting TF discovery and overcoming the limitations of traditional single gene deletion approach.

In addition to transcription factors, sugar transporters also play important roles in nutrient uptake and extracellular signal transduction associated with inhibiting or triggering the induction of lignocellulolytic enzymes (Gu et al., 2023). In *M. thermophila*, the L-arabinose transporter MtLat-1 has been recently illustrated to engaged in the repression of hemicellulase production when grown on arabinan (Gu et al., 2023). MtLat-1 acts as a transceptor that transports L-arabinose and transduces the molecular signal, leading to downstream suppression of hemicellulolytic gene expression. Notably, the expression of *Mtlat-1* was decreased in Δ*Mthac-1* mutant under cellulose conditions, indicating a possible role in cellulose utilisation. Similar to transcription factors, numerous putative sugar transporter genes also exhibited differential expression in the deletion strains of *Mtfkh1*, *Mthac-1*, and *Mtclr-2*, compared with WT. For example, 15 putative sugar transporter genes showed changed expression in the *Mtclr-2* disruption strain, including two upregulated and 13 downregulated genes. These predicted sugar transporters may affect cellulase and/or

xylanase production and merit future functional characterisation. Additionally, comparative transcriptomic analysis of *M. thermophila* growth between cellulose and glucose also revealed that eight putative sugar transporter genes were highly expressed under Avicel induction, suggesting their potential importance in the utilisation of lignocellulosic biomass and in the future strain engineering.

Finally, although this study elucidated the roles of three independent transcription factors (MtFKH1, MtHAC-1, and MtCLR-2) in the cellulase and xylanase production, their potential synergistic effects remain unexplored. A combination of disruption of *Mtfkh1* and *Mthac-1* together with overexpression of *Mtclr-2* is expected to further improve lignocellulolytic enzyme production in *M. thermophila*. In addition, future evaluation of these engineered strains in large-scale fermenters will be necessary to assess their industrial potential and feasibility for commercial biorefinery applications.

5.8 Conclusions

In this study, comparative transcriptomic analyses of *M. thermophila* cultivated in cellulose and glucose media identified multiple potential regulatory candidates involved in lignocellulolytic enzyme production. Using a newly established gene manipulation platform that integrates CRISPR/Cas9-based gene editing tool with a constitutive promoter (P*pdc*)-driven overexpression system, three transcription factors, MtFKH1, MtHAC-1, and MtCLR-2, were found to regulate cellulase and xylanase production. Through molecular genetic approaches and comparative transcriptomic analyses, the regulatory mechanisms of these three TFs involved in cellulase and xylanase expression were elucidated.

MtFKH1, the first forkhead transcription factor identified in *M. thermophila*, acts as a repressor of cellulase and xylanase biosynthesis. It negatively regulates the expression of major cellulase and xylanase genes by directly binding to their promoter regions and plays important roles in fungal sporulation.

The bZIP transcription factor MtHAC-1 exerts stage-dependent dual regulatory effects on cellulase and xylanase production, likely maintaining a balance between extracellular enzyme secretion and ER processing capacity. MtHAC-1 regulates

cellulase and xylanase gene expression through two mechanisms: by directly binding to the promoter regions of key cellulase and xylanase genes with different DNA motifs, and by modulating the expression of the crucial xylanolytic activator *Mtxyr1*. In addition, MtHAC-1 is associated with the 26S proteasome gene expression.

The Zn2Cys6-type transcription factor MtCLR-2 functions as a crucial activator of cellulase production. It regulates cellulase gene expression by directly binding to the promoter regions of major cellulase genes *egl2* and *bgl1*. Moreover, MtCLR-2 is also implicated in the regulation of ribosomal protein biosynthesis.

Overall, this thesis elucidates the molecular mechanisms governing cellulase and xylanase gene expression in *M. thermophila*. It expands the current repertoire of transcription factors known to regulate cellulolytic and xylanolytic gene expression and provides promising targets for engineering *M. thermophila* with enhanced lignocellulolytic enzyme production.

References

Adnan, M., Ma, X., Olsson, S., Wang, J., Liu, G., 2022. Promoter regulation and genetic engineering strategies for enhanced cellulase expression in *Trichoderma reesei*. Microbiol Res. 259, 127011.

Adnan, M., Zheng, W., Islam, W., Arif, M., Abubakar, Y.S., Wang, Z., Lu, G., 2017. Carbon Catabolite Repression in Filamentous Fungi. Int J Mol Sci. 19 (1).

Agrawal, R., Verma, A., Singhania, R.R., Varjani, S., Di Dong, C., Kumar Patel, A., 2021. Current understanding of the inhibition factors and their mechanism of action for the lignocellulosic biomass hydrolysis. Bioresour Technol. 332, 125042.

Ajeje, S.B., Hu, Y., Song, G., Peter, S.B., Afful, R.G., Sun, F., Asadollahi, M.A., Amiri, H., Abdulkhani, A., Sun, H., 2021. Thermostable Cellulases / Xylanases From Thermophilic and Hyperthermophilic Microorganisms: Current Perspective. Front Bioeng Biotechnol. 9, 794304.

Akram, F., Haq, I.u., Imran, W., Mukhtar, H., 2018. Insight perspectives of thermostable endoglucanases for bioethanol production: A review. Renewable Energy. 122, 225-238.

Al-Sheikh, H., Watson, A.J., Lacey, G.A., Punt, P.J., MacKenzie, D.A., Jeenes, D.J., Pakula, T., Penttilä, M., Alcocer, M.J., Archer, D.B., 2004. Endoplasmic reticulum stress leads to the selective transcriptional downregulation of the glucoamylase gene in *Aspergillus niger*. Mol Microbiol. 53 (6), 1731-1742.

Alazi, E., Ram, A.F.J., 2018. Modulating Transcriptional Regulation of Plant Biomass Degrading Enzyme Networks for Rational Design of Industrial Fungal Strains. Front Bioeng Biotechnol. 6, 133.

Alokika, Singh, B., 2019. Production, characteristics, and biotechnological applications of microbial xylanases. Appl Microbiol Biotechnol. 103 (21-22), 8763-8784.

Amorim, C., Silverio, S.C., Prather, K.L.J., Rodrigues, L.R., 2019. From lignocellulosic residues to market: Production and commercial potential of xylooligosaccharides. Biotechnol Adv. 37 (7), 107397.

Andlar, M., Rezic, T., Mardetko, N., Kracher, D., Ludwig, R., Santek, B., 2018. Lignocellulose degradation: An overview of fungi and fungal enzymes involved in lignocellulose degradation. Eng Life Sci. 18 (11), 768-778.

Antonieto, A.C., dos Santos Castro, L., Silva-Rocha, R., Persinoti, G.F., Silva, R.N., 2014. Defining the genome-wide role of CRE1 during carbon catabolite repression in Trichoderma reesei using RNA-Seq analysis. Fungal Genet Biol. 73, 93-103.

Aro, E.M., 2016. From first generation biofuels to advanced solar biofuels. Ambio. 45 Suppl 1 (Suppl 1), S24-31.

Aro, N., Saloheimo, A., Ilmen, M., Penttila, M., 2001. ACEII, a novel transcriptional activator involved in regulation of cellulase and xylanase genes of *Trichoderma reesei*. J Biol Chem. 276 (26), 24309-24314.

Aro, N., Ilmen, M., Saloheimo, A., Penttila, M., 2003. ACEI of Trichoderma reesei is a repressor of cellulase and xylanase expression. Appl Environ Microbiol. 69 (1), 56-65.

Ashokkumar, V., Venkatkarthick, R., Jayashree, S., Chuetor, S., Dharmaraj, S., Kumar, G., Chen, W.H., Ngamcharussrivichai, C., 2022. Recent advances in lignocellulosic biomass for biofuels and value-added bioproducts - A critical review. Bioresour Technol. 344 (Pt B), 126195.

Bach, D.H., Long, N.P., Luu, T.T., Anh, N.H., Kwon, S.W., Lee, S.K., 2018. The Dominant Role of Forkhead Box Proteins in Cancer. Int J Mol Sci. 19 (10).

Bajaj, P., Mahajan, R., 2019. Cellulase and xylanase synergism in industrial biotechnology. Appl Microbiol Biotechnol. 103 (21-22), 8711-8724.

Basit, A., Liu, J., Miao, T., Zheng, F., Rahim, K., Lou, H., Jiang, W., 2018. Characterization of Two Endo-beta-1, 4-Xylanases from *Myceliophthora thermophila* and Their Saccharification Efficiencies, Synergistic with Commercial Cellulase. Front Microbiol. 9, 233.

Basotra, N., Kaur, B., Di Falco, M., Tsang, A., Chadha, B.S., 2016. *Mycothermus thermophilus* (Syn. *Scytalidium thermophilum*): Repertoire of a diverse array of efficient cellulases and hemicellulases in the secretome revealed. Bioresour Technol. 222, 413-421.

Benocci, T., Aguilar-Pontes, M.V., Zhou, M., Seiboth, B., de Vries, R.P., 2017. Regulators of

plant biomass degradation in ascomycetous fungi. Biotechnol Biofuels. 10, 152.

Berka, R.M., Grigoriev, I.V., Otillar, R., Salamov, A., Grimwood, J., Reid, I., Ishmael, N., John, T., Darmond, C., Moisan, M.C., Henrissat, B., Coutinho, P.M., Lombard, V., Natvig, D.O., Lindquist, E., Schmutz, J., Lucas, S., Harris, P., Powlowski, J., Bellemare, A., Taylor, D., Butler, G., de Vries, R.P., Allijn, I.E., van den Brink, J., Ushinsky, S., Storms, R., Powell, A.J., Paulsen, I.T., Elbourne, L.D., Baker, S.E., Magnuson, J., Laboissiere, S., Clutterbuck, A.J., Martinez, D., Wogulis, M., de Leon, A.L., Rey, M.W., Tsang, A., 2011. Comparative genomic analysis of the thermophilic biomass-degrading fungi *Myceliophthora thermophila* and *Thielavia terrestris*. Nat Biotechnol. 29 (10), 922-927.

Berlin, A., 2013. No barriers to cellulose breakdown. Science. 342 (6165), 1454-1456.

Bernardi, A.V., Gerolamo, L.E., Uyemura, S.A., Dinamarco, T.M., 2021. A thermophilic, pH-tolerant, and highly active GH10 xylanase from Aspergillus fumigatus boosted pre-treated sugarcane bagasse saccharification by cellulases. Industrial Crops and Products. 170.

Bhardwaj, N., Kumar, B., Agrawal, K., Verma, P., 2021. Current perspective on production and applications of microbial cellulases: a review. Bioresour Bioprocess. 8 (1), 95.

Bhatia, S.K., Kim, S.-H., Yoon, J.-J., Yang, Y.-H., 2017. Current status and strategies for second generation biofuel production using microbial systems. Energy Convers Manage. 148, 1142-1156.

Blumer-Schuette, S.E., Brown, S.D., Sander, K.B., Bayer, E.A., Kataeva, I., Zurawski, J.V., Conway, J.M., Adams, M.W., Kelly, R.M., 2014. Thermophilic lignocellulose deconstruction. FEMS Microbiol Rev. 38 (3), 393-448.

Bok, J.W., Keller, N.P., 2004. LaeA, a regulator of secondary metabolism in *Aspergillus* spp. Eukaryot Cell. 3 (2), 527-535.

Bosio, M.C., Negri, R., Dieci, G., 2011. Promoter architectures in the yeast ribosomal expression program. Transcription. 2 (2), 71-77.

Brown, N.A., de Gouvea, P.F., Krohn, N.G., Savoldi, M., Goldman, G.H., 2013. Functional characterisation of the non-essential protein kinases and phosphatases regulating *Aspergillus nidulans* hydrolytic enzyme production. Biotechnol Biofuels. 6 (1), 91.

Cai, P., Wang, B., Ji, J., Jiang, Y., Wan, L., Tian, C., Ma, Y., 2015. The putative cellodextrin transporter-like protein CLP1 is involved in cellulase induction in *Neurospora crassa*. J Biol Chem. 290 (2), 788-796.

Cao, Y., Zheng, F., Wang, L., Zhao, G., Chen, G., Zhang, W., Liu, W., 2017. Rce1, a novel transcriptional repressor, regulates cellulase gene expression by antagonizing the transactivator Xyr1 in *Trichoderma reesei*. Mol Microbiol. 105 (1), 65-83.

Carlsson, P., Mahlapuu, M., 2002. Forkhead transcription factors: key players in development and metabolism. Dev Biol. 250 (1), 1-23.

Carvalho, N.D., Jørgensen, T.R., Arentshorst, M., Nitsche, B.M., van den Hondel, C.A., Archer, D.B., Ram, A.F., 2012. Genome-wide expression analysis upon constitutive activation of the HacA bZIP transcription factor in *Aspergillus niger* reveals a coordinated cellular response to counteract ER stress. BMC Genomics. 13, 350.

Chen, Y., Lin, A., Liu, P., Fan, X., Wu, C., Li, N., Wei, L., Wang, W., Wei, D., 2021. *Trichoderma reesei* ACE4, a Novel Transcriptional Activator Involved in the Regulation of Cellulase Genes during Growth on Cellulose. Appl Environ Microbiol. 87 (15), e0059321.

Coradetti, S.T., Xiong, Y., Glass, N.L., 2013. Analysis of a conserved cellulase transcriptional regulator reveals inducer-independent production of cellulolytic enzymes in *Neurospora crassa*. Microbiologyopen. 2 (4), 595-609.

Coradetti, S.T., Craig, J.P., Xiong, Y., Shock, T., Tian, C., Glass, N.L., 2012. Conserved and essential transcription factors for cellulase gene expression in ascomycete fungi. Proc Natl Acad Sci U S A. 109 (19), 7397-7402.

Craig, J.P., Coradetti, S.T., Starr, T.L., Glass, N.L., 2015. Direct target network of the *Neurospora crassa* plant cell wall deconstruction regulators CLR-1, CLR-2, and XLR-1. mBio. 6 (5), e01452-01415.

de Paula, R.G., Antonieto, A.C.C., Ribeiro, L.F.C., Srivastava, N., O'Donovan, A., Mishra, P.K., Gupta, V.K., Silva, R.N., 2019. Engineered microbial host selection for value-added bioproducts from lignocellulose. Biotechnol Adv. 37 (6), 107347.

de Souza, W.R., de Gouvea, P.F., Savoldi, M., Malavazi, I., de Souza Bernardes, L.A., Goldman,

M.H.S., de Vries, R.P., de Castro Oliveira, J.V., Goldman, G.H., 2011. Transcriptome analysis of *Aspergillus niger* grown on sugarcane bagasse. Biotechnol Biofuels. 4, 40.

Derntl, C., Rassinger, A., Srebotnik, E., Mach, R.L., Mach-Aigner, A.R., 2015. Xpp1 regulates the expression of xylanases, but not of cellulases in *Trichoderma reesei*. Biotechnol Biofuels. 8, 112.

Dominguez-Santos, R., Garcia-Estrada, C., Kosalkova, K., Prieto, C., Santamarta, I., Martin, J.F., 2015. PcFKH1, a novel regulatory factor from the forkhead family, controls the biosynthesis of penicillin in *Penicillium chrysogenum*. Biochimie. 115, 162-176.

Dos Santos Gomes, A.C., Falkoski, D., Battaglia, E., Peng, M., Nicolau de Almeida, M., Coconi Linares, N., Meijnen, J.P., Visser, J., de Vries, R.P., 2019. *Myceliophthora thermophila* Xyr1 is predominantly involved in xylan degradation and xylose catabolism. Biotechnol Biofuels. 12, 220.

Drescher, F., Li, Y., Villalobos-Escobedo, J.M., Haefner, S., Huberman, L.B., Glass, N.L., 2025. Transcriptomic and genetic analysis reveals a Zn2Cys6 transcription factor specifically required for conidiation in submerged cultures of *Thermothelomyces thermophilus*. mBio. 16 (1), e0311124.

Drula, E., Garron, M.L., Dogan, S., Lombard, V., Henrissat, B., Terrapon, N., 2022. The carbohydrate-active enzyme database: functions and literature. Nucleic Acids Res. 50 (D1), D571-D577.

Eveleigh, D.E., Mandels, M., Andreotti, R., Roche, C., 2009. Measurement of saccharifying cellulase. Biotechnol Biofuels. 2, 21.

Fan, F., Ma, G., Li, J., Liu, Q., Benz, J.P., Tian, C., Ma, Y., 2015. Genome-wide analysis of the endoplasmic reticulum stress response during lignocellulase production in *Neurospora crassa*. Biotechnol Biofuels. 8, 66.

Fordyce, P.M., Pincus, D., Kimmig, P., Nelson, C.S., El-Samad, H., Walter, P., DeRisi, J.L., 2012. Basic leucine zipper transcription factor Hac1 binds DNA in two distinct modes as revealed by microfluidic analyses. Proc Natl Acad Sci U S A. 109 (45), E3084-3093.

Frommhagen, M., Westphal, A.H., van Berkel, W.J.H., Kabel, M.A., 2018a. Distinct Substrate Specificities and Electron-Donating Systems of Fungal Lytic Polysaccharide

Monooxygenases. Front Microbiol. 9, 1080.

Frommhagen, M., Koetsier, M.J., Westphal, A.H., Visser, J., Hinz, S.W., Vincken, J.P., van Berkel, W.J., Kabel, M.A., Gruppen, H., 2016. Lytic polysaccharide monooxygenases from *Myceliophthora thermophila* C1 differ in substrate preference and reducing agent specificity. Biotechnol Biofuels. 9 (1), 186.

Frommhagen, M., Westphal, A.H., Hilgers, R., Koetsier, M.J., Hinz, S.W.A., Visser, J., Gruppen, H., van Berkel, W.J.H., Kabel, M.A., 2018b. Quantification of the catalytic performance of C1-cellulose-specific lytic polysaccharide monooxygenases. Appl Microbiol Biotechnol. 102 (3), 1281-1295.

Fujii, T., Inoue, H., Ishikawa, K., 2015. Decreased cellulase and xylanase production in the fungus *Talaromyces cellulolyticus* by disruption of tacA and tctA genes, encoding putative zinc finger transcriptional factors. Appl Biochem Biotechnol. 175 (6), 3218-3229.

Fujii, T., Inoue, H., Matsushika, A., 2021. The Transcription Factor Gene tclB2 Regulates Mannanolytic Enzyme Production in the Fungus *Talaromyces cellulolyticus*. Appl Biochem Biotechnol. 193 (10), 3163-3172.

Gao, B., Kunos, G., 2000. DNase I footprinting analysis of transcription factors recognizing adrenergic receptor gene promoter sequences. Methods Mol Biol. 126, 419-429.

Garcia-Huante, Y., Cayetano-Cruz, M., Santiago-Hernandez, A., Cano-Ramirez, C., Marsch-Moreno, R., Campos, J.E., Aguilar-Osorio, G., Benitez-Cardoza, C.G., Trejo-Estrada, S., Hidalgo-Lara, M.E., 2017. The thermophilic biomass-degrading fungus *Thielavia terrestris* Co3Bag1 produces a hyperthermophilic and thermostable beta-1,4-xylanase with exo- and endo-activity. Extremophiles. 21 (1), 175-186.

Ghose, T., 1987. Measurement of cellulase activities. Pure and applied Chemistry. 59 (2), 257-268.

Griffioen, G., Mager, W.H., Planta, R.J., 1994. Nutritional upshift response of ribosomal protein gene transcription in *Saccharomyces cerevisiae*. FEMS Microbiol Lett. 123 (1-2), 137-144.

Griffioen, G., Laan, R.J., Mager, W.H., Planta, R.J., 1996. Ribosomal protein gene transcription

in *Saccharomyces cerevisiae* shows a biphasic response to nutritional changes. Microbiology (Reading). 142 (Pt 8), 2279-2287.

Gu, S., Li, J., Chen, B., Sun, T., Liu, Q., Xiao, D., Tian, C., 2018. Metabolic engineering of the thermophilic filamentous fungus *Myceliophthora thermophila* to produce fumaric acid. Biotechnol Biofuels. 11, 323.

Gu, S., Zhao, Z., Xue, F., Liu, D., Liu, Q., Li, J., Tian, C., 2023. The arabinose transporter MtLat-1 is involved in hemicellulase repression as a pentose transceptor in *Myceliophthora thermophila*. Biotechnol Biofuels Bioprod. 16 (1), 51.

Gupta, A., Verma, J.P., 2015. Sustainable bio-ethanol production from agro-residues: A review. Renewable and Sustainable Energy Reviews. 41, 550-567.

Gupta, V.K., Kubicek, C.P., Berrin, J.G., Wilson, D.W., Couturier, M., Berlin, A., Filho, E.X.F., Ezeji, T., 2016. Fungal Enzymes for Bio-Products from Sustainable and Waste Biomass. Trends Biochem Sci. 41 (7), 633-645.

Hakkinen, M., Valkonen, M.J., Westerholm-Parvinen, A., Aro, N., Arvas, M., Vitikainen, M., Penttila, M., Saloheimo, M., Pakula, T.M., 2014. Screening of candidate regulators for cellulase and hemicellulase production in *Trichoderma reesei* and identification of a factor essential for cellulase production. Biotechnol Biofuels. 7 (1), 14.

Hetz, C., Papa, F.R., 2018. The Unfolded Protein Response and Cell Fate Control. Mol Cell. 69 (2), 169-181.

Himmel, M.E., Ding, S.Y., Johnson, D.K., Adney, W.S., Nimlos, M.R., Brady, J.W., Foust, T.D., 2007. Biomass recalcitrance: engineering plants and enzymes for biofuels production. Science. 315 (5813), 804-807.

Hogues, H., Lavoie, H., Sellam, A., Mangos, M., Roemer, T., Purisima, E., Nantel, A., Whiteway, M., 2008. Transcription factor substitution during the evolution of fungal ribosome regulation. Mol Cell. 29 (5), 552-562.

Hollenhorst, P.C., Bose, M.E., Mielke, M.R., Muller, U., Fox, C.A., 2000. Forkhead genes in transcriptional silencing, cell morphology and the cell cycle. Overlapping and distinct functions for FKH1 and FKH2 in *Saccharomyces cerevisiae*. Genetics. 154 (4), 1533-1548.

Huang, J., Cook, D.E., 2022. The contribution of DNA repair pathways to genome editing and evolution in filamentous pathogens. FEMS Microbiol Rev. 46 (6).

Huberman, L.B., Liu, J., Qin, L., Glass, N.L., 2016. Regulation of the lignocellulolytic response in filamentous fungi. Fungal Biology Reviews. 30 (3), 101-111.

Ichinose, S., Tanaka, M., Shintani, T., Gomi, K., 2018. Increased production of biomass-degrading enzymes by double deletion of creA and creB genes involved in carbon catabolite repression in *Aspergillus oryzae*. J Biosci Bioeng. 125 (2), 141-147.

Jadhav, R., Mach, R.L., Mach-Aigner, A.R., 2024. Protein secretion and associated stress in industrially employed filamentous fungi. Appl Microbiol Biotechnol. 108 (1), 92.

Jang, S.Y., Son, Y.E., Oh, D.S., Han, K.H., Yu, J.H., Park, H.S., 2023. The Forkhead Gene fkhB is Necessary for Proper Development in *Aspergillus nidulans*. J Microbiol Biotechnol. 33 (11), 1420-1427.

Joyia, M.A.K., Ahmad, M., Chen, Y.-F., Mustaqeem, M., Ali, A., Abbas, A., Gondal, M.A., 2024. Trends and advances in sustainable bioethanol production technologies from first to fourth generation: A critical review. Energy Convers Manage. 321, 119037.

Juturu, V., Wu, J.C., 2012. Microbial xylanases: engineering, production and industrial applications. Biotechnol Adv. 30 (6), 1219-1227.

Juturu, V., Wu, J.C., 2014. Microbial cellulases: Engineering, production and applications. Renewable and Sustainable Energy Reviews. 33, 188-203.

Kadowaki, M.A.S., Varnai, A., Jameson, J.K., AE, T.L., Costa-Filho, A.J., Kumagai, P.S., Prade, R.A., Polikarpov, I., Eijsink, V.G.H., 2018. Functional characterization of a lytic polysaccharide monooxygenase from the thermophilic fungus *Myceliophthora thermophila*. PLoS One. 13 (8), e0202148.

Karimi Aghcheh, R., Druzhinina, I.S., Kubicek, C.P., 2013. The putative protein methyltransferase LAE1 of *Trichoderma atroviride* is a key regulator of asexual development and mycoparasitism. PLoS One. 8 (6), e67144.

Karnaouri, A., Topakas, E., Antonopoulou, I., Christakopoulos, P., 2014. Genomic insights into the fungal lignocellulolytic system of *Myceliophthora thermophila*. Front Microbiol. 5, 281.

Karnaouri, A., Muraleedharan, M.N., Dimarogona, M., Topakas, E., Rova, U., Sandgren, M., Christakopoulos, P., 2017. Recombinant expression of thermostable processive MtEG5 endoglucanase and its synergism with MtLPMO from *Myceliophthora thermophila* during the hydrolysis of lignocellulosic substrates. Biotechnol Biofuels. 10, 126.

Kaufman, R.J., 1999. Stress signaling from the lumen of the endoplasmic reticulum: coordination of gene transcriptional and translational controls. Genes Dev. 13 (10), 1211-1233.

Kaufmann, E., Muller, D., Knochel, W., 1995. DNA recognition site analysis of *Xenopus* winged helix proteins. J Mol Biol. 248 (2), 239-254.

Kim, D., Langmead, B., Salzberg, S.L., 2015. HISAT: a fast spliced aligner with low memory requirements. Nat Methods. 12 (4), 357-360.

Kjaergaard, C.H., Qayyum, M.F., Wong, S.D., Xu, F., Hemsworth, G.R., Walton, D.J., Young, N.A., Davies, G.J., Walton, P.H., Johansen, K.S., Hodgson, K.O., Hedman, B., Solomon, E.I., 2014. Spectroscopic and computational insight into the activation of O2 by the mononuclear Cu center in polysaccharide monooxygenases. Proc Natl Acad Sci U S A. 111 (24), 8797-8802.

Klaubauf, S., Narang, H.M., Post, H., Zhou, M., Brunner, K., Mach-Aigner, A.R., Mach, R.L., Heck, A.J.R., Altelaar, A.F.M., de Vries, R.P., 2014. Similar is not the same: differences in the function of the (hemi-)cellulolytic regulator XlnR (Xlr1/Xyr1) in filamentous fungi. Fungal Genet Biol. 72, 73-81.

Kolbusz, M.A., Di Falco, M., Ishmael, N., Marqueteau, S., Moisan, M.C., Baptista, C.D.S., Powlowski, J., Tsang, A., 2014. Transcriptome and exoproteome analysis of utilization of plant-derived biomass by *Myceliophthora thermophila*. Fungal Genet Biol. 72, 10-20.

Korver, W., Roose, J., Clevers, H., 1997. The winged-helix transcription factor Trident is expressed in cycling cells. Nucleic Acids Res. 25 (9), 1715-1719.

Kumar, V., Binod, P., Sindhu, R., Gnansounou, E., Ahluwalia, V., 2018. Bioconversion of pentose sugars to value added chemicals and fuels: Recent trends, challenges and possibilities. Bioresour Technol. 269, 443-451.

Kun, R.S., Garrigues, S., Di Falco, M., Tsang, A., de Vries, R.P., 2021. Blocking utilization of major plant biomass polysaccharides leads Aspergillus niger towards utilization of minor components. Microb Biotechnol. 14 (4), 1683-1698.

Kun, R.S., Gomes, A.C.S., Hilden, K.S., Salazar Cerezo, S., Makela, M.R., de Vries, R.P., 2019. Developments and opportunities in fungal strain engineering for the production of novel enzymes and enzyme cocktails for plant biomass degradation. Biotechnol Adv. 37 (6), 107361.

Kun, R.S., Garrigues, S., Peng, M., Keymanesh, K., Lipzen, A., Ng, V., Tejomurthula, S., Grigoriev, I.V., de Vries, R.P., 2023. The transcriptional activator ClrB is crucial for the degradation of soybean hulls and guar gum in *Aspergillus niger*. Fungal Genet Biol. 165, 103781.

Lai, Y., Wang, J., Xie, N., Liu, G., Lacap-Bugler, D.C., 2025. Identification of a novel forkhead transcription factor MtFKH1 for cellulase and xylanase gene expression in *Myceliophthora thermophila* (ATCC 42464). Microbiol Res. 294, 128097.

Laissue, P., 2019. The forkhead-box family of transcription factors: key molecular players in colorectal cancer pathogenesis. Mol Cancer. 18 (1), 5.

Laoukili, J., Stahl, M., Medema, R.H., 2007. FoxM1: at the crossroads of ageing and cancer. Biochim Biophys Acta. 1775 (1), 92-102.

Lempiainen, H., Uotila, A., Urban, J., Dohnal, I., Ammerer, G., Loewith, R., Shore, D., 2009. Sfp1 interaction with TORC1 and Mrs6 reveals feedback regulation on TOR signaling. Mol Cell. 33 (6), 704-716.

Li, B., Dewey, C.N., 2011. RSEM: accurate transcript quantification from RNA-Seq data with or without a reference genome. BMC Bioinformatics. 12, 323.

Li, J., Lin, L., Li, H., Tian, C., Ma, Y., 2014. Transcriptional comparison of the filamentous fungus *Neurospora crassa* growing on three major monosaccharides D-glucose, D-xylose and L-arabinose. Biotechnol Biofuels. 7 (1), 31.

Li, J., Zhang, Y., Li, J., Sun, T., Tian, C., 2020a. Metabolic engineering of the cellulolytic thermophilic fungus *Myceliophthora thermophila* to produce ethanol from cellobiose. Biotechnol Biofuels. 13, 23.

Li, J., Lin, L., Sun, T., Xu, J., Ji, J., Liu, Q., Tian, C., 2020b. Direct production of commodity chemicals from lignocellulose using *Myceliophthora thermophila*. Metab Eng. 61, 416-426.

Li, J., Gu, S., Zhao, Z., Chen, B., Liu, Q., Sun, T., Sun, W., Tian, C., 2019. Dissecting cellobiose metabolic pathway and its application in biorefinery through consolidated bioprocessing in *Myceliophthora thermophila*. Fungal Biol Biotechnol. 6, 21.

Li, J., Wang, Y., Yang, K., Wang, X., Wang, Y., Zhang, H., Huang, H., Su, X., Yao, B., Luo, H., Qin, X., 2023a. Development of an efficient protein expression system in the thermophilic fungus *Myceliophthora thermophila*. Microb Cell Fact. 22 (1), 236.

Li, N., Kunitake, E., Aoyama, M., Ogawa, M., Kanamaru, K., Kimura, M., Koyama, Y., Kobayashi, T., 2016. McmA-dependent and -independent regulatory systems governing expression of ClrB-regulated cellulase and hemicellulase genes in *Aspergillus nidulans*. Mol Microbiol. 102 (5), 810-826.

Li, N., Liu, Y., Liu, D., Liu, D., Zhang, C., Lin, L., Zhu, Z., Li, H., Dai, Y., Wang, X., Liu, Q., Tian, C., 2022a. MtTRC-1, a Novel Transcription Factor, Regulates Cellulase Production via Directly Modulating the Genes Expression of the Mthac-1 and Mtcbh-1 in *Myceliophthora thermophila*. Appl Environ Microbiol. 88 (19), e0126322.

Li, X., Dilokpimol, A., Kabel, M.A., de Vries, R.P., 2022b. Fungal xylanolytic enzymes: Diversity and applications. Bioresour Technol. 344 (Pt B), 126290.

Li, X., Liu, Q., Sun, W., He, Q., Tian, C., 2020c. Improving cellulases production by *Myceliophthora thermophila* through disruption of protease genes. Biotechnol Lett. 42 (2), 219-229.

Li, X., Chomvong, K., Yu, V.Y., Liang, J.M., Lin, Y., Cate, J.H.D., 2015a. Cellobionic acid utilization: from *Neurospora crassa* to *Saccharomyces cerevisiae*. Biotechnol Biofuels. 8, 120.

Li, Y., Yan, P., Lu, X., Qiu, Y., Liang, S., Liu, G., Li, S., Mou, L., Xie, N., 2020d. Involvement of PaSNF1 in Fungal Development, Sterigmatocystin Biosynthesis, and Lignocellulosic Degradation in the Filamentous Fungus *Podospora anserina*. Front Microbiol. 11, 1038.

Li, Y., Song, W., Han, X., Wang, Y., Rao, S., Zhang, Q., Zhou, J., Li, J., Liu, S., Du, G., 2022c. Recent progress in key lignocellulosic enzymes: Enzyme discovery, molecular modifications, production, and enzymatic biomass saccharification. Bioresour Technol. 363, 127986.

Li, Y., Li, C., Muhammad Aqeel, S., Wang, Y., Zhang, Q., Ma, J., Zhou, J., Li, J., Du, G., Liu, S., 2023b. Enhanced expression of xylanase in *Aspergillus niger* enabling a two-step enzymatic pathway for extracting beta-glucan from oat bran. Bioresour Technol. 377, 128962.

Li, Z., Yao, G., Wu, R., Gao, L., Kan, Q., Liu, M., Yang, P., Liu, G., Qin, Y., Song, X., Zhong, Y., Fang, X., Qu, Y., 2015b. Synergistic and Dose-Controlled Regulation of Cellulase Gene Expression in *Penicillium oxalicum*. PLoS Genet. 11 (9), e1005509.

Liao, G.Y., Zhao, S., Zhang, T., Li, C.X., Liao, L.S., Zhang, F.F., Luo, X.M., Feng, J.X., 2018. The transcription factor TpRfx1 is an essential regulator of amylase and cellulase gene expression in *Talaromyces pinophilus*. Biotechnol Biofuels. 11, 276.

Liu, C.G., Xiao, Y., Xia, X.X., Zhao, X.Q., Peng, L., Srinophakun, P., Bai, F.W., 2019a. Cellulosic ethanol production: Progress, challenges and strategies for solutions. Biotechnol Adv. 37 (3), 491-504.

Liu, D., Garrigues, S., de Vries, R.P., 2023. Heterologous protein production in filamentous fungi. Appl Microbiol Biotechnol. 107 (16), 5019-5033.

Liu, G., Qu, Y., 2019. Engineering of filamentous fungi for efficient conversion of lignocellulose: Tools, recent advances and prospects. Biotechnol Adv. 37 (4), 519-529.

Liu, J., Chen, M., Gu, S., Fan, R., Zhao, Z., Sun, W., Yao, Y., Li, J., Tian, C., 2024. Independent metabolism of oligosaccharides is the keystone of synchronous utilization of cellulose and hemicellulose in *Myceliophthora*. PNAS Nexus. 3 (2), pgae053.

Liu, K., Dong, Y., Wang, F., Jiang, B., Wang, M., Fang, X., 2016. Regulation of cellulase expression, sporulation, and morphogenesis by velvet family proteins in *Trichoderma reesei*. Appl Microbiol Biotechnol. 100 (2), 769-779.

Liu, P., Lin, A., Zhang, G., Zhang, J., Chen, Y., Shen, T., Zhao, J., Wei, D., Wang, W., 2019b. Enhancement of cellulase production in *Trichoderma reesei* RUT-C30 by comparative

genomic screening. Microb Cell Fact. 18 (1), 81.

Liu, Q., Li, J., Gao, R., Li, J., Ma, G., Tian, C., 2019c. CLR-4, a novel conserved transcription factor for cellulase gene expression in ascomycete fungi. Mol Microbiol. 111 (2), 373-394.

Liu, Q., Zhang, Y., Li, F., Li, J., Sun, W., Tian, C., 2019d. Upgrading of efficient and scalable CRISPR-Cas-mediated technology for genetic engineering in thermophilic fungus *Myceliophthora thermophila*. Biotechnol Biofuels. 12, 293.

Liu, Q., Gao, R., Li, J., Lin, L., Zhao, J., Sun, W., Tian, C., 2017. Development of a genome-editing CRISPR/Cas9 system in thermophilic fungal *Myceliophthora* species and its application to hyper-cellulase production strain engineering. Biotechnol Biofuels. 10, 1.

Liu, Y.J., Li, B., Feng, Y., Cui, Q., 2020. Consolidated bio-saccharification: Leading lignocellulose bioconversion into the real world. Biotechnol Adv. 40, 107535.

Livak, K.J., Schmittgen, T.D., 2001. Analysis of relative gene expression data using real-time quantitative PCR and the 2(-Delta Delta C(T)) Method. Methods. 25 (4), 402-408.

Long, C., Cheng, Y., Cui, J., Liu, J., Gan, L., Zeng, B., Long, M., 2018. Enhancing Cellulase and Hemicellulase Production in *Trichoderma orientalis* EU7-22 via Knockout of the creA. Mol Biotechnol. 60 (1), 55-61.

Love, M.I., Huber, W., Anders, S., 2014. Moderated estimation of fold change and dispersion for RNA-seq data with DESeq2. Genome Biol. 15 (12), 550.

Lubeck, M., Lubeck, P.S., 2022. Fungal Cell Factories for Efficient and Sustainable Production of Proteins and Peptides. Microorganisms. 10 (4).

Ma, L., Chen, L., Zhang, L., Zou, G., Liu, R., Jiang, Y., Zhou, Z., 2016. RNA Sequencing Reveals Xyr1 as a Transcription Factor Regulating Gene Expression beyond Carbohydrate Metabolism. Biomed Res Int. 2016, 4841756.

Madhavan, A., Arun, K.B., Sindhu, R., Alphonsa Jose, A., Pugazhendhi, A., Binod, P., Sirohi, R., Reshmy, R., Kumar Awasthi, M., 2022. Engineering interventions in industrial filamentous fungal cell factories for biomass valorization. Bioresour Technol. 344 (Pt A), 126209.

Makela, M.R., Donofrio, N., de Vries, R.P., 2014. Plant biomass degradation by fungi. Fungal Genet Biol. 72, 2-9.

Maldonado-Bonilla, L.D., 2020. The endoribonuclease domain of IRE1 and its substrate HAC1 are structurally linked components of the unfolded protein response in fungi. Am J Biochem Biotechnol. 16, 482-493.

Mansour, A.A., Da Costa, A., Arnaud, T., Lu-Chau, T.A., Fdz-Polanco, M., Moreira, M.T., Cacho Rivero, J.A., 2016. Review of lignocellulolytic enzyme activity analyses and scale-down to microplate-based assays. Talanta. 150, 629-637.

Mao, Y., 2021. Structure, Dynamics and Function of the 26S Proteasome. Subcell Biochem. 96, 1-151.

Marion, R.M., Regev, A., Segal, E., Barash, Y., Koller, D., Friedman, N., O'Shea, E.K., 2004. Sfp1 is a stress- and nutrient-sensitive regulator of ribosomal protein gene expression. Proc Natl Acad Sci U S A. 101 (40), 14315-14322.

Marui, J., Kitamoto, N., Kato, M., Kobayashi, T., Tsukagoshi, N., 2002. Transcriptional activator, AoXlnR, mediates cellulose-inductive expression of the xylanolytic and cellulolytic genes in *Aspergillus oryzae*. FEBS Lett. 528 (1-3), 279-282.

Mattam, A.J., Chaudhari, Y.B., Velankar, H.R., 2022. Factors regulating cellulolytic gene expression in filamentous fungi: an overview. Microb Cell Fact. 21 (1), 44.

Mendonca, M., Barroca, M., Collins, T., 2023. Endo-1,4-beta-xylanase-containing glycoside hydrolase families: characteristics, singularities and similarities. Biotechnol Adv. 65, 108148.

Meng, J., Makela, M.R., de Vries, R.P., 2021. Molecular engineering to improve lignocellulosic biomass based applications using filamentous fungi. Adv Appl Microbiol. 114, 73-109.

Meng, Q., Abraham, B., Hu, J., Jiang, Y., 2025. Cutting-edge advances in strain and process engineering for boosting cellulase production in *Trichoderma reesei*. Bioresour Technol. 419, 132015.

Mohanty, S.K., Swain, M.R., 2019. Bioethanol Production From Corn and Wheat: Food, Fuel, and Future. In: Ray RC, Ramachandran S editors. Bioethanol Production from Food Crops: Academic Press. p. 45-59.

Montenegro-Montero, A., Goity, A., Larrondo, L.F., 2015. The bZIP Transcription Factor HAC-1 Is Involved in the Unfolded Protein Response and Is Necessary for Growth on Cellulose in *Neurospora crassa*. PLoS One. 10 (7), e0131415.

Morgenstern, I., Powlowski, J., Ishmael, N., Darmond, C., Marqueteau, S., Moisan, M.C., Quenneville, G., Tsang, A., 2012. A molecular phylogeny of thermophilic fungi. Fungal Biol. 116 (4), 489-502.

Mori, K., Ogawa, N., Kawahara, T., Yanagi, H., Yura, T., 1998. Palindrome with spacer of one nucleotide is characteristic of the cis-acting unfolded protein response element in *Saccharomyces cerevisiae*. J Biol Chem. 273 (16), 9912-9920.

Mulder, H.J., Nikolaev, I., 2009. HacA-dependent transcriptional switch releases hacA mRNA from a translational block upon endoplasmic reticulum stress. Eukaryot Cell. 8 (4), 665-675.

Mulder, H.J., Nikolaev, I., Madrid, S.M., 2006. HACA, the transcriptional activator of the unfolded protein response (UPR) in *Aspergillus niger*, binds to partly palindromic UPR elements of the consensus sequence 5'-CAN(G/A)NTGT/GCCT-3'. Fungal Genet Biol. 43 (8), 560-572.

Mulder, H.J., Saloheimo, M., Penttila, M., Madrid, S.M., 2004. The transcription factor HACA mediates the unfolded protein response in *Aspergillus niger*, and up-regulates its own transcription. Mol Genet Genomics. 271 (2), 130-140.

Naik, S.N., Goud, V.V., Rout, P.K., Dalai, A.K., 2010. Production of first and second generation biofuels: A comprehensive review. Renewable and Sustainable Energy Reviews. 14 (2), 578-597.

Nakari-Setala, T., Paloheimo, M., Kallio, J., Vehmaanpera, J., Penttila, M., Saloheimo, M., 2009. Genetic modification of carbon catabolite repression in *Trichoderma reesei* for improved protein production. Appl Environ Microbiol. 75 (14), 4853-4860.

Nanda, S., Rana, R., Sarangi, P.K., Dalai, A.K., Kozinski, J.A., 2018. A Broad Introduction to First-, Second-, and Third-Generation Biofuels. In: Sarangi PK,Nanda S, Mohanty P editors. Recent Advancements in Biofuels and Bioenergy Utilization. Singapore: Springer Singapore. p. 1-25.

Natarajan, K., Meyer, M.R., Jackson, B.M., Slade, D., Roberts, C., Hinnebusch, A.G., Marton, M.J., 2001. Transcriptional profiling shows that Gcn4p is a master regulator of gene expression during amino acid starvation in yeast. Mol Cell Biol. 21 (13), 4347-4368.

Nodvig, C.S., Nielsen, J.B., Kogle, M.E., Mortensen, U.H., 2015. A CRISPR-Cas9 System for Genetic Engineering of Filamentous Fungi. PLoS One. 10 (7), e0133085.

Noguchi, Y., Sano, M., Kanamaru, K., Ko, T., Takeuchi, M., Kato, M., Kobayashi, T., 2009. Genes regulated by AoXlnR, the xylanolytic and cellulolytic transcriptional regulator, in *Aspergillus oryzae*. Appl Microbiol Biotechnol. 85 (1), 141-154.

Ogawa, M., Kobayashi, T., Koyama, Y., 2012. ManR, a novel Zn(II)2Cys6 transcriptional activator, controls the beta-mannan utilization system in *Aspergillus oryzae*. Fungal Genet Biol. 49 (12), 987-995.

Ogawa, M., Kobayashi, T., Koyama, Y., 2013. ManR, a transcriptional regulator of the beta-mannan utilization system, controls the cellulose utilization system in *Aspergillus oryzae*. Biosci Biotechnol Biochem. 77 (2), 426-429.

Pakula, T.M., Laxell, M., Huuskonen, A., Uusitalo, J., Saloheimo, M., Penttila, M., 2003. The effects of drugs inhibiting protein secretion in the filamentous fungus *Trichoderma reesei*. Evidence for down-regulation of genes that encode secreted proteins in the stressed cells. J Biol Chem. 278 (45), 45011-45020.

Pant, S., Ritika, Nag, P., Ghati, A., Chakraborty, D., Maximiano, M.R., Franco, O.L., Mandal, A.K., Kuila, A., 2022. Employment of the CRISPR/Cas9 system to improve cellulase production in *Trichoderma reesei*. Biotechnol Adv. 60, 108022.

Park, H.S., Ni, M., Jeong, K.C., Kim, Y.H., Yu, J.H., 2012. The role, interaction and regulation of the velvet regulator VelB in *Aspergillus nidulans*. PLoS One. 7 (9), e45935.

Park, J., Kong, S., Kim, S., Kang, S., Lee, Y.H., 2014. Roles of Forkhead-box Transcription Factors in Controlling Development, Pathogenicity, and Stress Response in *Magnaporthe oryzae*. Plant Pathol J. 30 (2), 136-150.

Patel, A.K., Singhania, R.R., Sim, S.J., Pandey, A., 2019. Thermostable cellulases: Current status and perspectives. Bioresour Technol. 279, 385-392.

Patil, C.K., Li, H., Walter, P., 2004. Gcn4p and novel upstream activating sequences regulate

targets of the unfolded protein response. PLoS Biol. 2 (8), E246.

Petibon, C., Malik Ghulam, M., Catala, M., Abou Elela, S., 2021. Regulation of ribosomal protein genes: An ordered anarchy. Wiley Interdiscip Rev RNA. 12 (3), e1632.

Phillips, C.M., Beeson, W.T., Cate, J.H., Marletta, M.A., 2011. Cellobiose dehydrogenase and a copper-dependent polysaccharide monooxygenase potentiate cellulose degradation by *Neurospora crassa*. ACS Chem Biol. 6 (12), 1399-1406.

Porciuncula Jde, O., Furukawa, T., Mori, K., Shida, Y., Hirakawa, H., Tashiro, K., Kuhara, S., Nakagawa, S., Morikawa, Y., Ogasawara, W., 2013. Single nucleotide polymorphism analysis of a Trichoderma reesei hyper-cellulolytic mutant developed in Japan. Biosci Biotechnol Biochem. 77 (3), 534-543.

Powers, T., Walter, P., 1999. Regulation of ribosome biogenesis by the rapamycin-sensitive TOR-signaling pathway in *Saccharomyces cerevisiae*. Mol Biol Cell. 10 (4), 987-1000.

Raheja, Y., Gaur, P., Islam, T., Chaurasia, A.K., Gaur, V.K., Chadha, B.S., 2025. Advancement in lignocellulolytic enzyme production: tailored strategies to overcome challenges in biomass hydrolysis. Syst Microbiol Biomanuf. 5 (3), 948-968.

Raulo, R., Kokolski, M., Archer, D.B., 2016. The roles of the zinc finger transcription factors XlnR, ClrA and ClrB in the breakdown of lignocellulose by *Aspergillus niger*. AMB Express. 6 (1), 5.

Richie, D.L., Hartl, L., Aimanianda, V., Winters, M.S., Fuller, K.K., Miley, M.D., White, S., McCarthy, J.W., Latgé, J.P., Feldmesser, M., Rhodes, J.C., Askew, D.S., 2009. A role for the unfolded protein response (UPR) in virulence and antifungal susceptibility in *Aspergillus fumigatus*. PLoS Pathog. 5 (1), e1000258.

Ries, L., Pullan, S.T., Delmas, S., Malla, S., Blythe, M.J., Archer, D.B., 2013. Genome-wide transcriptional response of Trichoderma reesei to lignocellulose using RNA sequencing and comparison with *Aspergillus niger*. BMC Genomics. 14, 541.

Rubin, E.M., 2008. Genomics of cellulosic biofuels. Nature. 454 (7206), 841-845.

Rudra, D., Zhao, Y., Warner, J.R., 2005. Central role of Ifh1p-Fhl1p interaction in the synthesis of yeast ribosomal proteins. EMBO J. 24 (3), 533-542.

Sakata, E., Eisele, M.R., Baumeister, W., 2021. Molecular and cellular dynamics of the 26S

proteasome. Biochim Biophys Acta Proteins Proteom. 1869 (3), 140583.

Sakekar, A.A., Gaikwad, S.R., Punekar, N.S., 2021. Protein expression and secretion by filamentous fungi. Journal of Biosciences. 46 (1).

Saldarriaga-Hernandez, S., Velasco-Ayala, C., Leal-Isla Flores, P., de Jesus Rostro-Alanis, M., Parra-Saldivar, R., Iqbal, H.M.N., Carrillo-Nieves, D., 2020. Biotransformation of lignocellulosic biomass into industrially relevant products with the aid of fungi-derived lignocellulolytic enzymes. Int J Biol Macromol. 161, 1099-1116.

Saloheimo, A., Aro, N., Ilmen, M., Penttila, M., 2000. Isolation of the ace1 gene encoding a Cys(2)-His(2) transcription factor involved in regulation of activity of the cellulase promoter cbh1 of *Trichoderma reesei*. J Biol Chem. 275 (8), 5817-5825.

Saloheimo, M., Valkonen, M., Penttilä, M., 2003. Activation mechanisms of the HAC1-mediated unfolded protein response in filamentous fungi. Mol Microbiol. 47 (4), 1149-1161.

Sanchez, C., 2009. Lignocellulosic residues: biodegradation and bioconversion by fungi. Biotechnol Adv. 27 (2), 185-194.

Schmitt, E.K., Hoff, B., Kuck, U., 2004. AcFKH1, a novel member of the forkhead family, associates with the RFX transcription factor CPCR1 in the cephalosporin C-producing fungus *Acremonium chrysogenum*. Gene. 342 (2), 269-281.

Seiboth, B., Karimi, R.A., Phatale, P.A., Linke, R., Hartl, L., Sauer, D.G., Smith, K.M., Baker, S.E., Freitag, M., Kubicek, C.P., 2012. The putative protein methyltransferase LAE1 controls cellulase gene expression in *Trichoderma reesei*. Mol Microbiol. 84 (6), 1150-1164.

Shen, Q., Ruan, H., Zhang, H., Wu, T., Zhu, K., Han, W., Dong, R., Ming, T., Qi, H., Zhang, Y., 2024. Utilization of CRISPR-Cas genome editing technology in filamentous fungi: function and advancement potentiality. Front Microbiol. 15, 1375120.

Shi, Y.G., Tyler, B.M., 1991. Coordinate expression of ribosomal protein genes in *Neurospora crassa* and identification of conserved upstream sequences. Nucleic Acids Res. 19 (23), 6511-6517.

Shore, D., Zencir, S., Albert, B., 2021. Transcriptional control of ribosome biogenesis in yeast:

links to growth and stress signals. Biochem Soc Trans. 49 (4), 1589-1599.

Singh, B., 2016. *Myceliophthora thermophila* syn. *Sporotrichum thermophile*: a thermophilic mould of biotechnological potential. Crit Rev Biotechnol. 36 (1), 59-69.

Singhania, R.R., Sukumaran, R.K., Patel, A.K., Larroche, C., Pandey, A., 2010. Advancement and comparative profiles in the production technologies using solid-state and submerged fermentation for microbial cellulases. Enzyme and Microbial Technology. 46 (7), 541-549.

Soid-Raggi, G., Sanchez, O., Aguirre, J., 2006. TmpA, a member of a novel family of putative membrane flavoproteins, regulates asexual development in *Aspergillus nidulans*. Mol Microbiol. 59 (3), 854-869.

Sperandio, G.B., Filho, E.X.F., 2021. An overview of Trichoderma reesei co-cultures for the production of lignocellulolytic enzymes. Appl Microbiol Biotechnol. 105 (8), 3019-3025.

Stricker, A.R., Grosstessner-Hain, K., Wurleitner, E., Mach, R.L., 2006. Xyr1 (xylanase regulator 1) regulates both the hydrolytic enzyme system and D-xylose metabolism in *Hypocrea jecorina*. Eukaryot Cell. 5 (12), 2128-2137.

Sun, J., Glass, N.L., 2011. Identification of the CRE-1 cellulolytic regulon in *Neurospora crassa*. PLoS One. 6 (9), e25654.

Sun, J., Tian, C., Diamond, S., Glass, N.L., 2012. Deciphering transcriptional regulatory mechanisms associated with hemicellulose degradation in *Neurospora crassa*. Eukaryot Cell. 11 (4), 482-493.

Sun, X., Liang, Y., Wang, Y., Zhang, H., Zhao, T., Yao, B., Luo, H., Huang, H., Su, X., 2022. Simultaneous manipulation of multiple genes within a same regulatory stage for iterative evolution of *Trichoderma reesei*. Biotechnol Biofuels Bioprod. 15 (1), 26.

Sun, X., Zhang, X., Huang, H., Wang, Y., Tu, T., Bai, Y., Wang, Y., Zhang, J., Luo, H., Yao, B., Su, X., 2020. Engineering the cbh1 Promoter of *Trichoderma reesei* for Enhanced Protein Production by Replacing the Binding Sites of a Transcription Repressor ACE1 to Those of the Activators. J Agric Food Chem. 68 (5), 1337-1346.

Taha, M., Foda, M., Shahsavari, E., Aburto-Medina, A., Adetutu, E., Ball, A., 2016.

Commercial feasibility of lignocellulose biodegradation: possibilities and challenges. Curr Opin Biotechnol. 38, 190-197.

Tani, S., Hirose, S., Kawaguchi, T., 2024. Combinational manipulation of transcription factors, CreA and ClbR, is a viable strategy to improve cellulolytic enzyme production in *Aspergillus aculeatus*. J Biosci Bioeng. 138 (5), 361-368.

Tian, C., Kasuga, T., Sachs, M.S., Glass, N.L., 2007. Transcriptional profiling of cross pathway control in *Neurospora crassa* and comparative analysis of the Gcn4 and CPC1 regulons. Eukaryot Cell. 6 (6), 1018-1029.

van Peij, N.N., Gielkens, M.M., de Vries, R.P., Visser, J., de Graaff, L.H., 1998. The transcriptional activator XlnR regulates both xylanolytic and endoglucanase gene expression in *Aspergillus niger*. Appl Environ Microbiol. 64 (10), 3615-3619.

Visser, H., Joosten, V., Punt, P.J., Gusakov, A.V., Olson, P.T., Joosten, R., Bartels, J., Visser, J., Sinitsyn, A.P., Emalfarb, M.A., 2011. Development of a mature fungal technology and production platform for industrial enzymes based on a *Myceliophthora thermophila* isolate, previously known as Chrysosporium lucknowense C1. Industrial Biotechnology. 7 (3), 214-223.

Wang, B., Li, J., Gao, J., Cai, P., Han, X., Tian, C., 2017. Identification and characterization of the glucose dual-affinity transport system in *Neurospora crassa*: pleiotropic roles in nutrient transport, signaling, and carbon catabolite repression. Biotechnol Biofuels. 10, 17.

Wang, J., Gong, Y., Zhao, S., Liu, G., 2018. A new regulator of cellulase and xylanase in the thermophilic fungus *Myceliophthora thermophila* strain ATCC 42464. 3 Biotech. 8 (3), 160.

Wang, J., Wu, Y., Gong, Y., Yu, S., Liu, G., 2015. Enhancing xylanase production in the thermophilic fungus *Myceliophthora thermophila* by homologous overexpression of Mtxyr1. J Ind Microbiol Biotechnol. 42 (9), 1233-1241.

Wang, J., Wang, W., Wang, L., Zhang, G., Fan, K., Tan, H., Yang, K., 2011. A novel role of 'pseudo'gamma-butyrolactone receptors in controlling gamma-butyrolactone biosynthesis in *Streptomyces*. Mol Microbiol. 82 (1), 236-250.

Wang, K., Luo, H., Bai, Y., Shi, P., Huang, H., Xue, X., Yao, B., 2014. A thermophilic endo-1,4-beta-glucanase from *Talaromyces emersonii* CBS394.64 with broad substrate specificity and great application potentials. Appl Microbiol Biotechnol. 98 (16), 7051-7060.

Wang, S., Liu, G., Wang, J., Yu, J., Huang, B., Xing, M., 2013. Enhancing cellulase production in *Trichoderma reesei* RUT C30 through combined manipulation of activating and repressing genes. J Ind Microbiol Biotechnol. 40 (6), 633-641.

Wang, Y., Cen, X.F., Zhao, G.P., Wang, J., 2012. Characterization of a new GlnR binding box in the promoter of amtB in *Streptomyces coelicolor* inferred a PhoP/GlnR competitive binding mechanism for transcriptional regulation of amtB. J Bacteriol. 194 (19), 5237-5244.

Wimalasena, T.T., Enjalbert, B., Guillemette, T., Plumridge, A., Budge, S., Yin, Z., Brown, A.J., Archer, D.B., 2008. Impact of the unfolded protein response upon genome-wide expression patterns, and the role of Hac1 in the polarized growth, of *Candida albicans*. Fungal Genet Biol. 45 (9), 1235-1247.

Wosten, H.A.B., 2019. Filamentous fungi for the production of enzymes, chemicals and materials. Curr Opin Biotechnol. 59, 65-70.

Xia, X., 2019. Translation Control of HAC1 by Regulation of Splicing in *Saccharomyces cerevisiae*. Int J Mol Sci. 20 (12).

Xie, S., Shen, B., Zhang, C., Huang, X., Zhang, Y., 2014. sgRNAcas9: a software package for designing CRISPR sgRNA and evaluating potential off-target cleavage sites. PLoS One. 9 (6), e100448.

Xu, G., Li, J., Liu, Q., Sun, W., Jiang, M., Tian, C., 2018. Transcriptional analysis of *Myceliophthora thermophila* on soluble starch and role of regulator AmyR on polysaccharide degradation. Bioresour Technol. 265, 558-562.

Xu, W., Ren, Y., Xia, Y., Liu, L., Meng, X., Chen, G., Zhang, W., Liu, W., 2023. A novel transcriptional repressor specifically regulates xylanase gene 1 in *Trichoderma reesei*. Biotechnol Biofuels Bioprod. 16 (1), 161.

Xue, F., Zhao, Z., Gu, S., Chen, M., Xu, J., Luo, X., Li, J., Tian, C., 2023. The transcriptional

factor Clr-5 is involved in cellulose degradation through regulation of amino acid metabolism in *Neurospora crassa*. BMC Biotechnol. 23 (1), 50.

Xue, Y., Han, J., Li, Y., Liu, J., Gan, L., Long, M., 2020. Promoting cellulase and hemicellulase production from *Trichoderma orientalis* EU7-22 by overexpression of transcription factors Xyr1 and Ace3. Bioresour Technol. 296, 122355.

Yan, Y.S., Zhao, S., Liao, L.S., He, Q.P., Xiong, Y.R., Wang, L., Li, C.X., Feng, J.X., 2017. Transcriptomic profiling and genetic analyses reveal novel key regulators of cellulase and xylanase gene expression in *Penicillium oxalicum*. Biotechnol Biofuels. 10, 279.

Yang, F., Gong, Y., Liu, G., Zhao, S., Wang, J., 2015. Enhancing Cellulase Production in Thermophilic Fungus *Myceliophthora thermophila* ATCC42464 by RNA Interference of cre1 Gene Expression. J Microbiol Biotechnol. 25 (7), 1101-1107.

Yang, J., Yue, H.R., Pan, L.Y., Feng, J.X., Zhao, S., Suwannarangsee, S., Chempreda, V., Liu, C.G., Zhao, X.Q., 2023. Fungal strain improvement for efficient cellulase production and lignocellulosic biorefinery: Current status and future prospects. Bioresour Technol. 385, 129449.

Yao, C., Yan, M., Li, K., Gao, W., Li, X., Zhang, J., Liu, H., Zhong, Y., 2023. The ERAD Pathway Participates in Fungal Growth and Cellulase Secretion in *Trichoderma reesei*. J Fungi (Basel). 9 (1).

Yeoman, C.J., Han, Y., Dodd, D., Schroeder, C.M., Mackie, R.I., Cann, I.K., 2010. Thermostable enzymes as biocatalysts in the biofuel industry. Adv Appl Microbiol. 70, 1-55.

Yu, M., Zhou, X., Chen, D., Jiao, Y., Han, G., Tao, F., 2024. HacA, a key transcription factor for the unfolded protein response, is required for fungal development, aflatoxin biosynthesis and pathogenicity of *Aspergillus flavus*. Int J Food Microbiol. 417, 110693.

Zhang, C., Li, N., Rao, L., Li, J., Liu, Q., Tian, C., 2022. Development of an Efficient C-to-T Base-Editing System and Its Application to Cellulase Transcription Factor Precise Engineering in Thermophilic Fungus *Myceliophthora thermophila*. Microbiol Spectr. 10 (3), e0232121.

Zhang, F., Zhao, X., Bai, F., 2018. Improvement of cellulase production in *Trichoderma reesei*

Rut-C30 by overexpression of a novel regulatory gene Trvib-1. Bioresour Technol. 247, 676-683.

Zhang, J., Li, K., Sun, Y., Yao, C., Liu, W., Liu, H., Zhong, Y., 2024a. An efficient CRISPR/Cas9 genome editing system based on a multiple sgRNA processing platform in *Trichoderma reesei* for strain improvement and enzyme production. Biotechnol Biofuels Bioprod. 17 (1), 22.

Zhang, T., Liu, H., Lv, B., Li, C., 2020. Regulating Strategies for Producing Carbohydrate Active Enzymes by Filamentous Fungal Cell Factories. Front Bioeng Biotechnol. 8, 691.

Zhang, T., Mai, R.M., Fang, Q.Q., Ou, J.F., Mo, L.X., Tian, D., Li, C.X., Gu, L.S., Luo, X.M., Feng, J.X., Zhao, S., 2021. Regulatory function of the novel transcription factor CxrC in *Penicillium oxalicum*. Mol Microbiol. 116 (6), 1512-1532.

Zhang, X., Zhu, Y., Bao, L., Gao, L., Yao, G., Li, Y., Yang, Z., Li, Z., Zhong, Y., Li, F., Yin, H., Qu, Y., Qin, Y., 2016. Putative methyltransferase LaeA and transcription factor CreA are necessary for proper asexual development and controlling secondary metabolic gene cluster expression. Fungal Genet Biol. 94, 32-46.

Zhang, Z., Xing, J., Li, X., Lu, X., Liu, G., Qu, Y., Zhao, J., 2024b. Review of research progress on the production of cellulase from filamentous fungi. Int J Biol Macromol. 277 (Pt 4), 134539.

Zhao, S., Zhang, T., Hasunuma, T., Kondo, A., Zhao, X.Q., Feng, J.X., 2024a. Every road leads to Rome: diverse biosynthetic regulation of plant cell wall-degrading enzymes in filamentous fungi *Penicillium oxalicum* and *Trichoderma reesei*. Crit Rev Biotechnol. 44 (7), 1241-1261.

Zhao, S., Wang, J.X., Hou, R., Ning, Y.N., Chen, Z.X., Liu, Q., Luo, X.M., Feng, J.X., 2023a. Novel Transcription Factor CXRD Regulates Cellulase and Xylanase Biosynthesis in *Penicillium oxalicum* under Solid-State Fermentation. Appl Environ Microbiol. 89 (6), e0036023.

Zhao, S., Liu, Q., Wang, J.X., Liao, X.Z., Guo, H., Li, C.X., Zhang, F.F., Liao, L.S., Luo, X.M., Feng, J.X., 2019. Differential transcriptomic profiling of filamentous fungus during

solid-state and submerged fermentation and identification of an essential regulatory gene PoxMBF1 that directly regulated cellulase and xylanase gene expression. Biotechnol Biofuels. 12, 103.

Zhao, S., Yan, Y.S., He, Q.P., Yang, L., Yin, X., Li, C.X., Mao, L.C., Liao, L.S., Huang, J.Q., Xie, S.B., Nong, Q.D., Zhang, Z., Jing, L., Xiong, Y.R., Duan, C.J., Liu, J.L., Feng, J.X., 2016. Comparative genomic, transcriptomic and secretomic profiling of *Penicillium oxalicum* HP7-1 and its cellulase and xylanase hyper-producing mutant EU2106, and identification of two novel regulatory genes of cellulase and xylanase gene expression. Biotechnol Biofuels. 9, 203.

Zhao, X.Q., Liu, C.G., Bai, F.W., 2024b. Making the biochemical conversion of lignocellulose more robust. Trends Biotechnol. 42 (4), 418-430.

Zhao, Z., Gu, S., Liu, D., Liu, D., Chen, B., Li, J., Tian, C., 2023b. The putative methyltransferase LaeA regulates mycelium growth and cellulase production in *Myceliophthora thermophila*. Biotechnol Biofuels Bioprod. 16 (1), 58.

Zhou, B., Xie, J., Liu, X., Wang, B., Pan, L., 2016. Functional and transcriptomic analysis of the key unfolded protein response transcription factor HacA in *Aspergillus oryzae*. Gene. 593 (1), 143-153.

Zhu, G., Spellman, P.T., Volpe, T., Brown, P.O., Botstein, D., Davis, T.N., Futcher, B., 2000. Two yeast forkhead genes regulate the cell cycle and pseudohyphal growth. Nature. 406 (6791), 90-94.

Zhu, Z., Zhang, M., Liu, D., Liu, D., Sun, T., Yang, Y., Dong, J., Zhai, H., Sun, W., Liu, Q., Tian, C., 2023. Development of the thermophilic fungus *Myceliophthora thermophila* into glucoamylase hyperproduction system via the metabolic engineering using improved AsCas12a variants. Microb Cell Fact. 22 (1), 150.

Znameroski, E.A., Li, X., Tsai, J.C., Galazka, J.M., Glass, N.L., Cate, J.H., 2014. Evidence for transceptor function of cellodextrin transporters in *Neurospora crassa*. J Biol Chem. 289 (5), 2610-2619.

Zou, G., Shi, S., Jiang, Y., van den Brink, J., de Vries, R.P., Chen, L., Zhang, J., Ma, L., Wang, C., Zhou, Z., 2012. Construction of a cellulase hyper-expression system in

Trichoderma reesei by promoter and enzyme engineering. Microb Cell Fact. 11, 21.